FINAL REPORT

DESIGN FOR PRESSURE REGULATING COMPONENTS

March 1973

Prepared for:

Jet Propulsion Laboratory
California Institute of Technology

Contract No. 953383

The Marquardt Company
Van Nuys, California

FINAL REPORT

DESIGN FOR PRESSURE REGULATING COMPONENTS

By

H. Wichmann

March 1973

Prepared for:

Jet Propulsion Laboratory
California Institute of Technology

Contract No. 953383

The Marquardt Company
Van Nuys, California

1.

<u>FOREWORD</u>

This report is submitted by The Marquardt Company in accordance with the requirements of JPL Contract No. 953383 dated April 19, 1972. The work was administered by the Jet Propulsion Laboratory, California Institute of Technology, Pasadena, California, with Mr. George Yankura as the JPL Technical Manager.

This program was performed by the engineering department of The Marquardt Company at the Van Nuys facility. The Project Manager was Mr. H. Wichmann. Major contributors to this program were Mr. R. Braendlein, who performed all flow analyses and dynamic simulations on the analog computer, and Mr. A. Marderian, who prepared the regulator design layouts and the detailed design of the test fixture. Other contributors were Mr. I. Dickens, stress analysis; Mr. R. Loustau, liaison engineering; Mr. A. Malek, design management; and Mr. R. Dickinson, test.

2.
ABSTRACT

The design development for Pressure Regulating Components included a regulator component trade-off study with analog computer performance verification to arrive at a final optimized regulator configuration for the Space Storable Propulsion Module, under development for a Jupiter Orbiter mission. This application requires the pressure regulator to be capable of long-term fluorine exposure. In addition, individual but basically identical (for purposes of commonality) units are required for separate oxidizer and fuel pressurization. The need for dual units requires improvement in the regulation accuracy over present designs. An advanced regulator concept was prepared featuring redundant bellows, all metallic/ceramic construction, friction-free guidance of moving parts, gas damping, and the elimination of coil springs normally used for reference forces. The activities included testing of actual size seat/poppet components to determine actual discharge coefficients and flow forces. The resulting data was inserted into the computer model of the regulator. Computer simulation of the propulsion module perform-ance over two mission profiles indicated satisfactory minimization of propellant residual requirements imposed by regulator performance uncertainties. It is recommended that prototype units be fabricated and tested.

TABLE OF CONTENTS

TABLE OF CONTENTS
(Continued)

TABLE OF CONTENTS
(Continued)

APPENDICES:

3. PROGRAM SCOPE

The purpose of the program described in this report was the design and performance analysis of pressure regulating components which, with a minimum of modification and improvement, can be developed into flight hardware for the Space Storable Propulsion Module. The Space Storable Propulsion Module is the delta-V propulsion system to be employed in a spacecraft which will orbit the Planet Jupiter during the late seventies; this propulsion system utilizes advanced propellants and operates at a thrust level of 600 pounds. Approximately 90% of the subject program consisted of analytical, design, and study efforts with the remaining 10% devoted to the experimental determination of critical design criteria.

The design for pressure regulating components program consisted of four primary tasks. These tasks were:

  I   Pressure Regulator Design, Analysis, and Optimization

  II   Work Principles Proof

  III   Dynamic Modeling of the Propellant Feed System

  IV   Propulsion System Dynamic Modeling

Task I consisted of the design of a pressure regulator clearly capable of meeting the application requirements as defined in Section 4 of this report with a high degree of reliability and with low development risk. This effort included the trade-off of regulator components to arrive at the optimum configuration. During this task critical design criteria which were not amenable to analytical treatment alone and which required experimental verification to permit prediction of actual hardware performance within ± 10% were identified. These design criteria were experimentally determined during Task II.

Task II featured the design and fabrication of a test fixture with a poppet/seat interface identical to that of the optimized pressure regulator configuration. This test fixture further included a solenoid actuator to permit operation of the poppet/seat interface as well as means for the measurement of poppet actuation forces, poppet stroke, and gas flowrates. The test fixture was installed in a high pressure Helium flow facility and the poppet/seat discharge coefficient and poppet flow force were determined over the required inlet pressure operating range.

During Task III an analog model of one side (analogous to either oxidizer or fuel half) of the complete propellant feed system, including the optimized pressure regulator configuration, was prepared to permit the evaluation of the dynamic characteristics of this feed system. Operational modes such as inlet pressure surges due to the opening of upstream isolation valves during system arming (slam start), engine start and steady state operation, and system lock-up upon closing of the engine propellant valves were simulated.

1

Task IV consisted of the dynamic simulation of the complete propulsion system (two feed systems in parallel). For a possible 5% uncertainty in pressurant supply temperature and allowing for the maximum expected errors in component performance repeatability, the nominal and maximum pressurant and propellant loadings needed to assure completion of the mission as defined by two typical mission duty cycles were determined.

4.   TECHNICAL REQUIREMENTS

The primary requirement of the pressure regulating components is that they control the fuel and oxidizer feed pressures such that: (a) the amount of residual propellants that must be loaded, in addition to the nominal quantities, to guarantee against premature depletion of either propellant is tolerable, (b) variations in mixture ratio are maintained within thruster requirements, and (c) variations in total combined flow rate are minimized. As estimated from preliminary analyses, the desired limit on propellant residuals corresponds to that which would result were the feed pressures controlled to an accuracy of ± 1 percent of the nominal levels. The difficulty in achieving this degree of controlls compounded by: (a) the differences in the pressure and temperature levels of the individual pressurant supplies, (b) variations in the supply temperatures and pressures due to pressurant gas expansion, and (c) errors in the expected values due to uncertainties in vehicle thermal balance. The desired limits on the shifts in mixture ratio and total combined flow rate are not yet determined, however they appear to be minor constraints on component performance compared to the propellant residuals limitation.

Upon the cessation of propellant demand (coincident with engine shutdown) the regulator components must isolate the propellant tanks from the pressurant supplies. The maximum tolerable internal leakage is 45 scch Helium. The lockup pressure must not exceed approximately 1.05 times the nominal outlet pressure.

During launch and coast periods the regulator components will themselves be isolated from the pressurant supplies by shutoff valves. When the valves are opened, preparatory to an engine burn, the regulators must not permit pressure overshoot in the pressurant diffuser of the propellant tank to levels exceeding 280 psig, or cause the post-transient pressure to exceed the lockup pressure limit. The regulator response must not be adversely affected by the type of propellant acquisition device employed in the propellant tanks. Certain aquisition devices, which utilize only surface tension forces to orient the propellant in the tank, may permit migration of liquid into the pressurant lines and internal chambers in the regulator.

Upon engine start and shutdown the regulator components will experience a flow transient. Especially during engine start, any outlet pressure and/or flow instabilities must be minimized. No instabilities can be permitted, over any portion of the operation, which would result in a pressure oscillation in the propellant tanks in excess of ± 1/2 psi.

Another important requirement of the components is long life performance capability and compatibility with the respective propellants. The components must retain their design functional integrity for ten years in the space environment presented by the mission.

Because of the need for maximum thermal isolation of the fuel and oxidizer system, and also for the prevention of inter-leakage of propellants, any mechanical or pneumatic coupling between the respective pressure regulator components is undesirable.

Filtration required to protect the regulator components and assure satisfactory operation should be incorporated integrally.

The combined weight goal for the pressure regulator components is 4 pounds.

The Space Storable Propulsion Module will use either of two propellant combinations: FLOX*/monomethyl hydrazine or Fluorine/hydrazine. A schematic of the module is shown in Figure 4-I. A tabulation of the characteristics of the FLOX/MMH propulsion system is given in Table 4-I. A tabulation for the F_2/N_2H_4 system is given in Table 4-II. The pressure budget for the propulsion system components is given in Table 4-III. Two typical mission duty cycles for the FLOX/MMH system are listed in Table 4-IV. Computer printouts of these duty cycles were obtained from the Jet Propulsion Laboratory Univac 1108 Computer utilizing Program PSOP-C. This program is a single precision FORTRAN V Program, which is described in Reference 1. The program integrates a system of 16 first order differential equations to simulate the state variables of a propulsion subsystem for spacecraft before, during, and following an engine burn. The state variables include the temperature, pressure, flow rates, and related quantities of the oxidizer, fuel, and pressurization gas; additional quantities such as thrust are also computed.

The following characteristics also apply generally to the propulsion system:

(a)   The propellant feed systems must be capable of operating in the space environment, without venting, for ten years and be compatible with all aspects of the environments between the solar orbits of Venus and Pluto, and with the radiation environment due to an on-board Radioisotope Thermal-Electric Generator (RTG).

(b)   The system must be capable of multiple restarts in zero gravity.

(c)   The system must be designed for ground functional checkout, propellant loading, and mass and balance determinations prior to spacecraft shroud mounting and launch vehicle mating operations.

(d)   The system must withstand handling and shipping loads of the magnitudes listed in Table 4-V.

(e)   The system must withstand launch loads of the magnitudes listed in Table 4-VI.

(f)   The system must withstand flight loads of the magnitudes lised in Table 4-VII.

(g)   Filter elements are restricted to the stacked-disc type which provide full inspectability. The required filtration level of filter components in pressurant circuits is 10 microns absolute, or better.

---

* 88 percent Fluorine and 12 percent Oxygen

4

SPACE STORABLE PROPULSION SYSTEM SCHEMATIC
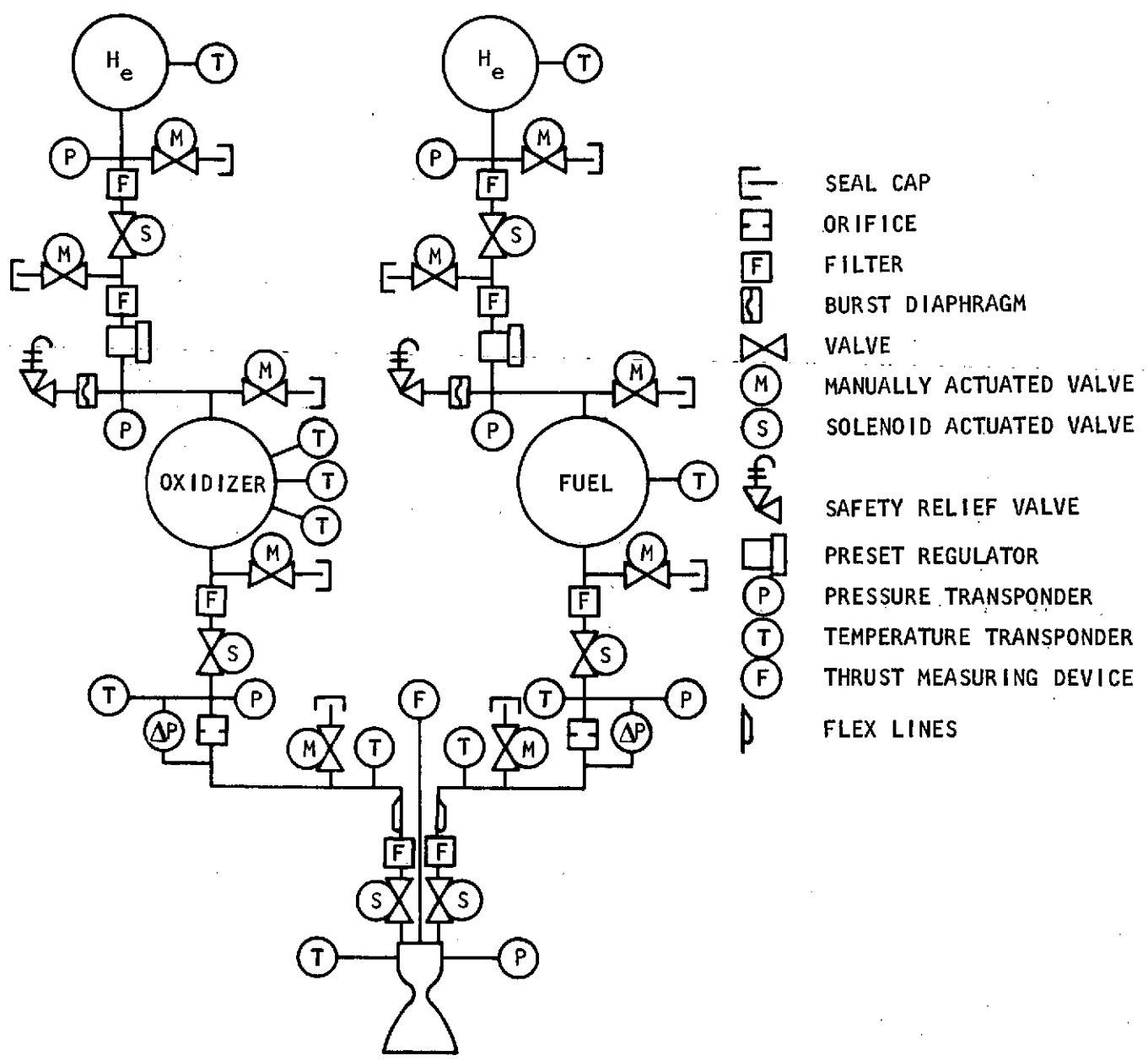
SEAL CAP

ORIFICE

FILTER

BURST DIAPHRAGM

VALVE

MANUALLY ACTUATED VALVE

SOLENOID ACTUATED VALVE

SAFETY RELIEF VALVE

PRESET REGULATOR

PRESSURE TRANSPONDER

TEMPERATURE TRANSPONDER

THRUST MEASURING DEVICE

FLEX LINES

Figure 4-1

TABLE 4-I

CHARACTERISTICS OF FLOX/MMH PROPULSION SYSTEM

ENGINE

Thrust (Vacuum)	600 lb$_f$
Chamber Pressure	100 psia
Specific Impulse	365 lb-sec/lb$_m$
Mixture Ratio (Overall)	2.6
Thrust Chamber Material	POCO Graphite/Carbon Cloth/ Silicia Insulator with either a L605 or Carbon Composite Skirt
Thrust Chamber Cooling	Barrier Cooling
Thrust Vector Control	Gimbals
Area Ratio	60:1
Fuel Flow Rate	0.441 lbm/sec
Oxidizer Flow Rate	1.142 lbm/sec
Combustion Gas Temperature	7600°R
Combustion Gas Molecular Weight	19.2
Ratio of Specific Heats (shifting)	1.15
Ratio of Specific Heats (frozen)	1.30
Throat Diameter	2.0 inches
Characteristic Length	30 inches
Characteristic Velocity	6280 ft/sec
Ignition Delay	Negligible (less than 1 ms)
Engine Valve Travel Time	20 ms

OXIDIZER FEED SYSTEM

Type of Propellant Feed	Gas Pressurization
Pressurization Gas	Helium
Pressurant Tank Volume	1.49 ft^3
Pressurant Tank Diameter	17 inches

TABLE 4-I (Continued)

CHARACTERISTICS OF FLOX/MMH PROPULSION SYSTEM

OXIDIZER FEED SYSTEM (Cont.)

Initial Pressurant Tank Pressure	4000 psia
Initial Pressurant Tank Temperature	150°R
Blowdown Ratio	10:1
Pressurant Line Size, and Material	3/8 in. O.D., 0.32" I.D., 347 ss
Mass of Gas	10.1 lbm
Pressurant Tank Material	Titanium, 6Al-4V
Pressurant Tank Mass	31.1 lbm
Regulator Outlet Pressure (Nominal)	240 psia
Regulator Flowrate (Nominal)	35.2 SCFM
Propellant Tank Volume	13 ft^3 (spherical)
Propellant Tank Diameter	35 inches
Ullage Volume	2.7 ft^3
Propellant Tank Design Pressure	375 psig
Propellant Tank Material	Aluminum 2219
GHe Prepressurization Level	26 psig
Usable Oxidizer Mass	915 lbm
Contingency Oxidizer Mass	36.6 lbm
Oxidizer Tank Mass	56.2 lbm
Propellant Acquisition	Surface Tension Device
Propellant Feed Line Size, and Material	3/4 in. O.D., 0.652 " I.D., 347 ss
Oxidizer Temperature (Nominal)	150°R
Propellant Valve	Solenoid actuated--not mechanically linked to fuel valve

TABLE 4-I (Continued)

CHARACTERISTICS OF FLOX/MMH PROPULSION SYSTEM

FUEL FEED SYSTEM

Type of Propellant Feed	Gas Pressurization
Pressurization Gas	Helium
Pressurant Tank Volume	0.586 ft^3
Pressurant Tank Diameter	12.5 in.
Initial Pressurant Tank Pressure	4000 psia
Initial Pressurant Tank Temperature	530°R
Blowdown Ratio	10:1
Pressurant Line Size, and Material	3/8 in. O.D., 0.32" I.D., 347 ss
Mass of Gas	1.4 lbm
Pressurant Tank Material	Titanium 6Al-4V
Pressurant Tank Mass	12.3 lbm
Regulator Outlet Pressure (Nominal)	216 psig
Regulator Flowrate (Nominal)	6.9 SCFM
Propellant Tank Volume	7.33 ft^3 (spherical)
Propellant Tank Diameter	29 in.
Ullage Volume	.59 ft^3
Propellant Tank Design Pressure	285 psia
Propellant Tank Material	Titanium 6Al-4V
GHe Prepressurization Level	100 psig
Usable Fuel Mass	352 lbm
Contingency Fuel Mass	14 lbm
Fuel Tank Mass	12.0 lbm
Propellant Acquisition	Surface Tension Device
Propellant Feed Line Size, and Material	3/4 in. O.D., 0.652 " I.D., 347 ss
Fuel Temperature (Nominal)	530°R
Propellant Valve	Solenoid actuated, not mechanically linked to the oxidizer valve

TABLE 4-I (Continued)

CHARACTERISTICS OF FLOX/MMH PROPULSION SYSTEM

<u>SYSTEM</u>

Nominal Number of Starts	26
Total Impulse	4.63×10^5 lb_f-sec
Life Time	10 years in the space environment
Thermal Control	Oxidizer pressurant and propellant tank to be covered with polyurethane foam ~ 1.5 in. thick. Fuel tank to be covered with 0.5 in. thick HPI. Oxidizer subsystem to be thermally isolated from the spacecraft and fuel subsystem. It appears passive methods will be sufficient to meet the requirements. The oxidizer subsystem will be maintained nominally at 150°R; the fuel at 530°R.

TABLE 4-II

CHARACTERISTICS OF F_2/N_2H_4 PROPULSION SYSTEM

ENGINE

Thrust (Vacuum)	600 lb_f
Chamber Pressure	100 psia
Specific Impulse (Nominal)	375 lb_f-sec/lbm
Mixture Ratio (Overall)	1.85
Thrust Chamber Material	POCO Graphite/Carbon Cloth/ Silica Insulator with either a L605 or Carbon Composite Skirt
Thrust Chamber Cooling	Barrier Cooling
Thrust Vector Control	Gimbals
Area Ratio	60:1
Fuel Flow Rate	0.561 lbm/sec
Oxidizer Flow Rate	1.039 lbm sec

OXIDIZER FEED SYSTEM

Type of Propellant Feed	Gas Pressurization
Pressurization Gas	Helium
Pressurant Tank Volume	1.24 ft^3 (spherical)
Pressurant Tank Diameter	16 in.
Initial Pressurant Tank Pressure	4000 psia
Initial Pressurant Tank Temperature	150°R
Blowdown Ratio	10:1
Pressurant Line Size, OD, and Material	3/8 in., 347 ss
Mass of Gas	8.6 lbm
Pressurant Tank Material	Titanium 6Al-4V
Pressurant Tank Mass	25.8 lbm
Regulator Outlet Pressure (Nominal)	232 psia
Regulator Flowrate (Nominal)	34.0 SCFM
Propellant Tank Volume	11.2 ft^3 (spherical)

TABLE 4-II (Continued)

CHARACTERISTICS OF F_2/N_2H_4 PROPULSION SYSTEM

OXIDIZER FEED SYSTEM (Cont.)

Propellant Tank Diameter	33.3 inches
Ullage Volume	2.32 ft^3
Propellant Tank Design Pressure	365 psig
Propellant Tank Material	Aluminum 2219
GHe Prepressurization Level	100 psig
Usable Oxidizer Mass	805.4 lbm
Contingency Oxidizer Mass	32.2 lbm
Oxidizer Tank Mass	46.9 lbm
Propellant Acquisition	Surface Tension Device
Propellant Feed Line Size, OD, and Material	3/4 in., 347 ss
Oxidizer Temperature (Nominal)	150°R
Propellant Valve	Solenoid actuated, not mechanically linked to the fuel valve

FUEL FEED SYSTEM

Type of Propellant Feed	Gas Pressurization
Pressurization Gas	Helium
Pressurant Tank Volume	0.63 ft^3
Pressurant Tank Diameter	12.8 in.
Initial Pressurant Tank Pressure	4000 psia
Initial Pressurant Tank Temperature	530°R
Blowdown Ratio	10:1
Pressurant Line Size. OD, and Material	3/8 in., 347 ss
Mass of Gas	1.51 lbm
Pressurant Tank Material	Titanium 6Al-4V
Pressurant Tank Mass	13 lbm

TABLE 4-II (Continued)

CHARACTERISTICS OF F_2/N_2H_4 PROPULSION SYSTEM

FUEL FEED SYSTEM (Cont.)

Regulator Outlet Pressure (Nominal)	217 psia
Regulator Flowrate (Nominal)	6.5 SCFM
Propellant Tank Volume	7.8 ft^3
Propellant Tank Diameter	30 in.
Ullage Volume	0.62 ft^3
Propellant Tank Design Pressure	285 psig
Propellant Tank Material	Titanium 6Al-4V
GHe Prepressurization Level	100 psig
Usable Fuel Mass	435.4 lbm
Contingency Fuel Mass	17.4 lbm
Fuel Tank Mass	12.6 lbm
Propellant Acquisition	Surface Tension Device
Propellant Feed Line Size, OD, and Material	3/4 in., 347 ss
Fuel Temperature (Nominal)	530°R
Propellant Valve	Solenoid actuated -- not mechanically linked to the oxidizer valve

SYSTEM

Number of starts	26
Total Impulse	466 x 10^5 lb$_f$-sec
Life Time	10 years in space environment

TABLE 4-II (Continued)

CHARACTERISTICS OF F_2/N_2H_4 PROPULSION SYSTEM

SYSTEM (Cont.)

Thermal Control

Oxidizer pressurant and propellant tank to be covered with polyurethane foam ~1.5 in. thick. Fuel tank to be covered with 0.5 in. thick HPI. Oxidizer subsystem to be thermally isolated from the spacecraft and fuel subsystem. It appears that passive methods will be sufficient to meet the requirements. The oxidizer subsystem will be maintained normally at 150°R; the fuel at 530°R.

TABLE 4-III

SYSTEM PRESSURE SCHEDULE

	FLOX	MMH	F_2	N_2H_4
P_c, psia	100	100	100	100
$\Delta P_{inj\ +\ manifold}$, psid	75	75	75	75
$\Delta P_{prop\ valve\ +\ filter}$, psid	14	4	11	5
$\Delta P_{iso\ valve\ +\ filter}$, psid	14	4	11	5
$\Delta P_{trimming\ device}$, psid	30	30	30	30
$\Delta P_{lines\ +\ trap}$, psid	7	3	5	2
$P_{tank} = P_c + \Sigma\Delta P$, psia	240	216	232	217
$P_{reg\ outlet}$, psia (Nominal)	240	216	232	217
$P_{reg\ lockup}$, psia (Maximum)	253	228	245	230
$P_{relief\ system}$, psia	365	278	357	280
$P_{tank\ design}$, psia	375	285	365	285

TABLE 4-IV

DUTY CYCLES

First Duty Cycle

Burn No.	Burn Time (sec)
1	10.2
2	20.2
3	420.2
4	20.2
5	14.65

Second Duty Cycle

1	10.2
2	10.2
3	361.2
4	157.2
5	166.2
6	66.2

NOTE: For the propulsion system modeling of these duty cycles, the ullage
was computed from the propellant tank volume and the propellant loaded as
specified in the computer printout. Also, the pressurant tank size was computed
from the pressurant mass as specified in the computer printout at a pressure of
4000 psia and a temperature of 560°R (fuel) and 150°R (oxidizer). Nominal
regulator set pressures were 233 psia for the oxidizer and 230 psia for the fuel.
All other system characteristics were in agreement with those listed in Table
4-I.

TABLE 4-V

HANDLING AND SHIPPING LOADS

(1)	Vibration	Frequency Range			Acceleration
		2.5	to	35 Hz	1.3 G peak
		35	to	48 Hz	3.0 G peak
		48	to	500 Hz	5.0 G peak

(2)	Shock	Mass			Drop Height
		0	to	20 lb_m	42 inches
		20	to	50 lb_m	36 inches
		50	to	250 lb_m	30 inches
		250	to	500 lb_m	24 inches
		500 and up lb_m			18 inches

TABLE 4-VI

LAUNCH LOADS

(1) Static Acceleration

	Thrust Axis	Lateral Axis
	+8, -4 G	+4, -4 G

(2) Sinusoidal Vibration

Frequency	Acceleration
5 to 30 Hz	4 G peak
30 to 2000 Hz	10 G peak

(3) Random Vibration

Frequency	Acceleration
100 to 1100 Hz	15 G RMS (.2 G^2/Hz flat)

(4) Acoustic

1/3 Octave Band Center Frequency	Sound Pressure Level (db ref. 2 X 10^{-4} bar)
50 Hz	132
100 Hz	136
200 Hz	139
400 Hz	139
800 Hz	138
1600 Hz	135
3150 Hz	132
6300 Hz	129
Overall	150

(5) Pyrotechnic Shock

Frequency	Peak Shock
10 to 22 Hz	20 G
22 to 1200 Hz	20 to 1000 G (linear)
1200 to 10,000 Hz	100 G

TABLE 4-VII

FLIGHT LOADS

(1) Acceleration   Engine Burn   –   0.225 G Maximum

                                 Attitude Change   – 22×10^{-6} rad/sec^2
                                 (Turn Rate is
                                 0.1°/sec)

                                 Cruise   – 1×10^{-7} G

(2) Shock   Engine Burn   –   To be determined

                                 Attitude Change   –   To be determined

                                 Cruise   –   To be determined

18

5. PRESSURE REGULATOR DESIGN, ANALYSIS AND OPTIMIZATION

The pressure regulation requirements of the Space Storable Propulsion System as defined in Section 4 of this report were carefully reviewed by The Marquardt Company. It was determined that of the four feed systems under consideration for this application the FLOX system requirements had the greatest impact on the design since they featured the highest flowrate and presented the most severe compatibility requirements. Consequently, Marquardt's study efforts were directed primarily towards satisfying the FLOX system requirements, and the particular pressure regulator design that evolved was then also evaluated for compatibility with the other three propellant systems. In this manner a single pressure regulator satisfying the performance requirements of all four feed systems was determined.
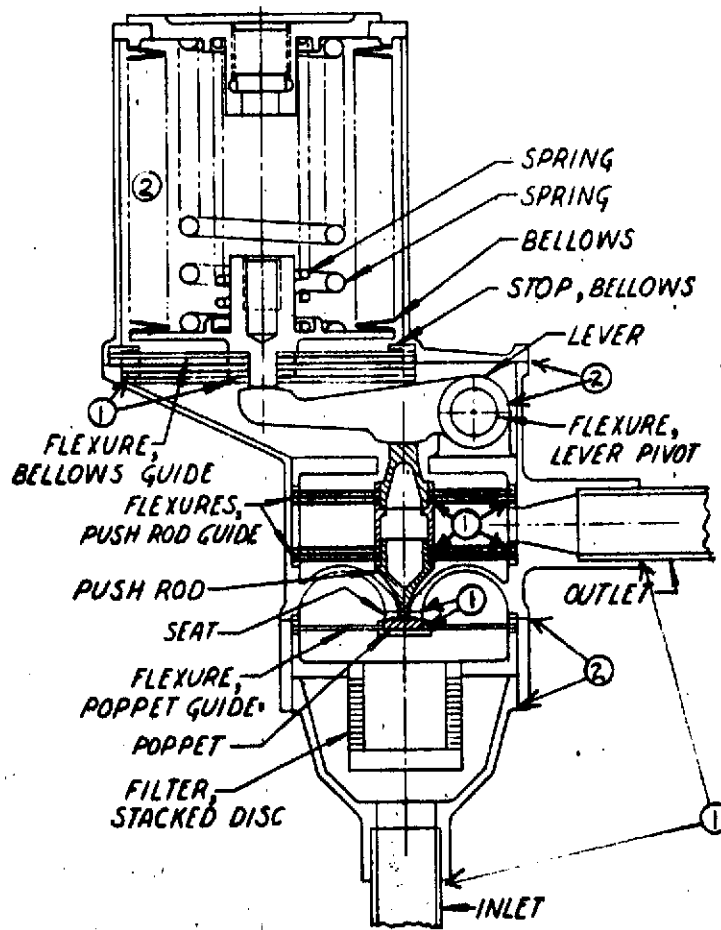
Based upon Marquardt's fluid system component technology and the current state-of-the-art of pressure regulators, a baseline design was conceived and analyzed in detail. The baseline design and its performance characteristics were subsequently presented to JPL technical personnel for their review. Based on this presentation it was decided that an optional task which involved the investigation of alternate designs should be implemented. Several alternate regulator components were subsequently incorporated into the design to arrive at the final regulator concept. Analytical models of the final regulator design were updated to include the experimental data generated during the Work Principles Proof task of this program. The final regulator design, which featured a pressure regulating accuracy of ±1% over the required inlet pressure and temperature range, was then integrated with the propellant feed system model to verify dynamic compatibility and with the propulsion system model to demonstrate satisfactory propellant and pressurant utilization for two typical mission duty cycles.

5.1 BASELINE DESIGN AND ANALYSIS

The selected baseline regulator concept is shown in Figure 5-1. The pressure regulator design is a unique concept which promises to exceed the cycle life capability, long term life capability, and propellant compatibility of current state-of-the-art regulators. This substantial increase in performance capability is made possible by a number of unique design features. These are:

1. Elimination of all sliding friction through the use of metallic flexures

2. Utilization of gas damping and solid damping only (no age/environment sensitive frictional damping)

3. All metallic/ceramic construction (no plastic or elastomeric materials)

4. Utilization of low leakage ceramic flat poppet/seat interface with impact control to prevent wear.

19

BASELINE REGULATOR DESIGN

SPRING
SPRING
BELLOWS
STOP, BELLOWS
LEVER
②
FLEXURE,
LEVER PIVOT
FLEXURE,
BELLOWS GUIDE
FLEXURES,
PUSH ROD GUIDE
PUSH ROD
OUTLET
SEAT
FLEXURE,
POPPET GUIDE
POPPET
FILTER,
STACKED DISC
INLET
②

① BRAZE JOINTS

② WELD JOINTS

Figure 5-1

Although the combination of these various unique features into a pressure regulator design had not previously been accomplished, the individual regulator components featured had been demonstrated by The Marquardt Company in other types of fluid system components. Thus, while the selected baseline regulator concept offers a substantial advance in the state-of-the-art of pressure regulator technology, the inherent development risks were considered to be relatively low.

The baseline regulator design features an unbalanced poppet which achieves effective sealing to the seat by means of the upstream pressure force. In addition, the poppet is also held against the seat by the axial guidance flexure. The actuation mechanism consists of a bellows which is exposed to space internally and to the regulator downstream pressure externally and which is held in the null position by one or more coil springs. If the regulator downstream pressure decreases from the preset pressure, the reference spring force overcomes the bellows pressure force and the actuator exerts a net opening force on the poppet through the lever arrangement. When this net force is greater than the poppet seating force, the poppet opens and allows pressurant gas to re-pressurize the downstream side of the regulator. When the downstream regulator pressure rises back up to the set pressure, the actuator returns to the null position and the poppet is returned to the seat by the axial guidance flexure spring force and the pressure differential across the poppet.

A Material Compatibility Study was performed to select the materials of construction of the pressure regulator and various analytical models were prepared to size the pressure regulator components. These analytical models served to determine the optimum poppet/seat interface configuration to meet the leakage and flow requirements as well as the regulator actuator requirements. A trade-off of the lever arm ratio, reference spring rate, and bellows area was performed to determine the sensitivity of dynamic characteristics and weight to these parameters. In addition, stress analyses of critically stressed elements of the regulator were performed and gas damping was investigated. Some of the analytical models were computerized; others were performed manually. A description of these analysis techniques is presented in the following sections.

5.1.1   Material Compatibility

The requirements of the "Design for Pressure Regulating Components" program include a specification that the regulator materials shall be compatible with the propellants presently under consideration for the Space Storable Propulsion System for a period of up to 10 years. These propellants are FLOX/MMH and fluorine/hydrazine. A review of available literature discloses that materials which are compatible with fluorine are also compatible with FLOX and, on the other hand, materials which are compatible with hydrazine are also compatible with monomethyl hydrazine. Consequently, fluorine and hydrazine compatibility were the criteria used in selecting materials.

In assessing 10-year compatibility with fluorine and hydraxine, it must be recognized that there is no actual data for this long of a time period available and that, in fact all compatibility determinations must still be based upon extrapolations of short-term data normally from several months to at best several years. For some materials this approach would result in predicted material corrosion or propellant decomposition rates which are too high for this application. However, recent data has shown that after a short induction period, the initially higher rates decrease to much lower values. Consequently, it would appear that the use of extrapolated short-term compatibility data generally tends to be conservative.

The baseline regulator design which is shown in Figure 5-1 includes call-outs for major regulator components and also identifies brazed joints and weld joints. A special effort was made to minimize the number of different materials utilized in this regulator and to thereby minimize the chances of employing a material which might not be compatible with the propellants as well as to minimize the potential for galvanic corrosion. Table 5-I lists all major regulator components, their materials of construction, the condition of their materials, the specification for these materials, the EMF based upon Reference 2, and the minimum wall thickness to be employed in the regulator. In reviewing this Table, it is evident that almost the entire regulator is made of Inconel 718 with the exception of the poppet and seat which are Tungsten Carbide, the stacked disc inlet filter which is Type 304L stainless steel, the brazing compound, which is a high nickel alloy, and the surface tension screen which may be required on the fluorine side and which is made from Nickel 200. These were the materials that needed to be considered for propellant compatibility. In assessing this compatibility, References 3 and 9 were used as primary sources and data listed in these reports is based on several other references, which are also referred to.

Fluorine Compatibility

Based on data presented in Reference 3, the nickel alloys received the highest compatibility rating. Consequently, the Inconel 718, nickel braze, and nickel 200 screen are ideally suited for this application. Fluorine compatibility data on ceramics and, in particular, on the tungsten carbide is very scarce. Reference 8 discusses the fact that aluminum oxide is compatible with gaseous fluorine at up to 1500 psia pressure. Consequently, tungsten carbide should definitely be compatible with fluorine at cryogenic temperature and lower pressures. Reference 9 includes a discussion which was originally obtained from Reference 10 to indicate that carbides of boron, tungsten, and silicone do not react with fluorine at ambient temperature. In addition, extensive testing by both Marquardt and the Air Force Rocket Propulsion Laboratory of tungsten carbide K96 and tungsten carbide K801 in chlorine-penta-fluoride and gaseous fluorine for periods of exposure up to one month disclosed no apparent problems in the area of propellant compatibility (Reference 22).

Fluorine is one of the most powerful oxidizing agents known and will react with practically all organic and inorganic substances. Consequently, component cleanliness is of utmost importance. The baseline regulator design was carefully reviewed to assure that all regulator components are accessible and can be cleaned. Flexure assemblies are to be brazed to

Eliminate possible crevices between flexure plates, and the welded bellows will be subjected to a cleaning cycle which includes stretching the bellows to the maximum allowable extension while subjecting it to the cleaning cycle to make the convolutions most accessible.

Another area of concern to the fluorine component designer is the use of relatively thin sections of materials. This concern is due to the fact that the activation energy to initiate combustion of materials is much lower with fluorine than with other oxidizers and that any excess localized energy must be dissipated quickly before ignition occurs. Thus, where relatively thin sections of material are used, they restrict the conduction of heat away from a reaction site, and increase the possibility of ignition. This situation can, of course, be improved by employing materials which feature a high coefficient of thermal conductivity and/or high heat capacity. Fortunately, the nickel alloys selected by Marquardt do have these features and thus are less likely to incur ignition. Also nickel has a high ignition point temperature compared to other structural metals. Minimum wall thicknesses presently under consideration for the baseline regulator design are 0.007 inches. Bellows of similar design and thickness have previously been employed in support of liquid fluorine technology programs sponsored by the NASA-Lewis Research Center.

According to Reference 9, exposure of nickel alloys to fluorine generally results in the formation of a fluoride at the surface of the nickel alloy. This fluoride reaches depths of approximately 2000 angstroms after several days exposure, but does not appear to grow in thickness appreciably thereafter. The fluoride film, in effect, acts as a barrier to prevent further reaction. Fluoride film thicknesses of 2000 angstroms are, of course extremely small in relation to the minimum wall thicknesses under consideration here and have no effect on the mechanical properties of the base material. There is also no evidence to indicate that these fluoride films will be damaged or lost during flexing of the base metal, such as occurs in a bellows or a flexure. On the other hand, Marquardt has shown that the type of impact loads incurred during closure of a poppet/seat interface can result in cracking and chipping of the fluoride films. The research effort described in Reference 9 investigated this phenomena in detail and developed criteria to assure reliable poppet/seat interface cycling of up to at least 100,000 cycles. One notable difference between the conditions under which the data were obtained by Marquardt during the investigation described in Reference 9 and the conditions of the proposed regulator application is the operating temperature. All extended cycling data (100,000 cycles or more) obtained by Marquardt was performed at ambient temperature, whereas the proposed application is at cryogenic temperature. Since both tungsten and carbide form volatile fluorides at room temperature, the only stable solid fluoride existing at the poppet/seat interface was that of the binder (6% cobalt or 6% nickel). At cryogenic temperatures, both carbide and tungsten form solid fluorides; however, the rate of formation of these fluorides as well as the binder's fluoride will be much lower. Consequently, since the amount of solid fluoride present at cryogenic temperature will be extremely small it is expected that the sealing surface behavior will be comparable to that previously evaluated at ambient temperature.

The utilization of relatively few materials minimizes shifts in the regulator operating characteristics over the ambient to cryogenic temperature range and also minimizes the potential galvanic corrosion. Based on Reference 2, it is considered good spacecraft design practice to limit the differences in EMF between adjacent materials to 0.25 volts. In accordance with Table 5-I, this has been effectively accomplished for the regulator. In summary, it is believed that the materials of construction chosen for the baseline regulator constitute a sound and logical choice based on all available compatibility data.

Hydrazine Compatibility

In assessing the compatibility of materials of construction with hydrazine, it must be recognized that two distinctly different compatibility modes are of concern. These are: (1) what effect does the hydrazine have on the material of construction, and (2) does the material of construction act as a catalyst and result in decomposition of the hydrazine. Unfortunately, most hydrazine compatibility data does not clearly distinguish between these two aspects. Thus, copatibility data tables are generally prepared to treat both aspect simultaneously. For the Space Storable Propulsion System Regulator, the effects of hydrazine on materials of construction are of primary concern and the extent of hydrazine decomposition is only a minor concern since the regulator will normally be subjected only to hydrazine vapor and since the decomposition of hydrazine vapor occurs at a much lower rate than that of hydrazine liquid according to experiments performed by Dr. P. J. Axworthy of Rocketdyne (Reference 23). Since there is actually no published data of hydrazine vapor decomposition rates with various materials, all of the following discussion will be based upon hydrazine liquid and must therefore be reviewed in a very conservative light.

According to Reference 3, uncontaminated hydrazine has little effect on metals. References 4 and 5 present data to indicate that nickel in general is assigned a rating of 3 (based on a point system from 1 to 4 where 1 is fully compatible and 4 is not acceptable) at 338°F and that the decomposition rate at this temperature is approximately 200 times that caused by glass or aluminum. References 6 and 7 state that hastalloy C, inconel, inconel-X, K-monel, monel, and nichrome braze are all compatible with hydrazine at 75°F. Since the operational temperature of the Space Storable Propulsion Fuel System is approximately at ambient temperature, it appears that the Inconel 718 is considered fully compatible with hydrazine. Similarly, the nickel braze appears to be compatible.

No hydrazine compatibility data with tungsten carbide was found. However, it is known that in general the ceramics, and particularly the carbides, are more inert than metals; and since the hydrazine has little effect on metals, it is expected to have even less effect on the tungsten carbide. Also, injector valves featuring tungsten carbide poppets have been employed successfully during the development of monopropellant rocket engines of various sizes, and in particular, for the P-95 program for which Lockheed Missiles and Space Corporation is responsible.

As mentioned previously, the choice of materials should minimize galvanic couples between all wetted materials in order to minimize potential galvanic corrosion. Based on the compatibility data reviewed, there is no indication of potential compatibility problems between the materials selected and the non-contaminated hydrazine liquid or vapor.

TABLE 5-I

MATERIALS LIST

COMPONENT	MATERIAL	MATERIAL CONDITION	PREF. SPEC	ALT. SPEC	EMF*	MIN. THICKNESS
Poppet & Seat	Tungsten Carbide	Sintered	K801	K96	+0.05	.040"
Poppet & Seat Carriers	Inco 718	Aged	AMS-5597A	AMS-5596C	-0.20	.030"
Poppet Flexure	Inco 718	Aged	AMS-5597A	AMS-5596C	-0.20	.010"
Housing	Inco 718	Aged & Welded	AMS-5597A	AMS-5596C	-0.20	.40"
Inlet & Outlet	Inco 718	Aged	AMS-5590	–	-0.20	.030"
Filter Element	304L SS	–	–	–	-0.20	.002"
Pushrod & Lever Arm	Inco 718	Aged	AMS-5597A	AMS-5596C	-0.20	.030"
Pushrod Flexures	Inco 718	Aged	AMS-5597A	AMS-5596C	-0.20	.008"
Lever Arm Flexure	Inco 718	Aged & Welded	AMS-5597A	AMS-5596C	-0.20	No Data
Bellows Assembly	Inco 718	Aged & Welded	AMS-5597A	AMS-5596C	-0.20	.007/.018"
Bellows Flexure	Inco 718	Aged	AMS-5597A	AMS-5596C	-0.20	.010/.040"
Reference Spring(s)	Inco 718	Aged	AMS-5597A	AMS-5596C	-0.20	.030"
Brazing**	Nickel	93.4 Ni, 3.5 Si, 1.6 Bo, 1.5 Fe	AMS-4779	AMS-4776	-0.15	–
Surface Tension Screen	Ni 200				-0.15	

*   Poppet, Seat, Flexures, Inlet and Outlet Tubing
**   Reference MSC Std. No. 63 (Silver is Zero Reference)

5.1.2   Flow Passage Sizing

To make certain that the regulator had sufficient flow capability to meet the requirements of any one of the four propellant feed systems presented in Section 4 of this report, the required pressurant flowrates in combination with the available pressure drop from the minimum 400 psia inlet pressure condition to the operating outlet pressure were determined. Based on this analysis it was found that the FLOX system required the largest flow passage. Consequently, the regulator poppet/seat interface was sized for this condition. Specific requirements were:

Helium Temperature	150°R
Inlet Pressure	400 psia
Outlet Pressure	240 psia

Volumetric Flowrate equivalent to 1.142 lb/sec of FLOX

Based on the discharge coefficient data available for similar poppet/seat interfaces from other Marquardt programs and utilizing Reference 11 the relative poppet strokes and seat diameters were computed. This relationship is shown in Figure 5-2. The possible relationships between stroke and seat hole diameter were subsequently iterated to determine the approximate actuator requirements. Since the baseline pressure regulator features essentially a brute force actuation approach, wherein actuation force and therefore actuator size are proportional to seat hole area, it was determined that a fairly small seating diameter was desirable. Furthermore, the fact that a push rod was required inside of this seating hole diameter resulted in the conclusion that a 0.063 inch diameter appeared to be optimum. Based on this choice, the variations in operating stroke as a function of inlet pressure and required propellant flowrate were determined utilizing the relationship:

$$A = \frac{\dot{W} \sqrt{T}}{P_1 \, C_m \, C_D}$$

where:

$$C_m = \sqrt{\frac{2g\gamma}{R(\gamma - 1)} \left[\left(\frac{P_2}{P_1}\right)^{\frac{2}{\gamma}} - \left(\frac{P_2}{P_1}\right)^{\frac{\gamma+1}{\gamma}} \right]}$$

(symbols are identified in Section 10)

The results from this analysis for the operating range is presented in Figure 5-3.
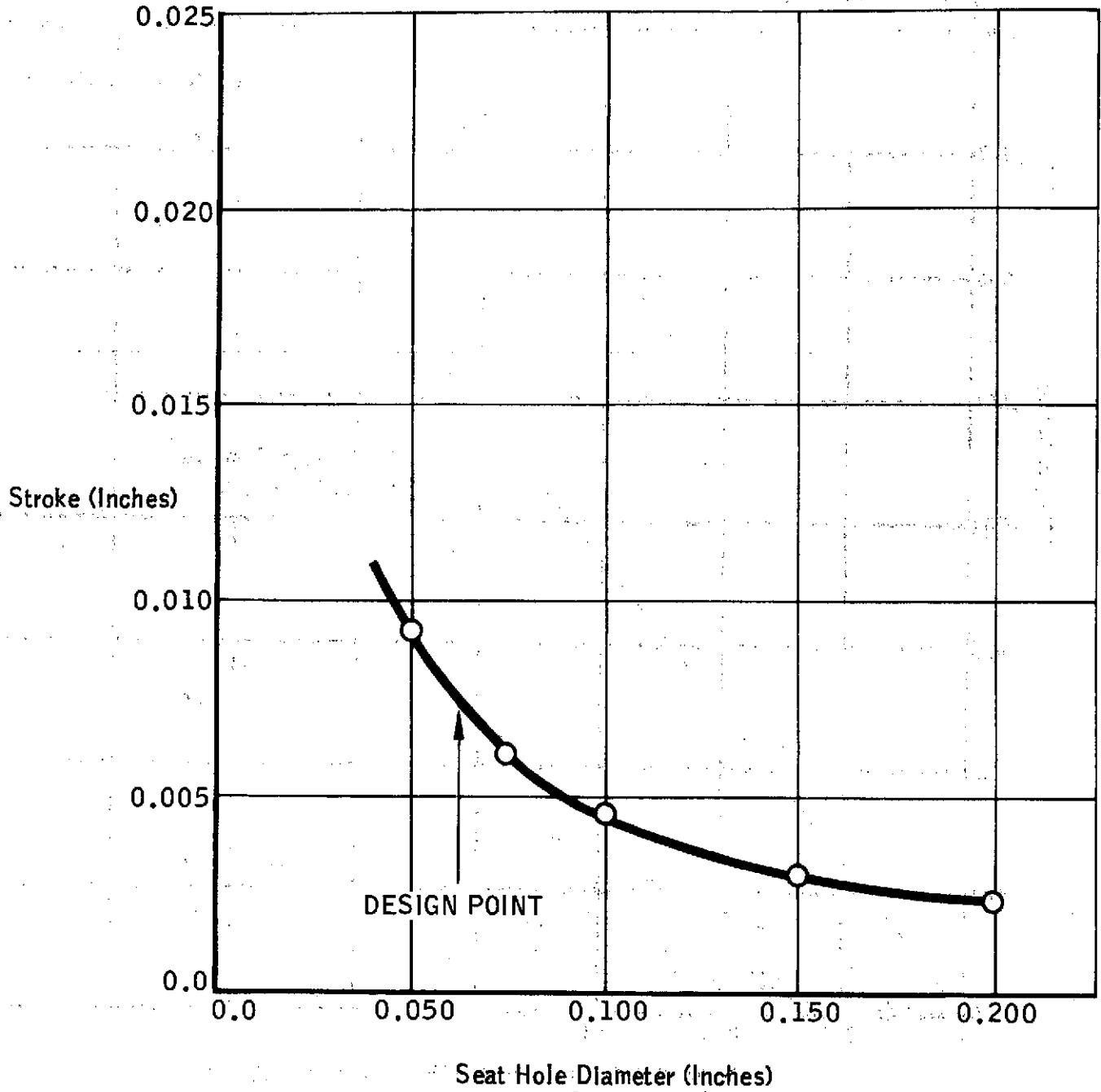
POPPET STROKE VS SEAT DIAMETER
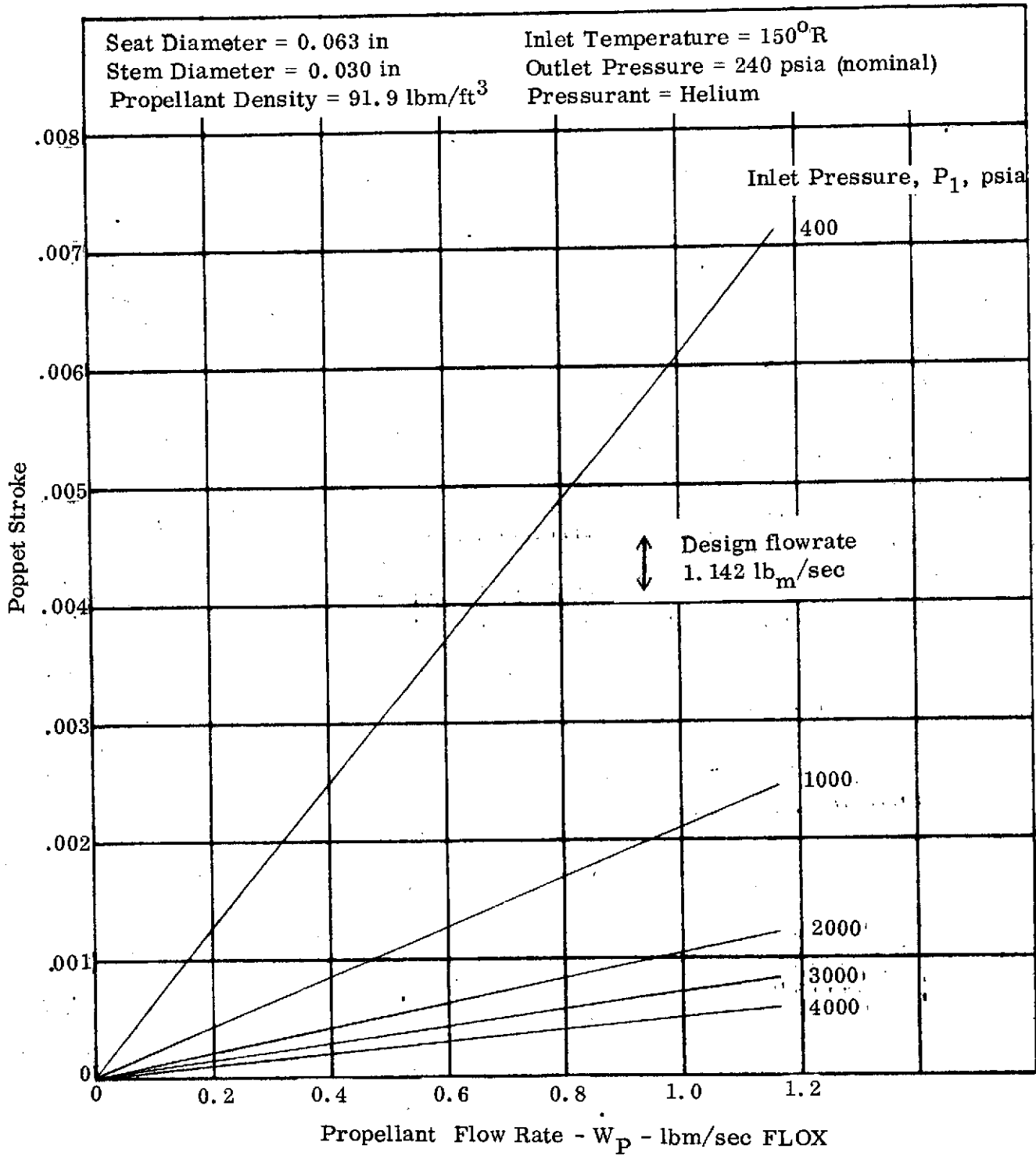

Figure 5-2

STEADY-STATE POPPET STROKE VS FLOX FLOW RATE

Seat Diameter = 0.063 in   Inlet Temperature = 150°R
Stem Diameter = 0.030 in   Outlet Pressure = 240 psia (nominal)
Propellant Density = 91.9 lbm/ft^3 Pressurant = Helium

Inlet Pressure, P_1, psia

Design flowrate
1.142 lb_m/sec

Poppet Stroke

Propellant Flow Rate - W_P - lbm/sec FLOX

Figure 5-3

28

5.1.3   Poppet/Seat Interface Configuration

Marquardt's investigations in the area of fluorine sealing technology des-
cribed in References 9 and 12. Since these investigations were very successful, the flat
poppet/seat interface utilized therein was also designated for the baseline regulator design.
The determination of the exact poppet/seat interface configuration involved three types of
analyses. These were a leakage analysis, the sizing of the seat support structure in com-
bination with the actual seat dimensions to limit poppet impact forces, and the dimension-
ing of a seat bumper to limit poppet-to-seat misalignment. The resultant seat detail
is shown in Figure 5-4.

Poppet/seat interface life or cycling capability is achieved through minimization
of impact stresses, assuring parallel mating between poppet and seat (no scrubbing) and
proper selection of materials. Based on the data generated in Reference 9, a maximum
total impact stress of 25,000 psi (due to impact and static forces) with a poppet-to-seat
parallelism within 2 minutes was selected to assure at least 100,000 cycles of life for the
tungsten carbide (with 6% binder) material without exceeding the 45 scc/hr helium
leakage rate. These requirements, as well as the flow orifice size, have dictated the
configuration shown in Figure 5-4. The bumper construction around the sealing land
assures pre-alignment between sealing surfaces during mating since the poppet will strike
the bumper first if it is out of parallel with the seat/bumper plane by more than 2 minutes
and will thereby be aligned to that plane. The impact stresses are controlled by designing
the seat support, see Figure 5-1, such that it is not absolutely rigid but rather that it
features a finite axial spring rate; thus poppet kinetic energy is transferred into potential
energy of the seat plate without generating high impact forces at the sealing surface. This
technique was successfully demonstrated in the investigation presented in Reference 9.
The actual calculations performed for the baseline regulator are presented in Appendix A
entitled "Calculations of Seat Impact Forces".

Good correlation between predicted leakage rates and actual leakage rates has been
achieved utilizing the following semi-empirical relationships (from Reference 12).

$$Q_u = \frac{100 \, D_s \, H^3 \left[P_1^2 - P_2^2\right]}{\mu \, L \, T \quad \sigma^{2/3}} \qquad Q_c = \frac{2 \, (10^4) \, D_s \, h^3 \left[P_1^2 - P_2^2\right]}{\mu \, L \, T \quad \sigma^{3/2}}$$

These relationships allow determination of volumetric leakage rates for unidirectional
and circular lay surfaces. In practice, the lapping techniques used by Marquardt result
in ramdom lay surfaces. Consequently, it has been found that actual leakage rates fall
on an average line between Q_u and Q_c. This average is plotted on log log paper as in Figure
5-5. The data in Figure 5-5 is based on operating pressures of 4000 and 400 psia inlet
and 240 psia outlet and a temperature of 150°R. As evident from this figure, a surface
finish of 3/4 AA (Arithmetic Average) is sufficient to assure less than 45 scc/hr of
leakage at 4000 psia (and much less leakage at 400 psia).

The flow limiting characteristics of the seat design shown in Figure 5-4 were also
determined assuming that the poppet was completely removed from the seat and that the
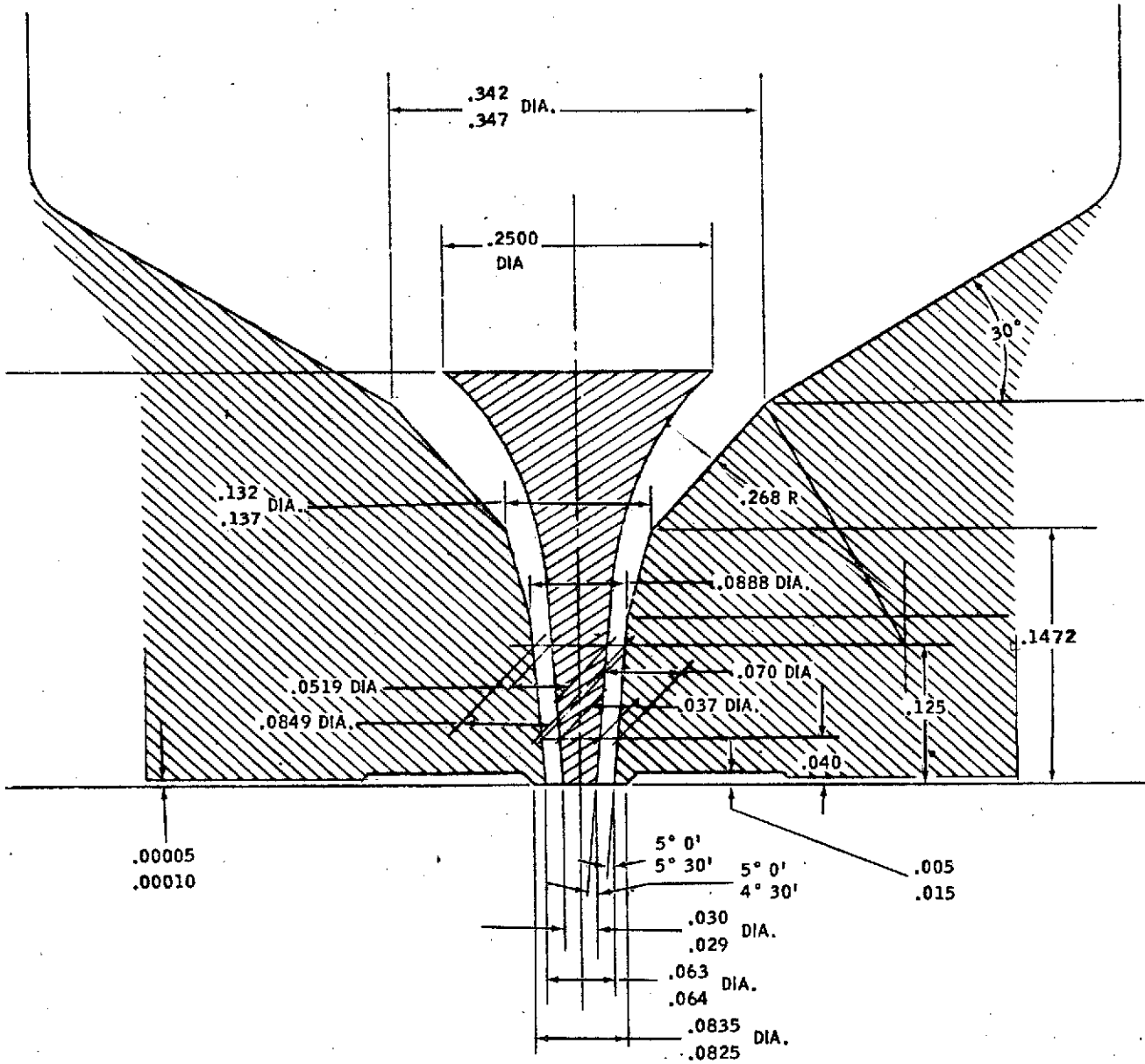
SEAT AND PUSH ROD DETAIL

.342 / .347 DIA.

.2500 DIA

30°

.132 / .137 DIA.

.268 R

.0888 DIA.

.1472

.0519 DIA.

.070 DIA

.0849 DIA.

.037 DIA.

.125

.040

.00005 / .00010

5° 0' / 5° 30'

5° 0' / 4° 30'

.005 / .015

.030 / .029 DIA.

.063 / .064 DIA.

.0835 / .0825 DIA.

Figure 5-4
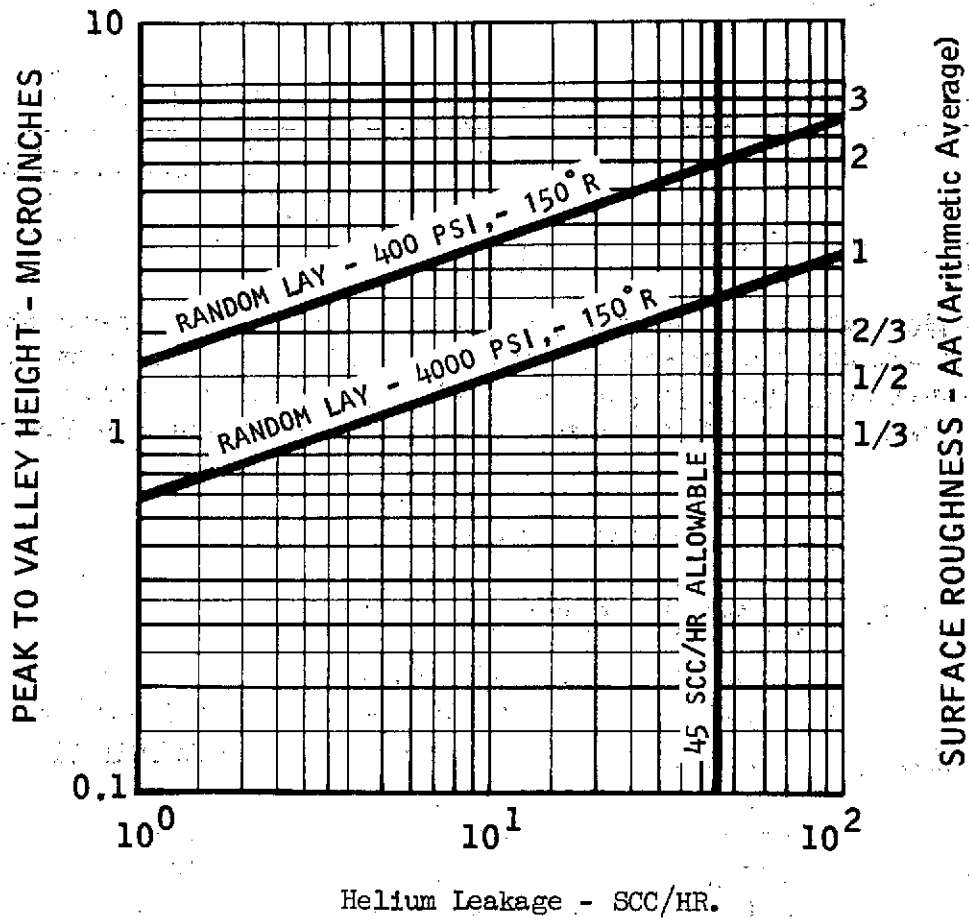
30

SURFACE FINISH VS LEAKAGE

Figure 5-5

31

seat with the push rod present simply acted as an orifice. Utilizing the flow relationship presented in Section 5.1.2 and choked flow at 4000 psia inlet pressure and $110^{\circ}R$ temperature it was determined that the maximum helium flow rate will be 0.20 lb per second. Thus, the relief systems on the space storable propulsion module should be sized to accommodate this helium flow rate.

5.1.4   Regulator Design APL Program (REG DES)

The regulator design APL program was prepared to size the regulator actuator and to permit a rapid tradeoff between such parameters as lever ratio, bellows area, spring preload, and spring rate. The REG DES Program consists of three force balance equations which define the poppet position at various strokes. These equations are:

$$A_B = A_s \frac{\left(P_{1max.} - P_{1min} + P_2\right)}{a/b \, \Delta P_2} \; ; \quad F_0 = P_2 A_B + \frac{A_s \left(P_{1max} - P_2\right)}{a/b}$$

$$K_S = \frac{F_0/X_{max} - \dfrac{\left(P_2 - \Delta P_2\right) A_B}{X_{max}} - \dfrac{\left(P_{1min} - P_2 + \Delta P_2\right) A_s \left(1 - \dfrac{4 D_{SE} X_{max}}{D_{SE}^2 - D_{st}^2}\right)}{a/b \, X_{max}}}{a/b}$$

By substituting the physical dimensions of the poppet/seat interface as discussed in Section 5.1.3, the required operating pressures, and the poppet flow forces as defined in Figure 5-6, the required bellows area, lumped spring preload, and lumped spring rate for lever ratios of 1, 2, 3, and 4 were determined. These values are listed in Table 5-II for a ± 1% accurate regulator.

TABLE 5-II

REGULATOR ACTUATOR DESIGN VALUES

Lever Ratio	Bellows Area (in	Lumped Spring Preload (lbf)	Lumped Spring Rate (lbf/inch)
1	8.121	1969.5	5484
2	4.061	984.7	1371
3	2.707	656.5	609
4	2.030	492.4	343

A sample print-out of the REG DES Program is presented in Table 5-III. The spring rate and spring preload data presented in Table 5-II was also determined for regulators featuring accuracies of ± 0.833 and ± 0.667% to determine sensitivity. These data are presented in Figures 5-6 and 5-7 as a function of the lever ratio. These data were subsequently used to size the coil springs, bellows, and flexures and to permit a weight trade-off as discussed in Section 5.1.8.

TABLE 5 – III

SAMPLE PRINTOUT – REGULATOR DESIGN PROGRAM

```
    REGDES
ENTER SET POINT PRESSURE-P2-PSIA
□:
    240
ENTER DEADBAND-ΔP-PSI
□:
    1.2
ENTER MAXIMUM INLET PRESSURE-P1MAX-PSIA
□:
    4000
ENTER MINIMUM INLET PRESSURE-P1MIN-PSIA
□:
    400
ENTER LEVER RATIO-A/B
□:
    1
ENTER SEAT DIAMETER-DS-INCHES
□:
    0.063
ENTER STEM DIAMETER-DST-INCHES
□:
    0.03
ENTER MAXIMUM STROKE-XMAX-INCHES
□:
    0.01
```

BELLOWS EFFECTIVE AREA, SQUARE INCHES	SPRING PRE-LOAD, POUNDS	SPRING RATE, POUNDS PER INCH
9.355	2256.9	2313

SPRING RATE PARAMETRICS

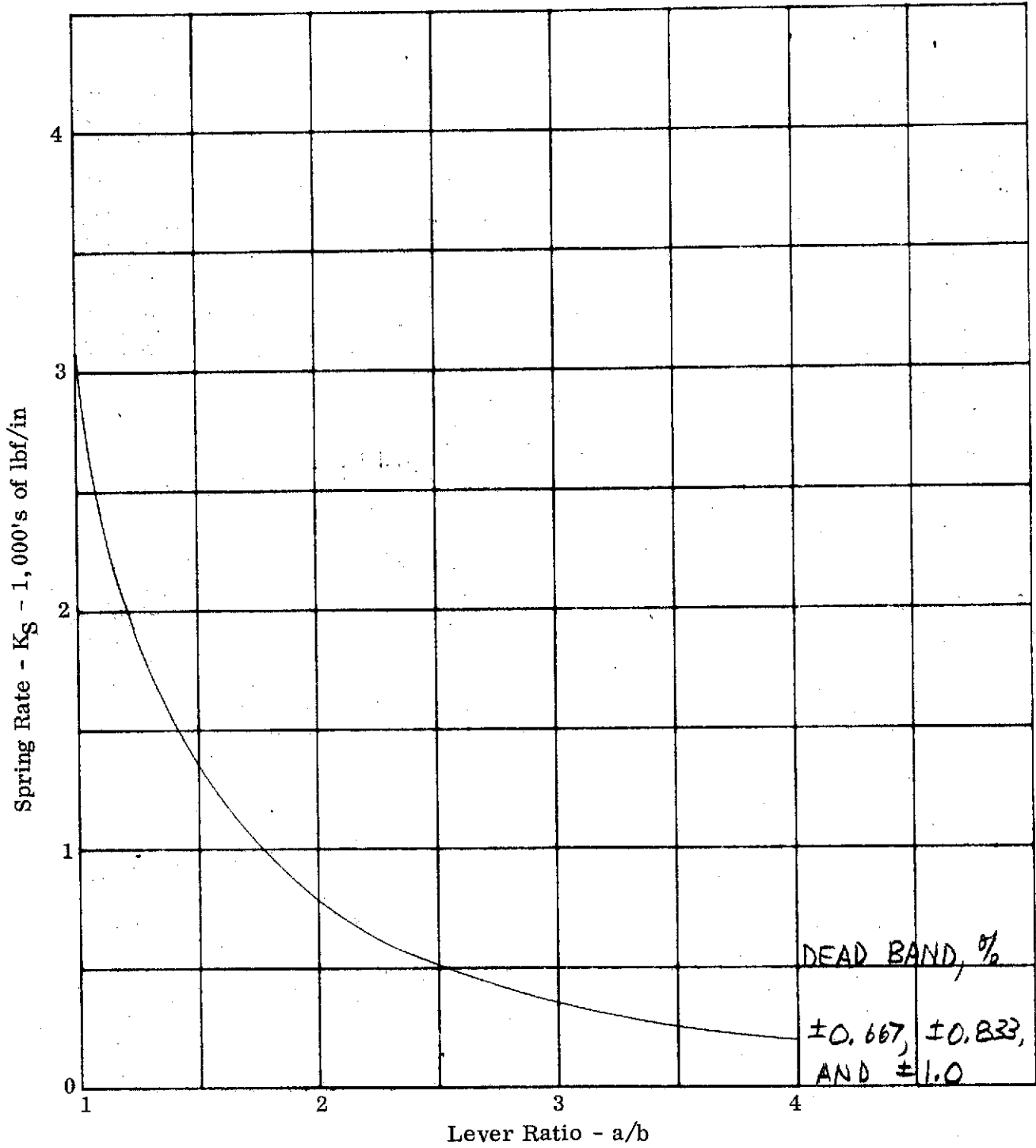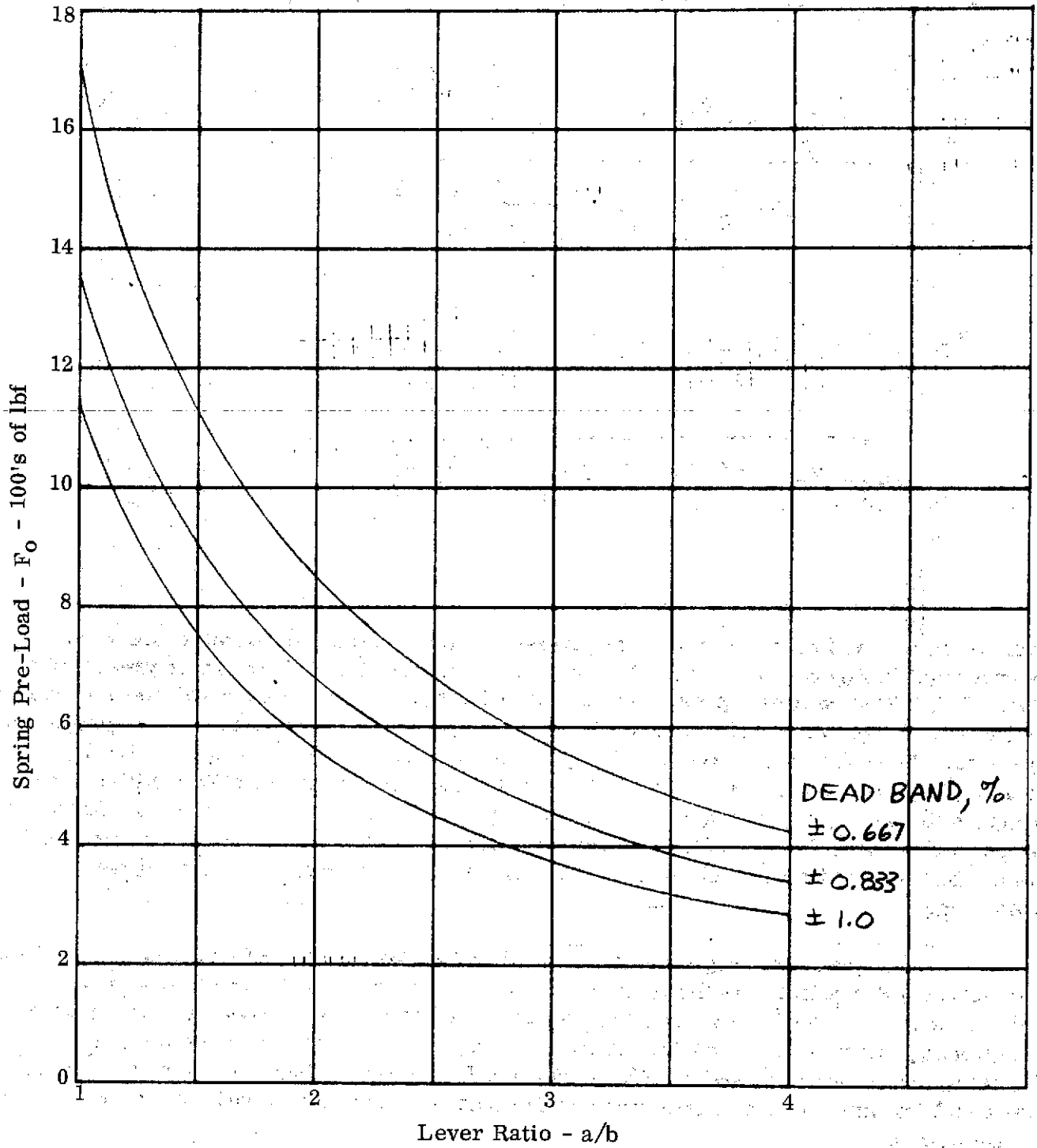

Figure 5-6

Figure 5-7

35

5.1.5 Regulator Performance APL Program (REG PERF)

To determine the regulated outlet pressure at any steady state flow rate of a particular design configuration the regulator performance APL Program (REG PERF) was developed. This program is based on the following relationships:

$$P_2 = \frac{a/b\, F_o - (a/b)^2 X_A K_S - P_1 A_S \left(1 - \dfrac{4\, D_S X_P}{D_{SE}^2 - D_{ST}^2}\right)}{a/b\, A_B - A_S \left(1 - \dfrac{4\, D_S X_P}{D_{SE}^2 - D_{ST}^2}\right)}$$

$$X_P = \frac{A_P}{\pi D_{SE}} \qquad A_P = \frac{\dot{W}\sqrt{T_1}}{P_1 C_m C_D}$$

$$C_m = \sqrt{\frac{2\, gr}{R\,(5-1)} \left[P_2/P_1^{\tfrac{2}{\alpha}} - (P_2 - P_1)^{\tfrac{\alpha+1}{\alpha}} \right]}$$

The discharge coefficient utilized in this expression was obtained from Reference 13 and is presented in Figure 5-8. A sample print-out of the REG PERF Program is presented in Table 5-IV. This computer program was then utilized to determine the regulator accuracies of the FLOX regulator sized in Section 5.1.4 for the MMH, hydrazine, and fluorine propellant systems. These data are presented in Figures 5-9 through 5-12. In comparing the input data for Figures 5-9 through 5-12 with the output parameters of the REG DES APL computer program (bellows area, spring rate, and spring preload) it should be noted that a slightly larger bellows area has been utilized since this specific bellow was available on the shelf from a bellows vendor and that the spring preload and spring rates have been adjusted accordingly.

The particular regulator performance data shown is for a lever ratio of 3, which was subsequently selected as the optimum lever ratio based on stability and weight considerations. As evident from these figures, the baseline regulator configuration featured a regulating accuracy of ± 0.9% for the flox system, ± 0.7% for the MMH system, ± 0.7% for the hydrazine system, and ± 0.8% for the fluorine system. Thus, it was shown that the flox regulator adequately met accuracy requirements of any of the propellant systems under consideration.

5.1.6 Stress Analysis of Flexures and Bellows

As evident from Figure 5-1, the baseline regulator design employees friction-free flexure guidance of all moving elements. Linear guidance flexures are employed for the actuator shaft, push rod, and poppet. A rotary flexure is employed for the lever arm.
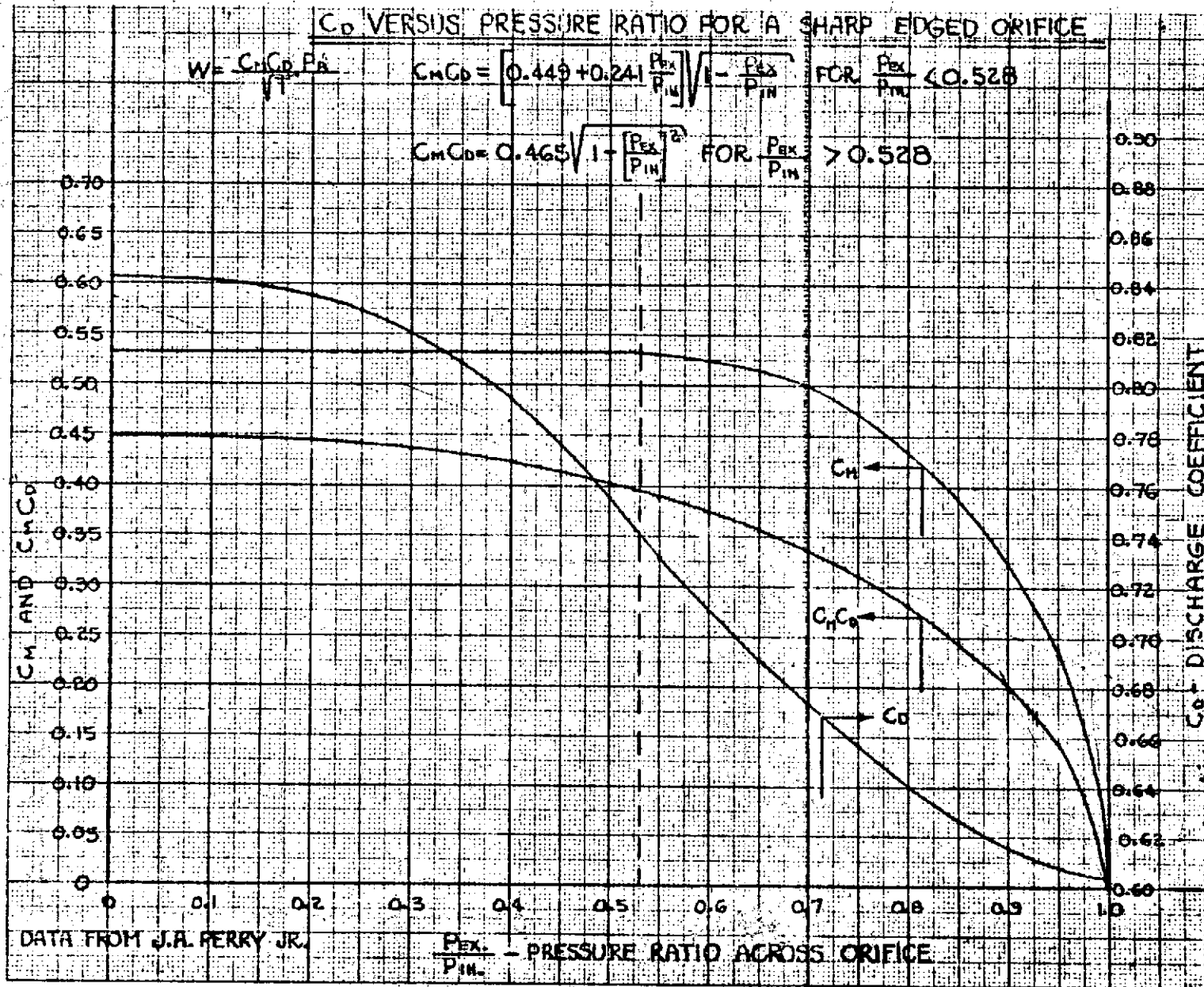
C_D VERSUS PRESSURE RATIO FOR A SHARP EDGED ORIFICE

$$W = \frac{C_M C_D P_R}{\sqrt{T}} \qquad C_M C_D = \left[0.449 + 0.241 \frac{P_{EX}}{P_{IN}}\right]\sqrt{1 - \frac{P_{EX}}{P_{IN}}} \qquad \text{FOR} \frac{P_{EX}}{P_{IN}} < 0.528$$

$$C_M C_D = 0.465 \sqrt{1 - \left[\frac{P_{EX}}{P_{IN}}\right]^2} \qquad \text{FOR} \frac{P_{EX}}{P_{IN}} > 0.528$$

DATA FROM J.A. PERRY JR.

$\frac{P_{EX}}{P_{IN}}$ — PRESSURE RATIO ACROSS ORIFICE

C_M AND $C_M C_D$

C_D — DISCHARGE COEFFICIENT

37

Figure 5-8

STEADY-STATE REGULATOR PERFORMANCE
FLOX SYSTEM

LEVER RATIO = 3
SPRING RATE = 592 LBF/IN.

SPRING PRE-LOAD = 688 LBF
SEAT DIAMETER = 0.066 IN.

STEM DIAMETER = 0.03 IN.
PROPELLANT DENSITY = 91.9 LBM/FT³

BELLOWS AREA = 2.84 IN²
INLET TEMP. = 150° R

+ 1%

INLET PRESSURE,
P_1, PSIA

1000
2500

4000

400

− 1%

↕ Design flowrate
1.142 lb_m/sec

OUTLET PRESSURE − P_2 − PSIA

PROPELLANT FLOW RATE − $\dot{W}_p$ − LBM/SEC FLOX

Figure 5-9

38
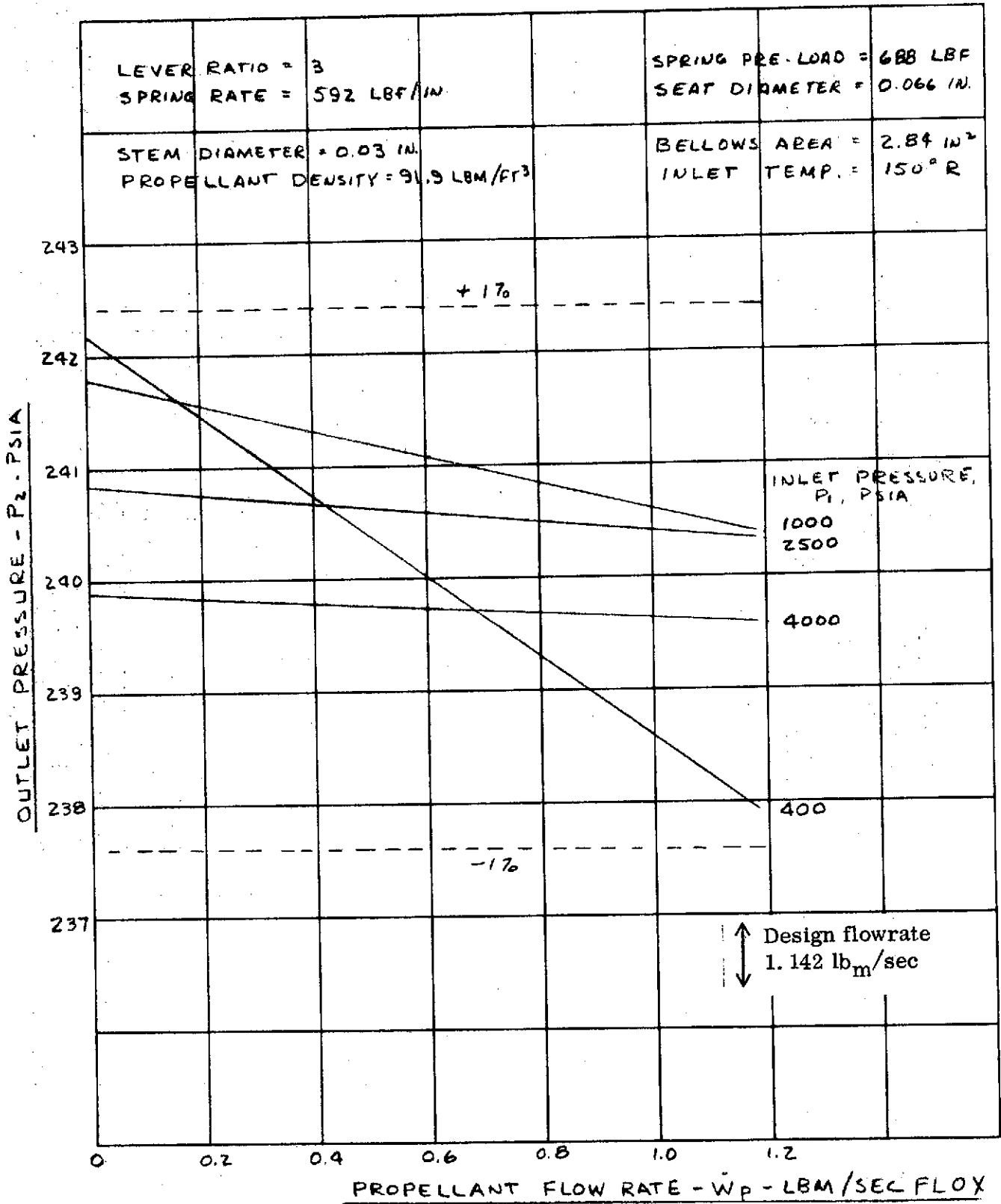
REGULATOR STEADY-STATE PERFORMANCE
MMH SYSTEM

LEVER RATIO = 3
SPRING RATE = 592 LBF/IN

SPRING PRE-LOAD 1626 LBF
SEAT DIAMETER = .066 IN

STEM DIAMETER = 0.03 IN
PROPELLANT DENSITY = 56.7 LBM/FT³

BELLOWS AREA = 2.84 IN²
INLET TEMP = 530 °R

INLET PRESSURE, Pi, PSIA

1000
400
2500
4000

1%

1%

Design flowrate
0.441 lb$_m$/sec MMH

OUTLET PRESSURE - P$_2$ - PSIA

PROPELLANT FLOW RATE - W$_P$ - LBM/SEC - MMH
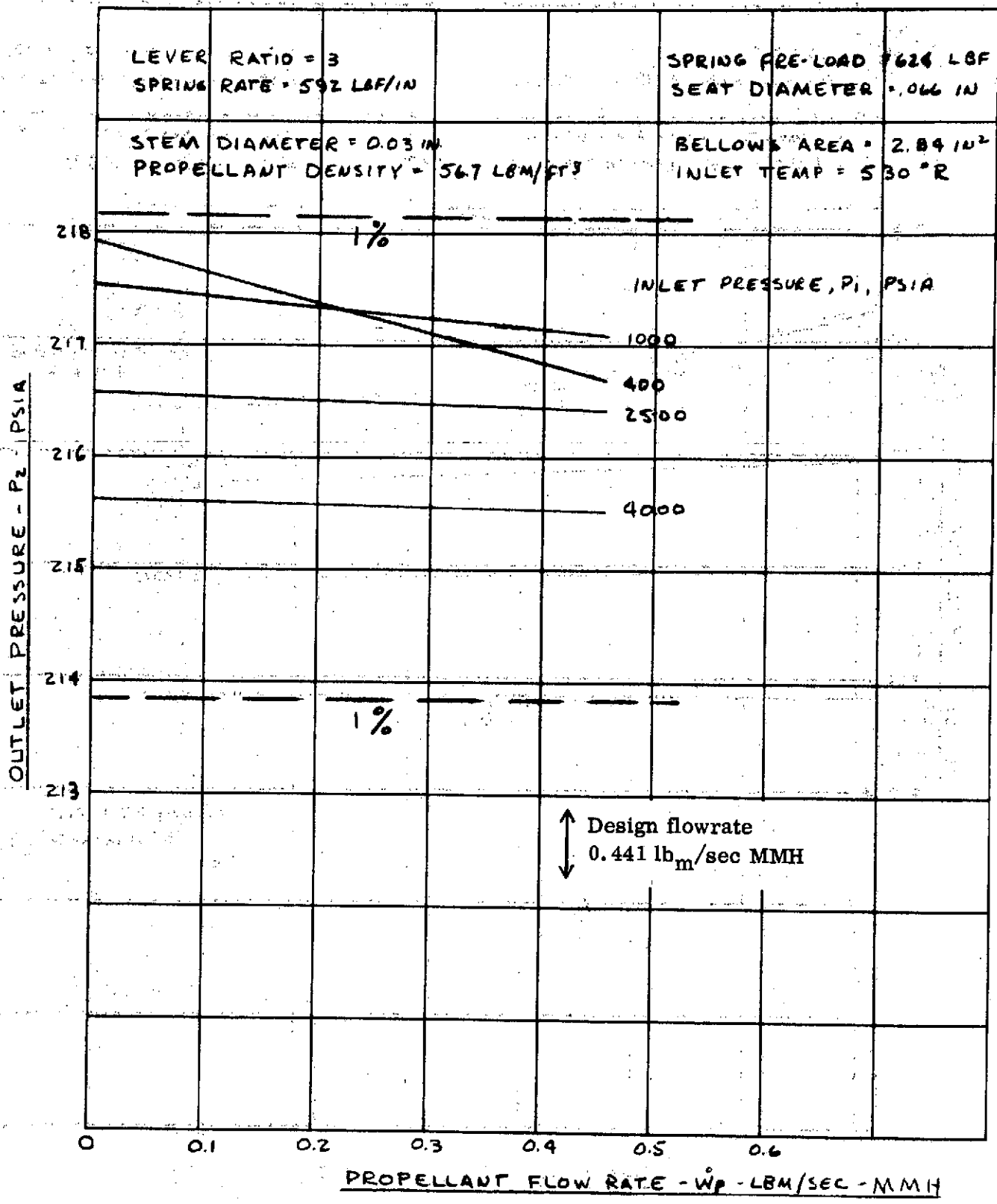
Figure 5-10

STEADY-STATE REGULATOR PERFORMANCE
HYDRAZINE SYSTEM

Figure 5-11

LEVER RATIO = 3
SPRING RATE = 592 LBF/IN

SPRING PRE-LOAD = 660 LBF
SEAT DIAMETER = 0.066 IN.

STEM DIAMETER = 0.03 IN.
PROPELLANT DENSITY = 94.5 LBM/FT³

BELLOWS AREA = 2.84 IN²
INLET TEMP = 150 °R

INLET PRESSURE, P_i, PSIA

1000
2500
4000
400

1%

Design flowrate
1.039 lb_m/sec F_2
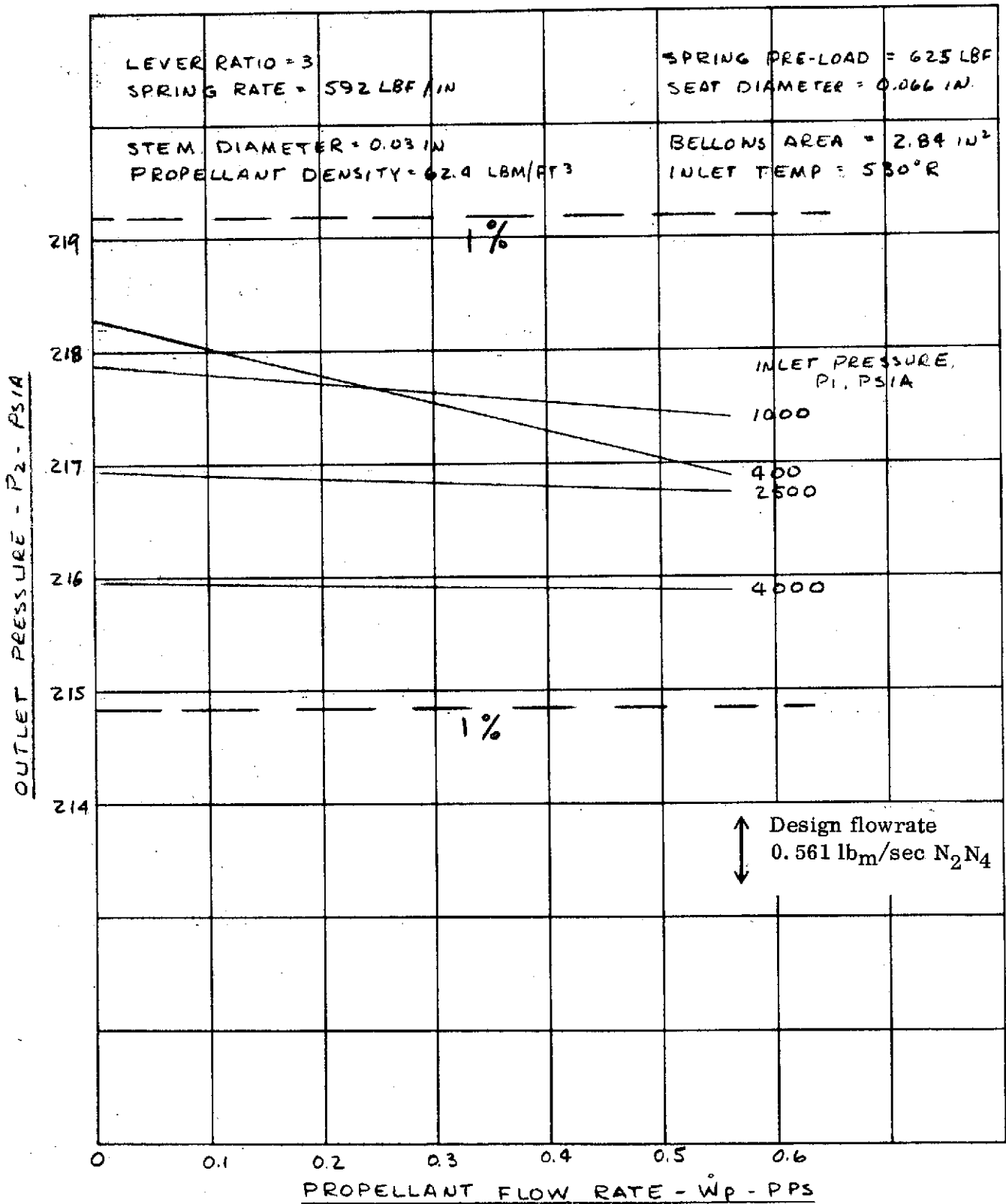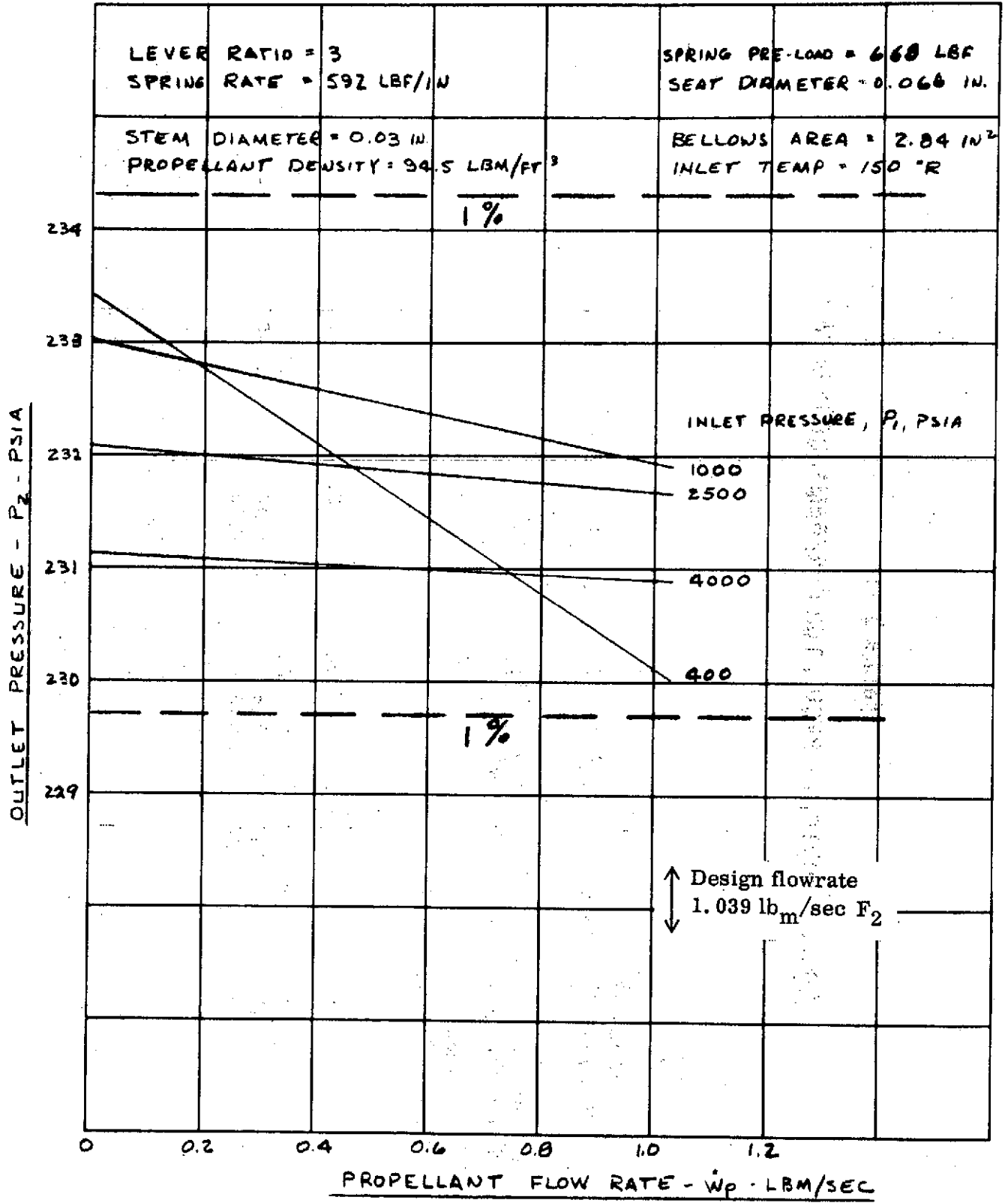
Figure 5-12

TABLE 5 – IV

SAMPLE PRINTOUT – REGULATOR PERFORMANCE PROGRAM

```
       X□
        ∇
        [9]←2500
       REGPERF
ENTER A/B, FO, KS, DS, DST, ABE, RHOP, T1, P1, DSE
□:
       □←X
3  666  592  0.083  0.03  2.84  94.5  150  2500  0.066
ENTER PROPELLANT FLOWRATES-WDOTP-PPS
□:
       WDOTP
ENTER SETPOINT-P2-PSIA
□:
       P2
```

P1	WDOTP	P2	XP	CM	CD
2500	0.000	233.07	0.00000	0.2097	0.953
2500	1.000	232.68	0.00072	0.2097	0.953
2500	1.100	232.64	0.00080	0.2097	0.953

Flexures were analyzed by means of the elastic energy methods developed by Reference 14. The results of these methods are simple relationships expressing the deflection, slope, and twist at the end of partial circular arc cantilever beams loaded transversely to the plane of curvature. Small deflection linear elastic theory is employed. Typical equations are:

$$\delta = \frac{Fr_a^3 K_\delta}{EI} \qquad \theta = \frac{Fr_a^3 K_\theta}{EI} \qquad \phi = \frac{Fr_a^3 K_\phi}{EI}$$

(These are relationships for the axial deflection (δ), slope (θ), and twist (ϕ) at the free end respectively; K is a theoretically derived constant as a function of arc included angle, load position, and section properties; F is the load at the free end of the arc; r_a is the mean radius of the arc; E is the modulus of elasticity; I is the moment of inertia of arc cross-section about the lateral axis.)

By using Maxwell's law of reciprocal deflections and/or choosing suitable inflection points, the effect of end fixities can be determined. To provide sufficient endurance life, the maximum stress from the combined effects of bending, shear, and torsion, coupled with any notch or surface stress concentration factors, is sized to be less than the fatigue or endurance stress allowed for the required number of cycles. The allowable endurance stresses are taken from such data as MIL Handbook 5-A or Aerospace Structural Metals Handbook (Syracuse Univ. Press).

Analysis of linear flexures at Marquardt has been accomplished for a number of configurations. One configuration used in the regulator which offers a high radial to axial stiffness ratio is identified as a 360° flexure. This flexure has generally been considered for use in a set of three wherein the flexures are rotated 120 degrees to one another to achieve nearly equal radial spring rate in all directions. The 360° flexure is particularly suitable for the regulator actuator shaft assembly since this assembly must support a significant side load. The push rod and poppet flexures are less critical due to the much lower side loads and were therefore designed to employ the three lobe configuration which features a symmetrical beam pattern and can be used singly rather than in sets of three as required for the 360° flexure. The criteria utilized in designing these flexures was a cycle life of 100,000 cycles, maximum radial deflection of 0.0001 in., minimum axial spring rates and the use of inconel 718 as the material of construction. Details of the stress analyses are presented in Appendix B.

The relationship of flexure plate thickness to radial and axial spring rates for the three lobe flexure, based on an outer diameter of 1.0 in., is shown in Figure 5-13. Flexure plate thicknesses selected during the analytical effort were 0.008 in. for the poppet flexure and a total of 4 flexure plates of 0.006 inch for the push rod flexure. Flexure plate thicknesses, as a function of outer diameter for the 360° flexures versus radial and axial spring rates, are shown in Figure 5-14. As indicated in Appendix B, a design point of 1-1/2 inches outer diameter and 0.016 inch flexure plate thickness were chosen.

The rotary pivot flexure required for the lever arm was selected on the basis of the design data listed in Reference 15 and several experimental data curves obtained from

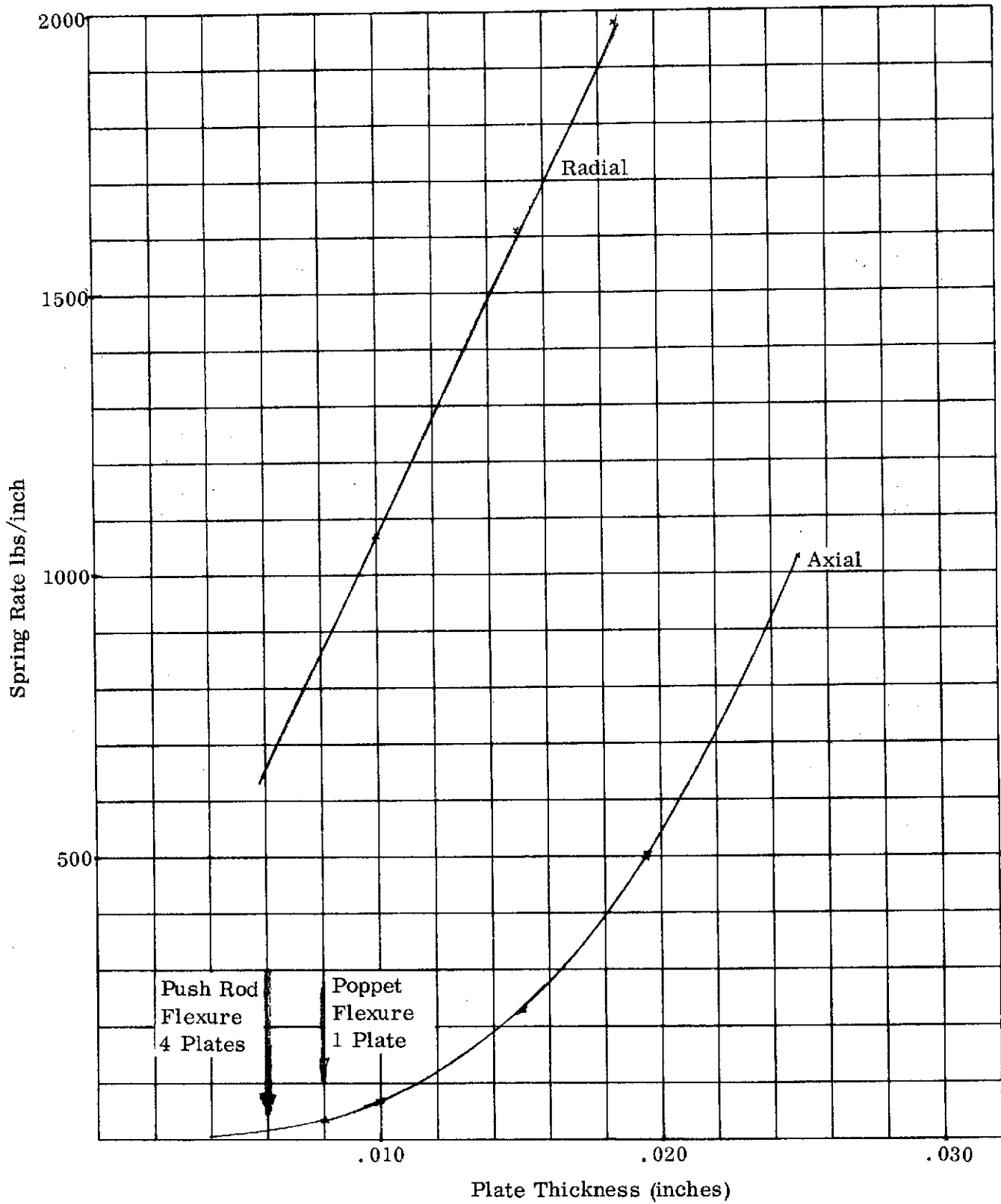# FLEXURE THICKNESS VS SPRING RATE
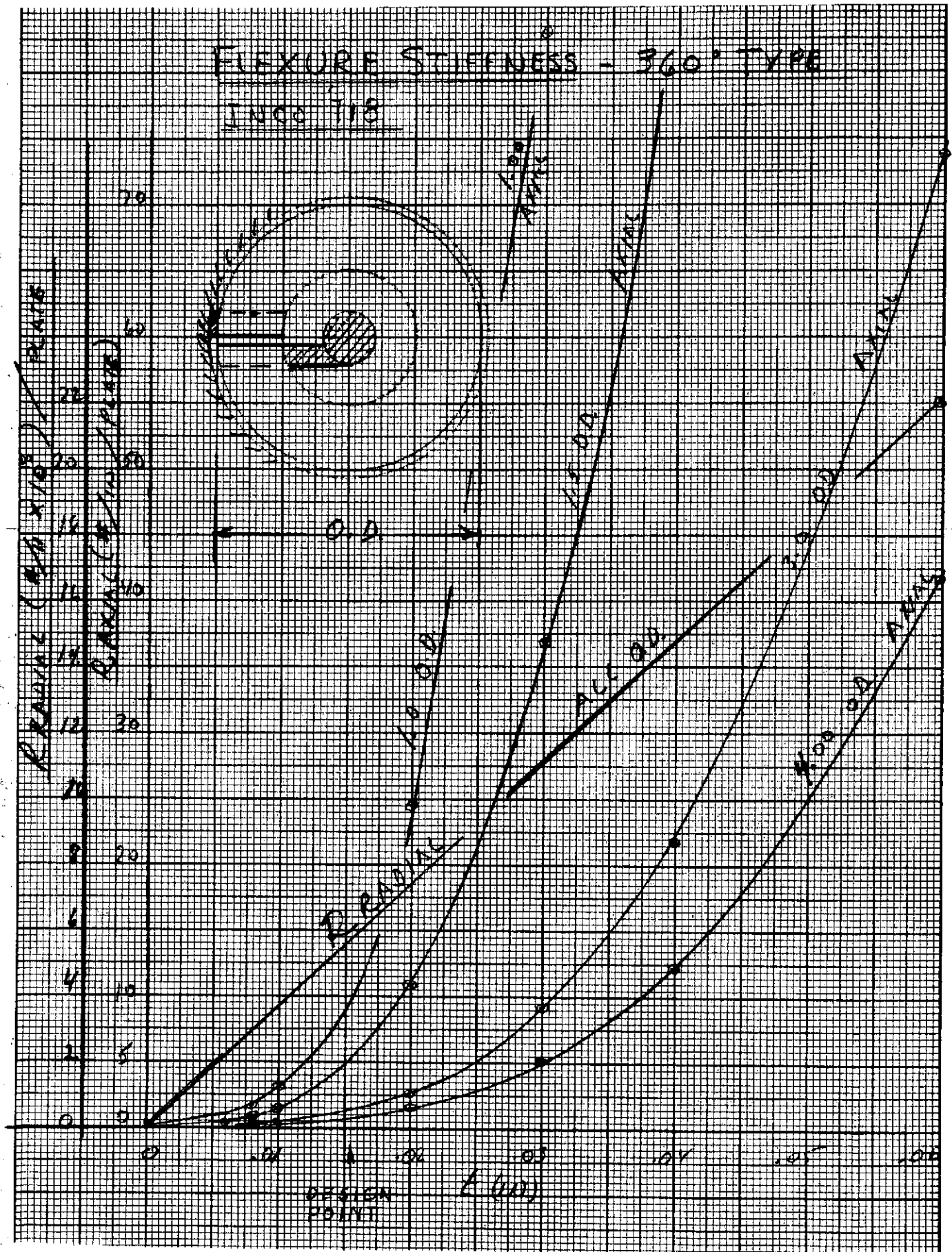## 3 LOBE TYPE - INCO 718

Figure 5-13

Figure 5-14

45

Bendix which define the flexure radial spring rates for given radial loads. The selected pivot flexure is a 1/4-inch series 600 flexure as listed in Reference 15. This particular flexure will assure an infinite flexure life.

A critical examination of the contact points between the actuator shaft assembly and the lever arm and between the push rod and the lever arm was also made. This examination served primarily to determine if any sliding friction would occur at those contact points during regulator operation. Analysis of the friction forces, relative motion, and stiffness of the guidance flexures resulted in the conclusion that as long as a minimum of 0.5 lb of force was maintained at the contact between the push rod and the lever arm no sliding motion would occur at that point. Consequently, the push rod flexures were designed into the baseline regulator such that this minimum force was always provided. Analysis of the contact point between the actuator shaft and the lever arm indicated that some sliding did occur. Consequently, the shaft immediately ahead of the contact point was slimmed down to permit minimal bending of the shaft at the contact point and to thereby eliminate this sliding characteristic.

Since the bellows performance characteristics play an important role in optimizing of the baseline regulator design, The Marquardt Company, early during the program, initiated contact with two suppliers of hydroformed bellows. A substantial number of bellow configurations and their performance characteristics were obtained from both of these suppliers and were utilized during the weight optimization of the baseline regulator. These bellow data are presented in Section 5.1.8 of this report. Upon completion of the weight optimization and selection of the 3:1 lever arm ratio, one bellow design applicable to this lever arm ratio was chosen from each of these suppliers and The Marquardt Company performed its own stress analysis of these bellow configurations. Specific bellow design parameters are listed in Table 5-V. In reviewing these design parameters, as well as the designs of other bellows supplied by these vendors, it is noted that Gardner tends to provide significantly higher stress margins than Stainless Steel Products, as shown in the Marquardt stress analysis in Appendix C. For a given spring rate the installed lengths of the bellows from the two vendors do not vary greatly; however, the reference force that could be obtained by compressing the bellows a given amount is substantially higher for the Stainless Steel Products bellows than for the Gardner bellows. This in turn would result in the requirement of a significantly smaller coil spring in combination with the Stainless Steel Products bellows, for the same envelope.

5.1.7   Dynamic Modeling

Regulator dynamics were simulated on Marquardt's Beckman Easy Model 1100 Analog Computer. The purpose of the analog simulations was to verify that the baseline regulator design is inherently stable, to compare regulator output pressure oscillations for baseline designs featuring four different lever arm ratios, and to evaluate the effects of friction and gas damping upon regulator performance. Dynamic analysis was performed for starting and stopping characteristics during typical rocket engine firings as well we for a so-called step response. The step response is a theoretical condition which is typically used in the analysis of dynamic components to simulate the worst case oscillation; however, in a practical system this degree of oscillation is never attained. In programming the step response on the analog computer, it is assumed that the regulator poppet is held in the closed

TABLE 5-V

BELLOWS DESIGN PARAMETERS

	Gardner	Stainless Steel Products
I. D.	1.60	1.74
O. D.	2.05	2.09
Effective Diameter	1.86	1.93
Number of Convolutions	30	20
Material Thickness	.008	.006
Spring Rate	105	105
Free Height	2.0	3.4
Allowable Compression (max.)	.3	1.5
Installed Length	1.7	1.9

position and is then suddenly released to instantaneously attain a position corresponding to nominal regulator flow conditions. The resulting poppet oscillations are observed to determine that they will damp out within a reasonable time.

The analog run matrix that was performed is shown in Table 5-VI. As indicated in this run matrix the variables included the lever ratio; minimum and maximum inlet pressures in combination with maximum and minimum ullage volumes, respectively; step response; motor firings; friction; and damping. The regulator dynamic analysis was performed by means of a non-linear, lumped parameter math model. The math model includes the gas dynamics and mechanical dynamics of the regulator, the gas dynamics of the propellant tank and the interaction between them. The downstream tank gas dynamics are included in the regulator math model, since this constitutes the feedback in the mechanism for the regulator. The gas dynamics include the non-linear equations of helium flow through the regulator valve variable-area ports and/or orifices and the flow-pressure relationships in several volumes, including the bellows actuator cavity and the propellant tank. The mechanical dynamics of the regulator relate force-mass to acceleration-velocity-position, and include spring/flexure damping and non-linear friction. The specific relationship used in the analog program are shown below:

Motion:

$$\ddot{Y} = \frac{g\left[P_2 A_B + YK_s - F_o - B\dot{Y} \pm F_f - \frac{(P_1 - P_2)A_s X_p}{a/b}\left[1 - \frac{4D_{SE}}{D_{SE}^2 - D_{ST}^2} \right] \right]}{W_T}$$

Mass:

$$W_T = \frac{W_{BS} + W_{BF}}{2} + W_{BP} + \frac{W_{WL}}{a/b^2} + \frac{W_P + W_{PR}}{a/b} + \frac{W_{PF} + W_{PRF}}{2\,a/b}$$

Poppet Flow:

$$\dot{W} = \frac{P_1 \pi D_{SE} C_m C_D X_P}{\sqrt{T_1}}$$

Propellant Tank:

$$\dot{P}_2 = \frac{RT_1}{V_T}\,\dot{W} - \frac{P_2}{V_T \rho_P}\,\dot{W}_P$$

TABLE 5-VI

ANALOG RUN MATRIX

Lever Ratio	Inlet Press. (psia)	Ullage (Ft^3)	Step Motor	Motor Firing	Friction	Gas Damping
1	4000	2.7	x	x		
1	400	13	x			
2	4000	2.7	x	x	x	
2	400	13	x		x	
3	4000	2.7	x	x		x
3	400	13	x			x
4	4000	2.7	x	x		
4	400	13	x			

Some of the regulator notations are shown in Figure 5-15. The remaining symbols are identified in Section 10. The regulator motion equation includes a damping term B which represents the lumped spring hysteresis, also referred to as solid damping. Solid damping occurs in all vibrating systems having elastic restoring forces, although it is not always large enough to be a deciding factor in limiting the amplitude. For simplicity of analysis the hysterisis is treated as a function of the amplitude only. This is permitted by the repeatability peculiar to all stress-strain diagrams when elastic members are cycled indefinitely between two limits. For example, when cycling a part between two limits the stress has a slightly higher value for the same strain when the stress is increasing than when it is decreasing, and this is true even when the maximum stress is below the elastic limit of the material. The area inside the hysteresis loop indicates the amount of energy dissipated (converted into heat) within the material during one cycle. According to References 16 and 17, solid damping may be represented by an effective damping ratio of 0.02 to 0.03 for most commonly employed engineering materials and this value was therefore used in the analog model. The analog computer diagram is shown in Figure 5-16.

To verify the applicability of the lumped parameter model to the baseline regulator design the natural frequencies of the various regulator elements that experience motion but are not mechanically coupled to one another were computed. These natural frequencies are listed in Table 5-VII. A review of Table 5-VII indicates that regardless of the lever ratio selected, the actuator assembly is always the lowest frequency element with the natural frequencies higher and increasing going from the lever to the push rod and to the poppet. This progression assures that the four regulator elements in contact with one another will always move synchronously with the actuator assembly and therefore verifies the validity of the lumped parameter model.

The dynamic analysis of the baseline regulator design featuring various lever ratios disclosed that there was no noticeable difference in the dynamic behavior of any of the lever arm ratios evaluated. All of the configurations were dynamically stable. Representative data of the regulator performance parameters that were monitored during the analog computer simulation are presented in Figures 5-17 through 5-22. Each of these figures shows the analog traces of poppet velocity, poppet position, helium flow rate, outlet pressure, and bellows position. Figure 5-17 shows the step response for the baseline regulator featuring a lever ratio of 3 for both the slowest and fastest system configuration. (The slowest configuration is achieved at the lowest inlet pressure and largest ullage, and the fastest configuration is achieved at the highest inlet pressure and smallest ullage volume). From Figure 5-17 can be seen that appreciable poppet oscillatory motion occurs for a period of approximately 20 milliseconds at the high inlet pressure and approximately 30 milliseconds at the low inlet pressure; however, outlet pressure remains very constant throughout these oscillations due to the large difference in the time constants of the regulator mechanism and the tank ullage volume. A typical motor firing is shown in Figure 5-18. For this run sequence the regulator is initially closed and at "motor on" liquid outflow of the propellant tank at the nominal flow rate is assumed. This liquid outflow causes the propellant tank pressure to decay as much as 0.2 psi at which time the regulator replenishes the pressurant at the nominal flow rate and no further changes in tank pressure occur. When the motor is turned off the regulator closes and the tank pressure returns to its original set pressure. As evident from Figure 5-18, this more realistic dynamic simulation of regulator behavior shows that no regulator poppet oscillations whatsoever normally occur.
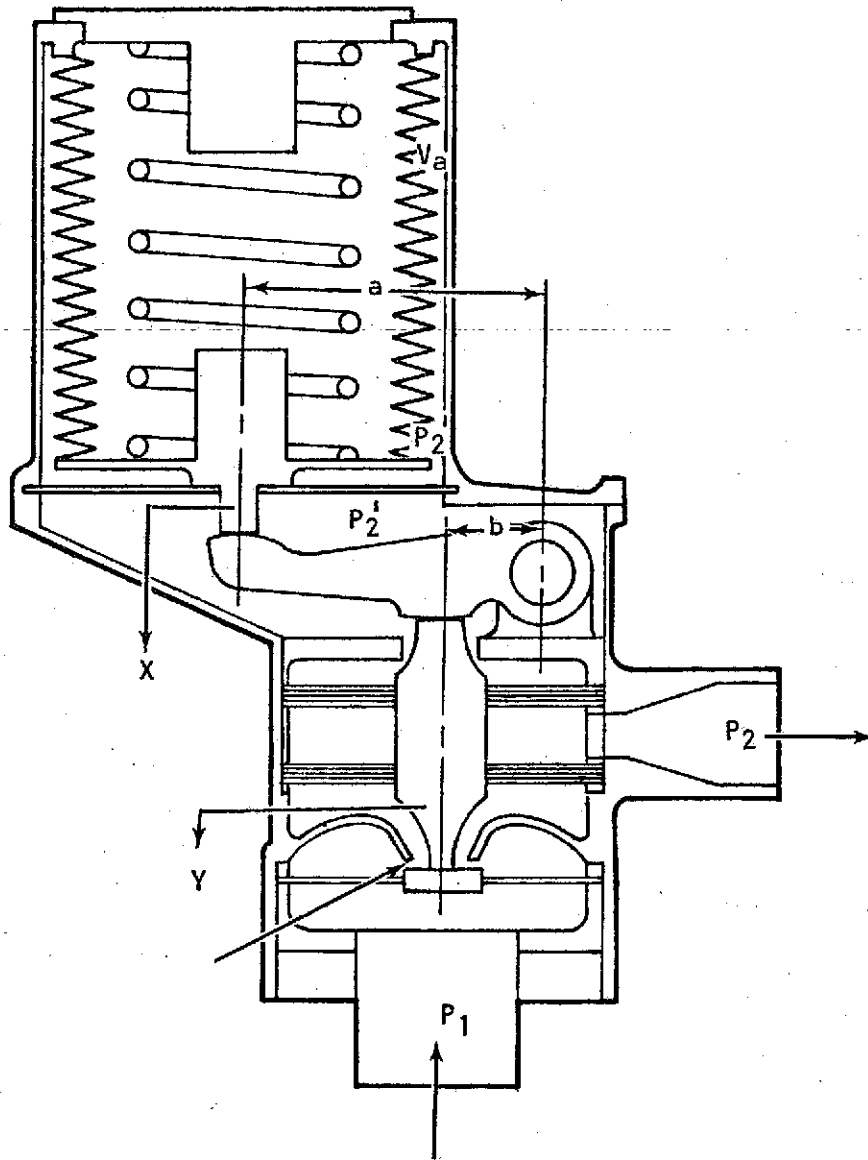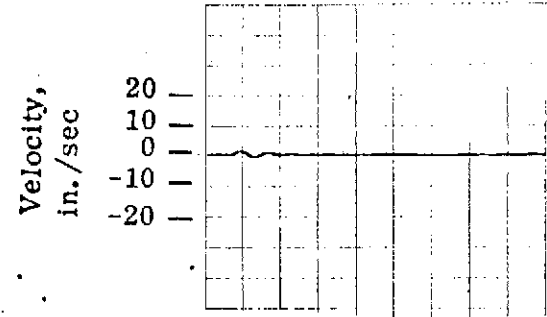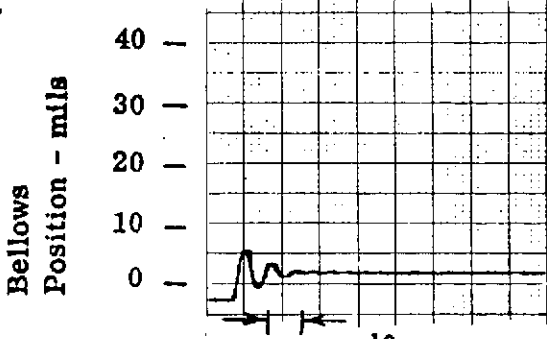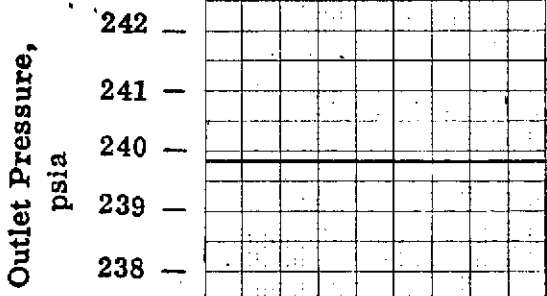
REGULATOR SCHEMATIC

Figure 5-15

ANALOG COMPUTER PROGRAM SCHEMATIC

Figure 5-16

Figure 5-17 Analog Computer Data

53

MOTOR FIRING   LEVER RATIO = 3   INLET PRESSURE = 4000 psia
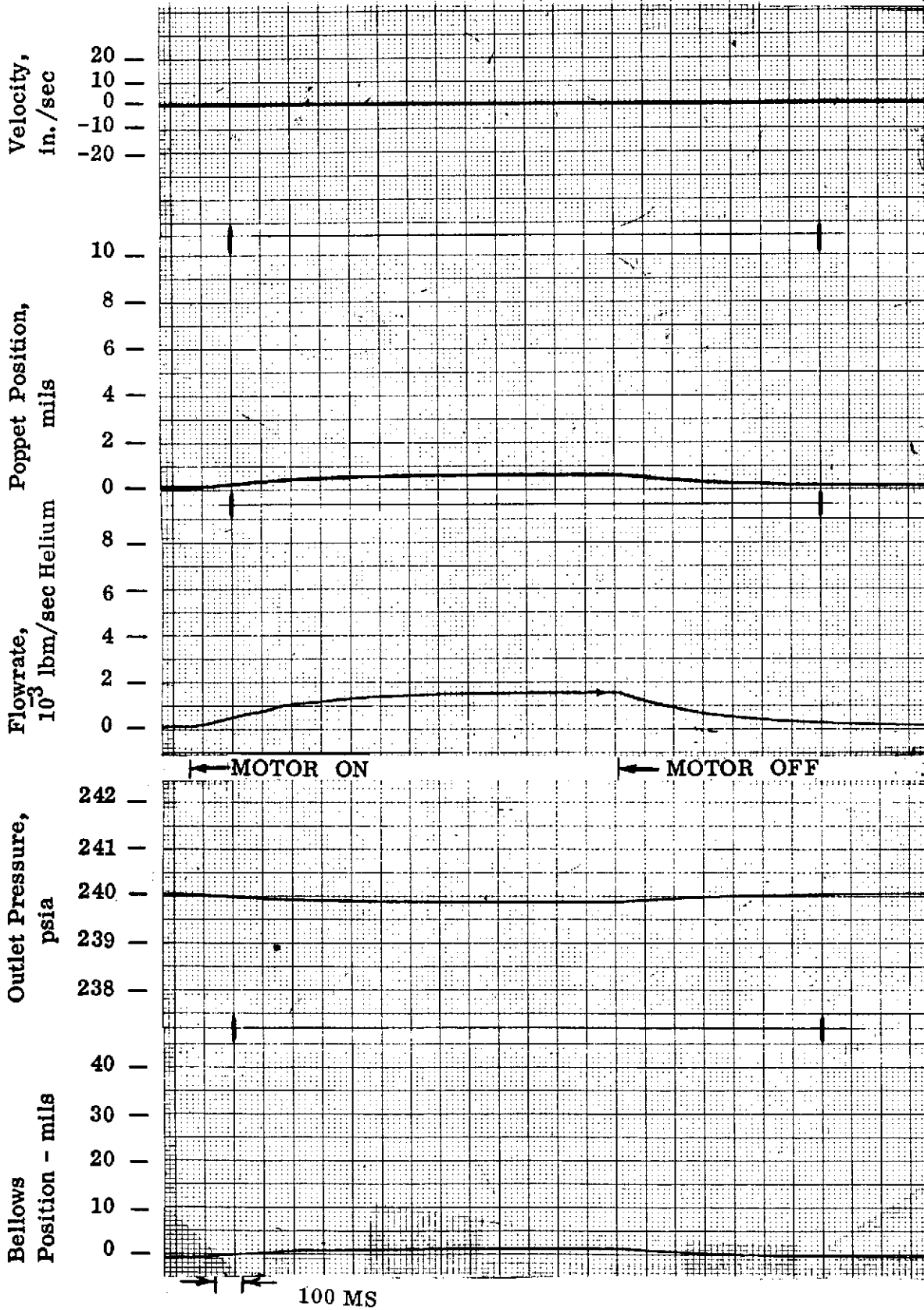
ULLAGE = 2.7 Cu.Ft.

Figure 5-18 Analog Computer Data
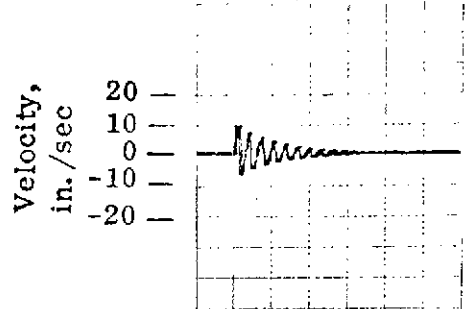
FRICTION SENSITIVITY   LEVER RATIO = 2   FRICTION = ± 2 LBF
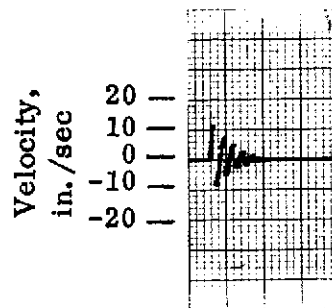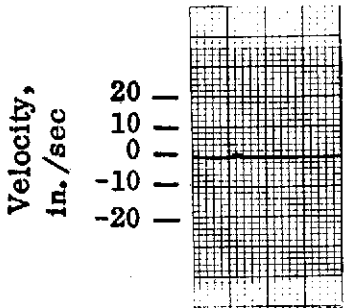
INLET PRESSURE = 4000 PSIA
ULLAGE - 2.7 CU.FT.

INLET PRESSURE = 400 PSIA
ULLAGE = 13 CU. FT.
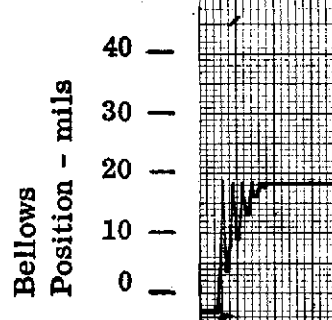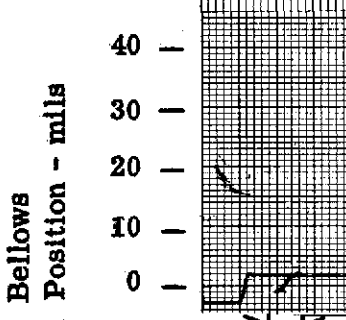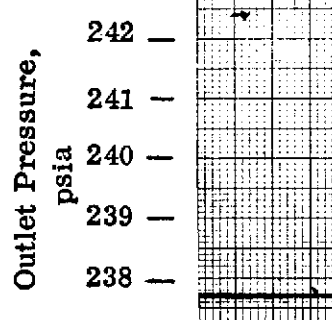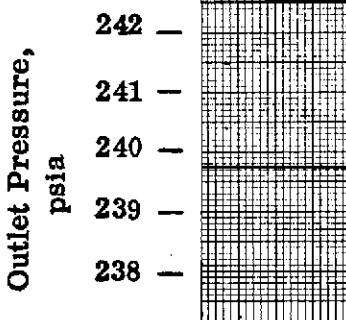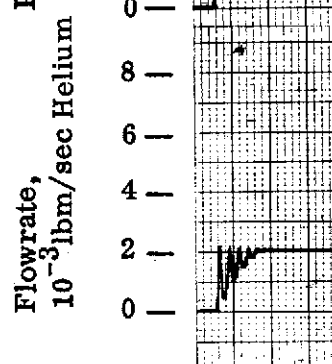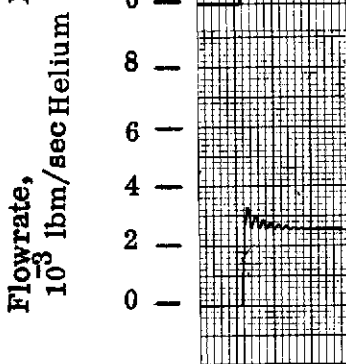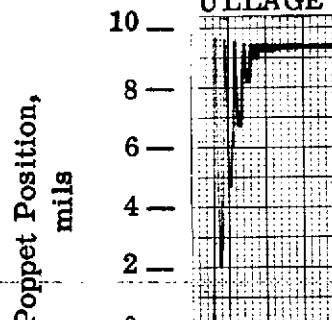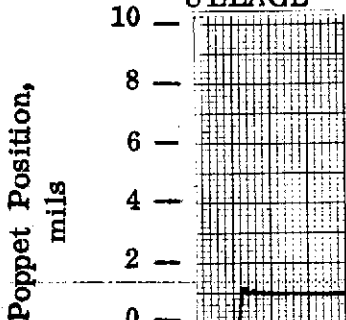
10 ms

Figure 5-19 Analog Computer Data

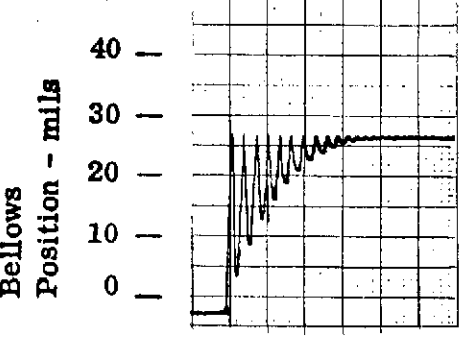FRICTION SENSITIVITY   LEVER RATIO = 2   FRICTION = ± 8 LBF
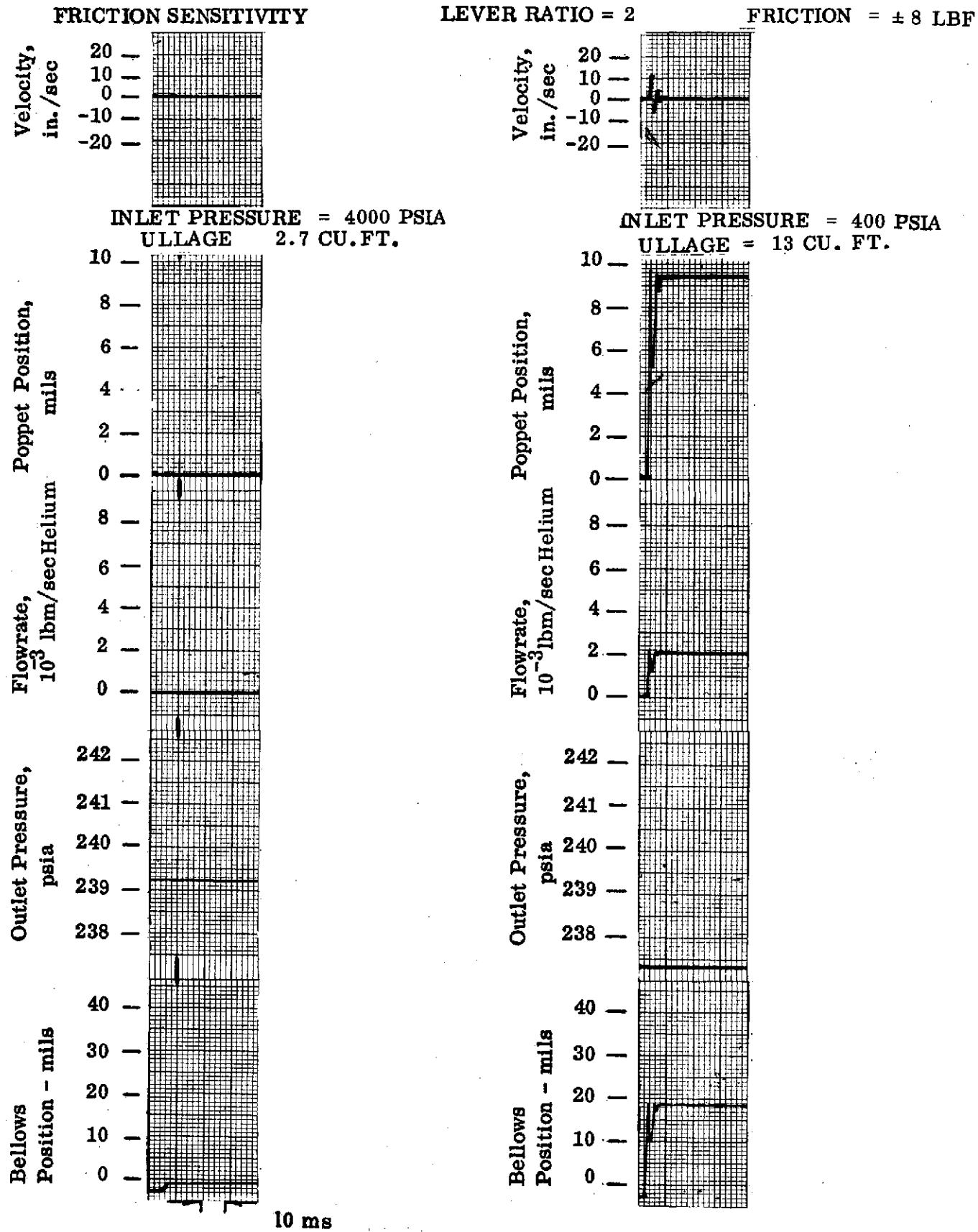
Figure 5-20 Analog Computer Data

GAS DAMPING   LEVER RATIO = 3   INLET PRESSURE = 400 psia

NO DAMPING   0.133" DIA. 0.059"DIA .0.042" DIA.
             ORIFICE   ORIFICE   ORIFICE
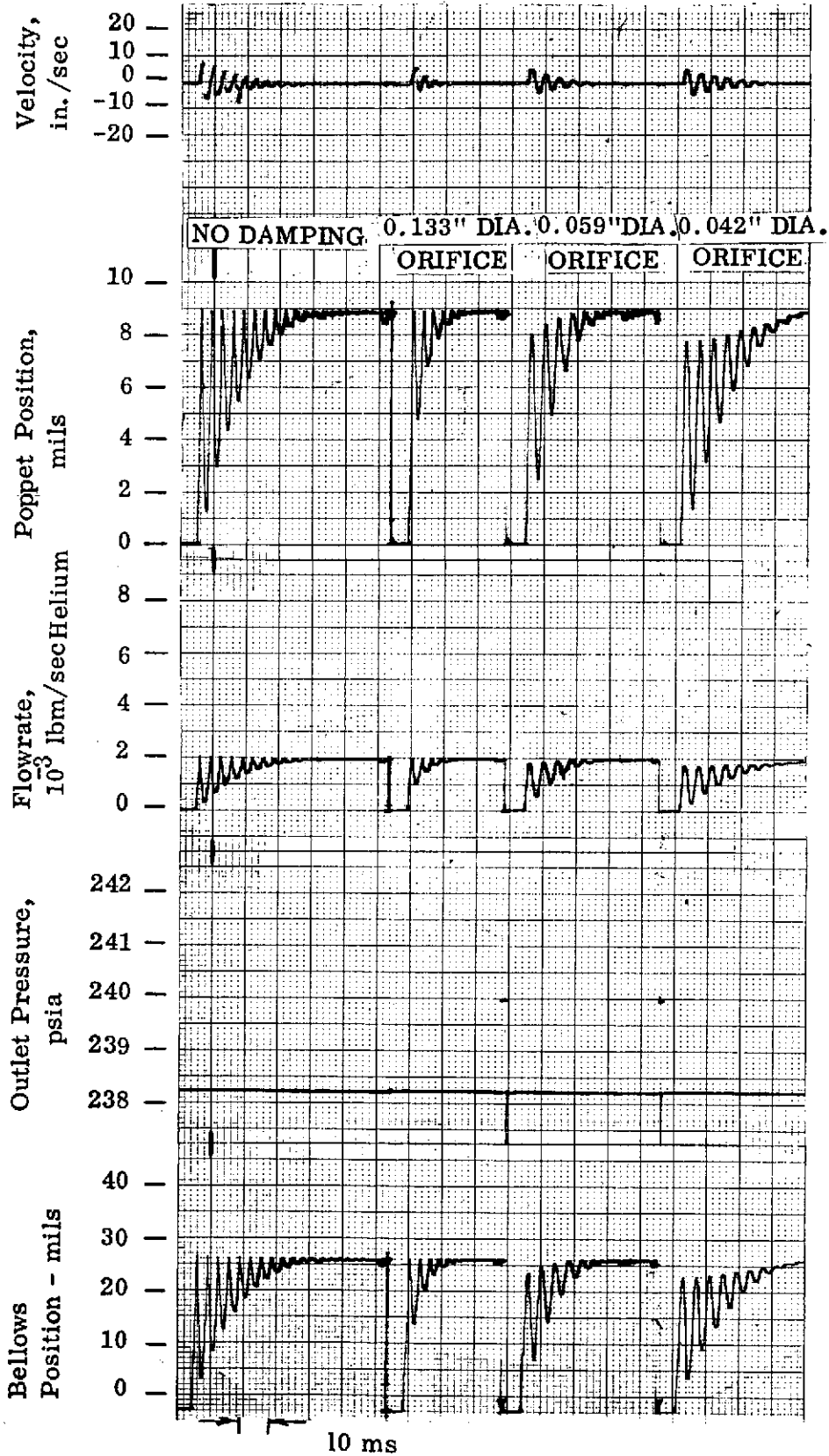
Figure 5-21 Analog Computer Data

57

GAS DAMPING   **LEVER RATIO = 3**   **INLET PRESSURE = 4000 psia**

Velocity, in./sec

Poppet Position, mils

NO DAMPING   0.133" DIA. ORIFICE   0.059" DIA. ORIFICE   0.42" DIA. ORIFICE

Flowrate, 10^3 lbm/sec Helium

Outlet Pressure, psia

Bellows Position - mils

10 ms
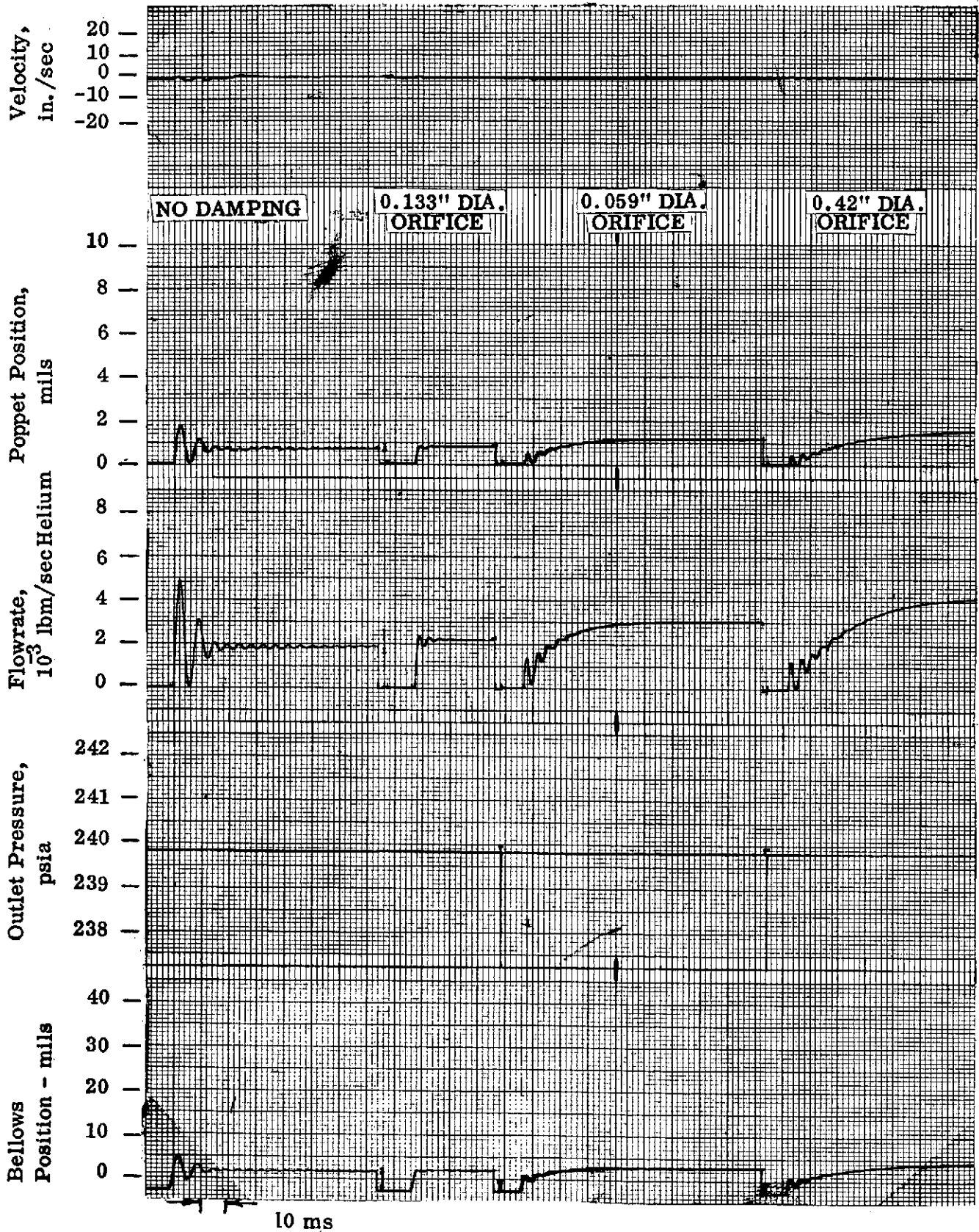
Figure 5-22 Analog Computer Data

58

TABLE 5-VII

NATURAL FREQUENCIES, BASELINE REGULATOR COMPONENTS

Item	Lever Ratio	Frequency (CPS)
Poppet	–	444
Pushrod	–	406
Lever	2	237
Lever	3	129
Lever	4	84
Actuator Assembly	1	221
Actuator Assembly	2	133
Actuator Assembly	3	93
Actuator Assembly	4	69

Figures 5-19 and 5-20 show the effects of two and eight pounds of inherent regulator friction on the baseline regulator dynamic behavior. As discussed previously, the baseline regulator design features zero friction; consequently, the data presented in Figures 5-19 and 5-20 are hypothetical cases to determine the degradation in the pressure set point accuracy that would occur as a result of friction, as well as the damping out of poppet oscillation for a step response. As seen from these figures, the outlet pressure changes by approximately 1/2 psi in going from the two-pound to the eight-pound friction configuration. Poppet oscillations are reduced under the same circumstances to approximately one single oscillation.

The effects of gas damping on poppet motion during step response were also evaluated. These data are presented in Figures 5-21 and 5-22. Gas damping was of interest since it could be incorporated into the baseline regulator very easily by simply controlling the clearance around the push rod where it enters the actuator cavity. Figures 5-21 and 5-22 show the effects of gas damping at inlet pressures of 400 and 4000 psi, respectively. Equivalent damping orifices of 0.042, 0.059 and 0.133 inch diameter were simulated. The analog data show that poppet oscillations are decreased appreciably by employing a 0.133 inch diameter orifice. By decreasing the orifice size even further, the poppet oscillations actually start to increase again since the gas damper is not a pure damping device, but rather a lead/lag device which becomes increasingly spring-like as the orifice gets smaller. Since the addition of this gas damping orifice of 0.133 inches in diameter did not complicate the baseline regulator design in any way it was decided to incorporate this particular feature.

5.1.8   Spring Analysis and Weight Considerations

A review of the baseline component weights indicated that the actuator assembly was by far the heaviest part of the regulator and that, in particular, the reference coil spring contributed a major portion of this weight. Consequently, it was decided to optimize the spring weight as much as possible in an effort to optimize the overall baseline regulator weight. This optimization was performed for each of the four lever ratios and included the analysis of single coil springs, zero twist springs featuring either two coil springs in series with oppositely wound helices or a machined spring featuring two sections with opposed helices. Details of this analysis are presented in Appendix D entitled "Spring Optimization."

To permit the sizing of the springs to fit within the bellows envelope, the bellow characteristics as supplied by the two vendors were plotted as shown in Figure 5-23. The results of the spring optimization are shown in Figures 5-24 and 5-25. The weight optimization concluded that a single coil spring is lighter than two coil springs in series with an opposite helix or a machined spring, for all of the lever ratios under consideration. The actual weight of the single coil spring for lever ratios of 2, 3, and 4 was determined to be relatively constant at approximately 0.85 pounds. The installed height of these springs was also minimum for the single coil spring and showed a gradual increase from 1.5 to 5.3 inches as the lever ratio increased from 1 to 4. Based on these installed heights, the actuator housings required to contain both the bellow assemblies and the coil springs were designed and their weight was determined. A summary of the combined actuator weights for each of the lever ratios is presented in Figure 5-26. From this figure it is evident that the minimum actuator weight is attained at lever ratios of 3 and 4. Since the lever ratio of 3 featured a shorter and therefore more attractive actuator package, it was selected for the final baseline regulator configuration.

60

BELLOWS CHARACTERISTICS
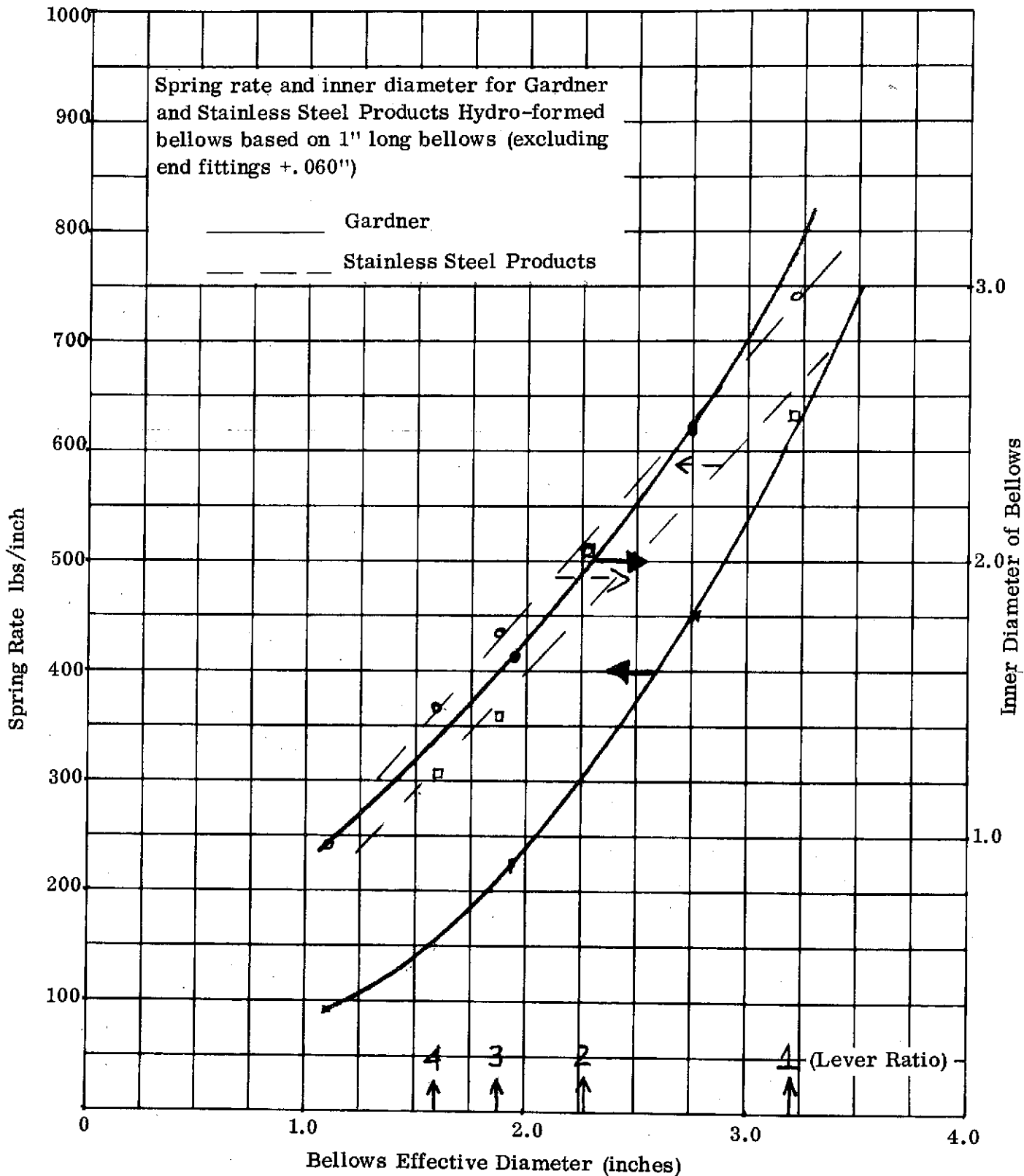
Figure 5-23

SPRING WEIGHT VS LEVER RATIO
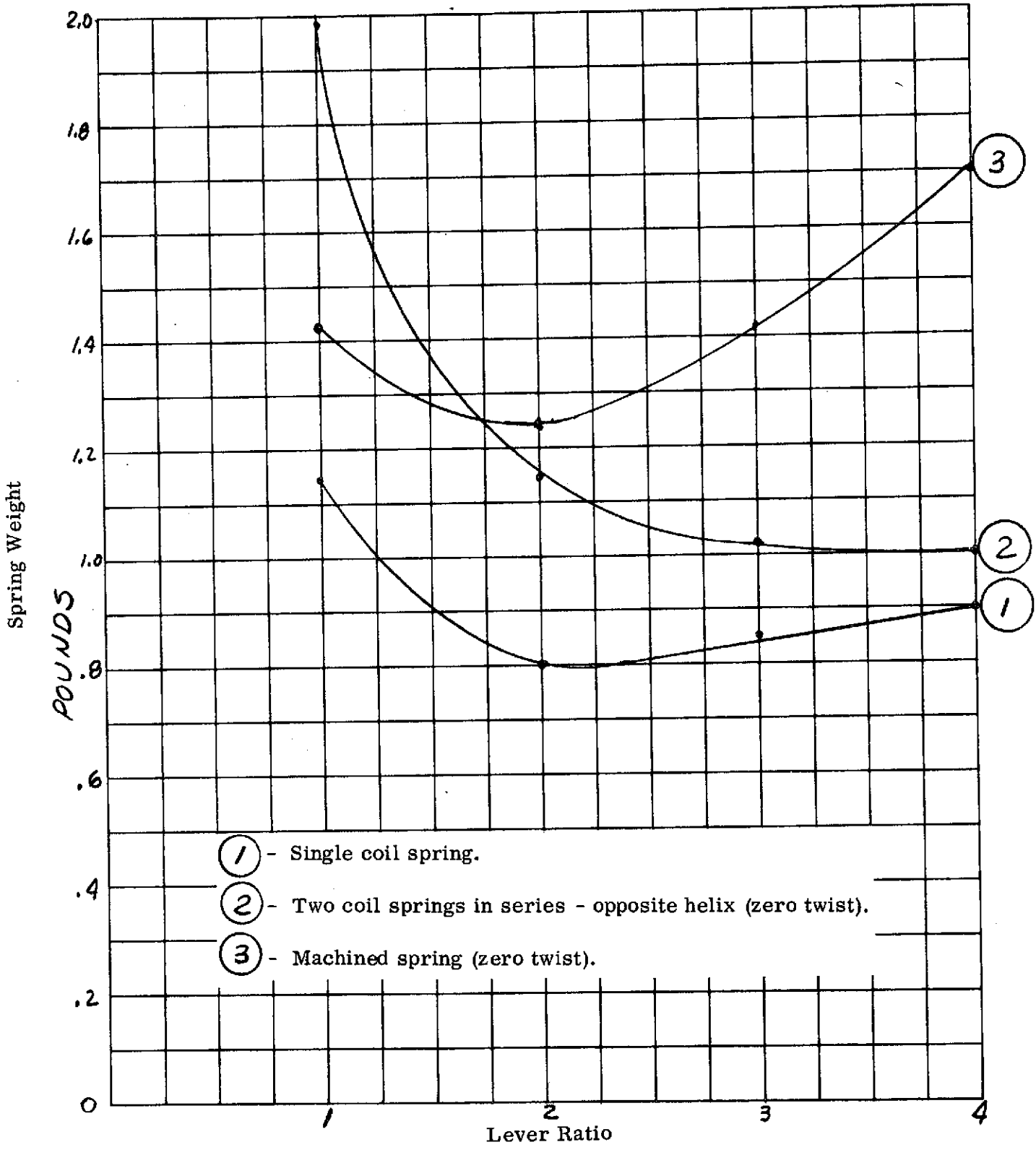
Figure 5-24

LEVER RATIO VS SPRING INSTALLED HEIGHT

① – Single coil spring.

② – Two coil springs in series – opposite helix (zero twist).
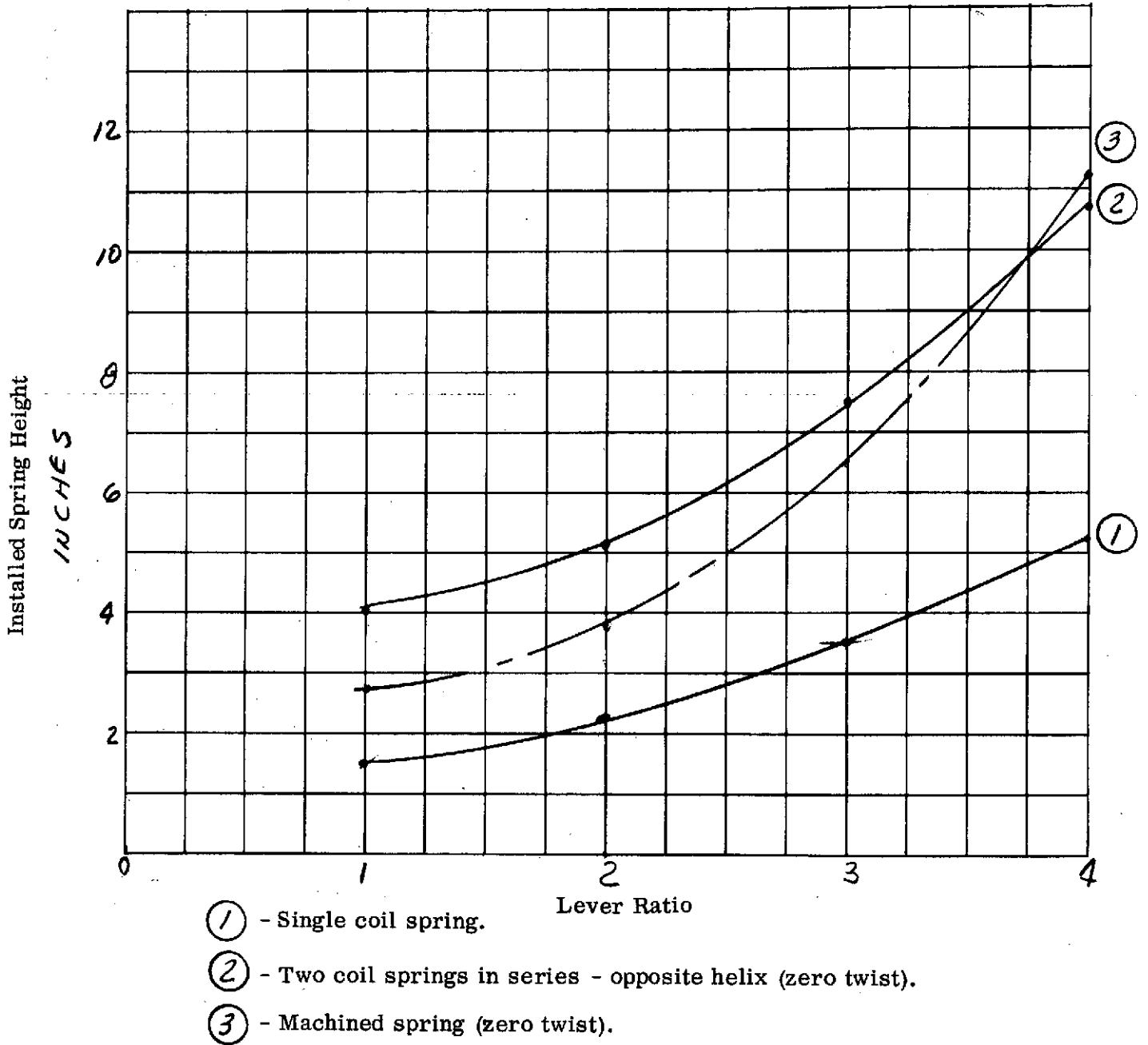
③ – Machined spring (zero twist).

Figure 5-25

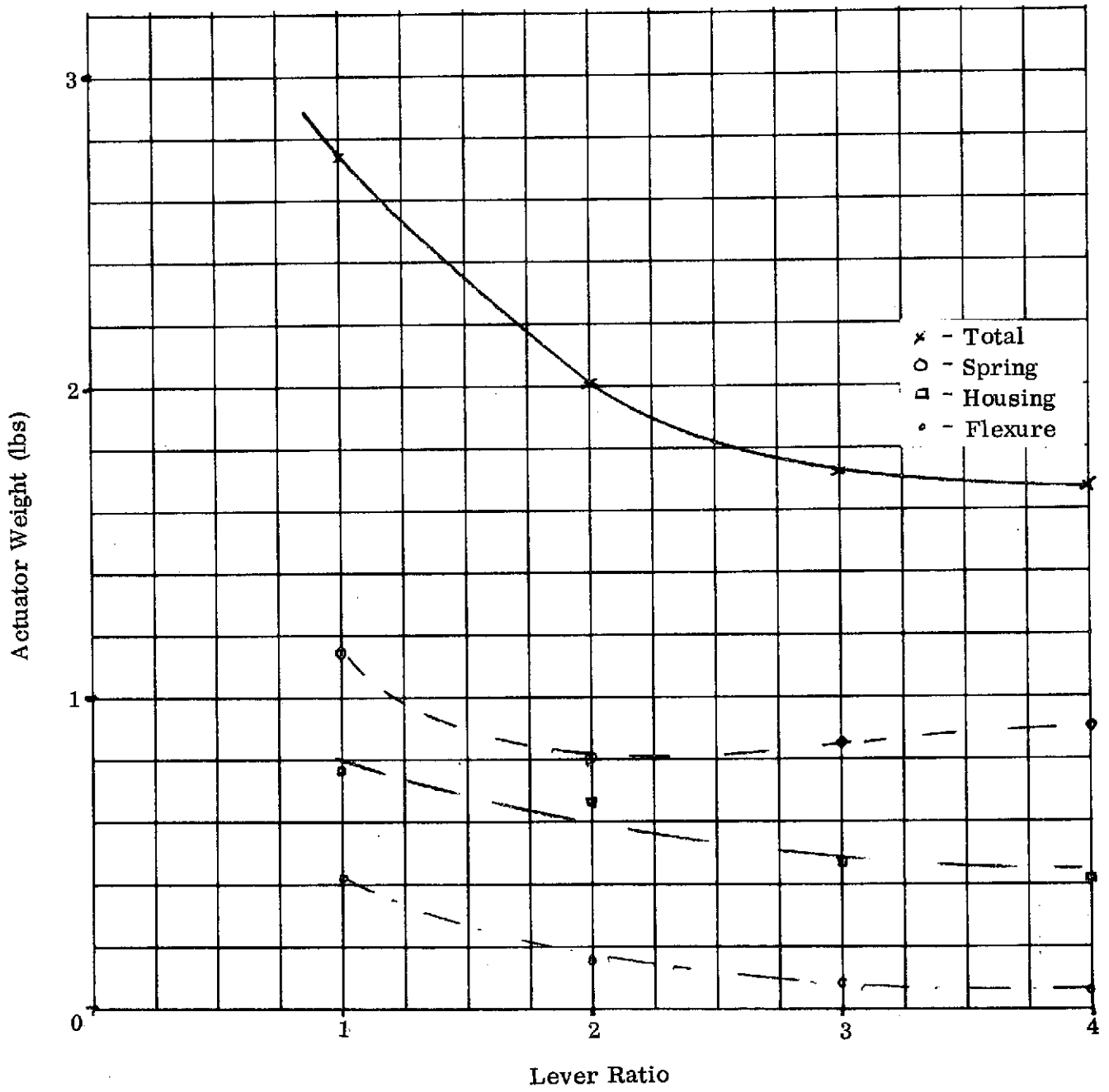# ACTUATOR WEIGHT VS LEVER RATIO

Figure 5-26

5.1.9   Design Layouts

Based upon the analyses presented in the preceding sections, the final spring rate and force budgets were prepared. These are shown in Table 5-VIII. Design layouts of the final baseline regulator utilizing a Gardner bellows and a Stainless Steel Products bellows were prepared and are shown in Figure 5-27. In comparing Figure 5-27 with Figure 5-1, which shows the baseline regulator design as conceived originally, it can be seen that the concept as such did not change appreciably as a result of the analytical optimizations discussed in the preceding sections. Notable differences are the utilization of two nested coil springs in place of the single coil spring, the inclusion of a shaft flexure at the actuator shaft to eliminate potential sliding friction between the actuator shaft and lever arm interface, and some minor configurational changes relating primarily to the assembly techniques to be employed in the fabrication of this baseline regulator. The utilization of two concentric coil springs constituted a further optimization of the weight tradeoff discussed in Section 5.1.8. The weight calculated for the baseline regulator was 2.76 pounds for the regulator featuring a Gardner bellows and 2.30 pounds for the regulator featuring a Stainless Steel Product bellows. The reason for this weight difference is explained in Section 5.1.6. As evident from Figure 5-27, there is also a one-inch difference in overall regulator height between the two regulator versions, that with the Stainless Steel Products bellows being the shorter.

Since the envelope and weight of the baseline regulator featuring the Stainless Steel Products bellows were superior to that of the Gardner bellows regulator, the former was selected as the recommended final baseline design. In assessing the performance margins of the baseline regulator, it was determined that the bellows and spring assemblies possessed the least margin, since both of these components were stressed closes to their yield strength,to minimize regulator weight and envelope. Additional concerns with both of these elements were the relatively thin wall thickness of the bellows (0.008 inch) and the possible degradation of this wall thickness during long-term fluorine exposure, and the possible relaxation of the coil springs over the extreme lifetime requirement. Other performance margins such as available flow area, stress levels in flexures, casings, and other structural components, as well as dimensional changes and physical property changes due to temperature, were considered to be more than adequate. As a result of some of these concerns expressed here, several alternate regulator components were investigated and these investigations are described in the next section.

5.2   ALTERNATE REGULATOR COMPONENTS

The purpose of investigating alternate components for the baseline regulator design was a desire to improve performance margins and reliability. Consequently, those components featuring the least margin were the primary candidates for this investigation. Specific alternate components analyzed included Belleville springs, actuator diaphragms, alternate bellows configurations, redundant bellows, welded versus brazed joints, and force mis-alignment in the actuator.

5.2.1   Belleville Springs

Belleville disc springs or coned disc springs, as they are more generally known, have been employed in numerous spring applications ever since Julian F. Belleville of Paris, France, obtained patents on this device over a century ago. The primary advantage in Belleville springs lies in the ability to shape the load versus deflection curve and to support relatively high loads within a very flat envelope. The primary disadvantage of Belleville

TABLE 5-VIII

SPRING RATE AND FORCE BUDGETS

Poppet Flexure	22 #/in	Reference Force Required		688#
Push Rod Flexure	40 "	Poppet Flexure Force		- 0.5#
Lever Arm Flexure	4 "	Push Rod Flexure Force		- 1.0#
Bellows Flexure	33 "	Bellows Flexure Force		+ 0.5#
Bellows	105 "	Stainless Steel Products Bellows Design:		
Springs	388 "	Bellows Force	+168#	
		Spring Force	+520#	
Lumped Spring Rate	592 "	Gardner Bellows Design:		
		Bellows Force	+ 38#	
		Spring Force	+650#	

FINAL BASELINE REGULATOR DESIGN LAYOUTS

SHORTENED 1.000"

2.75 DIA.

2.75 DIA.

7.63

6.63
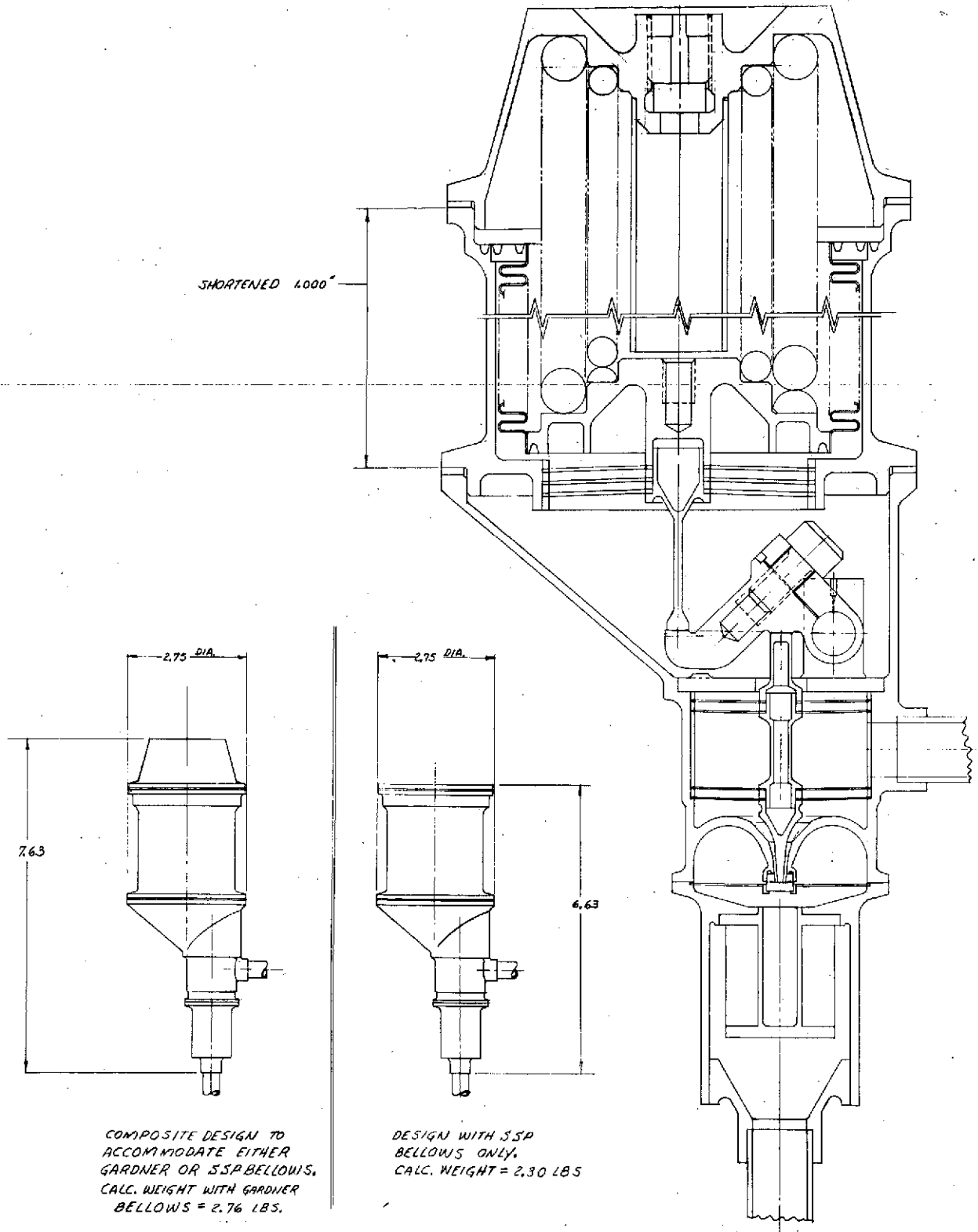
COMPOSITE DESIGN TO
ACCOMMODATE EITHER
GARDNER OR S.S.P. BELLOWS.
CALC. WEIGHT WITH GARDNER
BELLOWS = 2.76 LBS.

DESIGN WITH S.S.P.
BELLOWS ONLY.
CALC. WEIGHT = 2.30 LBS

Figure 5-27

67

springs is their inherent friction characteristics at the contact surfaces. In assessing the applicability of Belleville springs to the baseline regulator design, The Marquardt Company consulted a number of references. References 18 through 21 are the more noteworthy of these. According to Reference 19, the best utilization of the material (getting the most bounce per ounce) is obtained when the ratio of outer diameter to inner diameter is somewhere between 1.7 and 2.2, and the ratio of deflection to thickness is between 0.4 and 0.8. Within this range the spring will yield the greatest resiliency or energy storage capacity and the greatest fatigue life for its weight. Based on this criteria, Belleville washers were sized to fit inside the actuator bellows of the final baseline regulator design. These analyses are presented in Appendix E. To meet the required actuator spring rate it was necessary to employ the Belleville springs in a series stacked configuration rather than to use only a single Belleville spring. A summary of pertinent design data for the Belleville stacks is presented in Table 5-IX. In comparing the weight and height of these Belleville stacks with the weight and height of the two nested coil springs it was concluded that the Bellevilles are not only approximately 50% heavier, but are also taller in height. Thus, on the basis of weight and envelope, the Belleville springs were considered unattractive.

There was, however, a second reason which made Belleville springs even less attractive in comparison to coiled springs and this was the bearing edge inherent friction characteristic of Belleville springs. According to Reference 19, typical friction values for non-lubricated series stacked Belleville springs are approximately ±2 to 3% of axial load. Therefore, since the reference springs are required to provide a minimum force of 520 pounds, the Belleville spring friction characteristics are approximately 10 to 15 pounds. A friction force of this magnitude would degrade regulator accuracy by a factor of roughly 2. In addition, the friction characteristics of Belleville springs over a long time period and as a function of a large number of operating cycles are not very repeatable and could therefore result in considerable regulator setpoint variations.

5.2.2   Diaphragms for the Actuator

Diaphragms were investigated since they generally constitute a simpler flexible structural wall configuration than the bellows. Also it was of interest to determine whether the diaphragm thicknesses would be greater than those of the bellows and would therefore offer greater margin to possible material degradation due to the formation of fluoride during the long exposure period. In addition, their envelope might prove to be more attractive. Four types of diaphragms were investigated and were analyzed to varying degrees. These four configurations are shown in Figure 5-28. Diaphragm analyses are presented in Appendix F.

The design criteria for the diaphragms was the same as that for the bellows except that the diaphragms were not expected to provide the same level of reference force. This means that the diaphragms were required to deflect 0.015 inch for a change in pressure differential of 2.4 psi. The total pressure differential was 240 psi and the approximate effective area of the diaphragm was to be 2.8 square inches.

By treating the diaphragm of the plate type configuration as fixed (i.e., cantilevered) to the support at the outer circumference and also to the central plate, it was determined that (depending on the diaphram diameter) a wall thickness of 0.010 to 0.25 inches could not be exceeded to accomplish the 0.015 inch deflection at a change in pressure differential of 2.4 psi. Even with that constraint, the inherent stresses calculated for this plate configuration turned out to be in excess of 10^7 psi and this concept was therefore considered unfeasible.

TABLE 5-IX

BELLEVILLE SPRINGS SUMMARY

In Combination With Bellows

Belleville Parameter	Stainless Steel Products DO/DI = 2	Gardner DO/DI = 2	Gardner DO/DI = 3
Thickness	.039"	.067"	.069"
Number	38	60	55
Weight	1.20#	1.73#	1.93#
Height	2.83"	6.03"	5.69"
Edge Loading	280K PSI	300K PSI	347K PSI

DIAPHRAGM DESIGN CONCEPTS

Plate

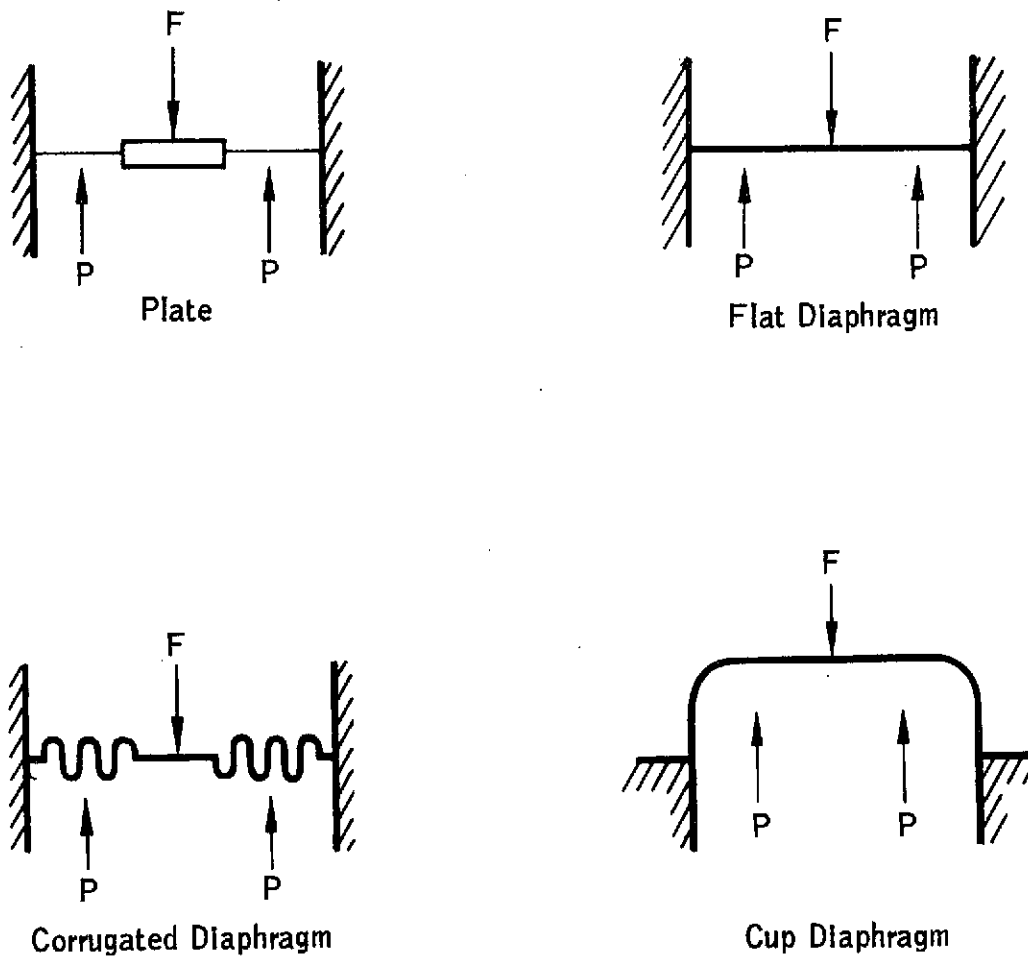Flat Diaphragm

Corrugated Diaphragm

Cup Diaphragm

Figure 5-28

70

Investigation of the corregated diaphragm disclosed that a wall thickness of about 0.007 inches for a 2-inch diameter diaphragm would satisfy the deflection requirement and that the stress level in the diaphragm would be reasonable. However, since the 0.007-inch thickness was actually slightly less than that for the bellows and since the diaphragm in combination with the required coil spring did not result in a weight savings, it was concluded that this concept did not offer a significant advantage. Furthermore, determining the effective diameter for this concept appeared to be difficult because it varied with stroke and the force contact point alignment in the center of the diaphragm where the reference spring load would be applied appeared to be very critical.

The results of the analysis for the flat diaphragm are similar to that of the corregated diaphragm and its performance characteristics are also similar. Like the corregated diaphragm, the flat diaphragm concept appeared feasible but, particularly in light of the difficulty of predicting the effective diameter and criticality of the force contact point, did not appear to offer sufficient advantage over the baseline regulator bellows design. The final design concept reviewed, but not analyzed in detail, was the cup diaphragm. It appeared to have the advantage of featuring a more readily definable effective diameter; however, it still had the inherent disadvantage of extremely critical force contact point. This criticality is evident from the centered load point design shown in Figure 5-29. As evident in this figure the shafts on both sides of the diaphragm must be perfectly aligned and guided to assure a single point contact at the center of each of the shafts. Single point contact in turn means very high local compressive stresses.

In conclusion it was determined that those diaphragm concepts which appear feasible do not offer any appreciable advantages over the bellows design and introduced additional complications such as the uncertainty in the effective diameter and the criticality of the load point. Consequently, further efforts with the diaphragm were discontinued.

5.2.3   Greater Margin Bellows

As discussed previously, it was considered desirable to investigate an alternate bellows configuration offering higher stress margins and greater wall thickness. A minimum allowable wall thickness of 0.010 inch was assumed and several bellows designs featuring this wall thickness were analyzed. The heavier wall thickness generally resulted in higher bellows spring rates, but also in higher load carrying capability of the bellows. This, in turn, required a resizing of the coil springs. Analyses supporting this effort are presented in Appendix G.

A comparison of the bellows originally selected for the baseline regulator design and the new heavy wall bellows characteristics, as well as the resultant overall regulator weight changes are presented in Table 5-X. As mentioned previously, the new bellows featured a 0.010 inch thickness and a greater bellows span (O.D. -I.D.). The greater span permitted a reduction in operating stresses from 132,000 to 115,000 psi. Surprisingly, the new bellows configuration required a significantly lighter spring and resulted in an overall regulator weight savings of 0.73 pound. Thus, the greater margin bellows analyses resulted in significantly more design margin as well as lower weight.

Subsequent to this analysis another concept offering even greater bellows reliability and the elimination of the coil spring altogether was investigated. This concept consisted of the utilization of redundant bellows (two bellows in series) and is discussed in the next section. The redundant bellows assembly was ultimately selected for the final regulator design.

CUP DIAPHRAGM CENTERED LOAD POINT DESIGN
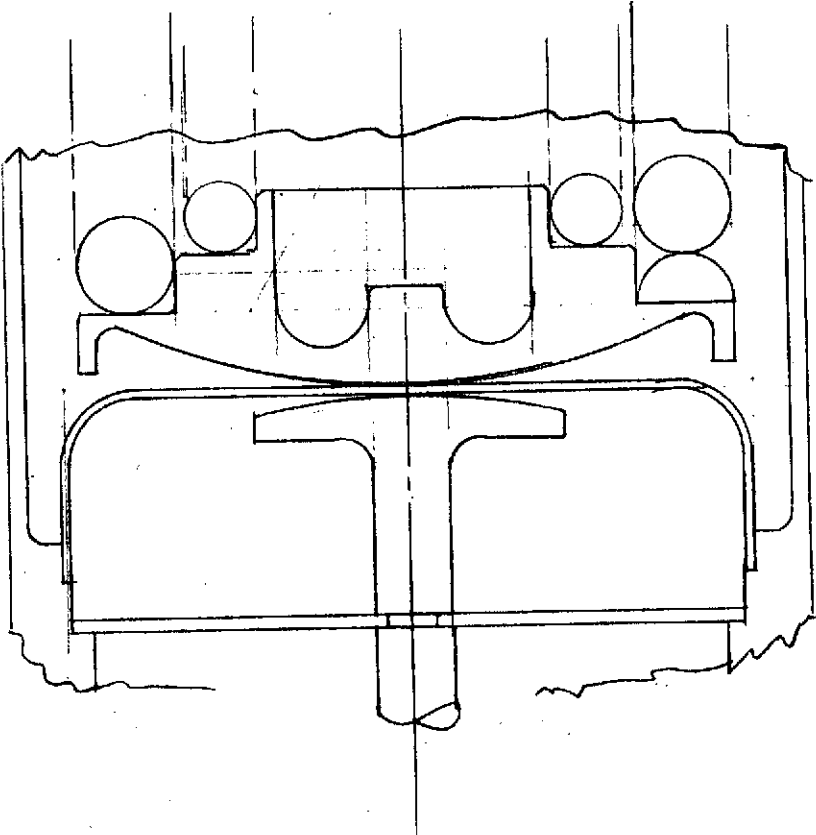
Figure 5-29

TABLE 5-X

GREATER MARGIN BELLOWS CHARACTERISTICS COMPARISON

	Original	New
Bellows thickness	0.006"	0.010"
Spring rate	105#/in	202#/in
Installed height	1.9"	1.9"
Inner diameter	1.74"	1.63"
Outer diameter	2.09"	2.11"
Effective diameter	1.93"	1.89"
Number of convolutions	20	19
Stress level	132K PSI	115K PSI
Bellows weight	0.26#	0.35#
Combined spring weight (2 springs)	0.85#	0.44#
Resulting total regulator weight	2.3#	2.0#

5.2.4 Redundant Bellows

Since the bellows assembly was still considered to be the most critical component in the baseline regulator design, ways of providing redundancy were investigated. Several arrangements were pursued and the two most promising arrangements are shown in Figures 5-30 and 5-31. The principal difference in these two concepts is the location of the gas damping orifice. In one case this orifice is located inside the bellows assembly and utilizes the regulator outlet pressure gas for operation; in the other case, the orifice is located outside the bellows assembly and utilizes prepressurized helium in the isolated actuator cavity. In this latter configuration (Figure 5-31) the gas damping orifice is exposed to pure helium only which eliminates any possibility of condensed propellant, or particulate contaminant in the pressurant or propellant from affecting this orifice. However, the regulator utilizing external damping is slightly heavier (3.02 pounds versus 2.84 pounds) and also slightly longer (9.83 inches versus 9.20 inches). in either case the pressurization of the actuator cavity surrounding the bellows was considered more desirable than leaving this cavity unpressurized, since the primary bellows (shown extended on the side of the push rod) was under these circumstances operating a zero pressure differential and the secondary bellows (shown in compression) was operating under external pressure. Utilization of bellows pressurized externally is considered a preferred design practice to internal pressurization since it eliminates the potential problems associated with bellows squirm.

Several design iterations took place in arriving at the final redundant bellows configuration. Bellows characteristics for this configuration are shown in Table 5-XI. The stress analysis supporting this configuration is presented in Appendix H. As noted in Table 5-XI, the material thickness of the redundant bellows is 0.012 inch which is an improvement over the 0.010 inch of the greater margin single bellows discussed in the preceding section; however, the operating stresses of the redundant bellows as determined in Appendix H are 137,600 psi, which is significantly greater than that of the greater margin single bellows. Nevertheless, the fact that the bellows arrangement as presented in Figures 5-30 and 5-31 offers full redundancy, is considered an improvement in overall actuator reliability compared to the greater margin single bellows.

5.2.5 Welded and Brazed Joints

The baseline regulator design features all welded or brazed construction and the elimination of all static seals. Because it is required that critical brazed and welded joints be verified to be structurally sound and leakproof, the design was reviewed for inspectable configuration. Experience in general has shown that welded joints tend to seal more reliably, particularly if it is possible to utilize X-ray inspection or an equivalent technique.

The review of joining techniques for the baseline regulator resulted in the conclusion that brazing should be used for the flexure cartridges and for the ceramic/Inco 718 joints at the poppet/seat interface. All other joints should be electron beam welded and arranged to permit the greatest possible X-ray analysis. The reason for selecting brazing for the flexures was the fact that the flexures are not required to provide a pressure seal and also because the braze would readily fill the crevices and thus minimize potential crevice corrosion. Brazing of the poppet and seat inserts to their support structure was considered necessary since the feasibility of welding ceramics to metallic structurs is beyond the current state-of-the-art.

PRESSURE REGULATOR

REDUNDANT BELLOWS ACTUATED, INTERNAL DAMPING
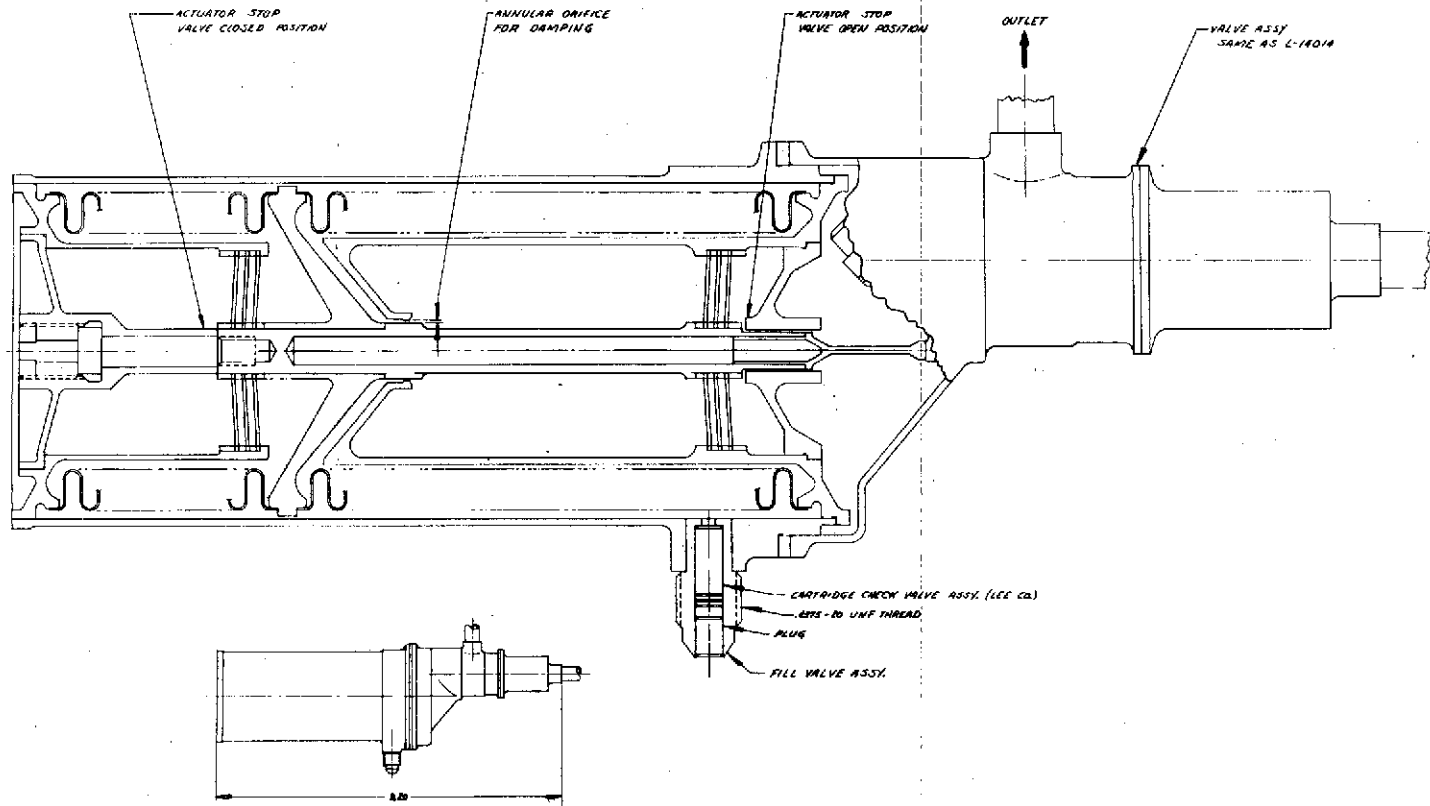
ACTUATOR STOP
VALVE CLOSED POSITION

ANNULAR ORIFICE
FOR DAMPING

ACTUATOR STOP
VALVE OPEN POSITION

OUTLET

VALVE ASSY
SAME AS L-14014

CARTRIDGE CHECK VALVE ASSY. (LEE Co.)

.8775 - 20 UNF THREAD

PLUG

FILL VALVE ASSY.

Figure 5-30

75

PRESSURE REGULATOR

REDUNDANT BELLOWS ACTUATED, EXTERNAL DAMPING

ACTUATOR STOP
VALVE CLOSED POSITION

ANNULAR ORIFICE
FOR DAMPING

ACTUATOR STOP
VALVE OPEN POSITION

OUTLET

VALVE ASSY.
SAME AS L-14014

FILL VALVE ASSY.
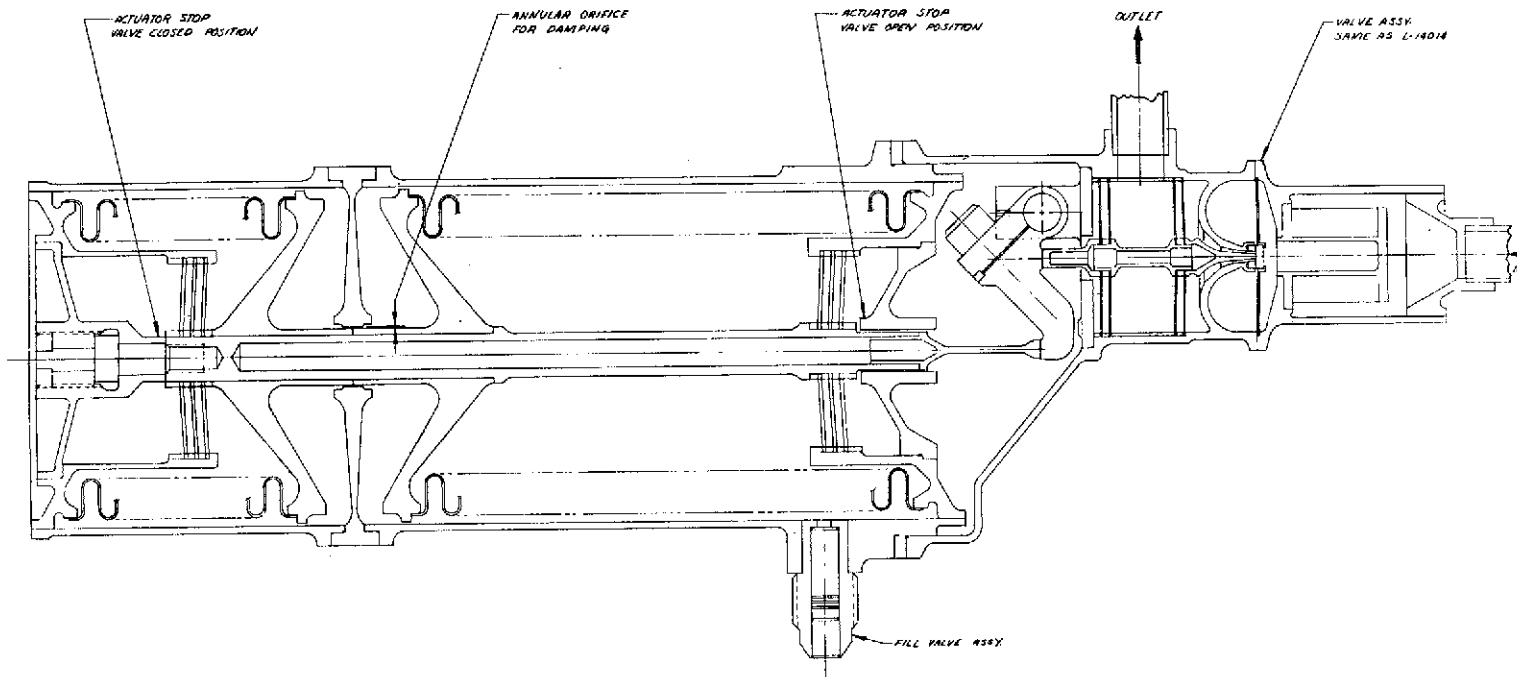
Figure 5-31

TABLE 5-XI

FINAL REDUNDANT BELLOWS CHARACTERISTICS

Effective Area	2.74 in^2
Spring Rate	696 lbs/in
Preload	657 lbs
Outer Diameter	2.11 in
Inner Diameter	1.56 in
Span	0.26 in
Material Thickness	0.012 in
Pitch	0.181 in
Free Length Per Bellows	2.28 in
Maximum Allowable Compression Per Bellows	1.023 in
Nominal Compression Per Bellows	0.94 in
Number of Convolutions Per Bellows	13
Squirm Pressure	618 psi
Weight	0.166 lbs

5.2.6   Coil Spring Eccentricity and Torsional Effects

During a review of the baseline regulator concept as shown in Figure 5-27, some concern was expressed regarding the possibility of coil spring force eccentricity and its effect upon regulator performance. Consequently, the maximum force vector eccentricities of both the outer and inner springs due to machining tolerances as well as inherent spring characteristics were determined to be 0.072 and 0.037 inches, respectively. This resulted in maximum moments of 16.5 and 4.5 inch pounds, respectively. These moments can be easily resisted by the flexures.

An analysis of the resisting moment of the combined bellows, flexure, and spring arrangement was made and is presented in Appendix I. This analysis disclosed the existing moment to be 4 inch pounds per degree. Thus, the maximum column flexure bending that could occur was determined to be 3 degrees. This amount of bending was considered excessive and it was therefore recommended to include a second guidance flexure at the top of the actuator in a manner similar to that shown for the redundant bellows actuator in Figure 5-31.

5.3   FINAL REGULATOR DESIGN

The final regulator design resulted from the initial conceptual design, analysis, and optimization as discussed in Section 5.1 of this report and the subsequent investigation of alternate regulator components as discussed in Section 5.2 of this report. The analytical models for the final regulator design were also updated to include the experimental data obtained during this program and described in Section 6. entitled "Work Principles Proof." This final regulator design was subsequently employed in the propellant feed system dynamic modeling and the propulsion system dynamic modeling to substantiate that the regulator's performance characteristics were sufficient to attain the desired minimum pressurant loadings and minimum residual propellants.

5.3.1   Configuration and Operational Description

The final regulator configuration is presented in Figure 5-32. The regulator is completely friction free and employs only solid damping and gas damping. It is of an entirely metallic/ceramic construction and utilizes Inco 718 throughout except for the use of Type 304L stainless steel in the screen and stacked disc filter elements, and the use of Tungsten Carbide for the poppet and seat interfaces. This choice of materials of construction and the elimination of plastics and elastomers has resulted in a component featuring wide temperature capability (-420°F to high temperatures which are limited only by propellant compatibility considerations above at least 300°F), fluorine and hydrazine compatibility, and long operational life.

As shown in Figure 5-32, the final regulator features redundant bellows which effectively eliminate the need for reference springs and result in a very simple and highly reliable design. The two identical bellows are installed in such a manner (one in compression and the other in tension) as to provide the reference force which is equal to the nominal regulato outlet pressure times the bellows effective area. The moving ends of the two bellows are attached to the actuator shaft which, in turn, is guided by means of two flexure assemblies. A pneumatic damping orifice has been installed at the actuator shaft between the two bellows

78

PRESSURE REGULATOR - REDUNDANT BELLOWS ACTUATED, EXTERNAL DAMPING

─── 9.83 In. ───

OUTLET

INLET

ACTUATOR STOP IN OPEN POSITION

ACTUATOR STOP IN CLOSED POSITION

FILL VALVE ASSEMBLY

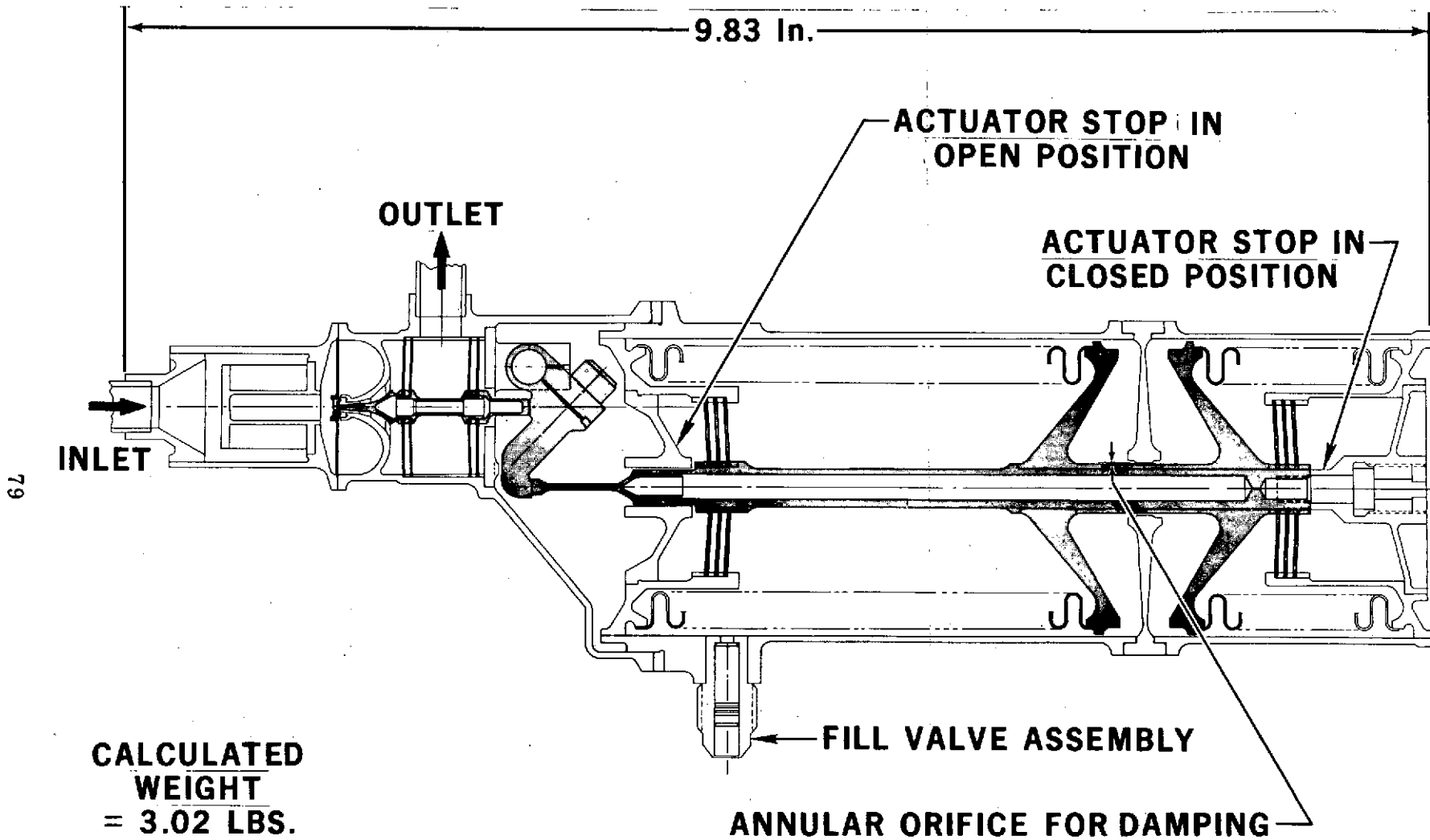ANNULAR ORIFICE FOR DAMPING

CALCULATED WEIGHT = 3.02 LBS.

Figure 5-32

assemblies such that the motion of the actuator causes a pumping action across the damping orifice. The cavity containing the damping orifice will be prepressurized with gaseous helium through a fill valve assembly to the same pressure as the nominal regulator outlet pressure (240 psia). Stops are incorporated in the actuator to prevent the poppet push rod from separating from the poppet by more than 0.003 inch and to limit the poppet stroke to 0.010 inch. A small screen filter is included in the reference cavity to minimize the introduction of contamination from the outside of the regulator into that cavity. The end of the actuator shaft applying the load to the lever arm has been slimmed down to allow a minimum amount of bending of the actuator shaft so that the shaft can follow the lever arm during regulator motion without resulting in sliding friction.

The lever arm features a ratio of 3.0 and utilizes a Bendix pivot flexure to eliminate all sliding friction. The lever arm serves to transmit the force from the actuator to the push rod assembly and to minimize reference force element (the bellows in this case) size. The push rod is guided by two small flexure assemblies and serves to apply the actuator load to the poppet. The push rod flexures are installed such as to always apply a minimum load of 0.5 pound to the push rod in the direction against the lever arm. In this manner, the push rod never separates from the lever arm and because of the stiff radial spring rates of the flexure assemblies also never incurs any sliding friction at its contact point with the lever arm. The push rod travel is controlled by the actuator travel.

The poppet/seat interface is of a flat design employing a 0.008 inch wide annular sealing surface land in the seat. The seat support structure has been designed with flexibility to minimize poppet impact loads at the sealing surface. The poppet is guided by means of a single plate flexure which serves as a return spring as well as a self-alignment device to assure effective sealing at all times. A stacked disc type fileter is installed upstream of the poppet/seat interface to prevent excessive contamination from entering the regulator.

The regulator operating principle is similar to that of other pressure regulators utilizing reference spring forces. the "null" position of the regulator is determined by the equalizing of the forces resulting from the outlet pressure acting on the actuator effective area plus the inlet pressure acting on the unbalanced portion of the poppet, and the reference force built into the precompressed bellows assemblies. If the nominal outlet pressure decreases, the pressure force acting on the bellows actuator also decreases and is overcome by the precompression force of the bellows. This causes the actuator shaft assembly and, in turn, the poppet to move in a direction so as to open the poppet. An open poppet results in flow into the regulator outlet and a corresponding increase in regulator outlet pressure. The exact regulator outlet pressure during flowing conditions is affected by how far the poppet has to be opened to re-establish a null condition because the loads exerted by the spring-like components in the assembly vary with stroke(i.e. have spring rate) and the fluid flows which also varies with stroke and pressure drop across the unit, exerts aerodynamic forces on the actuator parts. Regulator lock-up occurs when the downstream pressure exceeds the nominal regulating pressure and causes the actuator assembly to retract such that the push rod is no longer in contact with the poppet. Under this condition the pressure differential across the poppet, plus the poppet guidance flexure force, provide the necessary sealing closure forces to meet the leakage requirements.

The bellows reference force required in the final regulator is 657 pounds. The spring rates for the various spring elements in the regulator assembly are listed below:

Redundant Bellows Regulator L14020

Spring Rate Budget:

Poppet Flexure	5 lb/in
Push Rod Flexure	22 lb/in
Lever Arm Flexure	4 lb/in
Bellows Flexures	36 lb/in
Bellows Assembly	696 lb/in
Lumped Spring Rate	763 lb/in

5.3.2 Performance Characteristics

A summary of the performance characteristics of the final regulator design is presented in Table 5-XII. These performance characteristics fully meet the performance requirements originally set forth in the design specifications for the pressure regulating components program. Probably the most important regulator performance characteristic is its small variation in performance (outlet pressure regulation) over the range of operating conditions. This may be observed from the droop characteristics presented in Figure 5-33. This figure presents regulator outlet pressure at five regulator inlet pressures for the maximum temperature range, at the nominal volumetric flowrate, of the flox regulator. It is interesting to note that over most of the inlet pressure range (from 4000 to 1000 psi), and therefore during most of the mission, the regulator performance is extremely constant, being within 1 psi; however, between 1000 psia nad the lowest inlet pressure of 400 psia, significant variation does occur, such that the overall regulator accuracy, over the range of operating conditions, is ± 2.4 psi. As mentioned previously, the overall regulator weight was determined to be 3.02 pounds.

5.3.3 Dynamic Modeling

The final regulator, as shown in Figure 5-32, was dynamically analyzed to verify stable regulator operation during step response, motor start, steady state, and stop operating modes; and a sensitivity study was performed to determine the effects of ± 20% variations of the nominal spring rate and bellows diameter, independently, as well as the effects of ± 50% variations in the nominal damping orifice area. In addition, the dynamic behavior of the regulator when operating at minimum gas temperatures of 102°R for the flox system and 430.9°R for the MMH system was evaluated. Unlike the dynamic simulations which were performed during the baseline regulator studies with the FLOX system flow rates and volumes, it was decided to perform the final regulator dynamic simulations for the MMH system since this sytem featured the fastest transients because of smallest ullage and would therefore most readily exhibit pressure oscillations. Therefore, all the analog data presented in this section is for the MMH system with the exception of the one motor firing featuring the minimum gas temperature for the FLOX system (102°R).

The regulator dynamic performance math model differed from the model used in the baseline regulator tradeoff and screening studies in several factors:

- Final updated bellows area, spring rate, and masses from the mechanical design studies.

- Incorporation of experimental flow force/stroke and C_D test data.

- Double bellows gas damper.

TABLE 5-XII

FINAL REGULATOR PERFORMANCE CHARACTERISTICS

INLET PRESSURE .... 4000–400 PSIA

OUTLET PRESSURE .... 240 $\pm$ 2.4 PSIA

LOCK UP PRESSURE .... 252 PSIA, MAXIMUM

INTERNAL LEAKAGE .... 45 SCC/HR HELIUM MAXIMUM

FLOW CAPABILITY .... 0.75 FT.^{3}/MIN HELIUM
AT 150 °R

LIFE .... 10 YEARS AND 100,000
CYCLES, ZERO MAINTENANCE

MATERIAL COMPATABILITY WITH .... FLOX (82% F_2, 18% O_2
F_2, N_2H_4, MMH, HELIUM

TEMPERATURE OPERATING RANGE .... 142 – 158 °R OXIDIZER
503 – 557 °R FUEL

INTEGRAL FILTER .... 10 μ ABSOLUTE RATING

DROOP CHARACTERISTICS
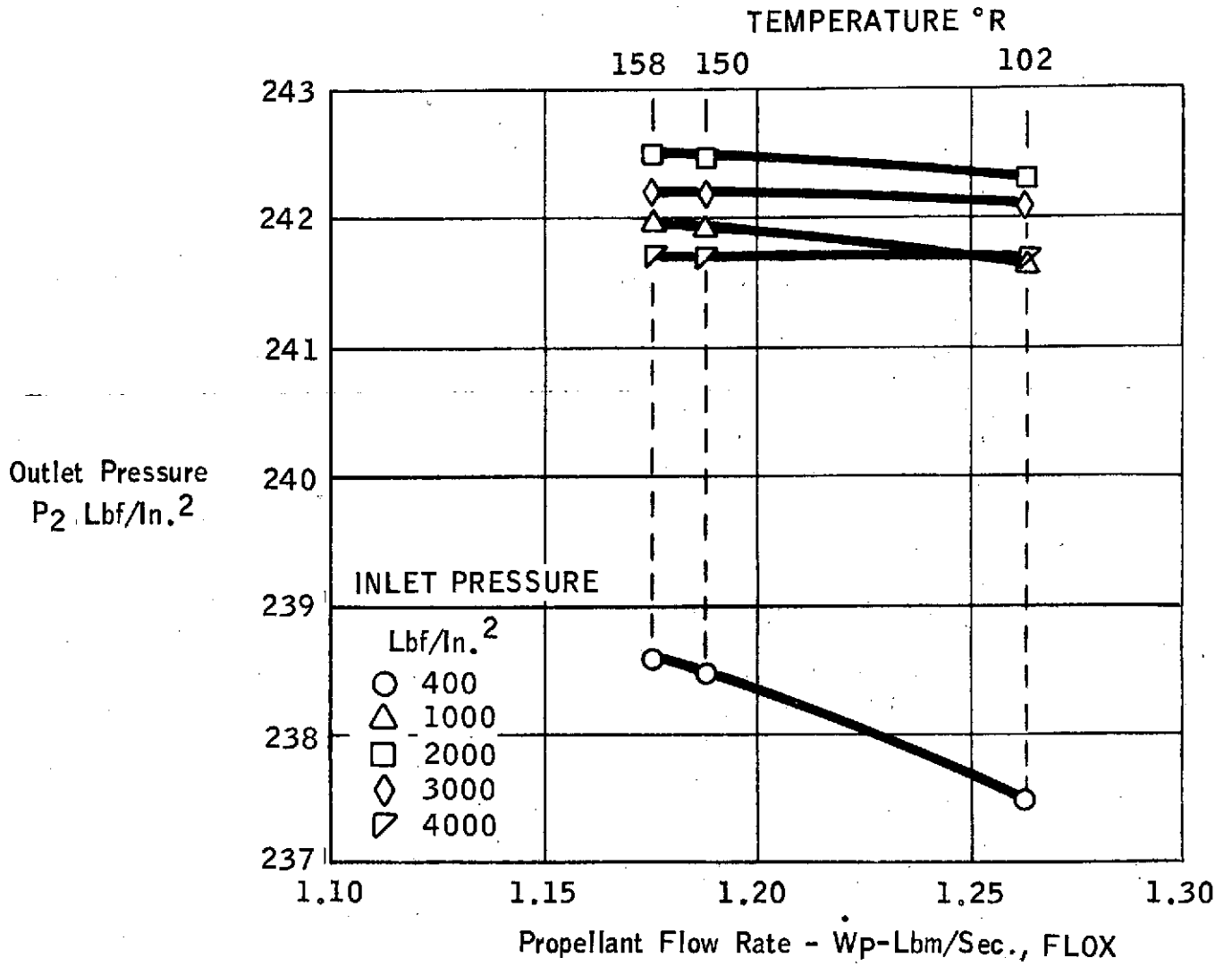
Space Storable Propulsion System Regulator

Figure 5-33

83

The physical equations are summarized in Tabe 5-XIII describing the regulator force balance dynamics, component masses, helium flowrate, propellant tank gas dynamics, and gas damper functions. The force balance dynamics include the bellows, spring preload, spring rate, solid damping, flow, and gas damping forces. The flow force relationship was modified from the original characteristics which were based on published data, in accordance with the experimental results of the force/stroke tests. The mass budget accounts for the inertial effects of the various components including the bellows assembly, bellows flexure, bellows end plate, lever, poppet, push rod, poppet flexure, and push rod flexure. The helium flowrate description through the poppet/seat interface uses compressible flow relationships including the empirical discharge coefficient as derived from the C_D test data. The propellant tank gas dynamics account for the effects of helium flow into the ullage and propellant flow out of the tank. The gas damping physical equations describe the effects and relationships of gas flow between the two gas damper cavities and the volume change in the cavities due to bellows motion.

The regulator math model is shown schematically in Figure 5-34 as programmed on the electronic analog computer. In addition to the physical equations described in Table 5-XIII, the computer setup also provides for open and closed high spring rate stops on bellows travel, clearance between the bellows and lever when the poppet is in the closed position, and a provision for turning propellant flowrate on and off. The potentiometer schedule used in the computer setup is shown in Table 5-XIV defining the physical parameters. The discharge coefficient math model as derived from the poppet/seat interface tests is shown in Figure 5-35. The model mechanizes the empirical function for C_D shown in Table 5-XIII and was used to produce the results shown in Figure 5-36.

The final regulator data inputs that were utilized in the dynamic simulation are presented in Table 5-XV. A summary of the analog data obtained is presented in Figures 5-37 through 5-46. The technique by which a step response is obtained on the analog was previously discussed in Section 5.1.7. As evident from Figure 5-37 and from Figure 5-38, there are no noticeable pressure oscillations or appreciable poppet motion during typical motor firings in the time scale of interest. The poppet positions corresponding to nominal flow conditions are not achieved in the portion of the printout shown because the system time constant even for the minimum volume of 0.59 cubic ft is 1.45 seconds. Thus, typical motor start, steady state, and stop simulation data for the sensitivity studies presented in Figures 5-39 through 5-45 are equally uninteresting and are therefore not included. The step response data under nominal conditions shows two or three oscillations before the steady poppet position is reached and no noticeable pressure oscillations in the tank, either at the fastest system response condition (4000 psi inlet pressure and 0.59 cubic ft ullage volume) or the slowest system response condition (400 psi inlet pressure and 733 cubic ft ullage volume).

Figures 5-39 and 5-40 show the regulator dynamic behavior when the nominal spring rate is increased or decreased by 20%, respectively. No significant changes in dynamic behavior were observed. Figures 5-41 and 5-42 show the regulator dynamic behavior when the bellows diameter is increased or decreased by 20%. A slight increase in poppet oscillation is noted with the 20% larger bellows diameter; however, the regulator is still completely stable.

Figures 5-43 and 5-44 present the analog traces for the final regulator configuration

ANALOG COMPUTER WIRING DIAGRAM - PROPELLANT FEED SYSTEM
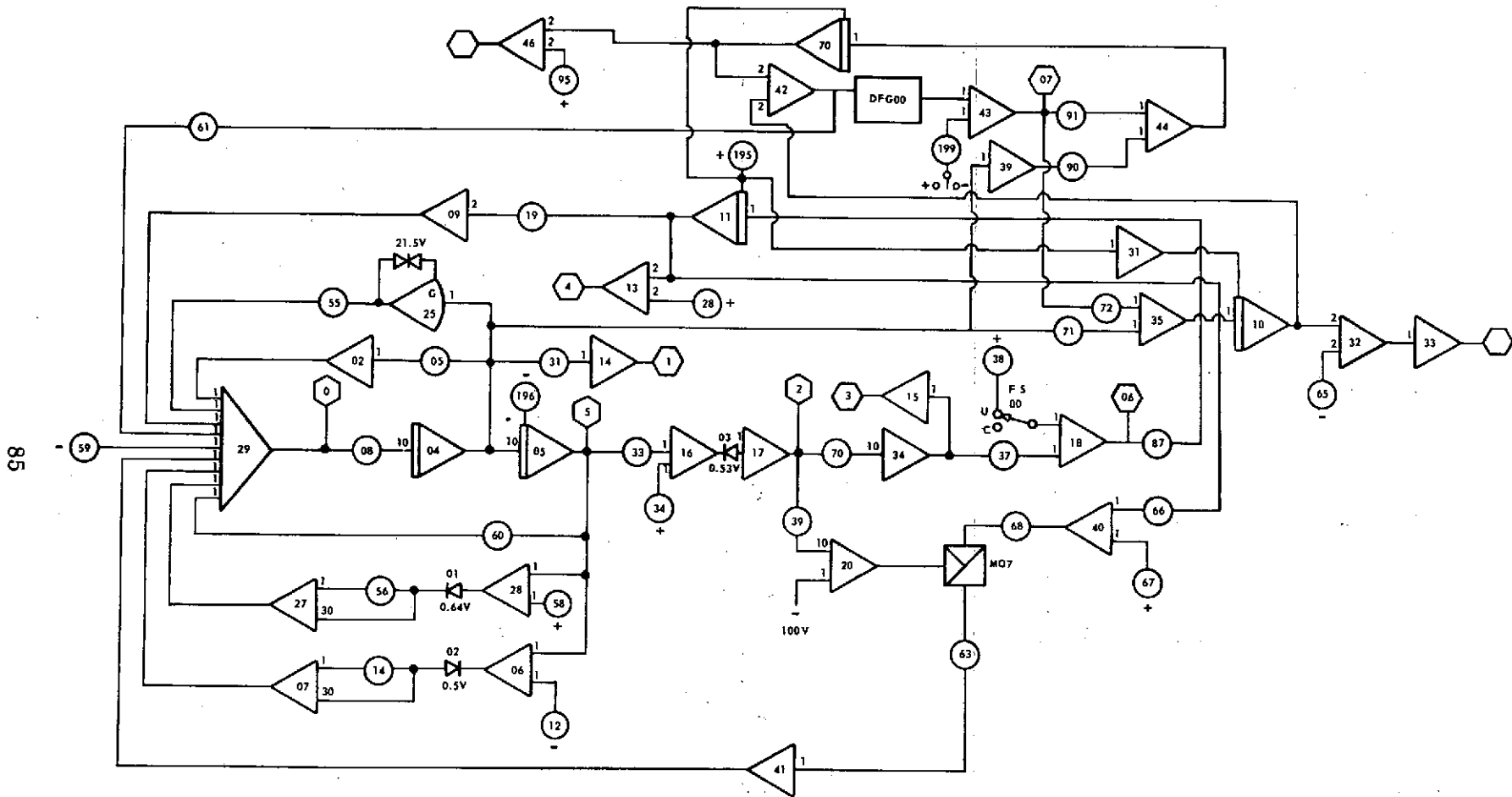
Figure 5-34

A72-11-370-54

DISCHARGE COEFFICIENT MATH MODEL
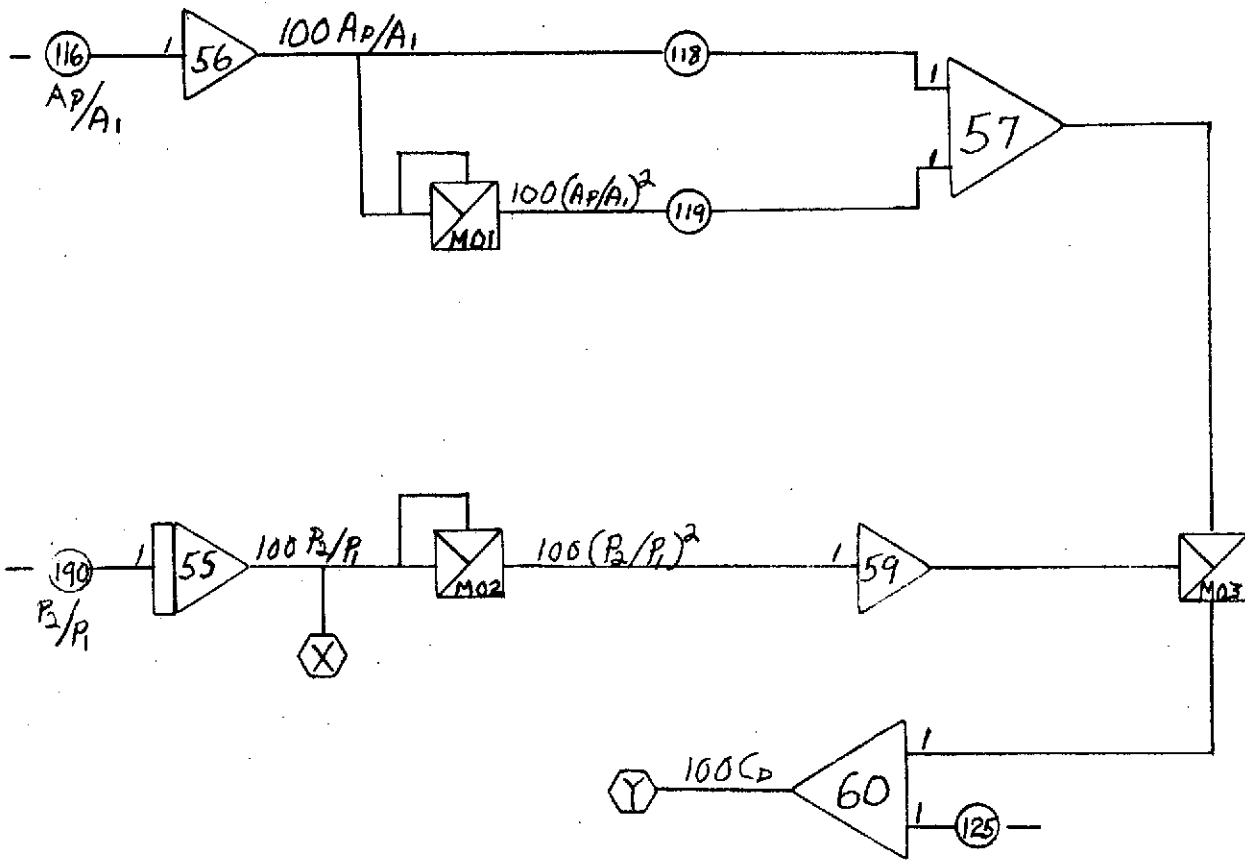
Figure 5-35

EXPERIMENTAL DISCHARGE COEFFICIENT VERSUS PRESSURE RATIO
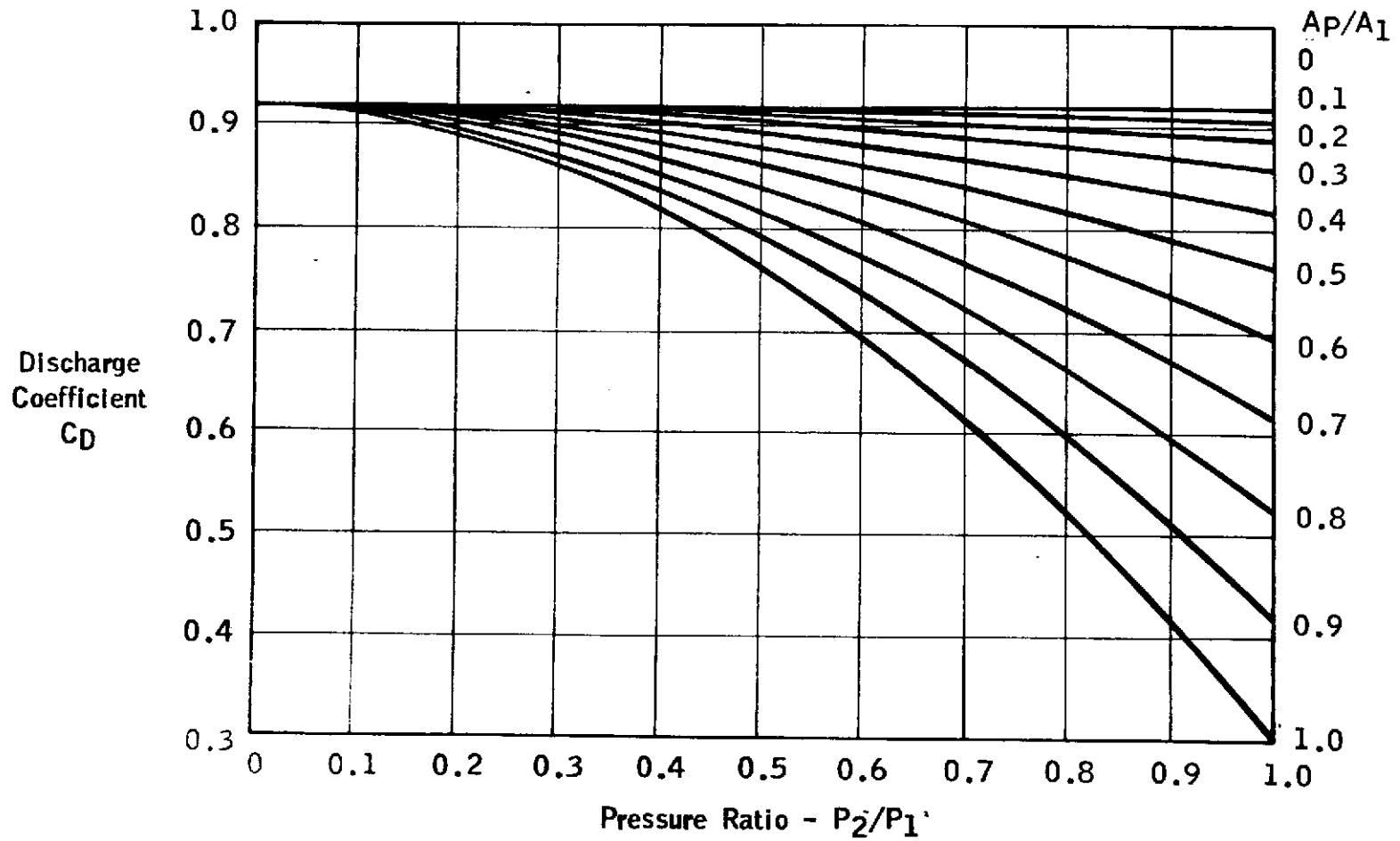
Figure 5-36

STEP RESPONSE, MOTOR START, STEADY STATE, AND STOP

MMH SYSTEM $P_1 400$ $V_T = 7.33 \, \text{ft}^3$
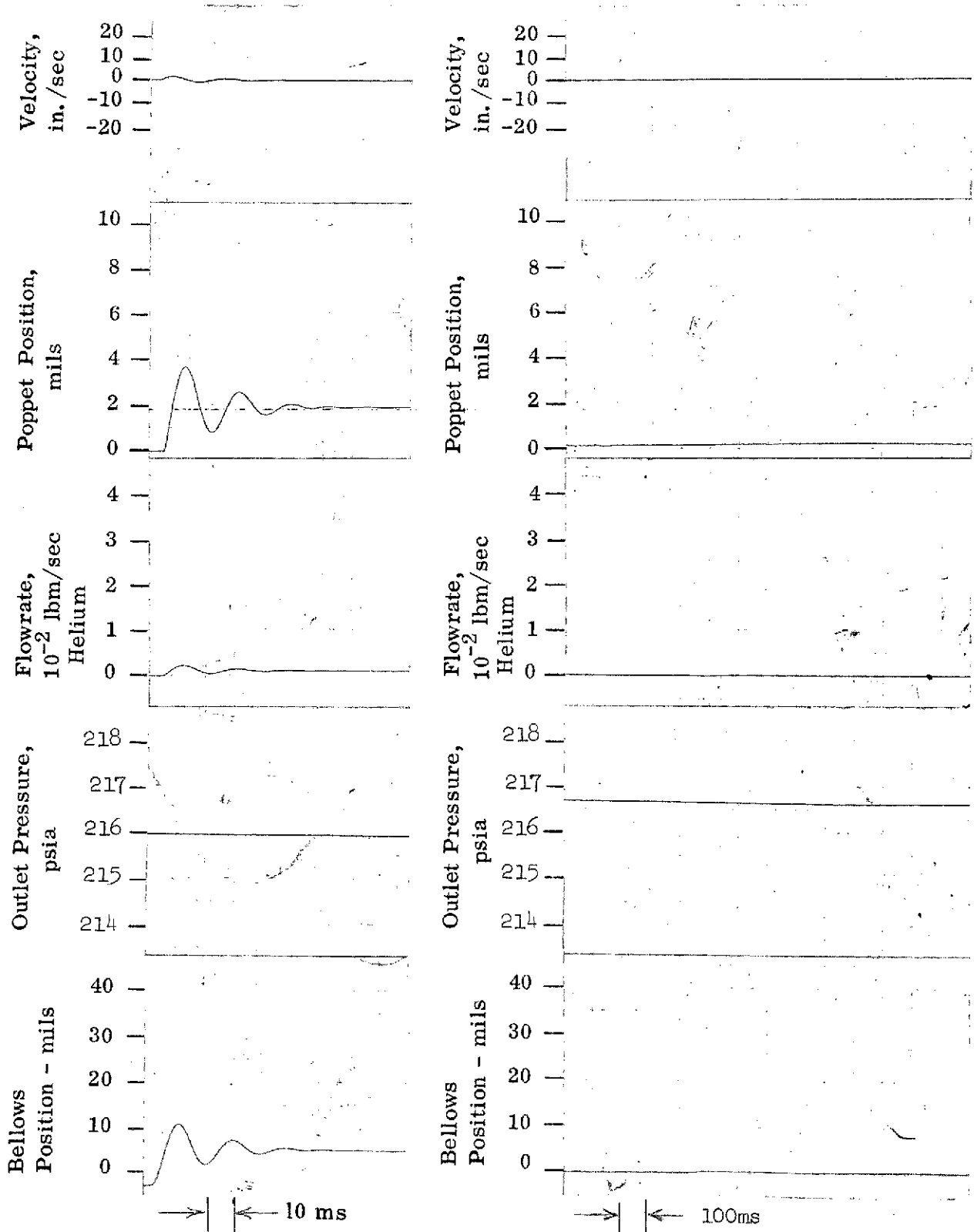
Figure 5-37 Analog Data – Final Regulator

88

STEP RESPONSE, MOTOR START, STEADY STATE, AND STOP

MMH SYSTEM $P_1 = 4000$ $V_T = 0.59$ FT.^{3}
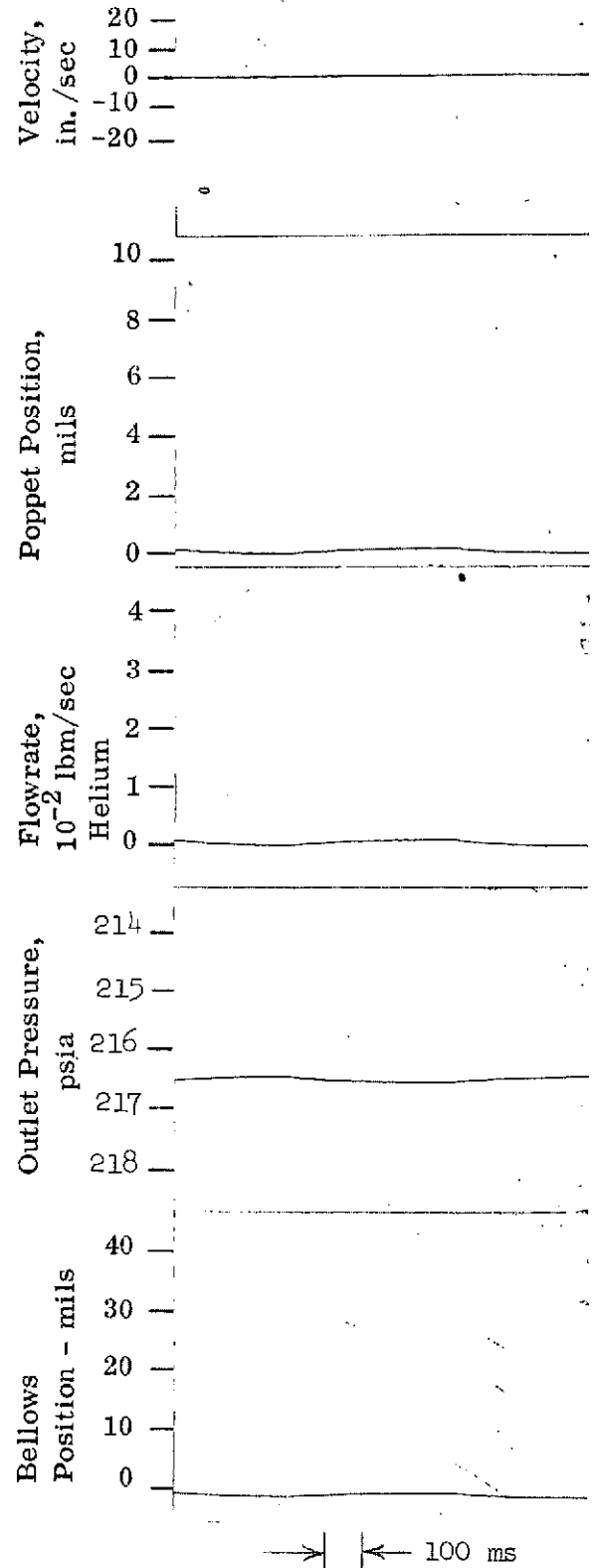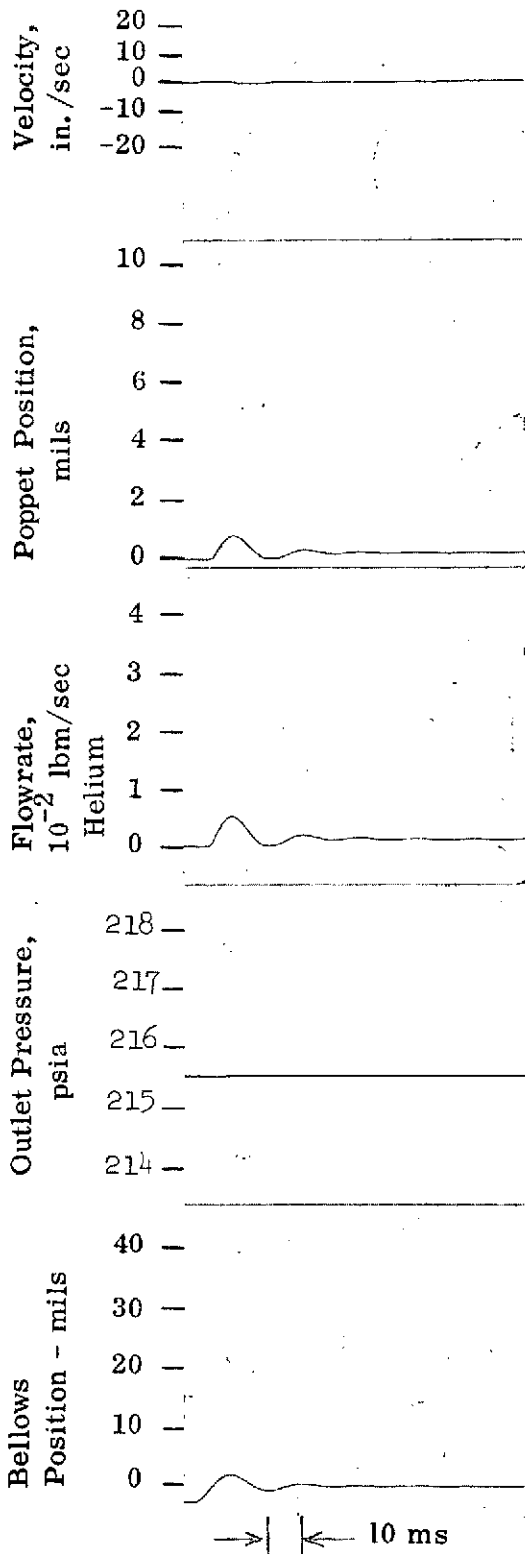
Figure 5-38 Analog Data - Final Regulator

STEP RESPONSE
+20% K_s, MMH SYSTEM

P_1 = 400 PSI V_T = 7.33 FT.^{3} P_1 = 4000 PSI V_T = 0.59 FT.^{3}
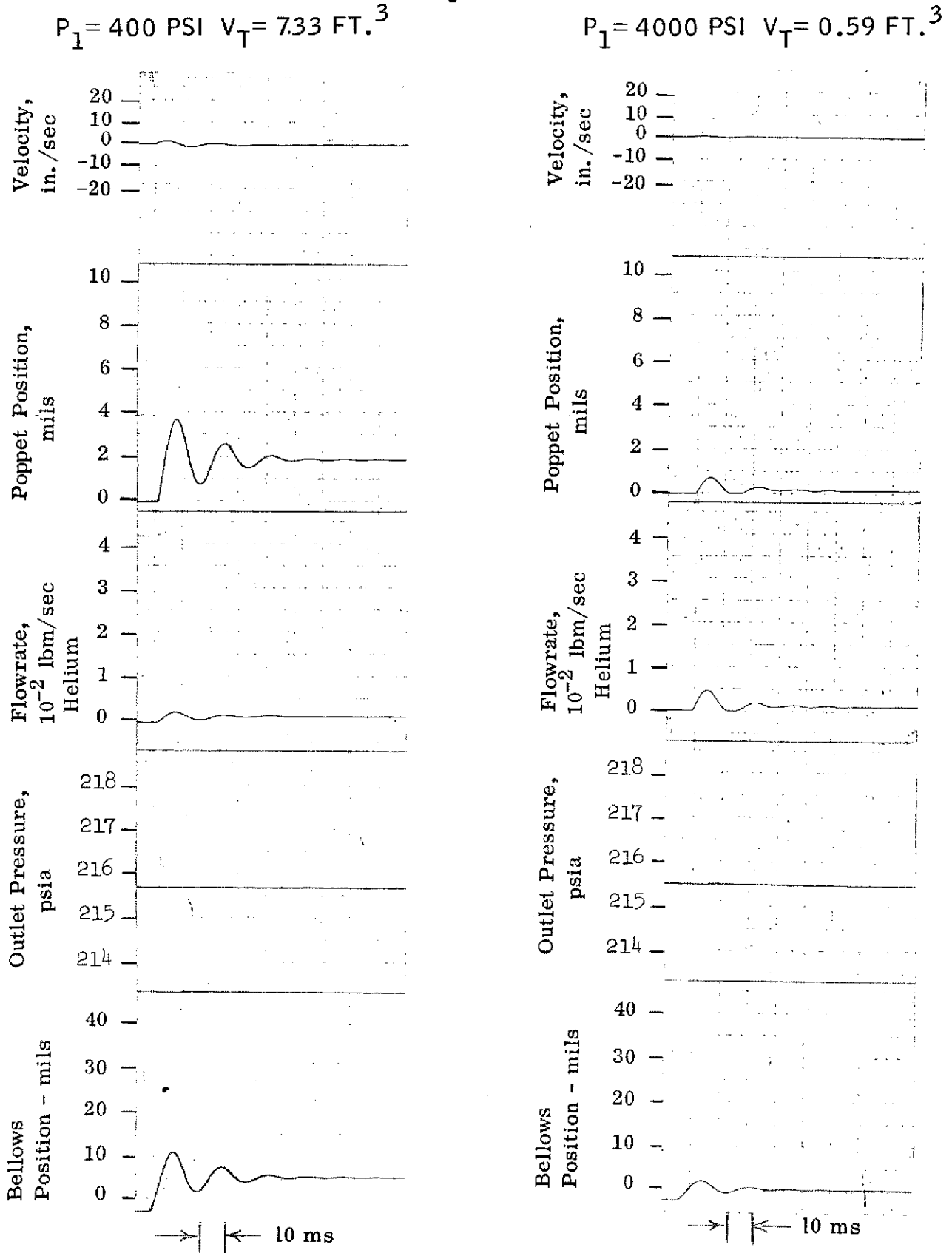
Figure 5-39 Analog Data – Final Regulator

90

STEP RESPONSE
-20% K_s, MMH SYSTEM

$P_1 = 400$ PSI, $V_T = 7.33$ ft^3 $P_1 = 4000$ PSI - V_T 0.59 FT^3
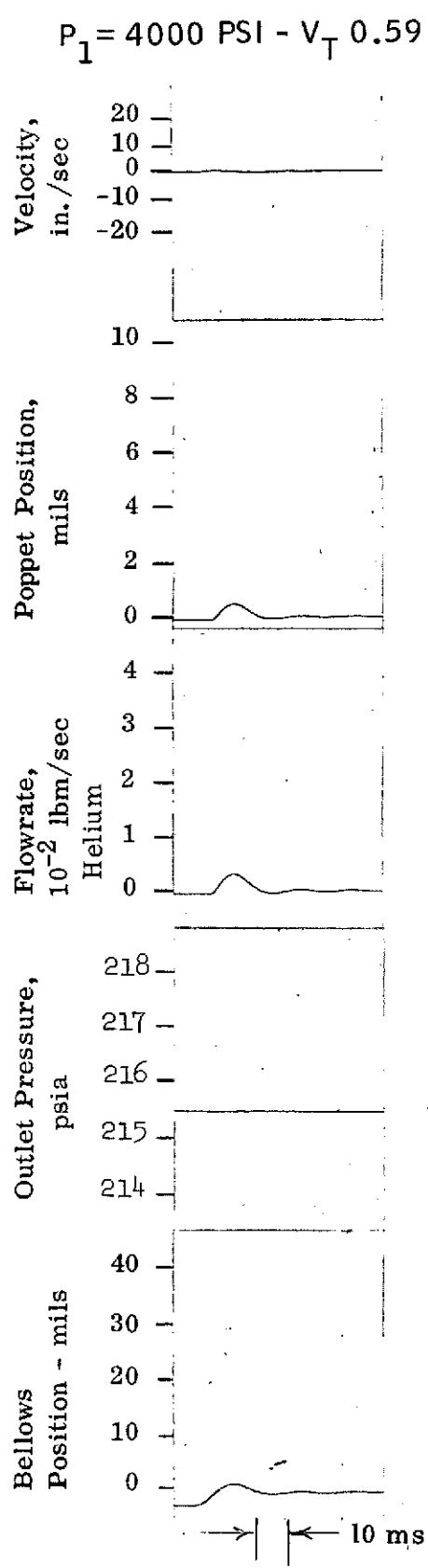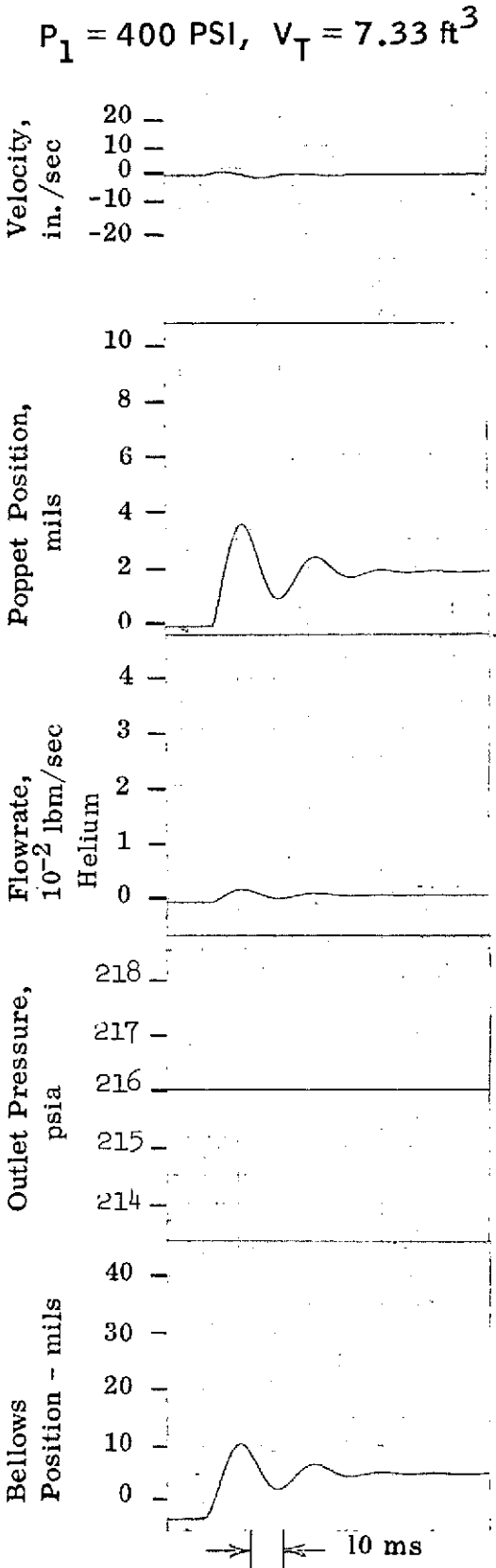
Figure 5-40 Analog Data - Final Regulator

91

STEP RESPONSE

+20% BELLOWS DIAM., MMH SYSTEM

P_1 4000 PSI - V_T = 0.59

P_1 400 PSI V_T = 7.33 ft^3

Velocity, in./sec

Poppet Position, mils

Flowrate, 10^{-2} lbm/sec Helium

Outlet Pressure, psia

Bellows Position – mils

10 ms
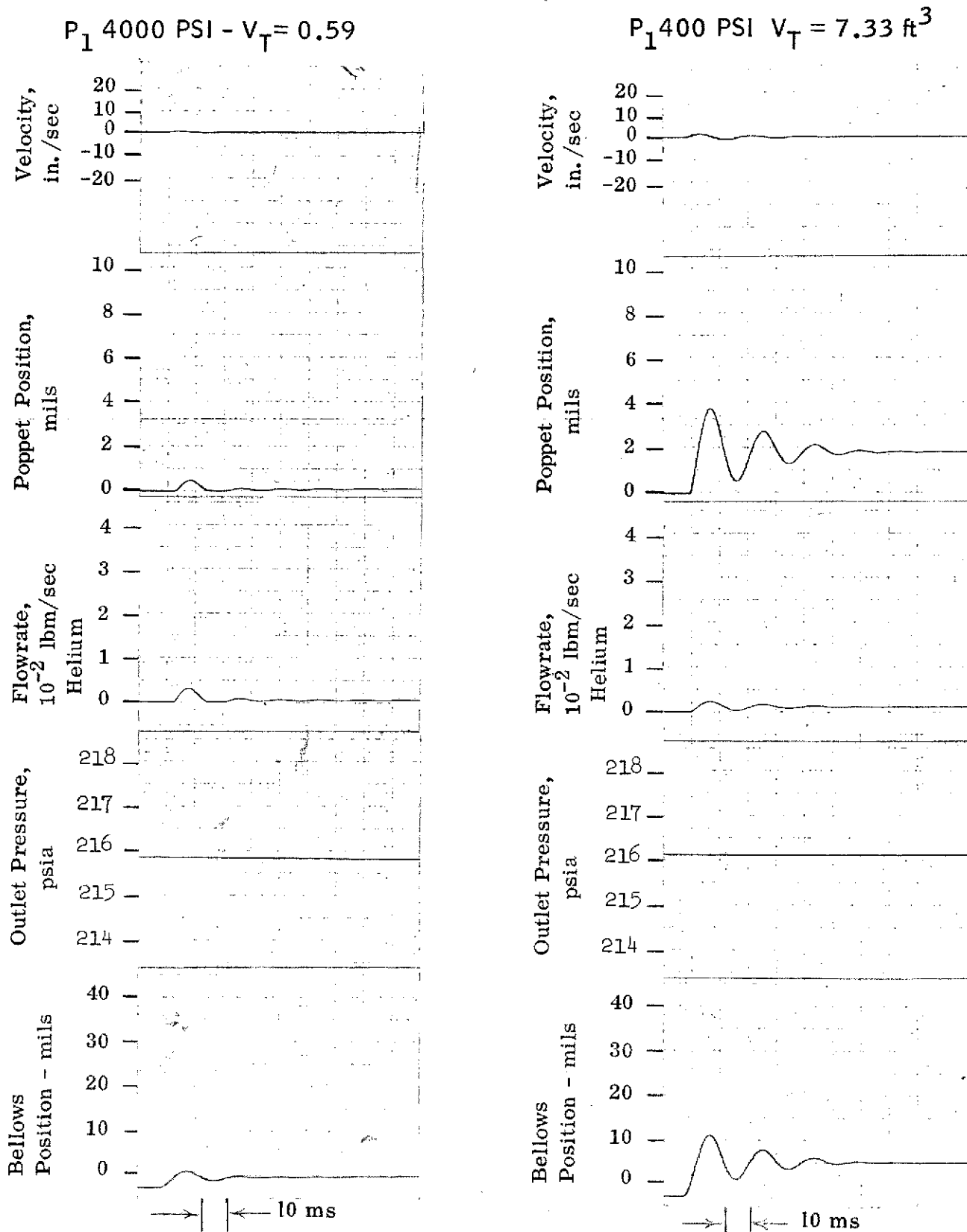
Figure 5-41 Analog Data – Final Regulator

92

STEP RESPONSE
-20% BELLOWS DIAM., MMH SYSTEM

$P_1 = 4000$ $\qquad\qquad\qquad$ $P_1 = 400$ PSI $\quad$ $V_T = 7.33$ ft^3
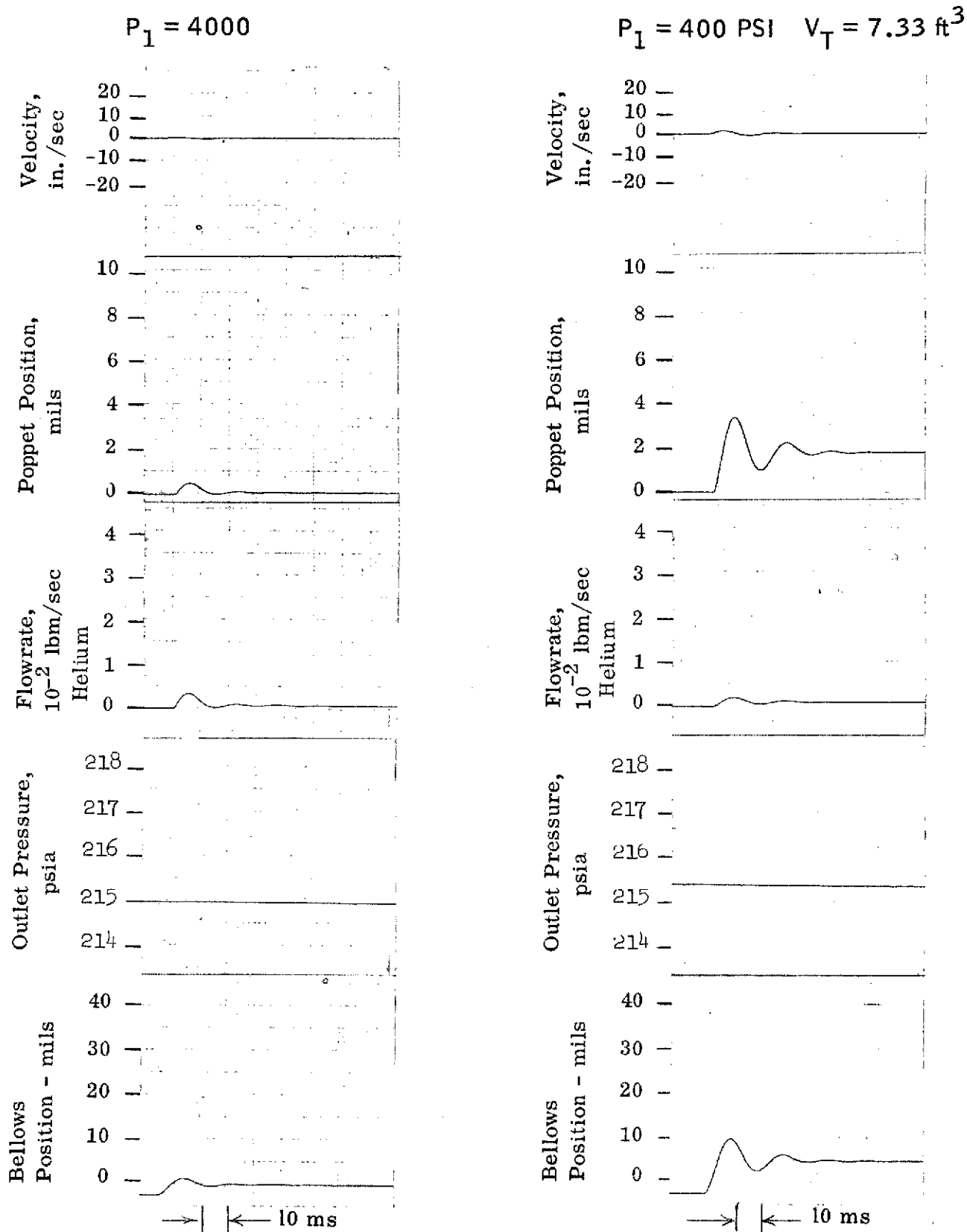
Figure 5-42 Analog Data – Final Regulator

93

STEP RESPONSE

+50% DAMPING ORIFICE AREA, MMH SYSTEM

$P_1 = 400$ PSI

P_1 4000 PSI $V_T = 0.59$ ft^3
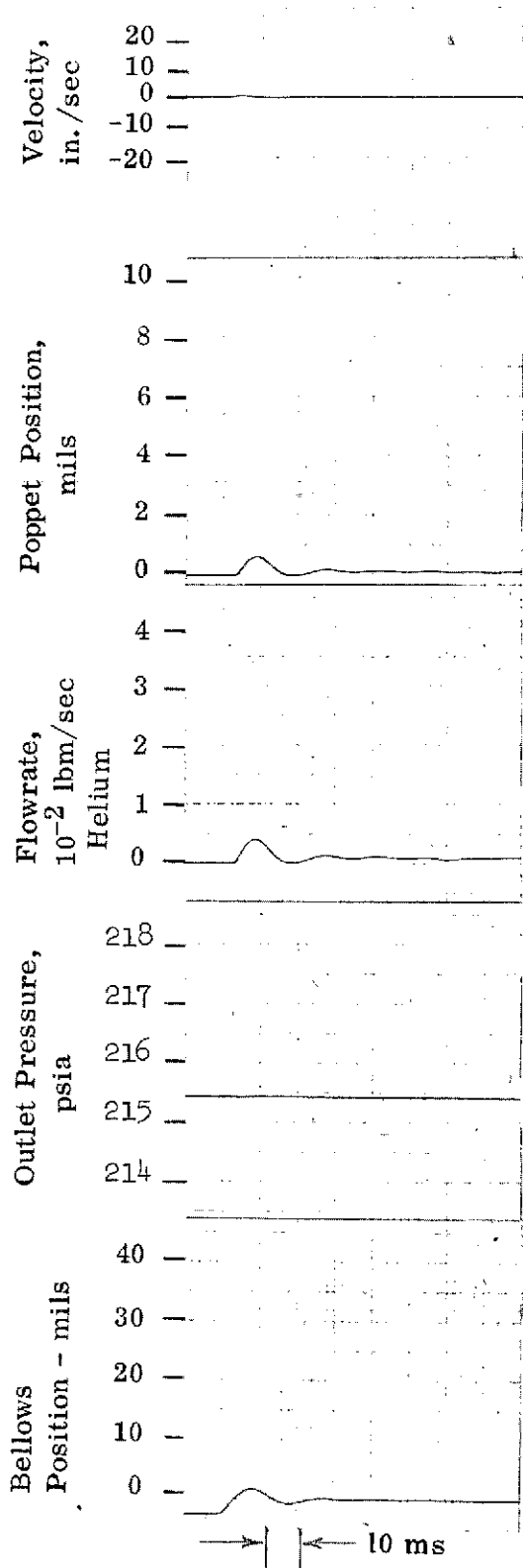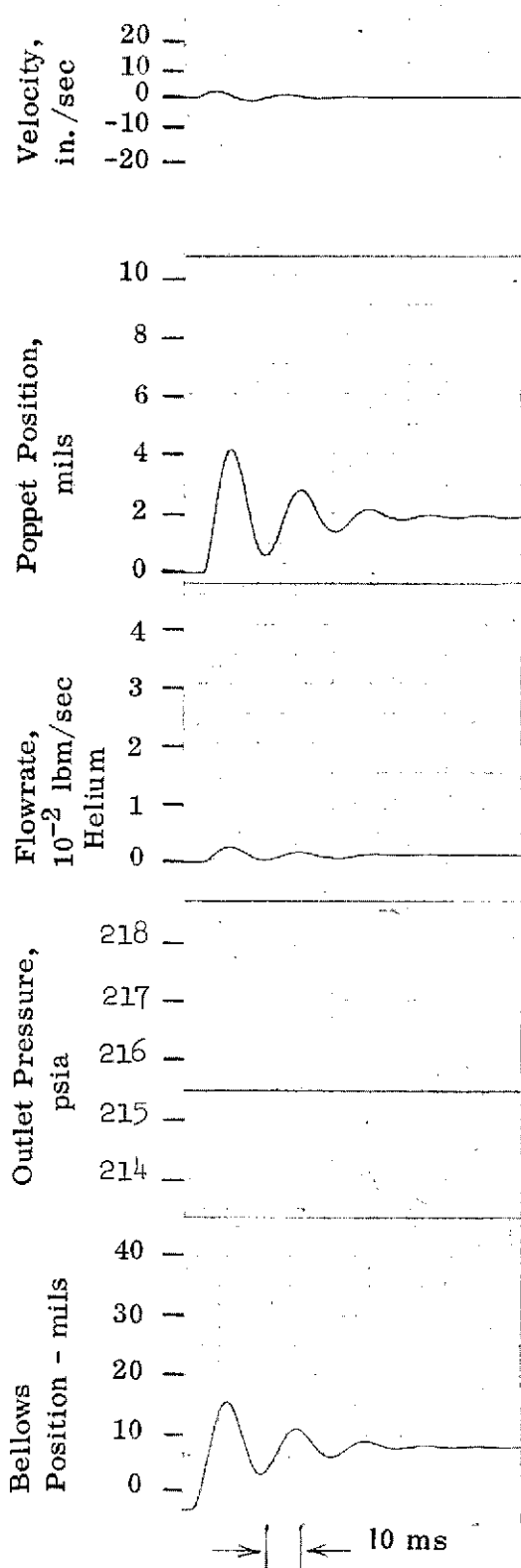
Figure 5-43 Analog Data - Final Regulator

STEP RESPONSE

-50% DAMPING ORIFICE AREA - MMH SYSTEM

$P_1 = 4000$ PSI, $V_T = 0.59$ ft^3 $P_1 = 4000$ PSI, $V_T = 7.33$ ft^3
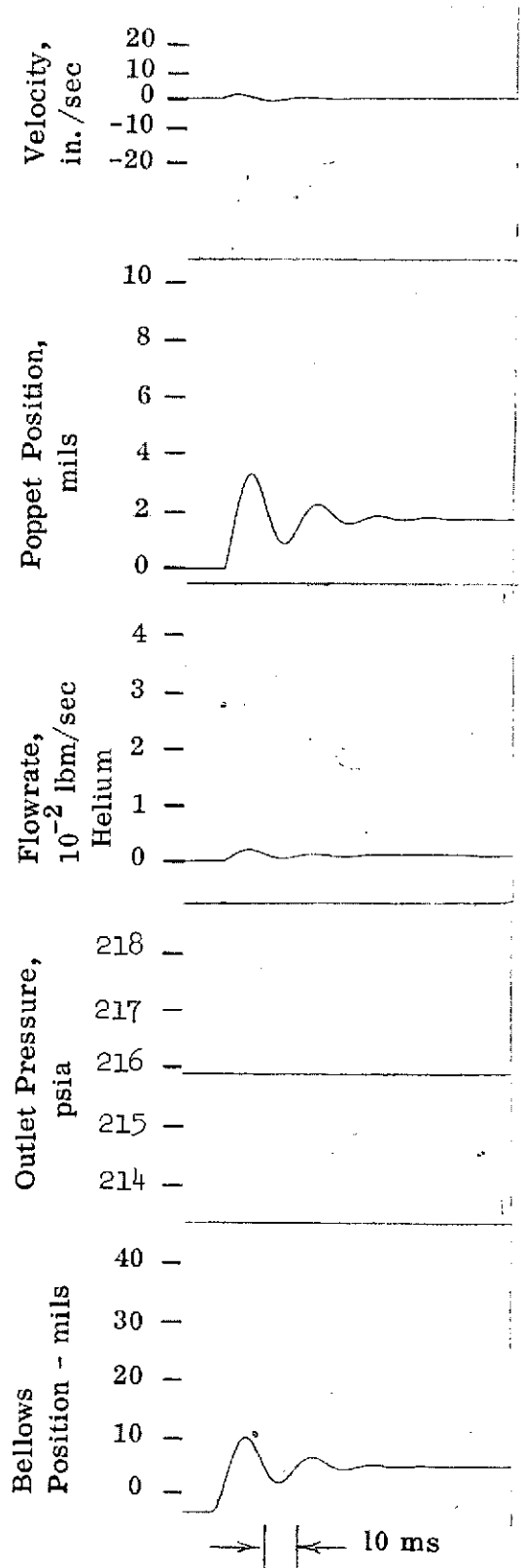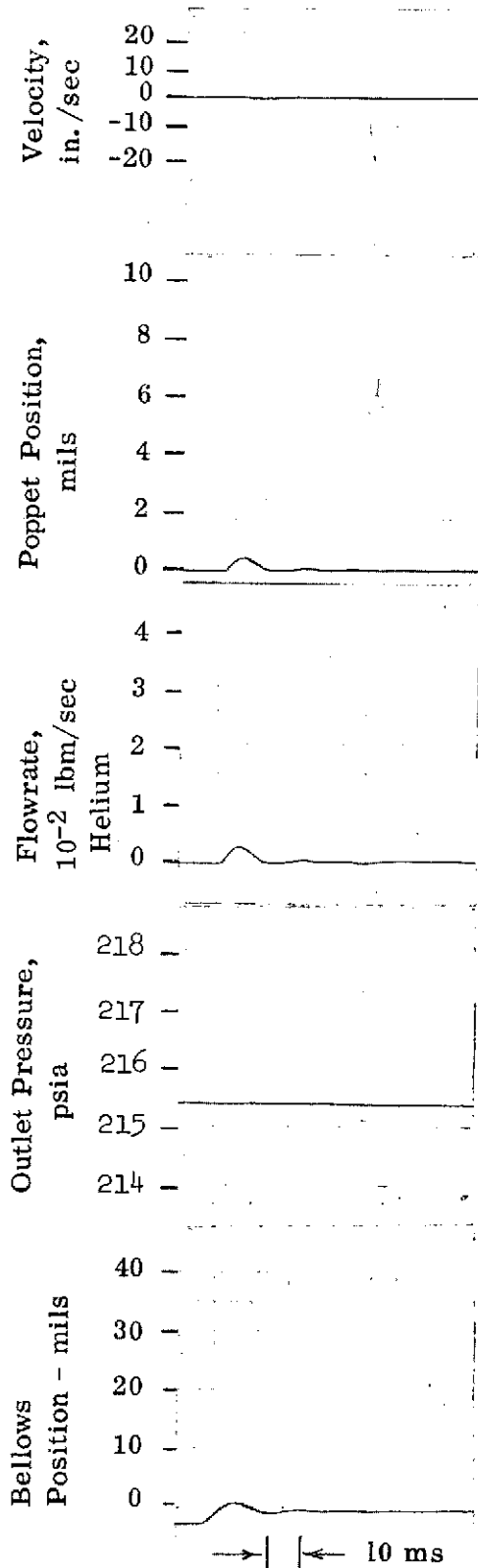
Figure 5-44 Analog Data - Final Regulator

95

STEP RESPONSE

$T_1 = 430.9°R -$ MMH SYSTEM
$P_1 = 400$ PSI, $V_T = 7.33$ ft^3

$T_1 = 430.9°R -$ MMH SYSTEM
$P_1 = 4000$ PSI, $V_T = 0.59$ ft^3
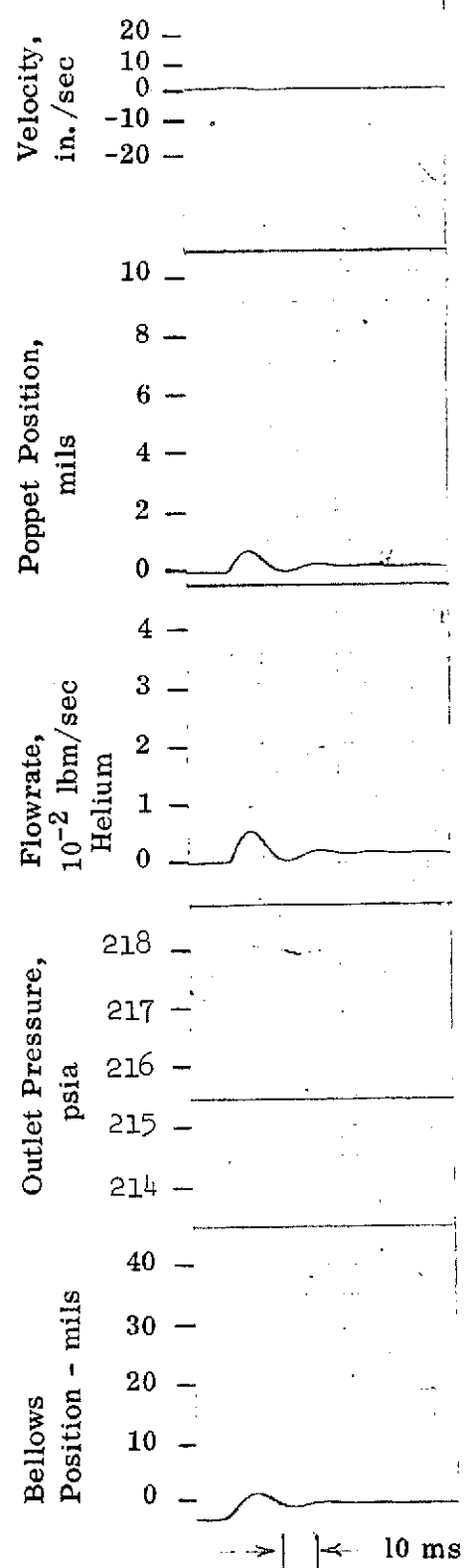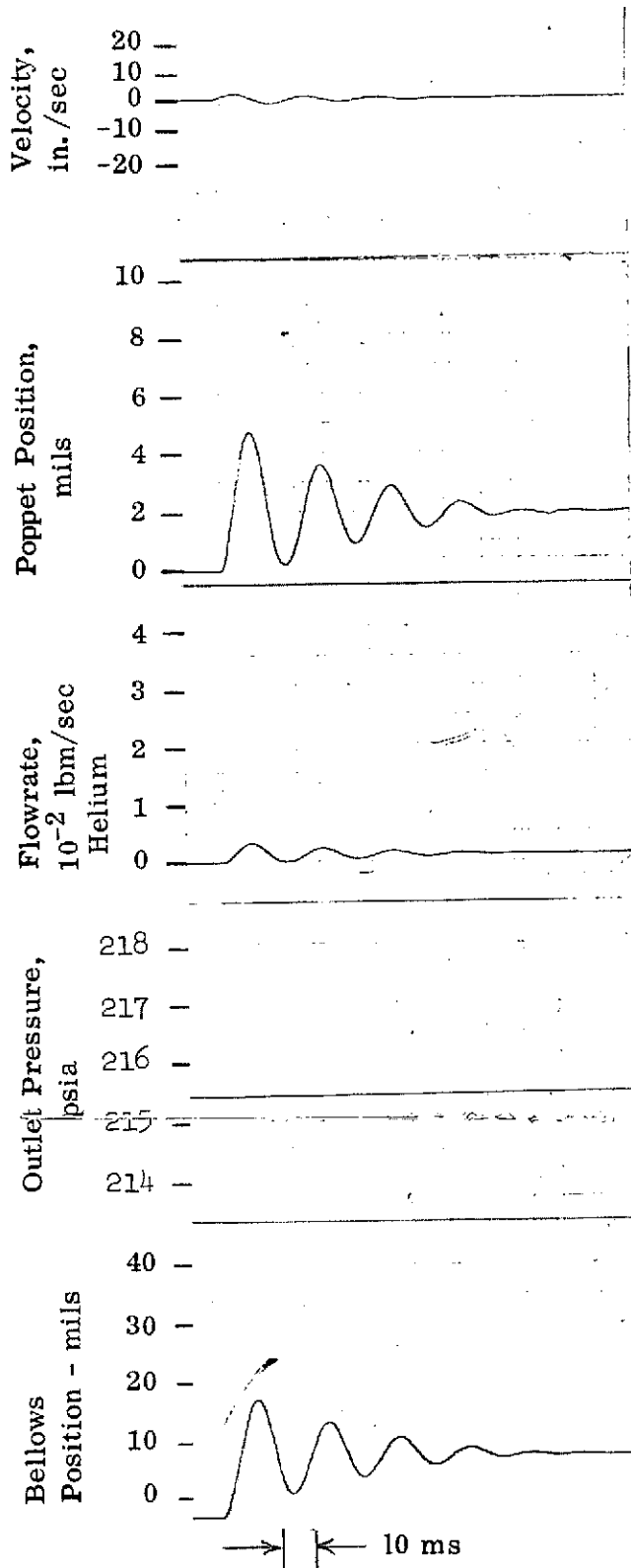
Figure 5-45

MOTOR START - STOP

$T_1 = 102°R$ - FLOX SYSTEM

$P_1 = 4000$ PSIA $V_T = 2.7$ ft^3
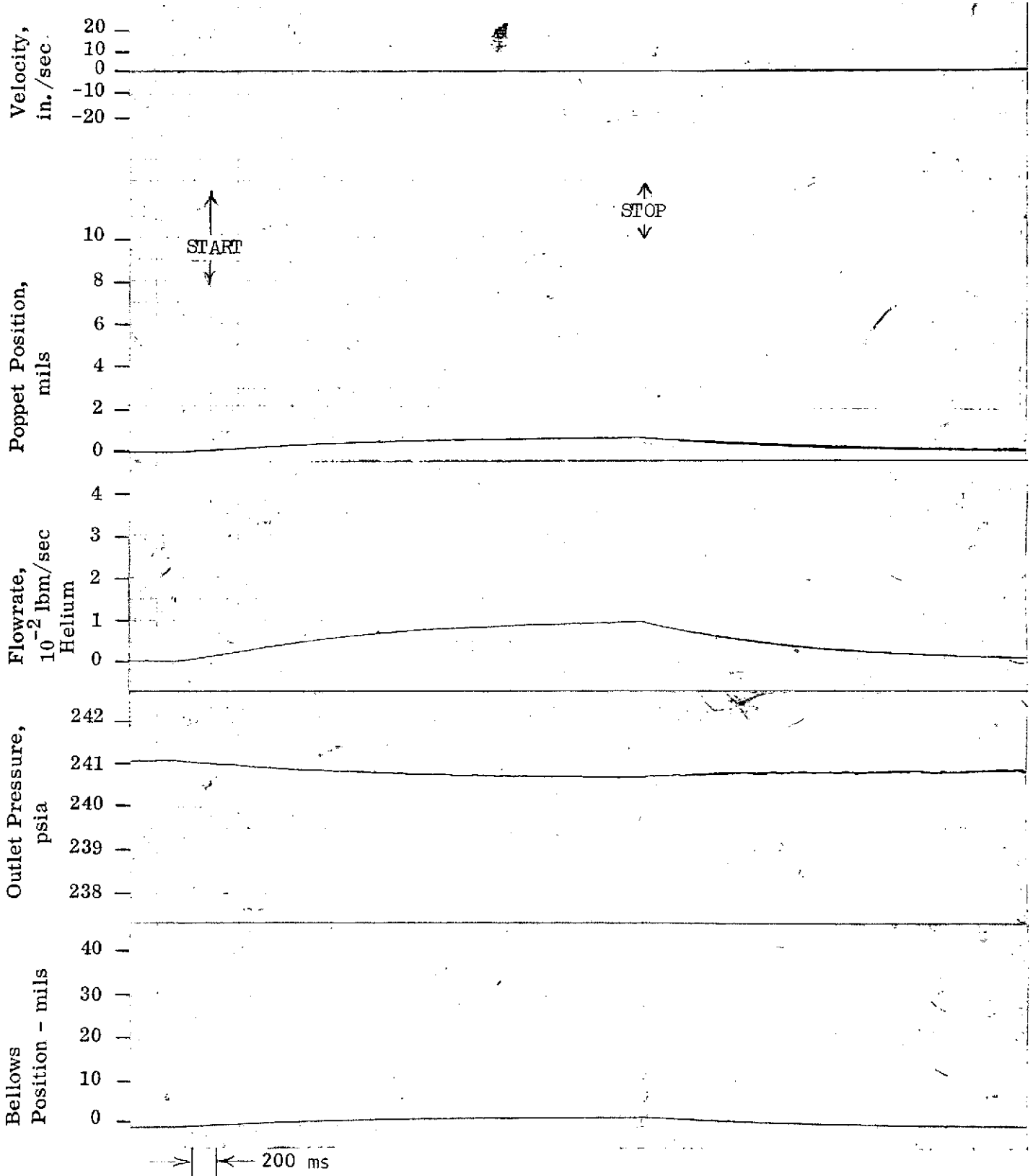
Figure 5-46 Analog Data – Final Regulator

97

TABLE 5-XIII

PHYSICAL EQUATIONS - FINAL REGULATOR

Force Balance

$$\ddot{Y} = \frac{g\left[P_2 A_B - F_o + Y K_s - \dot{Y} B + \frac{\left(P_1 - P_2\right)A_s X_p}{a/b} \left[1 - \frac{4K_1 D_{SE}}{D_{SE}^2 - D_{ST}^2} \right] - \left(P_2'' - P_2'\right)A_B \right]}{W_T}$$

$$\dot{Y} = \dot{Y}_i + \int_0^t \ddot{Y} \, dt$$

$$Y = Y_i + \int_0^t \dot{Y} \, dt$$

$$A_s = \frac{\pi}{4} D_s^2$$

Mass

$$W_T = \frac{W_{BS} + W_{BF}}{2} + W_{BP} + \frac{9 W_L}{(a/b)^2} + \frac{W_P + W_{PR}}{a/b} + \frac{W_{PF} + W_{PRF}}{2 \, a/b}$$

Poppet Flow:

$$\dot{W} = \frac{P_1 \, \pi \, D_{SE} \, C_m \, C_D \, X_P}{\sqrt{T_1}}$$

$$C_m = \sqrt{\frac{2 g \gamma}{R (\gamma - 1)} \left[\left(P_2/P_1\right)^{\frac{\gamma}{2}} - \left(P_2/P_1\right)^{\frac{\gamma + 1}{\gamma}} \right]}$$

$$C_D = 0.9171 - \left[0.010954 \, \frac{4 D_{SE} X_P}{D_{SE}^2 - D_{ST}^2} + 0.60053 \left(\frac{4 D_{SE} X_P}{D_{SE}^2 - D_{ST}^2}\right)^2 \right] \left(P_2/P_1\right)^2$$

$$X_P = \frac{Y}{a/b}$$

TABLE 5-XIII (Continued)

Propellant Tank:

$$\dot{P}_2 = \frac{R\,T_1}{V_T}\,\dot{W} - \frac{P_2}{V_T\,\rho_P}\,\dot{W}_P$$

$$P_2 = P_{2i} + \int_o^t \dot{P}_2 \; dt$$

Gas Damping:

$$\dot{P}_2{}' = \frac{R\,T_1}{V_2{}'}\,\dot{W}_2{}' - \frac{P_2{}'\,A_B}{V_2{}'}\,\dot{Y}$$

$$\dot{W}_2{}' = C_D\,A_o\sqrt{\frac{2\,g\,P_2{}'\left(P_2{}'' - P_2{}'\right)}{R\,T_1}}$$

$$P_2{}' = P_{2i}{}' + \int_o^t \dot{P}_2{}' \; dt$$

$$\dot{P}_2{}'' = \frac{R\,T_1}{V_2{}''}\,\dot{W}_2{}'' - \frac{P_2{}''\,A_B}{V_2{}''}\,\dot{Y}$$

$$\dot{W}_2{}'' = C_D\,A_o\sqrt{\frac{2\,g\,P_2{}''\left(P_2{}' - P_2{}''\right)}{R\,T_1}}$$

$$P_2{}'' = P_{2i}{}'' + \int_o^t \dot{P}_2{}'' \; dt$$

TABLE 5-XIV

POTENTIOMETER SCHEDULE - FINAL REGULATOR

Potentiometer * Number	Parameter	Units
05	$B/2$	lbf-sec/in.
08	$g/5,000\ W_T$	in./lbf-sec^2
12	$10\ Y_{max} - \Delta V_2/100$	in.
14	$K_{ss} - 6 \times 10^5/2 \times 10^4$	lbf/in.
19	$A_B/10$	in.^{2}
28	$(P_2)_{ref}/400$	lbf/in.^{2}
31	$1/a/b$	–
33	$1/a/b$	–
34	$\Delta V_3/100$	volts
37	$R\ T_1/4,000\ V_T$	lbf/lbm-in.^{2}
38	$P_2\ \dot{W}_P/800\ V_T\ \rho_P$	lbf/in.^{2}-sec
39	$4K_1\ D_{SE}/100\ (D_{SE}^2 - D_{ST}^2)$	1/in.
56	$K_{ss} - 6 \times 10^5/2 \times 10^4$	lbf/in.
58	$10\ \Delta Y - \Delta V_1/100$	in.
59	$F_o/2,000$	lbf
60	$K_s/20,000$	lbf/in.
61	$A_B/10$	in.^{2}
63	$1/40\ a/b$	–
65	$(P_2)_{ref}/400$	lbf/in.^{2}
66	$1/12.5$	–
67	$P_1/5,000$	lbf/in.^{2}
68	$100\ A_s$	in.^{2}
70	$P_1\ \pi\ D_{SE}\ C_m\ C_D/20\ \sqrt{T_1}$	lbm/sec-in.

*Reference Figure 5-34

TABLE 5-XIV (Continued)

Potentiometer Number	Parameter	Units
71	$P_2'' \, A_B / 400 \, V_2''$	lbf/in.^3
72	$C_D A_o \sqrt{4 g P_2'' R T_1 / 4,000 V_2''}$	$(\text{lbf/in.}^2)^{1/2}/\text{sec}$
87	$8/4,000$	-
90	$P_2' \, A_B / 400 \, V_2'$	lbf/in.^3
91	$C_D A_o \sqrt{4 g P_2' R T_1 / 4,000 V_2'}$	$(\text{lbf/in.}^2)^{1/2}/\text{sec}$
95	$(P_2)_{\text{ref}}/400$	lbf/in.^2
195	$P_{2i}/400$	lbf/in.^2
196	$10 \, Y_i$	in.
199	ΔV_4	volts

TABLE 5-XV

FINAL REGULATOR DATA INPUTS

Lumped Spring Rate:	763 lbf/in
Bellows Effective Area:	2.741 in^2
Lever Arm Ratio:	3
Spring Preload:	657 lbf
Bellows Mass:	0.34 lbm
Bellows Flexure Mass:	0.03 lbm
Bellows Shaft & Piston Mass:	0.43 lbm
Lever Mass:	0.06 lbm
Poppet Mass:	0.003 lbm
Push Rod Mass:	0.007 lbm
Push Rod Flexure Mass:	0.003 lbm
Poppet Seating Diameter:	0.083 in
Poppet Stem Diameter:	0.030 in
Poppet Seat Hole Diameter:	0.062 in
Upper External Bellows Volume:	2.535 in^3
Lower External Bellows Volume:	4.765 in^3
Discharge Coefficient:	See Figure 6-6
Flow Force on Poppet:	See Figure 6-9
Gas Damping Orifice:	0.133 in dia.

Figures 5-43 and 5-44 present the analog traces for the final regulator configuration featuring either a 50% increase or 50% decrease in the damping orifice area. Again, very little change in the dynamic behavior of the regulator is observed. Figure 5-45 shows the regulator operation with the helium gas temperature of 430.9°R. Interestingly enough, the lower gas temperature does result in somewhat greater poppet oscillations; however, the outlet pressure still does not exhibit any oscillations and the regulator is still completely stable. Figure 5-45 is in a different time scale ans shows the FLOX regulator outlet pressure during a motor start, steady state, and stop sequence when the helium temperature has reached its coldest condition of 102°R. As shown in this data, the regulator outlet pressure at 240.7 psia is well within the pressure regulation band. Furthermore, no undesirable pressure oscillations are observed.

In summary, the dynamic data for the final redundant bellows regulator configuration disclosed the regulator to be very stable over a wide range of regulator component performance characteristics variations.

5.3.4 Unit-to-Unit Variables

The final regulator design was reviewed to determine those component part variables that might cause unit-to-unit performance variations or affect regulator stability. the largest variable identified was that of the lumped spring rate. Variations in the lumped spring rate, in turn, are primarily due to variations in the manufacture of the bellows assemblies which constitute approximately 85% of the total lumped spring rate. The bellows are a procured component and discussions with several vendors have indicated that a tolerance of ± 15% for the spring rate is a reasonable assumption. Discussions with the same vendors also disclosed that the bellows effective area can be maintained within ± 5%.

A review of the matching tolerances to be employed in fabricating the poppet/seat interface indicated that the controlling flow area and the effective seating diameter would both be held within ± 5%. Machining tolerances affecting the lever ratio would result in a ± 3% variation. Other unit-to-unit variables such as the modulii of the materials, variations in the thermal coefficient of expansion of the materials, etc., were determined to be less than 3% and were therefore considered to be negligible. As discussed in the preceding section, the more important variables such as spring rate and bellows effective area were evaluated during sensitivity studies in support of the dynamic modeling. These studies indicated a completely stable regulator configuration regardless of these variations. Further investigations to determine whether these variations have significant effects on the minimum amount of pressurant loaded or propellant residuals are discussed in Section 8 of this report.

5.3.5 Failure Modes and Effects Analysis

In accordance with generally accepted reliability practices a failure modes and effects analysis was prepared. This analysis served as a review of each impact and regulator component, its function, its possible failure mechanism, the possible cause of the failure, the effect of such a failure and inherent compensating provisions. Details of the analysis follow on pages 104 through 109.

ITEM NAME AND PART NUMBER	BLOCK DIAGRAM REF. NO.	FUNCTION	ASSUMED FAILURE	POSSIBLE CAUSES	EFFECTS AND CONSEQUENCES	INHERENT COMPENSATING PROVISIONS	REMARKS		
Regulator Case		To provide the pressure shell for the mechanical valve components	External leakage	1. Improper welding of mating sections	1. Loss of the supply pressure	1. None	1. Each regulator valve will be proof pressure tested to verify structural integrity. All material processes will be controlled by detailed procedures.		
				2. Material imperfections	2. Loss of the supply pressure	2. None	2. Each regulator valve will be proof pressure tested to verify structural integrity. All weld processes and inspection will be controlled by detailed procedures.		
Valve Seat and Poppet		To provide the sealing surface between inlet and regulated pressure supplies and provide the metering orifice system for pressure regulation as commanded by the regulator system	Internal gas leakage	1. Contamination entrapped between the seat and poppet	1. The regulated pressure system will be exposed to the inlet pressure level. There will be a loss of regulator sealing function until the contamination has been removed from the seat/poppet sealing surface.	1. Any entrapped contamination will be blown from the seat after one cycle of the poppet.	1. The gas fluid will be filtered prior to entry into the valve. The assembly and weld procedures will preclude introduction of contamination during regulator assembly. Filter size is sufficient to exclude all particles that would cause leakage.		
				2. Seat or poppet wear of the micro-finish	2. The regulated pressure system will be exposed to the inlet pressure level. There will be a permanent loss of the regulator sealing function.	2. The system should include a relief valve.	2. The selected material and seat design will preclude excessive or premature wear on sealing surface of either the poppet or valve seat. Verified through type approval/margin limit testing.		
Stacked Disc Filter		To provide the contamination control for the valve system	1. Contamination within the valve	1. Damaged filter element	1. If the contamination is entrapped at the valve seat, internal gas leakage will occur. The regulated pressure system will be exposed to the inlet pressure level. There will be a loss of regulator function until the contamination has been removed from the seat/poppet sealing surface.	1. The possibility of a particle both passing thru a damaged filter section and being entrapped on the valve seat is remote. Any entrapped contamination will be blown from the seat after one cycle of the poppet.	1. The filter will be acceptance tested as an individual component to verify integrity and cleanliness. Verify no particle generation through type approval/ margin limit testing.		

ITEM NAME AND PART NUMBER	BLOCK DIAGRAM REF. NO.	FUNCTION	ASSUMED FAILURE	POSSIBLE CAUSES	EFFECTS AND CONSEQUENCES	INHERENT COMPENSATING PROVISIONS	REMARKS		
Stacked Disc Filter (Continued)			2. Limited gas flow from the inlet into the valve	2. Contaminated filter	2. The regulated pressure response rate will be decreased but the regulator will remain functional. Inlet/outlet characteristics will vary	2. The filter has been sized to accommodate more contamination than specification limits dictates.	2. The filter will be acceptance tested as an individual component to verify integrity and cleanliness.		
Push Rod Guide Flexures and Poppet Guide Flexure	-	To provide the alignment of the push rod and poppet for the poppet alignment with the valve seat	1. Gas leakage past the seat	1. Fatigue fracture of the push rod guide or poppet guide flexures	1. Proper alignment may not be maintained between the seat and poppet and leakage across the seat will occur..	1. There are five flexures; the loss of any one, except for the poppet flexure, would not prevent continued use of the regulator although degradation of performance may occur due to frictional drag of fractured flexure.	1. The selected material, the processing and assembly control will preclude premature fatigue fractures. Verify through type approval/margin limit testing.		
			2. Low or high regulated pressure	2. Improper assembly of the flexure including welding. This will result in frictional drag in the push rod guide or poppet guide flexures.	2. Decrease in the accuracy of the regulated pressure due to the frictional drag within the flexure system	2. The driving forces are sufficient to overcome any drag forces in the push rod guide flexures	2. Sufficient misalignment may result in fatigue fracture of the flexure. The acceptance test of the regulator will determine any gross flexure assembly problems as evident from excessive droop characteristics and a lack of repeatability.		
Push Rod		To provide the drive linkage abetween the lever and the poppet	1. Poppet partially opens	1. Push rod wear on the bearing surface	1. The regulated pressure level will be decreased.	1. The push rod flexures are installed with a 0.5 pounds load applied through the push rod into the lever. With the radial spring rates of the flexure assemblies no sliding friction is imposed on the push rod at the lever contact point.	1. The selected material and stress level will preclude any premature wear on the lever/push rod bearing surface. Cyclic operation will be performed during acceptance testing to assure wear condition is not present		
			2. Poppet does not open	2. Fracture of the push rod	2. Loss of the regulated pressure level. The supply pressure will not be depleted by this condition but will be maintained by the closed valve seat condition.	2. None.	2. The selected material will preclude fatigue fracture. The acceptance test will verify assembly integrity. Verify through type approval/margin limit testing		

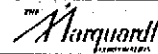| ITEM NAME AND PART NUMBER	BLOCK DIAGRAM REF. NO.	FUNCTION	ASSUMED FAILURE	POSSIBLE CAUSES	EFFECTS AND CONSEQUENCES	INHERENT COMPENSATING PROVISIONS	REMARKS		
Lever		To provide the 3 to 1 mechanical gain for the force balance between poppet push rod and the actuator	1. Low or no regulated pressure	1. Lever wear on the bearing surface	1. The regulated pressure level will be decreased.	1. The push rod flexures are installed with a 0.5 pounds load applied through the push rod into the lever. With the radial spring rates of the push rod flexures and the actuator rod no sliding friction is imposed on the lever at push rod or actuator rod contact points.	1. The selected material will preclude any premature wear on the bearing surface. Verified by type approval/margin limit testing.		
			2. No regulated pressure	2. Fracture of the lever	2. Loss of the regulated pressure level. The supply pressure system will not be depleted by this condition but will be maintained by the closed valve seat condition.	2. None.	2. The selected material will preclude fatigue fracture. The acceptance test will verify assembly integrity. Verified by type approval/margin limit testing.		
Lever Pivot Flexure		To provide the pivot point for the lever	1. Lever will not pivot	1. Fracture of the lever pivot flexure	1. The pressure supply system will be sealed with no regulation of the pressure possible. The supply pressure system will not be depleted by this condition but will be maintained by the closed valve seat.	1. None.	1. The maximum rotational travel of the flexure is approximately .005 of an inch. The selected material will preclude fatigue fracture. Verified by type approval/margin limit testing.		
			2. Limited or slow response of the lever movement	2. Frictional drag in the lever pivot flexure from assembly damage	2. Decrease in the regulated pressure	2. The driving forces are sufficient to overcome any drag forces in the lever pivot flexure without significant decreases in regulated pressure.	2. Sufficient assembly damage may result in subsequent fatigue fracture. Inspection of the flexure will limit the possibility of structural damage during assembly. The acceptance test will verify any gross assembly damage.		

ITEM NAME AND PART NUMBER	BLOCK DIAGRAM REF. NO.	FUNCTION	ASSUMED FAILURE	POSSIBLE CAUSES	EFFECTS AND CONSEQUENCES	INHERENT COMPENSATING PROVISIONS	REMARKS		
Bellows Guide Flexures		To provide the guide force and coupling between the actuator shaft and the bellows assemblies	1. Low regulated pressure	1. Improper assembly of the bellows guide flexure including welding	1. Decrease in regulated pressure level. The misalignment flexure/actuator shaft assembly will prevent proper loading of the lever.	1. None	1. The capability of the bellows guide flexures will be demonstrated during acceptance testing. Verified through type approval/margin limit testing. The assembly processes will be controlled by detailed procedures.		
			2. Loss of regulated presure	2. Fatigue fracture of the bellows guide flexure	2. Loss or decrease of the regulated presure	2. There are three flexures for each bellows; the loss of any one would not normally prevent continued use of the regulator although degradation of performance may occur due to frictional drag of fractured flexure. It is possible that fracture of flexure could cause the unit to jam in any position from full open to full closed but the supply pressure should cause the unit to closed by over-pressurizing the bellows	2. The selected material, the processing and assembly control will preclude premature fatigue fractures. Verified through type approval and/or margin limit testing.		
Actuator Stops		To provide the stops for the actuator shaft and thereby limit the poppet stroke.	Increased actuator shaft stroke	1. Wear of the actuator stop contact surfaces	1. The regulator tends to overshoot and regulated pressure has a higher variation in the amplitude and rate of change.	1. The annular orifice will tend to dampen any rapid pressure variations.	1. The selected material will preclude excessive or premature wear on these contact surfaces. Verified through type approval/margin limit testing.		
				2. Fracture of the actuator stops	2. The regulator will overshoot causing wide variation in the regulated pressure amplitude and rate of change. Stroke overshoot may be sufficient to cause flexure damage or excessive impact loads on the poppet/valve seat sealing surface.	2. The annular orifice will tend to dampen any rapid pressure variations to prevent poppet/valve seat impact damage.	2. The selected material will preclude fatigue failure from the impact loads. Verified through type approval/margin limit testing.		

FAILURE MODE AND EFFECT ANALYSIS   Marquardt

ITEM NAME AND PART NUMBER	BLOCK DIAGRAM REF. NO.	FUNCTION	ASSUMED FAILURE	POSSIBLE CAUSES	EFFECTS AND CONSEQUENCES	INHERENT COMPENSATING PROVISIONS	REMARKS		
Tension Loaded Bellows		To provide a flexible isolate between the regulated pressure source and reference pressure sources and supply a portion of the preload force on the lever	1. Leakages across the bellows walls	1. Fatigue fracture or improper assembly including welding	1. The reference pressure becomes the same as the regulated pressure and the regulator pressure amplitude and rate of change becomes a function of the variations within this same regulated pressure.	1. None. The regulator will function, but the regulated pressure will have a wider amplitude variation and will be shifted from the original nominal setting.	1. Proof pressure and leak tests during acceptance will verify bellows integrity. Material and process control will assure uniformity and repeatability of the production lot. The selected material will preclude fatigue fracture. Verified through type approval/margin limit tests.		
			2. Improper spring rate	2. Bellows damaged during assembly or improper machining of the bellows	2. Dependant upon the extent of damage or improper machining, the discrepant bellows may not be noted in acceptance test. Any discrepancy not noted during acceptance test will cause the life of the bellows to be fatigue life limited.	2. None. No evident performance change will be noted until there is a fatigue failure of the bellows. When the fatigue failure occurs, the regulator will function but the regulated pressure will have a wider amplitude variation and will be shifted from the original nominal setting.	2. Proof pressure and leak tests during acceptance will verify bellows integrity. Material and process control will assure uniformity and repeatability of the production lot. Verified through type approval/margin limit testing.		
Compression Loaded Bellows		To provide a flexible isolate between the reference pressure source and external environment and supply a portion of the preload force on the lever.	1. Leakages across the bellows walls	1. Fatigue fracture or improper assembly including welding	1. Loss of reference pressure through expulsion to external environment.	1. None. The regulator will function but the regulated pressure will be shifted from the nominal setting. The decrease in reference pressure will also limit the effective of the annular orifice damping and wider variations in the regulated pressure will occur.	1. Proof pressure tests during acceptance will verify bellows integrity. Material and process control will assure uniformity and repeatability of the production lot. The selected material will preclude fatigue fracture.		
			2. Improper spring rate	2. Bellows damaged during assembly or improper machining of the bellows	2. Dependant upon the extent of damage or improper machining, the discrepant bellows may not be noted in acceptance test. Any discrepancy not noted during acceptance test will cause the life of the bellows to be fatigue life limited.	2. None. No evident performance change will be noted until there is a fatigue failure of the bellows. When the fatigue failure occurs, the regulator will function but the regulated pressure will be shifted from original nominal setting and the effectivity of the annular orifice damping will be limited.	2. Proof pressure tests during acceptance will verify bellows integrity. Material and process control will assure uniformity and repeatability of the production lot.		

FAILURE MODE AND EFFECT ANALYSIS

Marquardt

ITEM NAME AND PART NUMBER	BLOCK DIAGRAM REF. NO.	FUNCTION	ASSUMED FAILURE	POSSIBLE CAUSES	EFFECTS AND CONSEQUENCES	INHERENT COMPENSATING PROVISIONS	REMARKS		
Annular Orifice		To provide a system of damping to limit the rate of regulated pressure change	Wider pressure variations in the regulated pressure	1. Frictional drag between the annular orifice and the actuator shaft due to contamination entrapment.	1. Sufficient contamination entrapment could cause the actuator shaft to bind in the annular orifice with the regulated pressure increasing to inlet pressure	1. None. Sufficient drive force is available to move the actuator shaft for minimal shaft lock-up due to contamination.	1. The assembly and weld procedures will preclude introduction of contamination during regulator assembly. The only other potential source of contamination is through the reference pressure fill valve. This source will be filtered to preclude contamination of the regulator cavity.		
Reference Pressure Fill Valve		To provide a source for pressurizing the reference pressure cavity	External Leakage	1. Contamination entrapped between the ball and the seat	1. Loss of reference pressure through expulsion to external environment	1. None	1. Following the pressurizing of the reference pressure cavity, the leakage rate of the reference pressure fill valve will be verified. Since the valve is cycled only at the time filling, no subsequent leakage is anticipated.		
Vent Screen		To provide a contamination free vent source to the environmental side of the compression loaded bellows	1. Wider pressure variations in the regulated pressure	1. Contaminated filter	1. The regulator system becomes over-damped and a wider variation in the regulated pressure occurs.	1. The exhaust of gas from the bellows cavity tends to clean the vent screen. This occurs once for each regulator cycle.	1. The possibility of sufficient contamination being entrapped in the vent screen to cause a restriction in the flow through the screen is remote.		
			2. Contamination within the environmental side of the bellows cavity.	2. Damaged filter element.	2. Sufficient contamination could cause damage to the compression loaded bellows flexures.	2. None	2. The possibility of sufficient contamination of sufficient size being entrapped in environmental side of the compression loaded bellows is remote. The regulator system under normal environmental conditions would operate continually without a vent screen.		

109

5.3.6   System Compatibility and Use Limitations

Throughout the analysis and conceptual design effort that resulted in the final regulator configuration the technical requirements as set forth in Section 4 of this report were continuously reviewed to ascertain that the final regulator design is fully compatible with its intended usage. In particular, such performance characteristics as operating pressures, flowrates, temperatures, cycle life, propellant compatibility, regulator stability, and such environmental factors as vibration, acceleration, shock, long-term life, and the humid air environment during ground operations were continually being considered. Also, as discussed in Section 7 of this report the possibility of the regulator being filled with liquid propellants was evaluated. On the basis of these reviews and evaluations, it was concluded that the final regulator design was fully compatible with all of the requirements set forth in Section 4. Upon completion of the analytical efforts in support of this program and as a result of other pressure regulator technology programs at The Marquardt Company, there were, however, two additional analytical efforts identified which should be performed to eliminate even the least amount of doubt. These efforts are discussed in Section 9 of this report.

5.3.7   Fabrication State-of-the-Art and Development Risks

Throughout the design effort which resulted in the final regulator configuration as shown in Figure 5-32, consideration was given to the inclusion of design features that would reflect the state-of-the-art and minimize development risks. It is believed that this approach has been successful. The design concepts of all of the regulator components have been demonstrated by The Marquardt Company in the development of other fluid system components. Fabrication techniques for flexures, ceramic poppets and seats, and the joining of various regulator elements by brazing or electron beam welding are all state-of-the-art at The Marquardt Company. A review of procured regulator components and materials was made to identify long lead time items. This review indicated that all vendor-supplied hardware can be procured within a period of two months with the exception of the Bendix pivot flexure. The Bendix pivot flexure is available off-the-shelf made from 400 series stainless steel; however, for the flight regulator configuration, because of the low temperature operating environment of the FLOX regulator, this flexure will be made from Inco 718. Unfortunately, the best quote received from Bendix to date for this special pivot flexure is for a six months delivery. Thus, a prototype pressure regulator utilizing the stock pivot flexure could be fabricated approximately four months after completion of this design effort, whereas the prototype regulator featuring the special Inco 718 pivot flexure would require approximately seven months.

6.   WORK PRINCIPLES PROOF

An experimental investigation was conducted to determine the poppet flow forces and the poppet/seat discharge coefficient for the selected final regulator configuration. This effort consisted of the design and fabrication of a test fixture and subsequent tests with this fixture in a helium flow facility. The determination of the poppet flow force was made both under steady state and dynamic flow conditions. Dynamic flow conditions were achieved by opening the poppet with a solenoid actuator whose response was varied by varying the voltage to the solenoid. All data were obtained at the various inlet pressures of interest and ambient temperature.

110

6.1   TEST FIXTURE DESCRIPTION AND OPERATION

The test fixture for this experimental investigation is shown in Figure 6-1. The test fixture duplicates the poppet/seat interface shown in Figure 5-4 and provides the necessary actuation mechanism and force and stroke measurements for the poppet. As shown in Figure 6-1, the poppet/seat interface is located in the bottom of the test fixture. The poppet is simply a cylinder which is spring loaded by means of a small coil spring and is guided by the bottom portion of the housing which is removable. The sealing surface of the poppet cylinder was lapped to a finish of approximately 4; the poppet is opened by means of a push rod which is a part of the moving element of the actuator assembly.

The moving element of the actuator assembly consists of a total of 7 parts. These are in order of the stackup starting with the push rod which contacts the poppet:

1.   Push rod, guided by an electrolized bushing

2.   Load cell for force measurements

3.   Load cell to solenoid armature connecting rod

4.   Connecting rod to armature adapter

5.   Solenoid armature

6.   Coupling

7.   LVDT armature

Guidance of this moving element stack occurs at the push rod bushing, at the connecting rod, at the solenoid armature, and at the LVDT armature. The cavity surrounding the load cell is pressurized to the outlet pressure of the poppet/seat interface (240 psia) and an O-ring seal at the connecting rod prevents this pressure from escaping outside of that cavity. The stackup of load cell, solenoid actuator, and LVDT permits the measurement of the force applied by the solenoid to the poppet in lifting the poppet off the seat and at the same time permits position monitoring of the poppet. The solenoid actuator employed was the same as that used in Marquardt's P/N 228683 valve. The load cell was the Bytrex Model JP-50 unit manufactured by Kavlico Electronics, Inc., to Marquardt Drawing No. X28959.

6.2   TEST SYSTEM DESCRIPTION

The test system for the Work Principles Proof Testing is shown schematically in Figure 6-2. Photographs of the test system, test fixture, and instrumentation and controls are shown in Figures 6-3, 6-4, and 6-5. The helium supplied to the flow system consisted of several K bottles pressurized to approximately 2000 psi. Helium from these bottles was pumped up to approximately 5000 psi by means of a high pressure helium pump. The high pressure helium was stored in a 4.5 cubic ft bottle and was subsequently regulated by means of a facility regulator to the required test fixture operating pressure. The helium pump as we as the high pressure storage bottle may be seen on the right side of Figure 6-3. The facility regulator is located in front of the storage bottle near the ground level. Helium from the regulator was then routed through a shutoff valve to the test fixture. The test fixture was supported on a 6-inch column and may also be seen in Figures 6-3 and 6-4. Downstream of the test fixture the helium was routed through a throttling valve and a flow measuring

TEST FIXTURE
POPPET VALVE, HELIUM REGULATOR
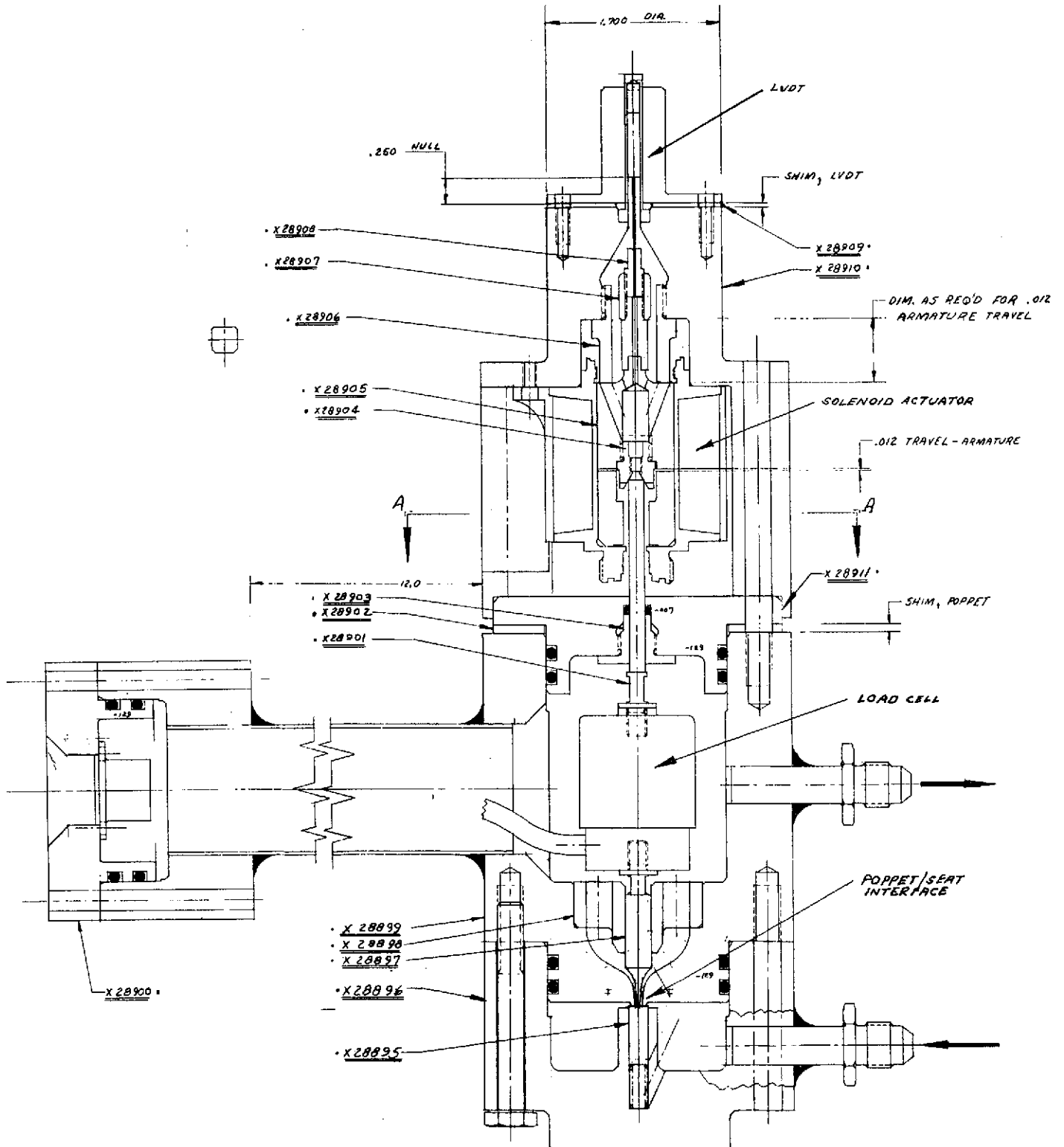
Figure 6-1

112

FLOW SYSTEM SCHEMATIC
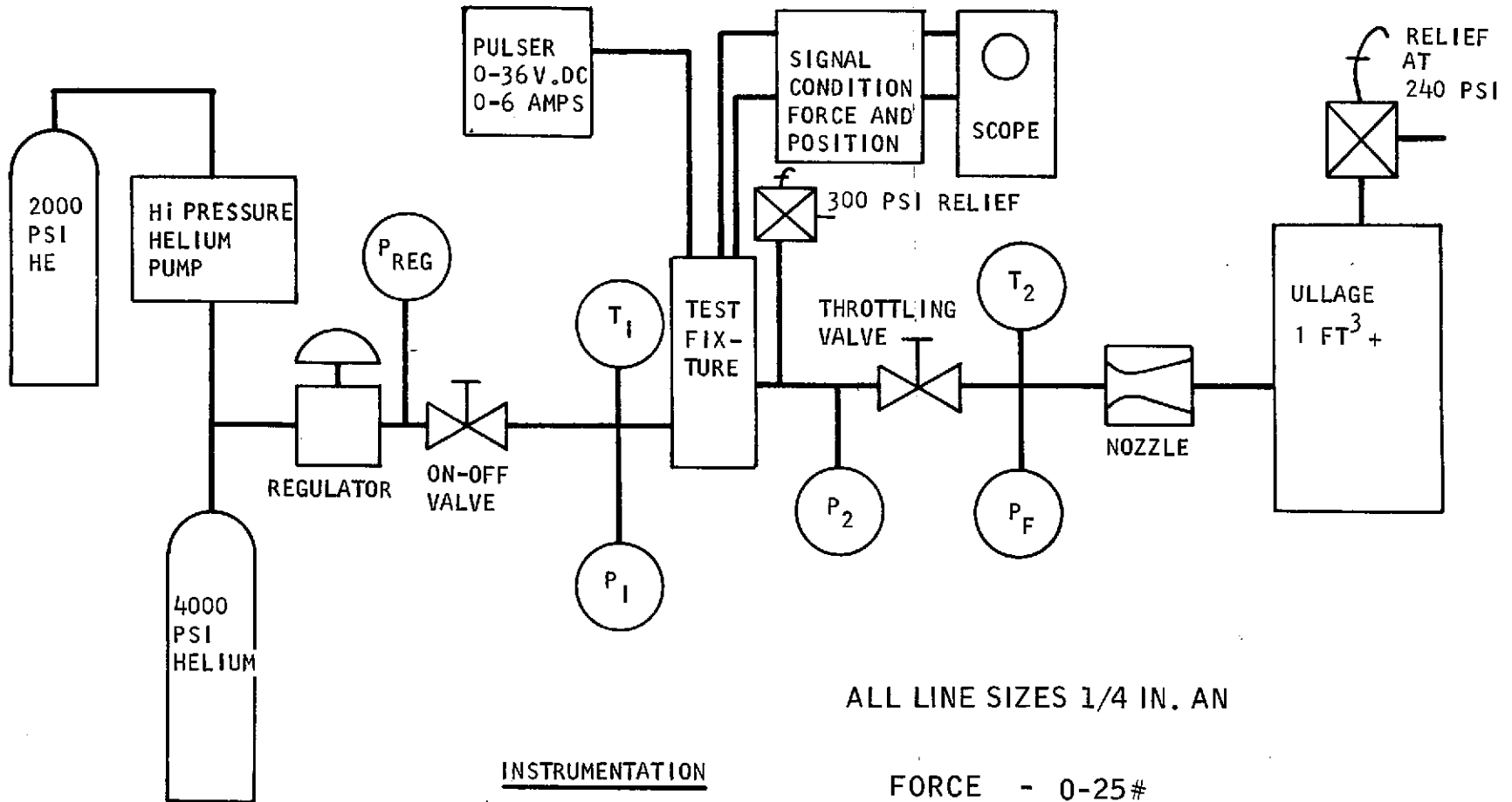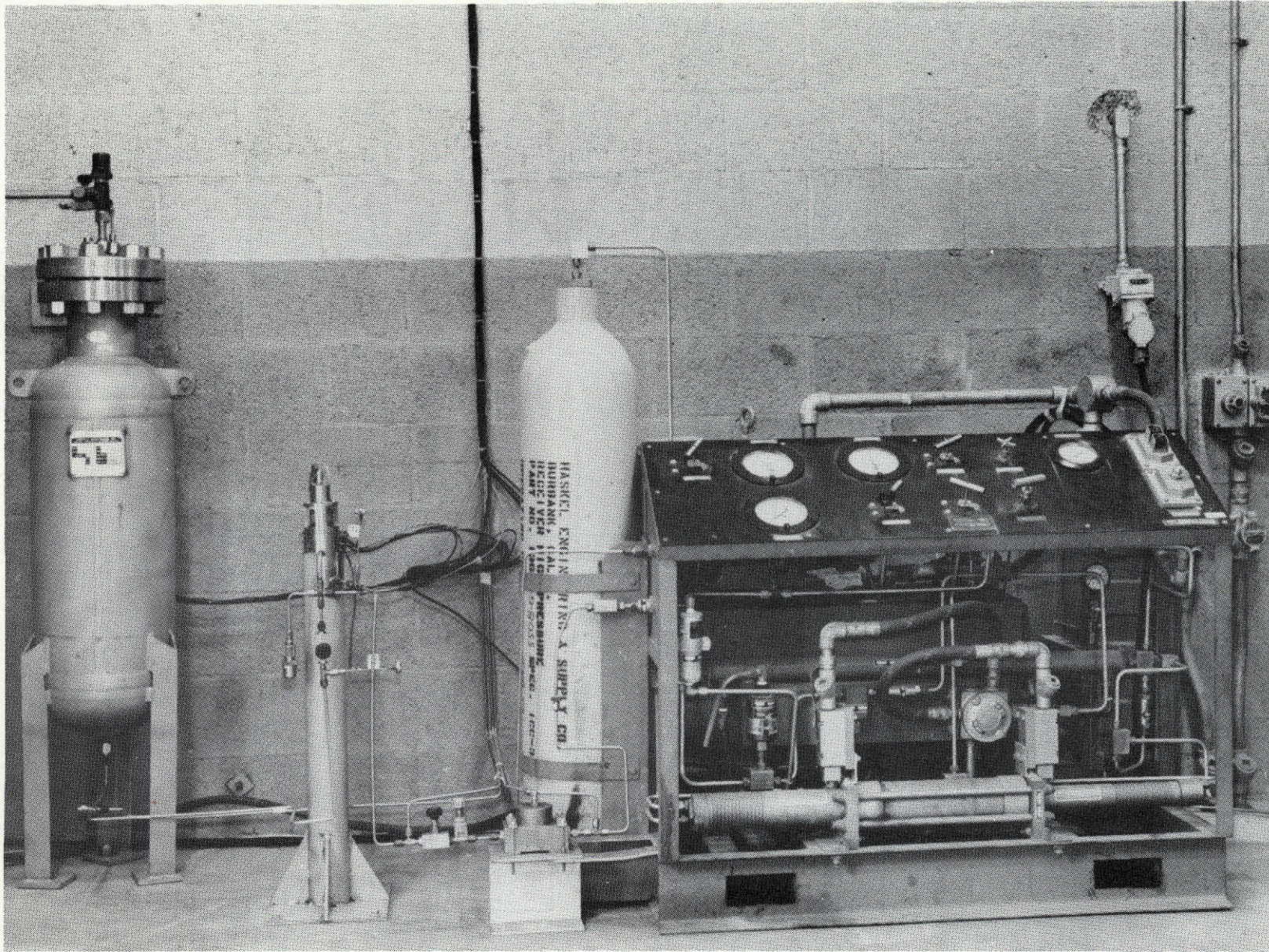
Figure 6-2

Figure 6-3   JPL Helium Regulater Program-Test Setup

NEG. 72-231-2
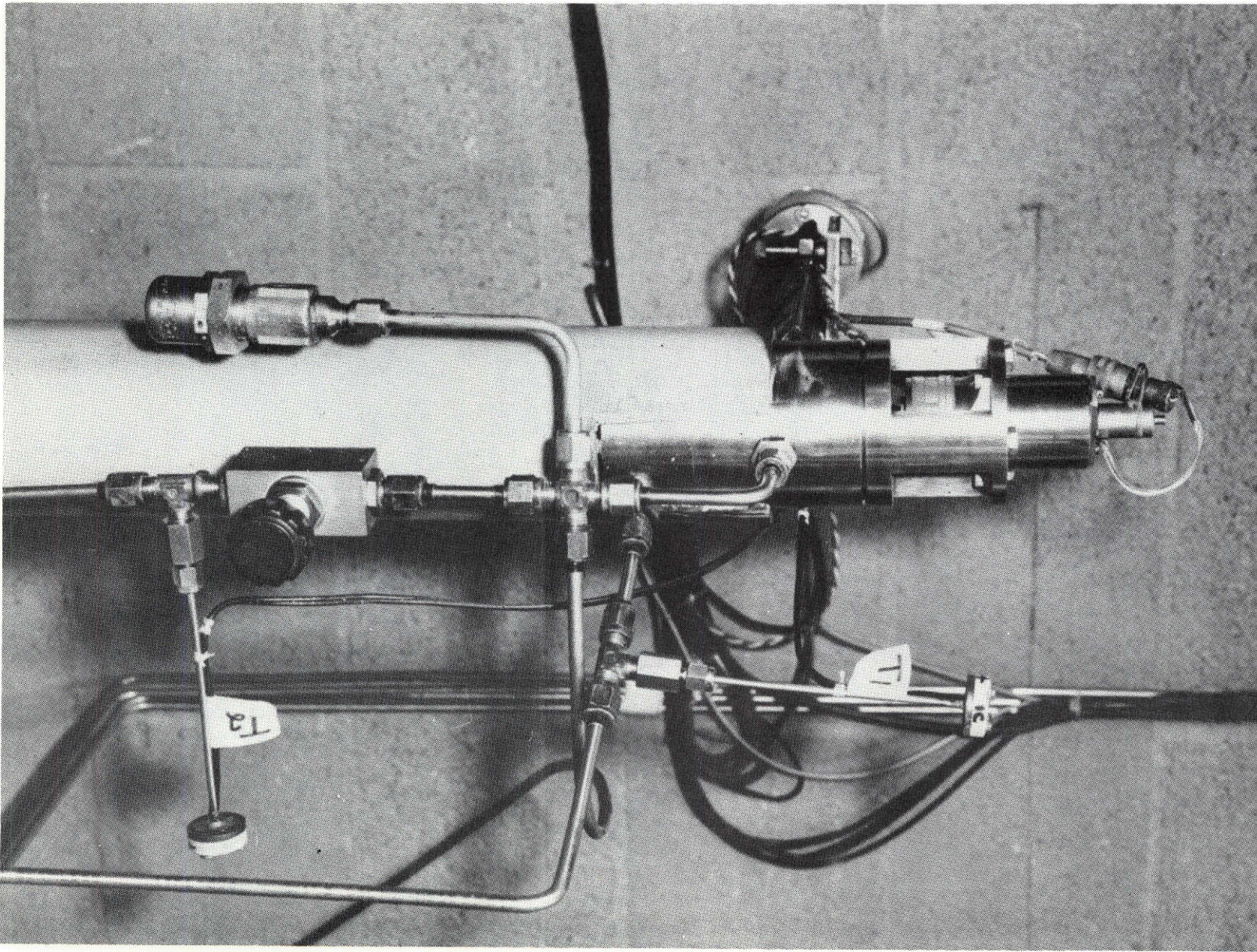
A73-6-477-5

Figure 6-4   JPL Helium Regulator Program-Test Fixture

NEG. 72-231-3
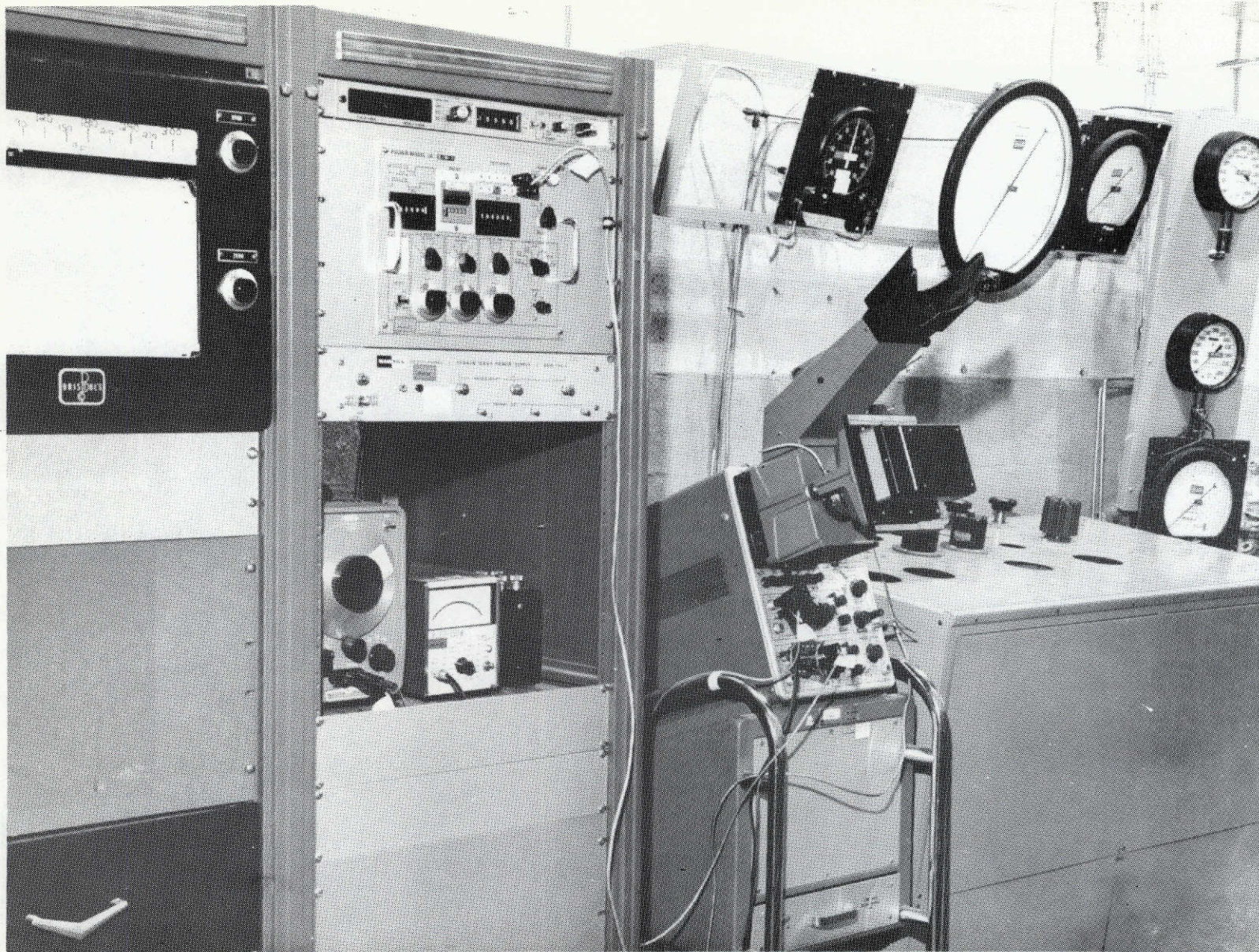
A 73-6-477-7

Figure 6-5   JPL Helium Regulator Program-Control Panel

nozzle to an ullage tank wherein the helium back pressure was controlled to approximately 240 psia by means of a relief valve. This ullage tank is also visible on the left side of Figure 6-3.

Figure 6-4 is a closeup of the test fixture as installed in the helium flow system. The inlet line to the flow fixture approaches the flow fixture from the right and the outlet line can be seen leaving the flow fixture in a direction which is almost perpendicular to the plane in the picture. The LVDT position transducer may be seen on top of the flow fixture and the solenoid actuator through the cutouts near the center of the flow fixture. Other components recognizable in Figure 6-4 are the upstream and downstream thermocouples, and the throttling valve and the relief valve located downstream of the test fixture.

Instrumentation and controls for the helium flow system are shown in Figure 6-5. The first rack on the left side of the picture holds the temperature recorder. The second rack contains the pulser required for solenoid operation as well as the signal condition equipment for the LVDT transducer. Also evident in the picture are the oscilloscope used for recording position and force traces, several pressure gages, and the controls for the facility helium regulator.

The sequence of operation for the flow system generally consisted of initially setting the facility regulator to a pressure of approximately 250 psi and opening both the manual and the test fixture valves to prepressurize the ullage tank. Subsequently, the test fixture valve was closed again and the facility regulator run up to the required operating pressure. The test fixture solenoid was then actuated again and steady state pressure drop measurements as well as dynamic and steady state force measurements were made. After the data was obtained, the facility shutoff valve was closed and the system downstream of the shutoff valve bled down.

6.3   TEST RESULTS

6.3.1   Discharge Coefficient Determination

The discharge coefficient for the regulator poppet/seat interface was determined by flowing helium through the test fixture at ambient temperature and at inlet pressures of 4000, 2500, 1000, and 400 psia. The test fixture had been designed so that by substituting a specific spacer the operating stroke of the poppet could be varied. Spacers had been fabricated to permit strokes of 0.001, 0.002, 0.005 and 0.010. Tests were performed for flowrates of up to 50% in excess of nominal flowrates. This meant that at the 4000 psia inlet pressure condition data was obtained for only the two shortest strokes; however, at the 400 psia inlet pressure, data was obtained for all strokes. These data and computer fitted curves are shown in Figure 6-6.

To permit plotting of the data in Figure 6-6, the actual flow area of the poppet/seat interface had to be determined. This flow area is a function of the poppet stroke and the seat diameter. While the seat diameter can be measured very precisely, some problems were encountered in accurately determining the poppet stroke at very short strokes. The technique utilized for measuring this stroke for steady state test was to physically remove

117

EXPERIMENTAL DISCHARGE COEFFICIENT
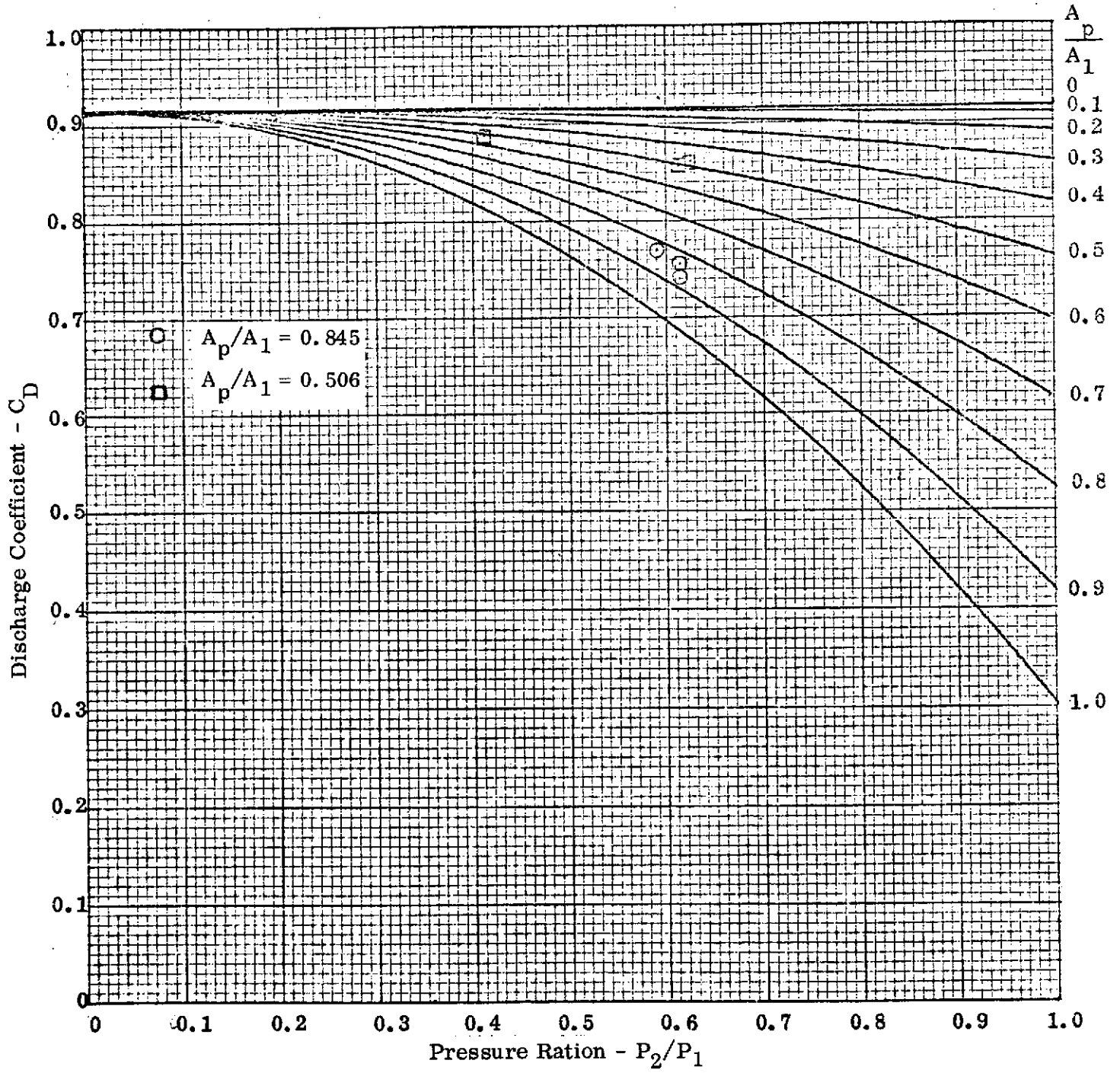
Figure 6-6

the inlet housing of the test fixture. This, in effect, removed the poppet as well as per-mitted direct access to the seat surface and the push rod. To measure the strokes, the solenoid actuator of the test fixture was energized, thereby causing the push rod to protrude out of the seat by the particular stroke dimension. A micrometer was then utilized to measure the height of the push rod above the seat surface. These measurements were repeated several times for each stroke. In making these measurements it became evident that the measurement was only accurate to within approximately 0.0005 inch. This inherent inaccuracy substantially affected the area determination for very short strokes. Thus, for a 0.001 inch stroke, the possible maximum flow area error was 50%; for a 0.002 inch stroke, it was 25%.

As a result of the inaccuracy of determining flow area at very short strokes, considerable scatter in the data obtained was observed. Nevertheless, the data obtained at the larger strokes is believed to be sufficient to permit the fitup of the curves as shown in Figure 6-6. As evident from this figure, the discharge coefficient varies between 0.915 for very low pressure ratios and low area ratios to approximately 0.7 at the higher pressure ratios and higher area ratios of interest.

6.3.2   Flow Force Data

Poppet flow forces were measured at 4000 psia, 2500 psia, and 400 psia inlet pressure and ambient temperature. Both dynamic flow force data and steady state flow force data were obtained. The reason for making both dynamic and steady state measure-ments was the concern expressed by some dynamic analysts that it appeared possible that during the opening motion the shock waves generated in the poppet/seat area as the gas decelerates from supersonic to subsonic conditions would probably not be stationary and therefore might have an influence on the flow force. However, based on the test data obtained during this program, this concern did not seem to be warranted, since no measurable differences between steady state and dynamic flow force data were noted.

Dynamic flow force data was obtained by recording the LVDT output and the load cell output on the oscilloscope. Several precautions were taken to assure that the frequency response to these transducers and their signal condition was sufficient to measure the relatively fast 2 - 5 ms response of the poppet. As the result of a number of checkout tests, several improvements were made to the signal conditioning equipment to obtain time constants of 0.1 millisecond. Figure 6-7 shows two oscilloscope pictures at time constants of 0.4 and 0.1 milliseconds and at an operating pressure of 2500 psia. These data are also representative of the type of traces obtained during the test program. A brief explanation of the traces is in order.

During the dynamic testing it became evident that depending on the inlet pressure and on the operating voltage of the solenoid (which determined the response of the solenoid and, in turn, of the poppet) that the actuator moving element stack exhibited two types of motion. For the higher pressures and the lower operating voltages (slower response), the moving stack initially traversed the clearance between the push rod and the poppet at no load and then came to rest against the poppet as the load exerted on the push rod increased; after the push rod force reached the required poppet lift-off force the motion again proceeded to accelerate until the poppet reached the full open position as determined by the solenoid armature in the actuator hitting its stop. This type of motion is shown in both of the pictures of Figure 6-7. It is also evident from these pictures that as the actuator hits the poppet and then subsequently hits the armature stop, considerable ringing in the force measurement is

DYNAMIC FORCE DATA - FREQUENCY RESPONSE
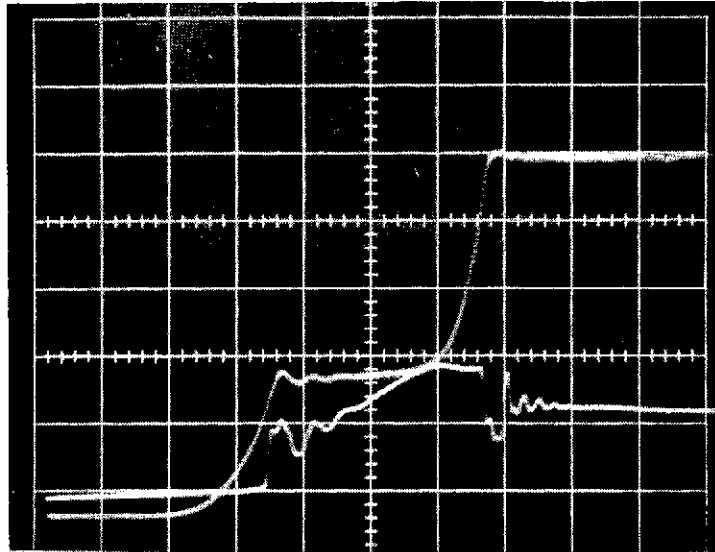
0.4 ms Time Constant
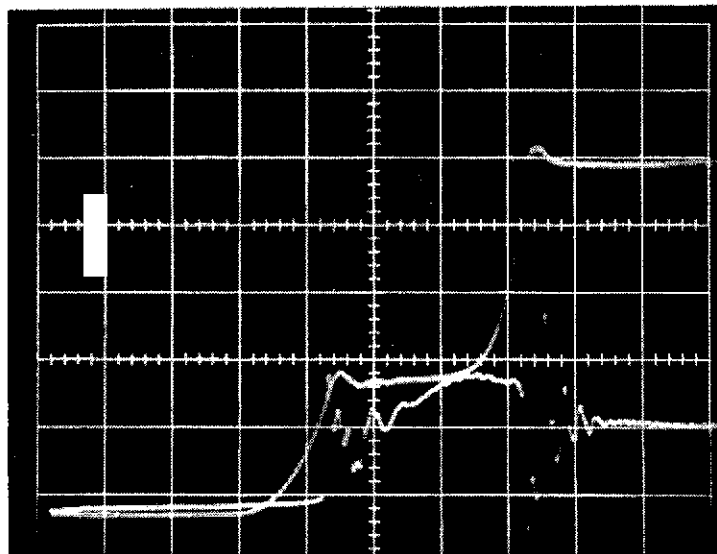
0.1 ms Time Constant

OUTLET PRESSURE 2500 PSIA, SWEEP RATE - 2ms/cm

UPPER TRACE AT START: LOAD CELL FORCE OUTPUT

LOWER TRACE AT START: LVDT POSITION

Figure 6-7

120

observed. A comparison of the type of motion just described and the second type of motion may be seen in Figure 6-8. This figure shows a full pulse (opening and closing motion) at an operating pressure of 1000 psia. The upper photograph shows operation at 36 volts and the lower photograph at 15 volts. Corresponding poppet motion times are 2 milliseconds and 4 milliseconds. As evident from the upper picture, the actuator moving stack does not stop when it comes in contact with the poppet, but rather has sufficient momentum to carry it on to the full open position. The traces for this type of motion were somewhat more difficult to analyze since considerable ringing in the force measuring transducer was occurring during the poppet motion. The data presented in Figures 6-7 and 6-8 are typical of the dynamic force data obtained during this program.

To determine the net flow force on the poppet, similar force versus stroke data was obtained at zero psia inlet conditions. The forces thus measured were considered tear forces due to spring, friction, and acceleration forces inherent in the test fixture and were subtracted from the total forces measured at the various inlet pressures. The net force was therefore the actual flow force. The same technique was utilized in determining the steady state flow forces. As mentioned previously, no significant differences between steady state and dynamic flow forces were observed.

A summary of the flow force data is presented in Figure 6-9. The data is plotted at various inlet pressures as a function of poppet stroke. This data was subsequently incorporated into the final regulator steady state and dynamic performance models.

7. PROPELLANT FEED SYSTEM DYNAMIC MODELING

To determine inlet pressure surges due to the opening of upstream isolation valves, engine start and steady state operation, and system lockup upon closing of the engine propellant valves, a complete propellant feed system was modeled on the analog computer. This feed system model included the final regulator dynamic model as discussed in Section 5.3.3 of this report. The dynamic behavior of the feed system was determined at both nominal and minimum helium gas temperatures for both the MMH and flox systems. Dynamic simulation included both the motor firing mode as well as the step response mode defined previously in Section 5.1.7 of this report. In addition, slam starts due to the opening of the upstream isolation valves, were simulated as well as the effects of liquid in the gas damping orifice.

7.1 FEED SYSTEM CONFIGURATION AND ITS ANALOG MODEL

The quantitative performance model described a single circuit of the bipropellant feed system, either fuel or oxidizer. A schematic of the physical system is shown in Figure 7-1. The gas circuit consists of the pressurant tank, line filter, helium isolation valve regulator (with internal filter), and ullage in the propellant tank. The propellant circuit consists of the feed line with a series of flow impedances including two propellant filters, two valves (isolation and propellant), trim orifice, injector/manifold, and rocket motor. The math model of the feed system is also shown in Figure 7-1. In the helium circuit, the pressurant tank, regulator and ullage is mathematically described. The helium line filter effects were considered to be negligible and were omitted. However, the modeling did include

DYNAMIC FORCE DATA – FULL PULSE
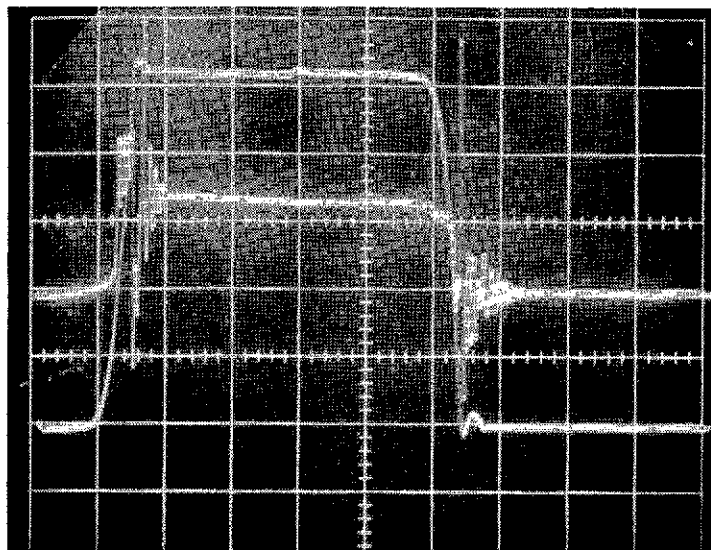
36 Volt Solenoid Operation
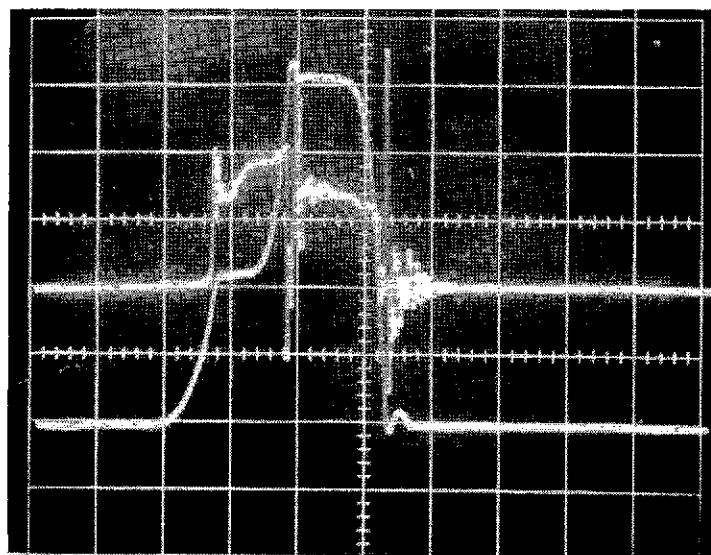
15 Volt Solenoid Operation

OUTLET PRESSURE 1000 PSIA, SWEEP RATE – 10ms/cm
UPPER TRACE AT START: LOAD CELL FORCE OUTPUT
LOWER TRACE AT START: LVDT POSITION

Figure 6-8

122

FLOW FORCE VS STROKE
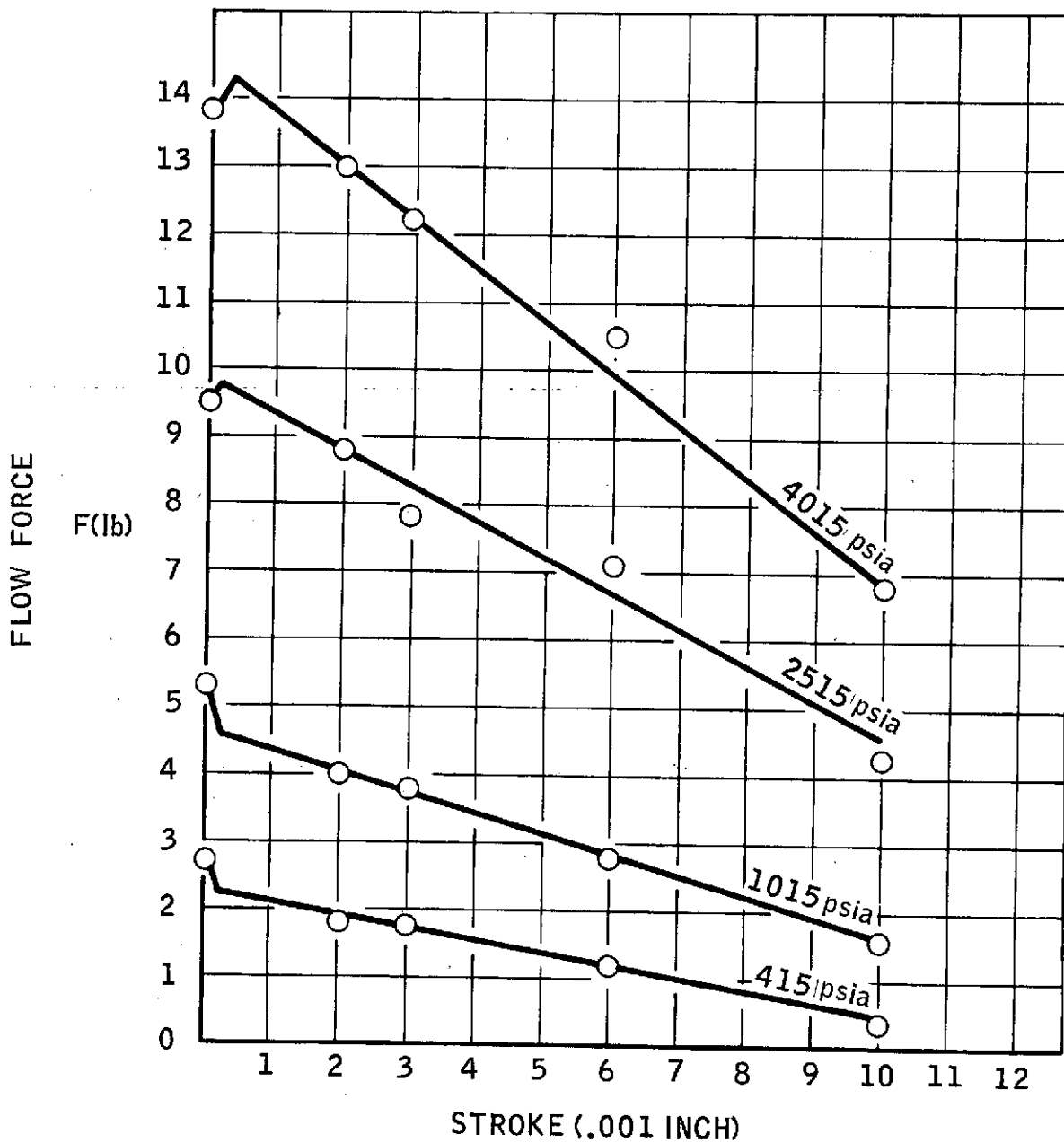
Figure 6-9

FEED SYSTEM SCHEMATIC AND MATH MODEL

PHYSICAL SYSTEMS
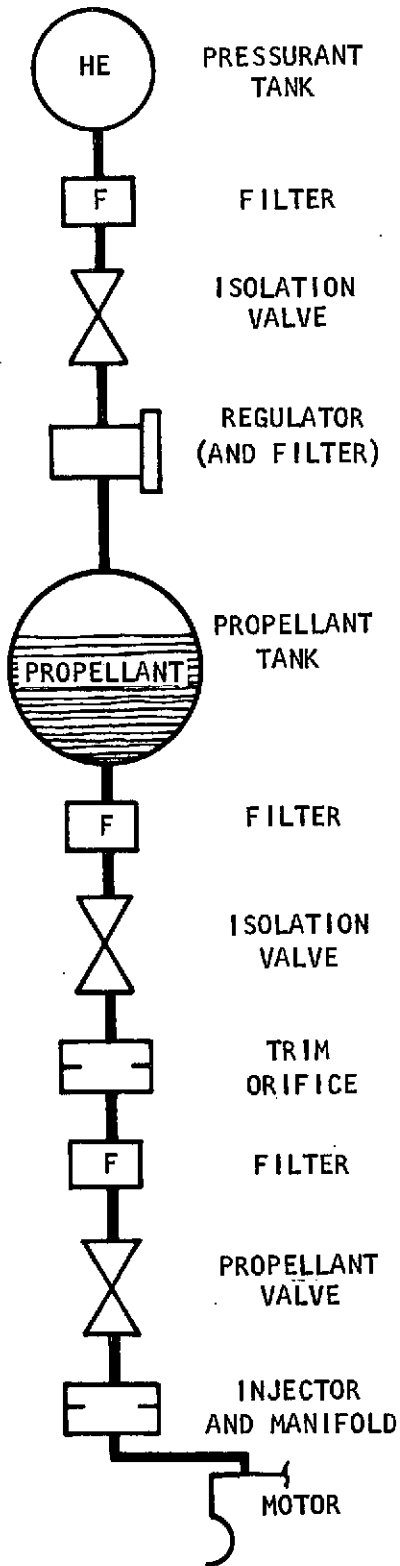
MATH MODEL
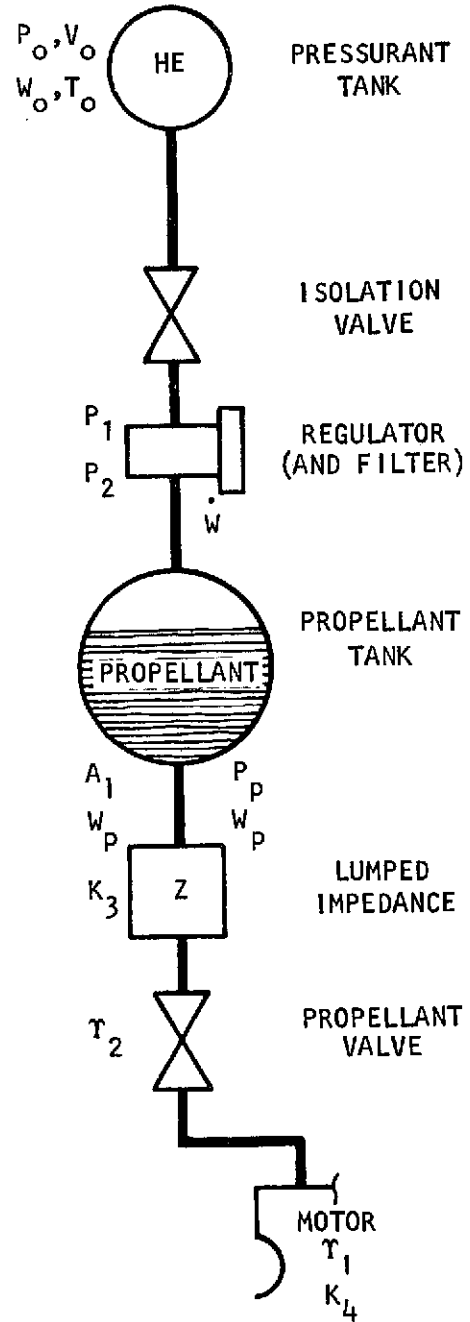
Figure 7-1

the internal regulator filter. The propellant circuit included the feed line, propellant valve, motor dynamics, and a lumped impedance representing the cumulative flow characteristics of the two in-line propellant filters, isolation valve, trim orifice, and injector and manifold.

The added physical equations which complete the feed system are shown in Table 7-I. These equations are in addition to those utilized in the regulator and propellant tank modeling previously summarized in Table 5-XIII. The pressurant tank equations account for the helium compressibility, helium mass flow from the tank, and helium temperature drop due to adiabatic expansion. The temperature rate is arbitrary. The regulator internal filter characteristics are based upon a laminar flow model. The propellant line dynamics include the acceleration of the fluid column in the propellant feed line between the propellant tank and motor and the lumped flow impedance characteristics. The engine dynamics are linearized from the fill dynamics of the motor chamber. The propellant valve dynamics are also linearized where the valve time constant is arbitrary. Provisions were made to include modeling of the damper in the regulator in the eventuality that it were to become filled with propellant. In the slam start model, the gas volume downstream of the regulator poppet/seat interface was divided into two parts, the volume within the regulator between the poppet/seat interface and outlet port and the volume comprised by the helium line between the outlet port and ullage. The helium pressure in the regulator internal volume was determined by the net mass storage within that volume.

The complete quantitative performance computer model is shown in Figure 7-2, and the setup for slam starts is shown in Figure 7-3. The slam start circuit includes provisions for providing multi-value step pressure inputs to the regulator as determined by the application of shock tube theory for the helium line between the helium isolation valve and the upstream side of the regulator internal filter. The potentiometer schedule for the additional components of the feed system is shown in Table 7-II.

7.2 SLAM START SIMULATION

Slam starts were simulated by assuming that the regulator outlet pressure was initially at 0 psia and that the isolation valves upstream of the regulator were suddenly opened to admit the 4000 psi pressurant and supply pressure into the regulator. The primary reason for this simulation was the concern that a momentary overpressure might result in the outlet housing of the pressure regulator which could conceivably damage the actuator bellows. Also of concern is a momentary overpressure (>280 psia in this case) in line from the regulator outlet, which might prematurely actuate the burst/relief device normally incorporated at this location (see Figure 4-1). Data from the analog simulation is presented in Figure 7-4. As a result of shock waves traveling back and forth in the feed line between the isolation valve and the regulator inlet, the initial inlet pressure felt at the regulator poppet/seat interface is approximately 2700 psi for a period of 8 milliseconds. Upon cessation of these shock waves the inlet pressure returns back up to the 4000 psi pressurant supply tank pressure. The regulator internal pressure at the outlet side meanwhile rises at first to a maximum pressure of 112 psia, then continues gradually to the lockup condition. It was therefore concluded that for this particular regulator configuration, overpressure during slam start was not a problem.

Figure 7-2

A72-11-370-49
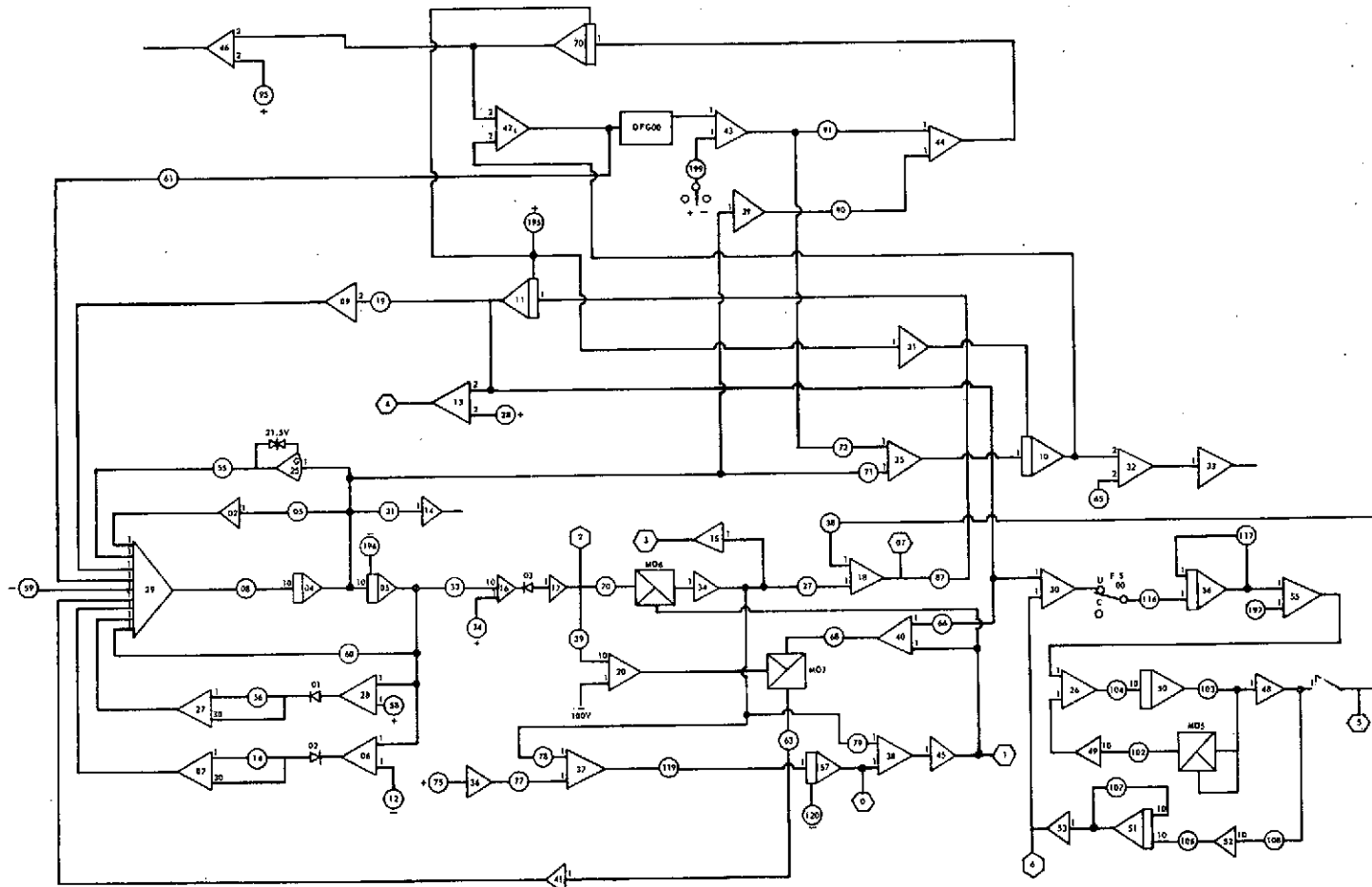
CIRCUIT ADDITION FOR SLAM STARTS
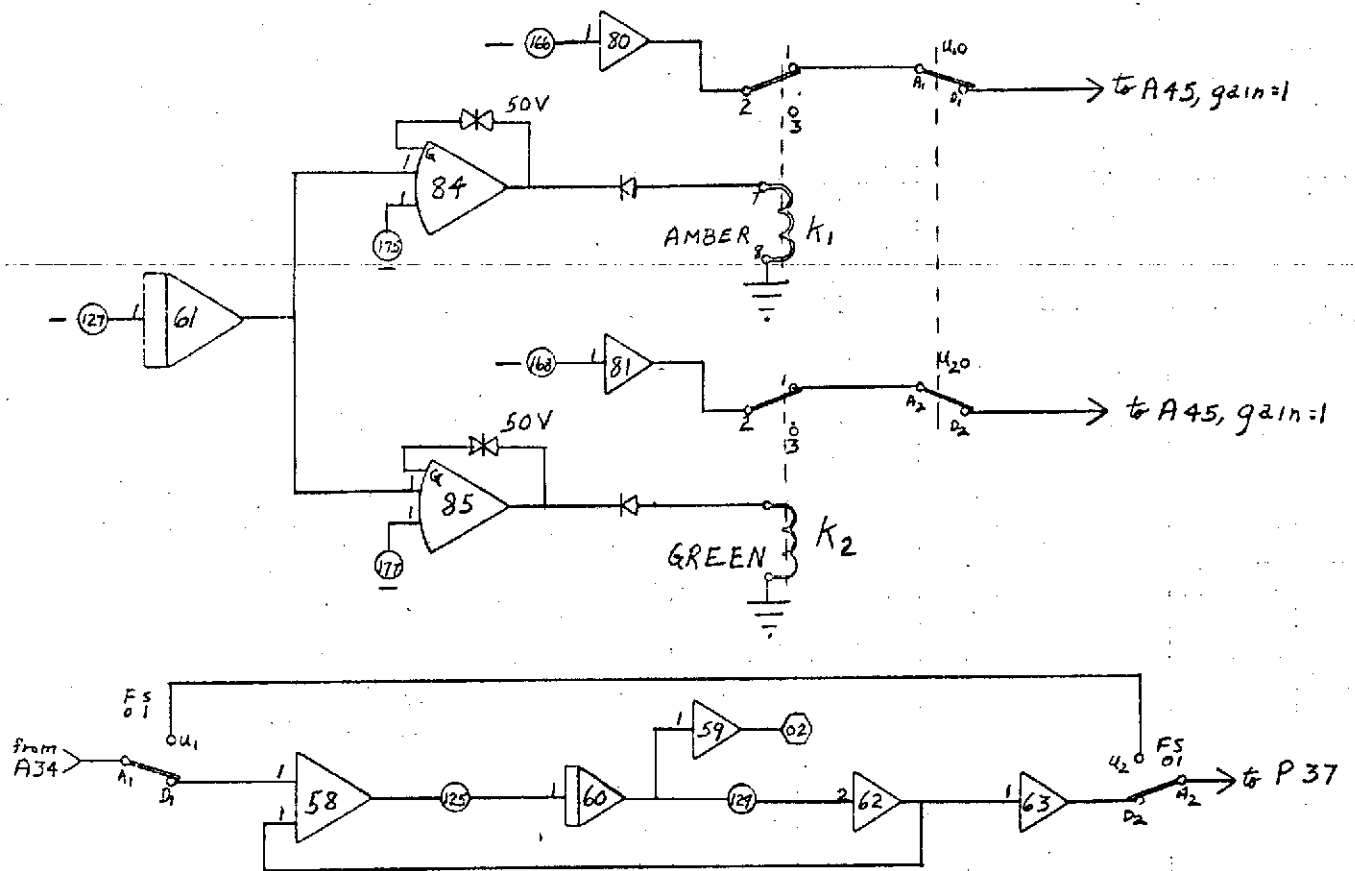
Figure 7-3

SLAM START ANALOG SIMULATION

FLOX, $T = 150°R$, $P = 4000$ psia, $V_T = 1.769$ ft^3

Tank Pressure, P_0, psia

Regulator Inlet Pressure, P_1, psia

Regulator Internal Pressure, P_2 psia

10 ms
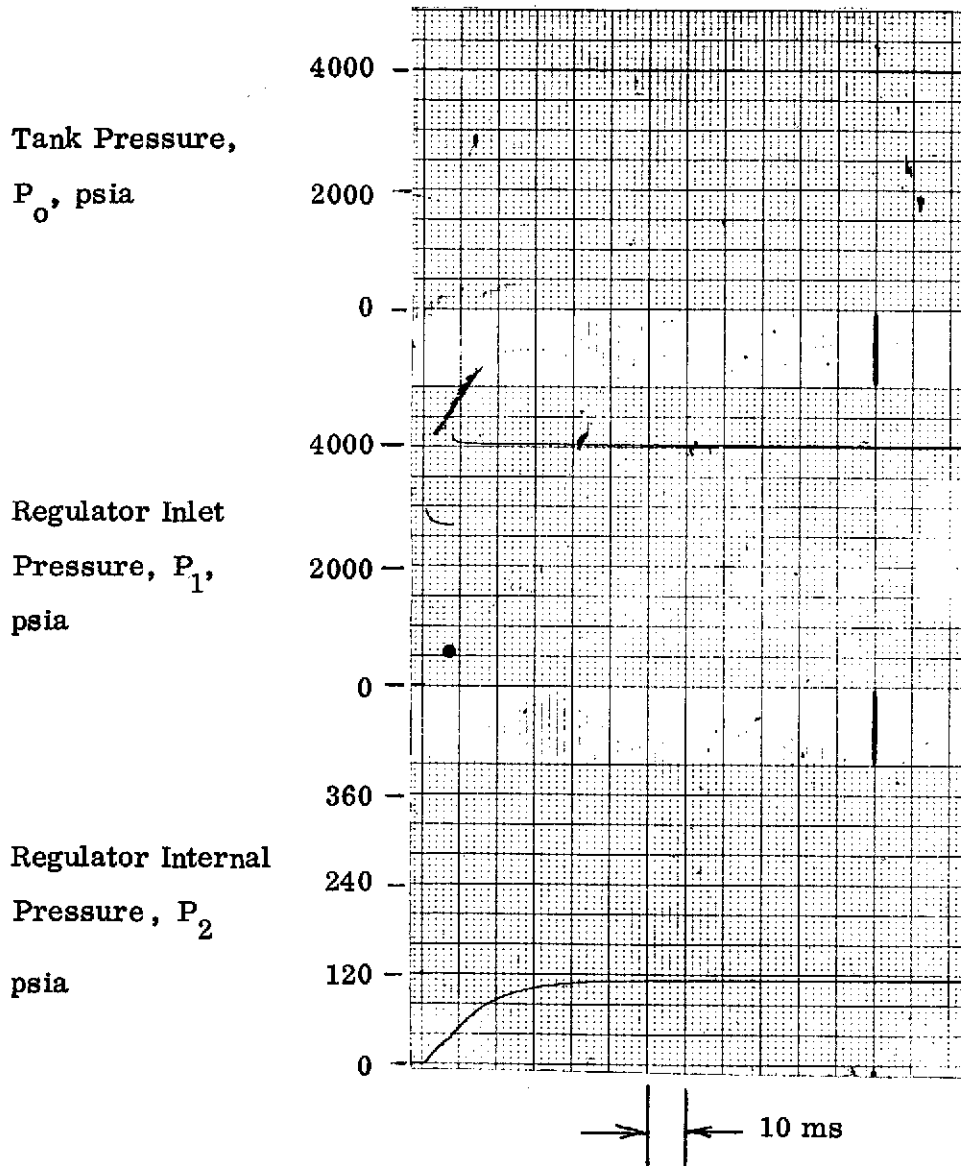
Figure 7-4

TABLE 7-I

FEED SYSTEM - ADDED PHYSICAL EQUATIONS

Pressurant Tank:

$$\dot{P}_o = - \frac{ZR\,T_o}{V_o}\,\dot{W} - \frac{ZR\,W_o}{V_o}\,\dot{T}_o$$

$$\dot{T}_o = \text{Constant}$$

$$P_o = P_{oi} + \int_o^t \dot{P}_o \; dt$$

Regulator Filter (Laminar):

$$P_o - P_1 = \frac{R\,T_o\,\dot{W}}{K_2\,P_o}$$

Propellant Line Dynamics:

$$\dot{V}_p = (P_2 - P_3)\,\frac{A_L\,g}{W_p}$$

$$V_p = V_{pi} + \int_o^t \dot{V}_p \; dt$$

$$\dot{W}_P = V_p\,\rho_P\,A_L$$

$$P_2 - P_3 = K_3\,\dot{W}_P^2$$

Engine Dynamics:

$$\frac{P_3(S)}{\dot{W}_P(S)} = \frac{K_4}{1 + \tau_1\,S}$$

$$\tau_1 = \frac{V_e}{R_e\,\sqrt{T_e}\,(C_m\,C_D)\,A_T^*}$$

TABLE 7-I (Continued)

Propellant Valve Dynamics:

$$\frac{\dot{W}_p(s)}{e_i(s)} = \frac{1}{1 + \tau_2 S}$$

$$\tau_2 = \text{Specified}$$

Liquid-Filled Damper (Laminar):

$$\dot{W}_{p_2} = \dot{Y} A_B \rho_p$$

$$P_2'' - P_2' = \frac{32 \ L \ \mu}{\rho_p \pi \ C^4 \ g} \ \dot{W}_{p_2}$$

Slam Start:

$$\dot{P}_{21} = \frac{R \ T_o}{V_R} \left(\dot{W} - \frac{P_{21} A_R \ C_m \ C_D}{\sqrt{T_o}} \right)$$

$$P_{21} = P_{21_i} + \int_o^t \dot{P}_{21} \ dt$$

130

TABLE 7-II

FEED SYSTEM – ADDITIONAL POTENTIOMETER SCHEDULE

Potentiometer * Number	Parameter	Units
11	$32\,L\,\mu\,A_B^2/160\,\pi\,C^4\,g$	lbf-sec/in.
38	$P_2/400\,V_T\,\rho_P$	lbf/in.^{2}-lbm
70	$250\,\pi\,D_{SE}\,C_m\,C_D/\sqrt{T_1}$	in.-lbm/lbf-sec
75	$\dot{T}_0/10^4$	°R/sec
77	$ZR\,W_0/100\,V_0$	lbf/in.^{2}-°R
78	$ZR\,T_0/5,000\,V_0$	lbf/in.^{2}-lbm
79	$R\,T_0/K_2\,P_0$	lbf-sec/in.^{2}-lbm
102	$K_3/1000$	lbf-sec^2/in.^{2}-lbm^2
103	$50\,\rho_P\,A_L$	lbm/in.
104	$A_L\,g/2,500\,W_p$	in.^{3}/lbf-sec^2
106	$1/10\,\tau_1$	1/sec
107	$1/10\,\tau_1$	1/sec
108	$K_4/2000$	lbf-sec/in.^{2}-lbm
116	$1/\tau_2$	1/sec
117	$1/\tau_2$	1/sec
118	$1/5,000$	–
125	$R\,T_0/2\times10^6\,V_R$	lbf/lbm-in.^{2}
127	$\dot{t}/10^8$	–
129	$1000\,A_R\,C_m\,C_D/\,T_0$	lbm-in.^{2}/sec-lbf
166	$P_{01}/5,000$	lbf/in.^{2}
168	$P_{02}/5,000$	lbf/in.^{2}
175	$t_1/104$	sec
177	$t_2/104$	sec

* Reference Figure 7-2

7.3 ENGINE START, STEADY STATE AND STOP SIMULATION

Typical motor start, steady state, and stop, as well as step response data are presented in Figures 7-5 through 7-13. The step response data is presented primarily because the typical motor start and stop data proved to be rather uninteresting dynamically. Figure 7-5 shows regulator operation at 4000 psi inlet pressure and with a 0.2942 cubic ft ullage for both nominal and minimum helium gas temperatures. As evident from this figure, outlet pressure variations are less than 0.1 psia during this motor firing cycle. To determine what type of poppet motion would be experienced for both the fastest MMH system (4000 psi inlet pressure and 0.2942 cubic ft ullage) and the slowest MMH system (400 psia inlet pressure and 4.5882 cubic ft ullage) step responses were simulated. These data are shown in Figure 7-6. As evident from this figure, the poppet motion damps out very rapidly and no variations in regulator outlet pressure are noted. Figure 7-7 presents the same simulation as Figure 7-6, except that the helium gas operating temperature is 430.9°R instead of 530°F and also shows that poppet motion is damped out very rapidly.

Figures 7-8 and 7-9 are motor start and stop simulations of the flox feed system operating at an inlet pressure of 4000 psia, an ullage volume of 1.769 cubic ft and both nominal and minimum helium gas temperatures. These data also show very steady outlet pressure with no overshoot characteristics upon motor termination. Since these data are again rather uninteresting, the step response for the flox system was also determined and is presented in Figures 7-10 and 7-11. As for the MMH system, the poppet motion is also damped out very rapidly for the flox system and no noticeable outlet pressure oscillations occur.

7.4 SIMULATION OF LIQUID-FILLED DAMPING ORIFICE

Although the final regulator design as described in Section 5.3 of this report featured the gas damping orifice in a separate prepressurized cavity such that there is no possibility of liquid being introduced into the damping orifice, as a matter of interest a condition where the entire cavity would be filled with liquid rather than with gas was also simulated. Since the step response mode (described in Section 5.1.7) simulates the worst possible dynamic condition, this mode was run on the analog computer for the MMH system for both the slowest and fastest configuration at nominal temperature. These data are presented in Figures 7-12 and 7-13. As evident from these figures, even a liquid-filled damping orifice will not result in any noticeable outlet pressure oscillations since the damping orifice is rather large and the time constant for the pressure regulator with the liwuid-filled damping orifice is still considerably faster than that for the entire feed system.

In conclusion it may be stated that it is apparent that under all of the operating conditions considered, the rather rapid response characteristics of the regulator in combination with the fairly slow response characteristics of the entire feed system effectively eliminate overshoot characteristics during both startup and shutdown conditions even when the damping orifice is filled with liquid.

MOTOR START AND STOP
MMH SYSTEM

4000 PSI Inlet Pressure, 0.2942 ft^3 Ullage
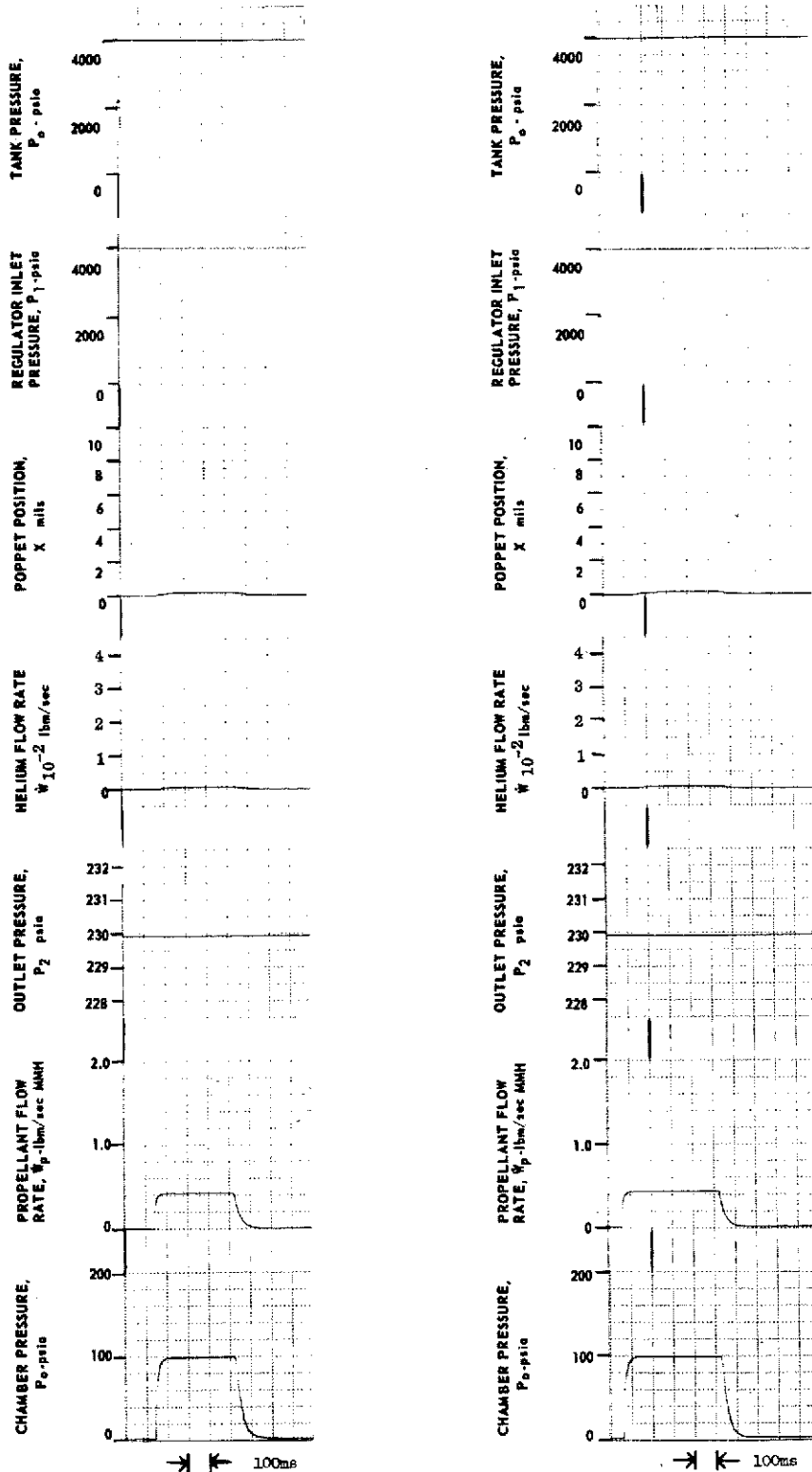
Figure 7-5

STEP RESPONSE
MMH FEED SYSTEM, 530°R

400 PSI $V_T = 4.5882$ ft^3 4000 PSI V_T 0.2942
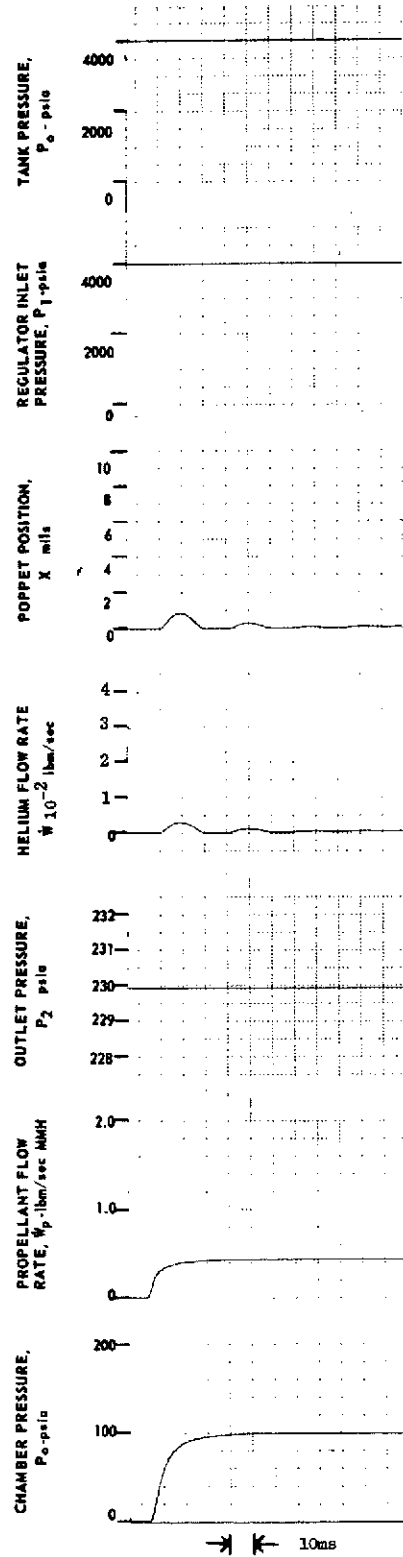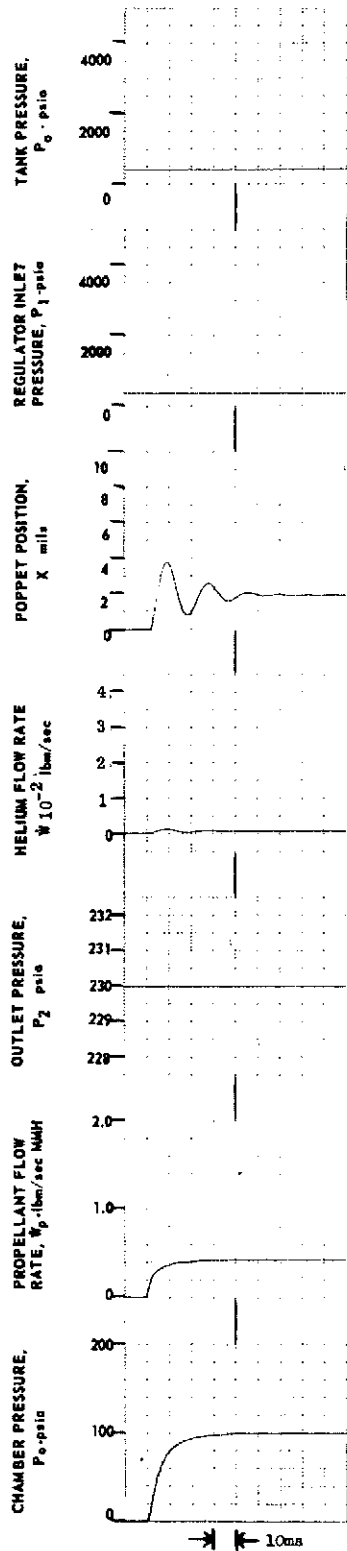
Figure 7-6

STEP RESPONSE
MMH SYSTEM, 430.9°R

$4000 \text{ PSI} \quad V_T = 0.2942 \text{ ft}^3 \quad 400 \text{ PSI} \quad T = 4.5882 \text{ ft}^3$

Figure 7-7

135
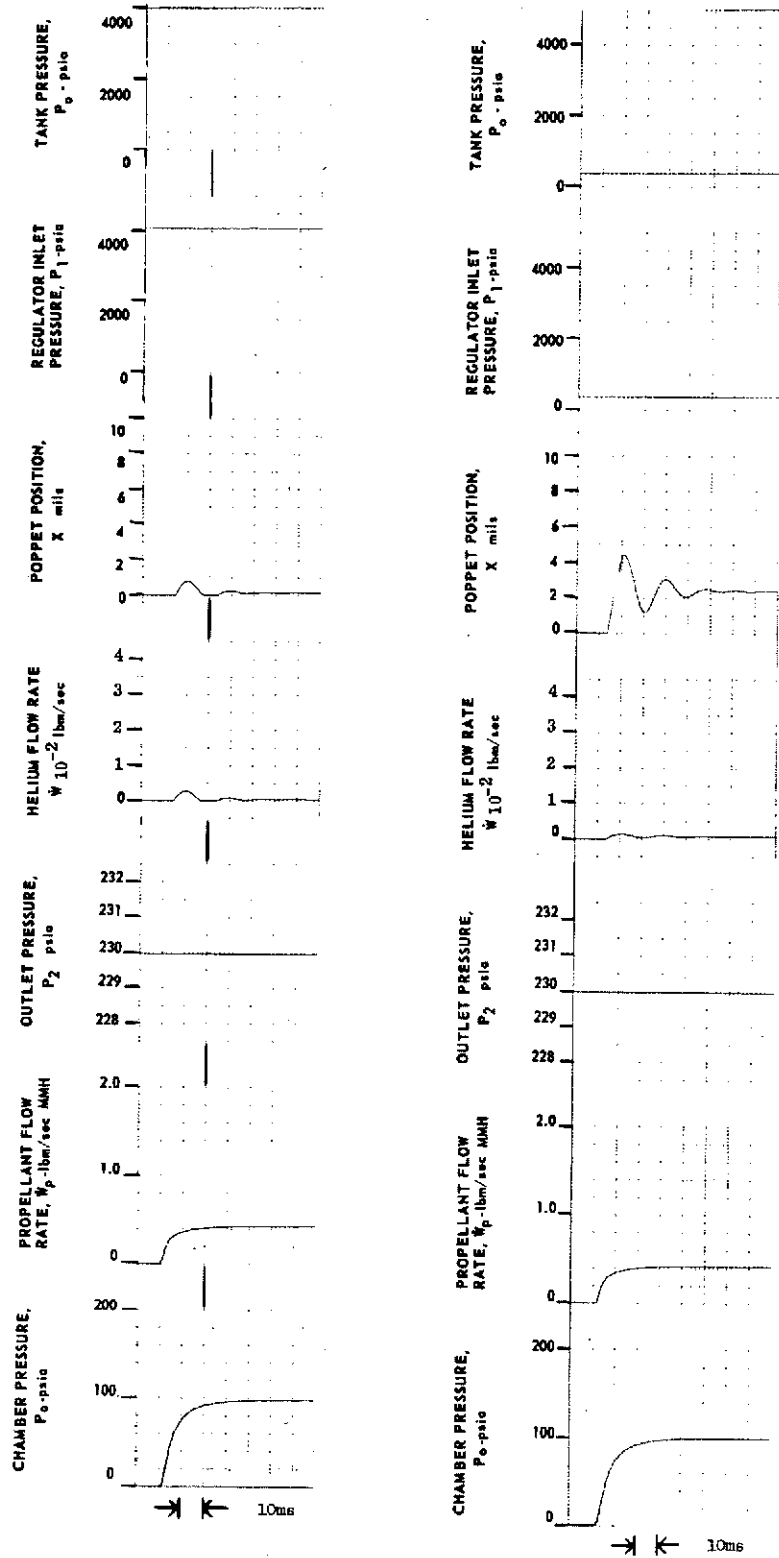
MOTOR START AND STOP
FEED SYSTEM - FLOX, 150°R

4000 PSIA $V_T = 1.769$ ft^3

Figure 7-8

136
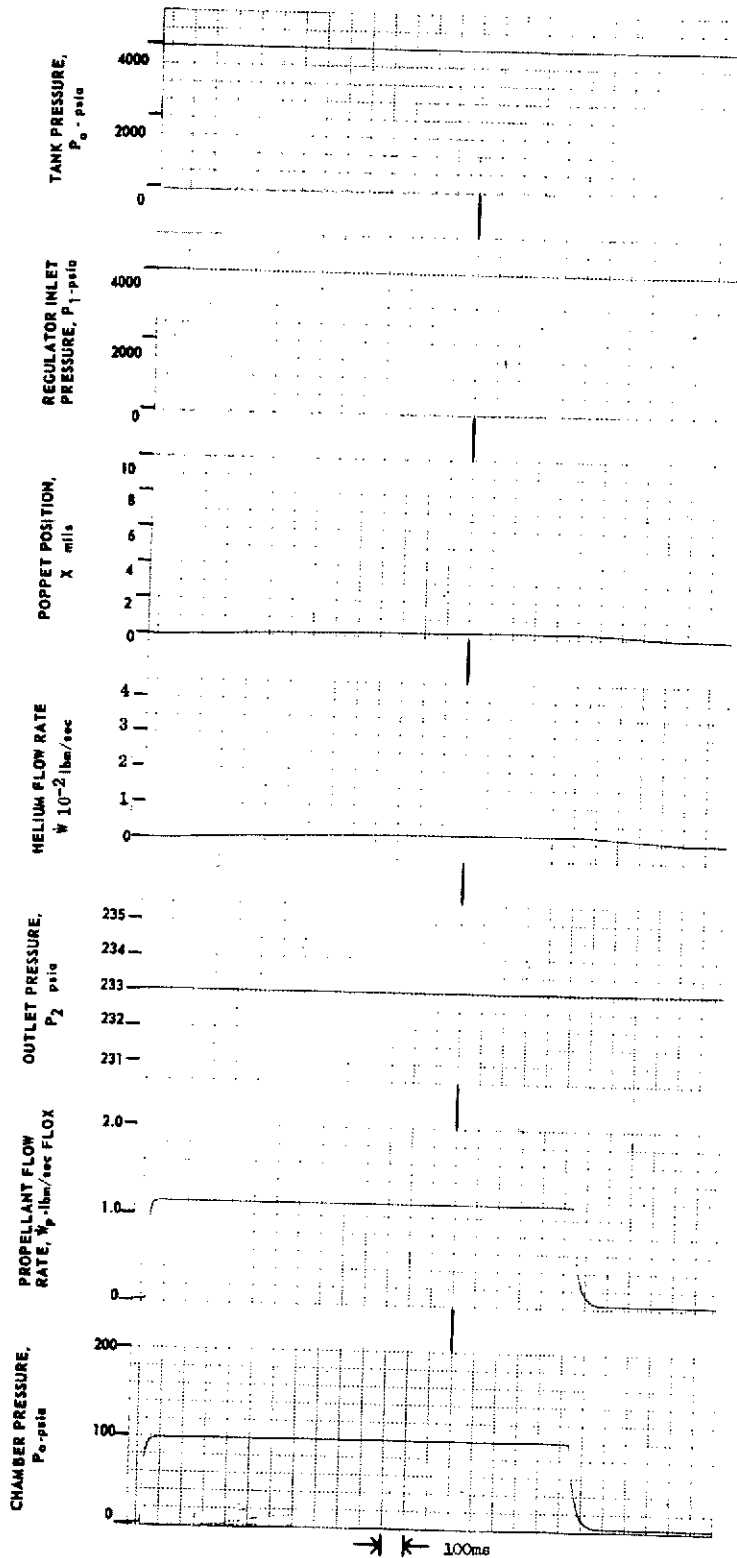
MOTOR START AND STOP
FEED SYSTEM - FLOX

4000 PSI $T_O = 102°R$ $V_T = 1.769$ ft^3

Figure 7-9

137
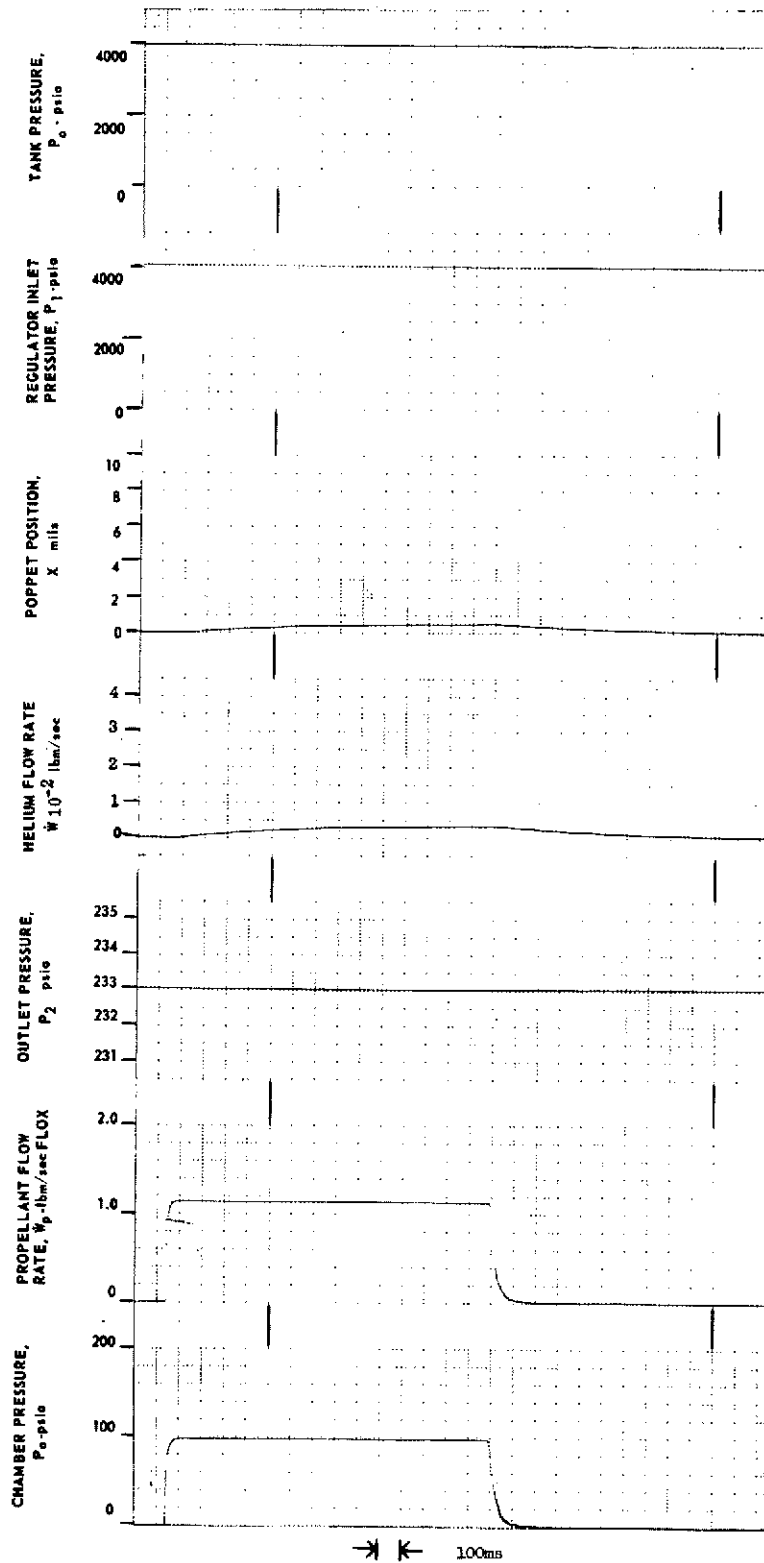
STEP RESPONSE
FLOX SYSTEM, 150°R

A73-6-477-44

400 PSI $V_T = 7.856$ ft^3 **4000 PSIA** $V_T = 1.769$ ft^3

Figure 7-10

138
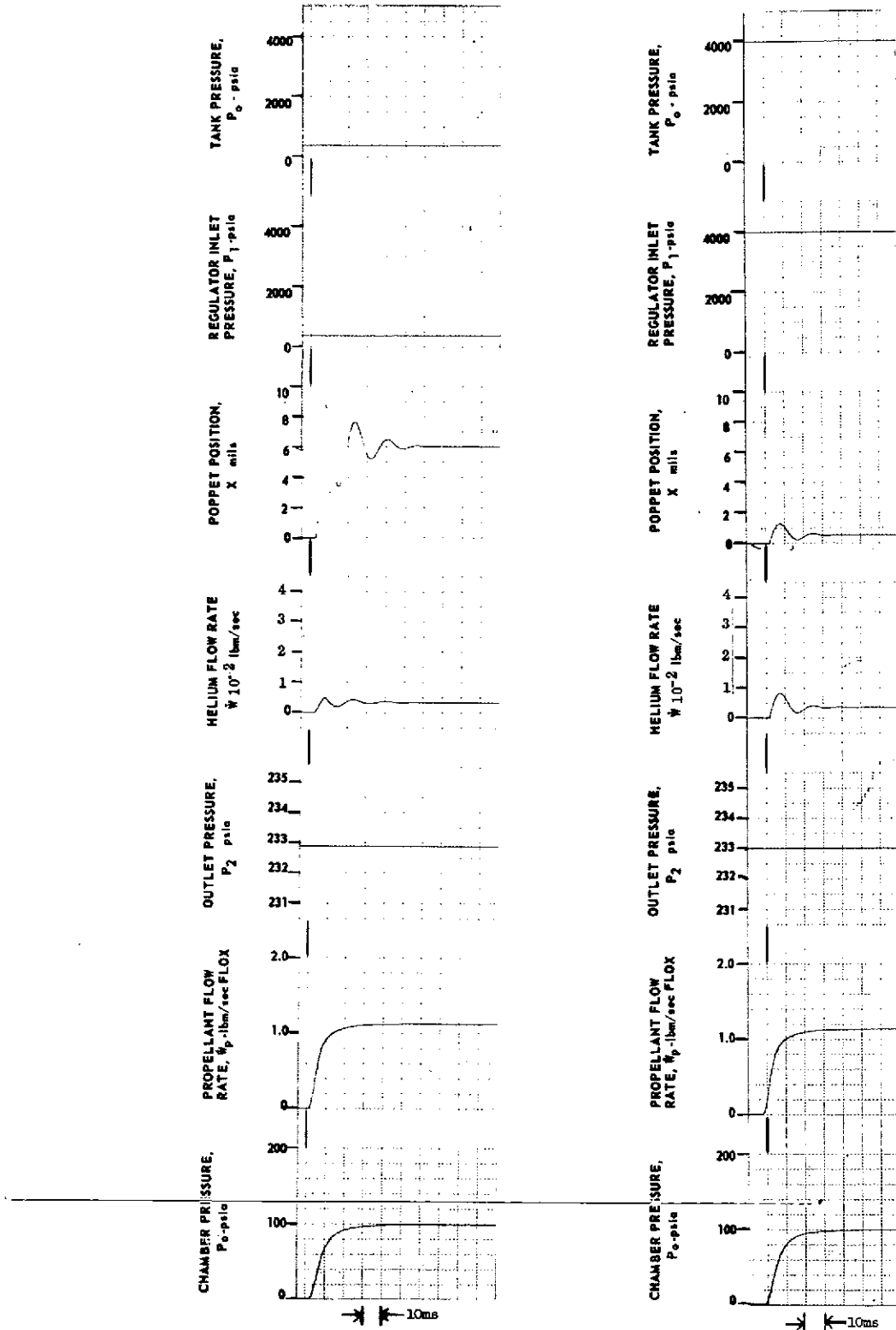
STEP RESPONSE
FLOX FEED SYSTEM, 102°R

4000 PSI, $V_T = 1.769$ ft^3 400 PSI $V_T = 7.856$ ft^3
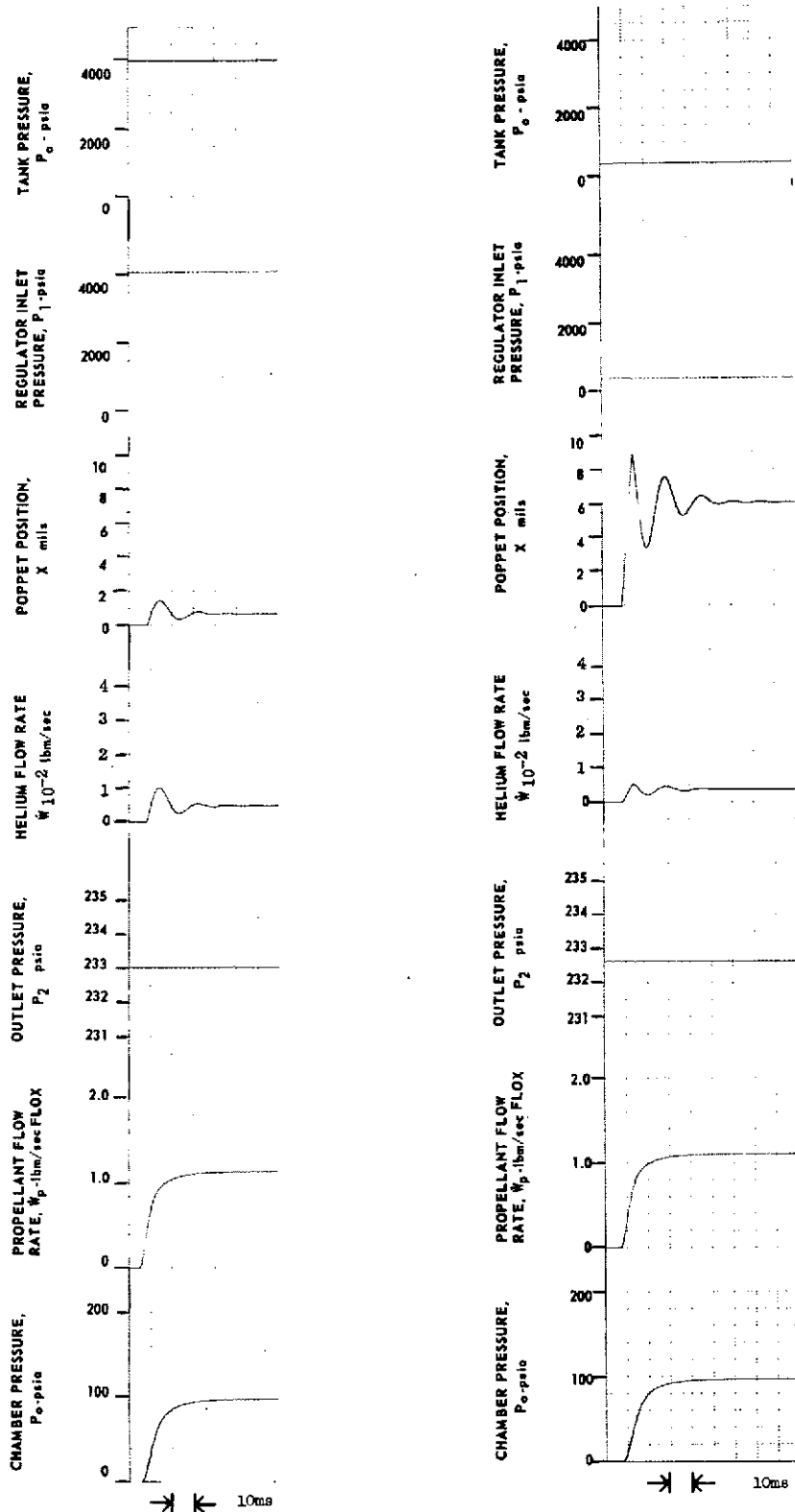
Figure 7-11

STEP RESPONSE - LIQUID FILLED DAMPER (LAMINAR)
MMH SYSTEM
4000 PSI, $T_0 = 530°R$, $V_T = 0.2942$ ft^3

Figure 7-12

140
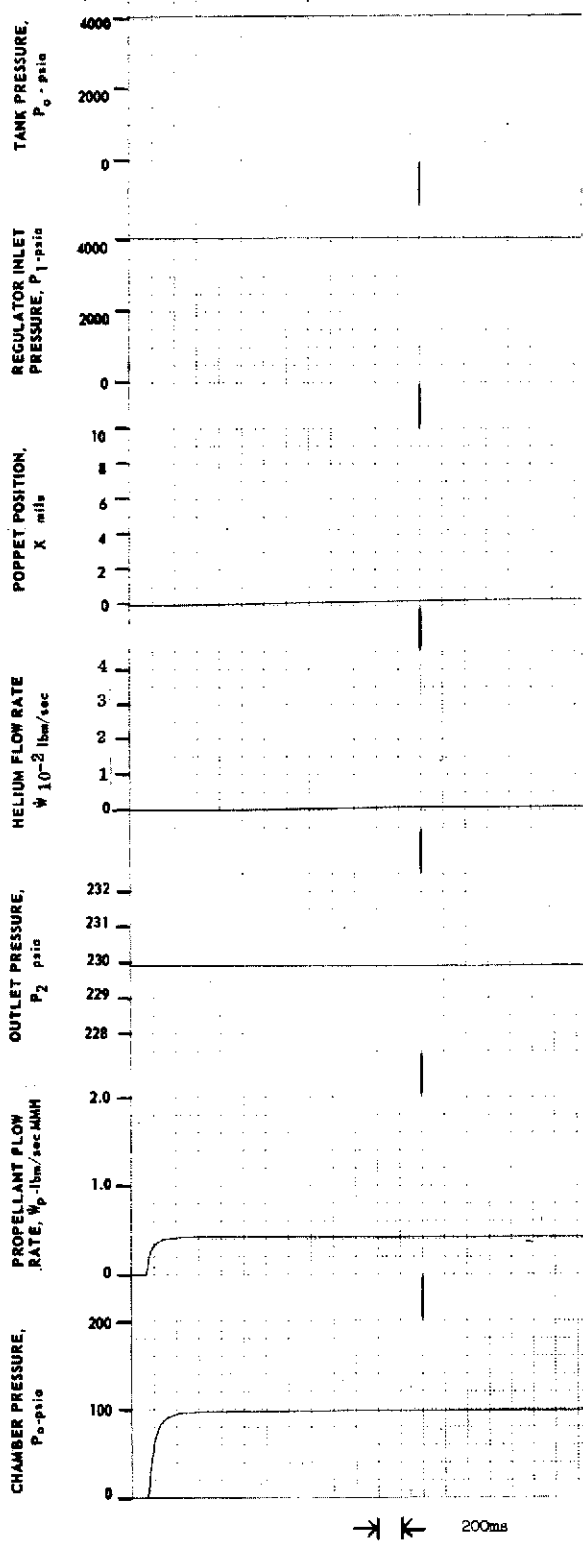
STEP RESPONSE – LIQUID FILLED DAMPER (LAMINAR)
MMH FEED SYSTEM

400 PSI, $T_0 = 530°R$, $V_T = 4.5882$ ft^3

A73-6-477-41

Figure 7-13

141
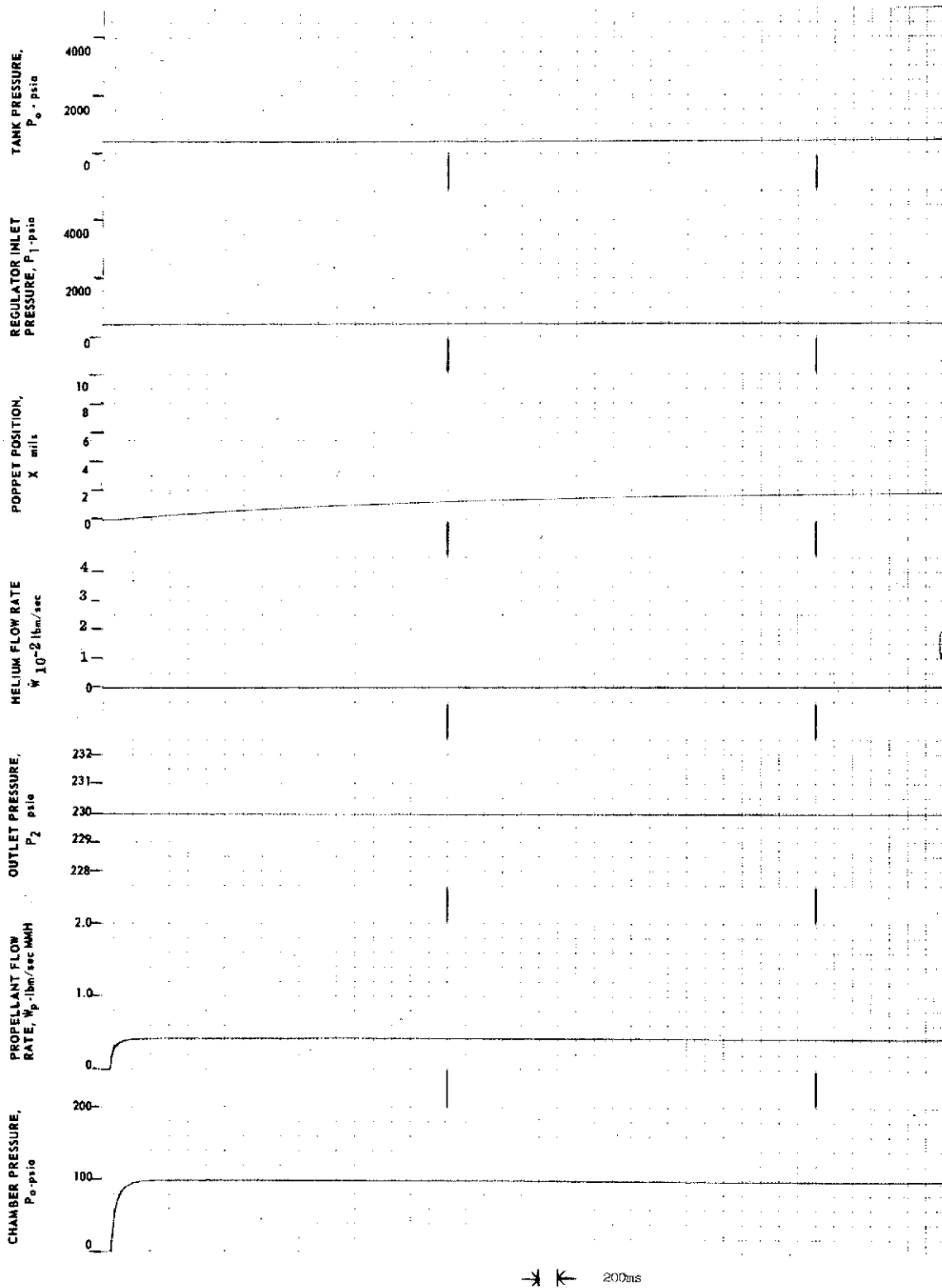
8. PROPULSION SYSTEM DYNAMIC MODELING

The complete propulsion system, including oxidizer feed system and fuel feed system, was modeled on the analog computer and two typical Jupiter Orbiter Missions as supplied by the Jet Propulsion Laboratory were simulated to determine propellant residuals at the end of the missions. To assess the possible range of propellant residuals requirements for any one mission as they are affected by regulator unit-to-unit variables such as spring rates, bellows effective area, effective seating diameter, deffective seat flow orifice, actuator stop in relation to the poppet in the seated position, and inlet gas temperature variations, three mission simulations were performed for each mission specified. The difference between these three mission simulations was the fact that one mission was performed with completely nominal regulator performance characteristics, one mission was performed utilizing an oxidizer regulator featuring the most droop and a fuel regulator featuring the least droop, and one mission was performed utilizing a fuel regulator featuring the most droop and an ozidizer regulator featuring the least droop. In addition the propellant temperatures were adjusted, for the off-nominal cases, to either the high or low extreme to further bias the results towards minimum and maximum propellant utilization.

Most droop and least droop regulator models were defined by choosing the unit-to-unit variables mentioned in the preceding paragraph in such a manner that their tolerance extreme would either increase or decrease droop, respectively. The specific values for the parameters of the regulator model presented in Section 5.3.3 were adjusted as shown in Table 8-I to obtain the most droop and least droop regulators.

TABLE 8-I

Most Droop Oxidizer Regulator			Least Droop Fuel Regulator		
K_s	=	0.85 x nominal	1.15	x	nominal
A_B	=	1.05 x "	0.95	x	"
A_{SE}	=	0.95 x "	1.05	x	"
A_s	=	1.05 x "	0.95	x	"
ΔY	=	nominal + .001	nominal	−	.001

Least Droop Oxidizer Regulator			Most Droop Fuel Regulator		
K_s	=	1.15 x nominal	0.85	x	nominal
A_B	=	0.95 x "	1.05	x	"
A_{SE}	=	1.05 x "	0.95	x	"
A_s	=	0.95 x "	1.05	x	"
ΔY	=	nominal − .001	nominal	+	.001

8.1 PROPULSION SYSTEM CONFIGURATION AND ITS ANALOG MODEL

The propulsion system model consists of two feed systems in parallel, oxidizer and fuel. The schematic of the physical system is shown in Figure 8-1. It consists of the respective tanks, filters, regulators, valves, and orifices for the two propellant circuits. The math model of the propulsion system is made up of the pressurant tank, isolation valve, regulator, propellant tank, lumped impedance, and propellant valve for each of the feed systems.

The propulsion system physical equations are summarized in Table 8-II. The helium tank dynamics include the effects of compressibility, flowrate, and temperature changes rate on instantaneous helium pressure, where the temperature rate is arbitrary. The regulator characteristics are defined by the force balance and helium flow through the poppet/seat interface. The bellows position is defined by the bellows feedback force, (outlet pressure X bellows effective area), spring preload and rate, and poppet flow force as determined from the flow force tests. The helium compressible flow relationship includes the results of the C_D tests. The propellant tank gas dynamics account for the helium flowrate into the ullage and the change in ullage due to propellant usage. Propellant flowrate is defined as being equal to a reference flowrate when the outlet pressure of the regulator is equal to the nominal value. To this is added a linearized increment in flowrate when the regulated pressure deviates from the nominal outlet pressure.

The analog computer model of the physical equations is shown in Figure 8-2. The diagram is divided into the two propellant circuits, fuel and oxidizer. Each feed system is further divided into the helium tank, regulator, and propellant tank (ullage gas and propellant). The potentiometer schedule for the propulsion system is summarized in Table 8-III, along with a description of each coefficient.

In the use of the analog computer circuits shown in Figure 8-2, the initial pressure of the helium in each propellant tank at the beginning of the next burn (P_{2i}) and the initial helium pressure in the pressurant tank (P_{oi}) are both computed from the following relationships in order to account for the helium reheat as the systems re-establishes thermal equilibrium during coast between burns:

$$P_{2i} = P_{2f} \frac{T_{2i}}{T_{2f}}$$

$$P_{oi} = \frac{Z R W_{of} T_{oi}}{V_o}$$

The analysis is dependent upon the final pressure and temperature at the end of the prior burn, pressurant tank volume, ullage, and gas phase properties (gas constant and compressibility). This included pressurization of the ullages above regulator lockup, due to re-establishment of temperature equilibrium of the ullage gas with the propellant prior to each succeeding burn. Analog equipment component accuracies are presented in Table 8-IV.

143

PROPULSION SYSTEM SCHEMATIC

A73-6-477-14

Figure 8-1

144
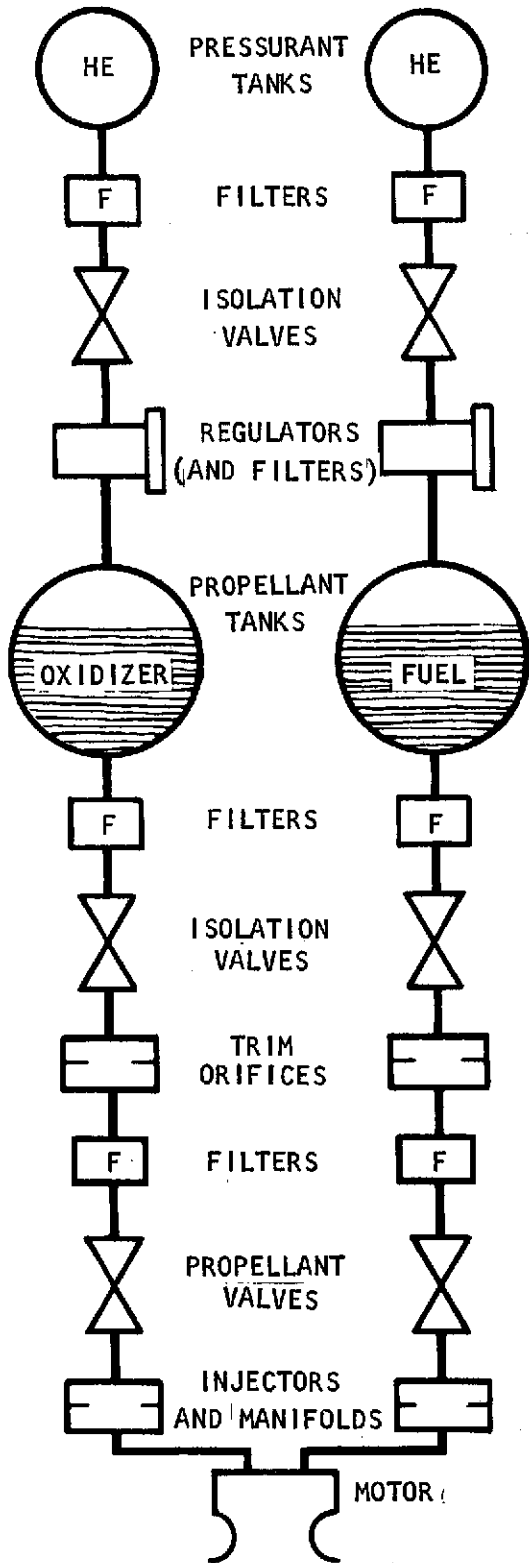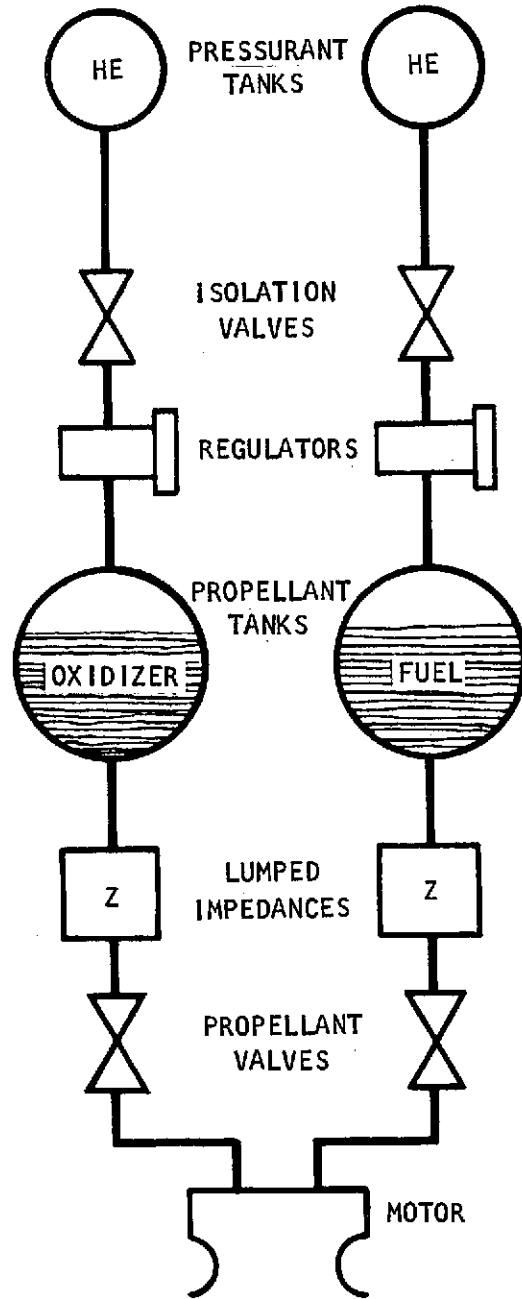
SPACE STORABLE PROPULSION SYSTEM – ANALOG WIRING SCHEMATIC
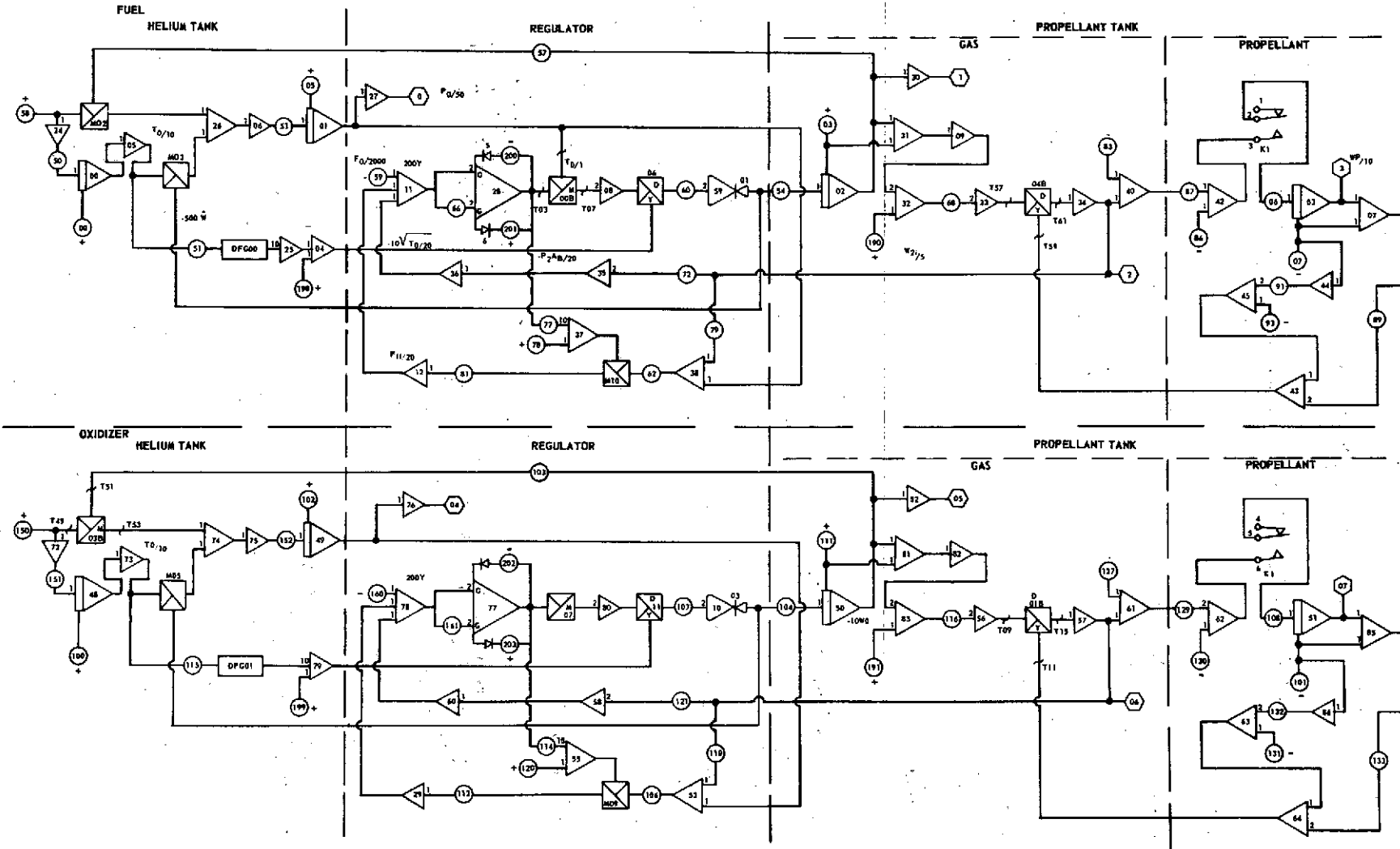
Figure 8-2

TABLE 8-II

PROPULSION SYSTEM PHYSICAL EQUATIONS

Helium Tank

$$\dot{P}_o = -\frac{Z R T_o}{V_o} \dot{W} - \frac{Z W_o R}{V_o} \dot{T}_o,$$

$$P_o = P_{oi} - \int_o^t \dot{P}_o dt$$

$$\dot{T}_o = \text{Constant},$$

$$W_o = W_{oi} - \int_o^t \dot{W} dt$$

$$T_o = T_{oi} - \int_o^t \dot{T}_o dt$$

Regulator

Force Balance:

$$Y = \frac{1}{K_s} \left[P_2 A_B - F_o + \left(1 - \frac{4K D_{SE} Y}{(D_{SE}^2 - D_{ST}^2) \, a/b} \right) \frac{(P_o - P_2) A_s}{a/b} \right]$$

Flow:

$$\dot{W} = \frac{P_o \pi D_{SE} Y C_m C_D}{a/b \sqrt{T_o}}$$

TABLE 8-II (Continued)

Propellant Tank

Gas:

$$\dot{W}_2 = W_{2i} + \int_o^t \dot{W} dt$$

$$P_2 = \frac{W_2 R T_2}{V_2}$$

$$V_2 = V_{2i} + \frac{1}{\rho_p} \int_o^t \dot{W}_p dt$$

Propellant:

$$W_p = W_{pi} - \int_o^t \dot{W}_p dt$$

$$\dot{W}_p = (\dot{W}_p)_{REF} + \left[(P_2)_{REF} - P_2 \right] \Delta \dot{W}_p / \Delta P_2$$

$$\Delta \dot{W}_p / \Delta P_2 = 1/2 K_3 (\dot{W}_p)_{REF} - K_4$$

PROPULSION SYSTEM POTENTIOMETER SCHEDULE

Potentiometer * Number	Parameter	Description
Fuel - MMH		
00	$T_{oi}/1000$	Initial helium temperature
03	$W_{oi}/1000$	Initial helium mass
05	$P_{oi}/5000$	Initial helium pressure
06	$1/500$	Scaling
07	$W_{pi}/1000$	Initial propellant mass
50	$1/1000$	Scaling
51	$1/2$	Scaling
52	$1/20$	Scaling
53	$Z\,R/25\,V_o$	Helium properties and pressurant tank volume
54	$1/50$	Scaling
58	$\dot{T}_o$	Rate of change of helium temperature with time
59	$F_o/1000$	Regulator spring preload
60	$\dfrac{1.25\,\pi\,D_{SE}\,C_m\,C_D\,250}{\sqrt{20}\;a/b}$	Poppet/seat interface flow characteristics

* Refer to Figure 8-1.

TABLE 8-III (Continued)

PROPULSION SYSTEM POTENTIOMETER SCHEDULE

Potentiometer Number	Parameter	Description
62	$100\ A_s$	Poppet/seat area
66	$\left[2000 - 2\ K_s\right]/K_s$	Regulator spring rate
68	$R\ T_2/3.2 \times 10^6$	Helium temperature in propellant tank
72	$A_B/5$	Bellows effective area
77	$4\ KD_{SE}/100\ a/b\ (D_{SE}^2 - D_{ST}^2)$	Flow force
78	$1/5$	Scaling
79	$1/12.5$	Scaling
81	$1/4\ a/b$	Lever ratio
83	$(P_2)_{REF}/400$	Reference propellant tank pressure
86	$(\dot{W}_p)_{REF}/2$	Reference propellant flow rate
87	$200/\left[2\ K_3\ (\dot{W}_p)_{REF} - K_4\right]$	$\Delta \dot{W}_p/\Delta P_2$ Rate of change of fuel flow rate with respect to tank pressure
89	$1/40\ \rho_p$	Propellant density
91	$1/40\ \rho_p$	Propellant density
93	$V_T/2 \times 10^4$	Propellant tank volume
190	$W_{2i}/5$	Initial helium mass in propellant tank

TABLE 8-III (Continued)

PROPULSION SYSTEM POTENTIOMETER SCHEDULE

Potentiometer Number	Parameter	Description
Oxidizer		
100	$T_{oi}/1000$	Initial helium temperature
101	$W_{pi}/1000$	Initial propellant mass
102	$P_{oi}/5000$	Initial helium pressure
103	$1/20$	Scaling
104	$1/50$	Scaling
106	$100\ A_s$	Poppet/seat area
107	$\dfrac{1.25\ \pi\ D_{SE}\ C_m\ C_D\ 250}{20\ a/b}$	Poppet/seat interface flow characteristics
108	$1/500$	Scaling
110	$1/12.5$	Scaling
111	$W_{oi}/10$	Initial helium mass
112	$1/4\ a/b$	Lever ratio
114	$4\,K D_{SE}/100\ a/b\ (D_{SE}^{2} - D_{ST}^{2})$	Flow force
115	$1/2$	Scaling
116	$R\,T_{2}/3.2 \times 10^{6}$	Helium temperature in propellant tank
120	$1/5$	Scaling

TABLE 8-III (Continued)

PROPULSION SYSTEM POTENTIOMETER SCHEDULE

Potentiometer Number	Parameter	Description
121	$A_B/5$	Bellows effective area
127	$(P_2)_{REF}/400$	Reference propellant tank pressure
129	$100/\left[2\,K_3\,(\dot{W}_p)_{REF} - K_4\right]$	$\Delta\dot{W}_p/\Delta P_2$ Rate of change of oxidizer flow rate with respect to tank pressure
130	$(\dot{W}_p)_{REF}/2$	Reference propellant flow rate
131	$V_T/2 \times 10^4$	Propellant tank volume
132	$1/40\,\rho_p$	Propellant density
133	$1/40\,\rho_p$	Propellant density
150	$\dot{T}_o$	Rate of change of helium temperature with time
151	$1/1000$	Scaling
152	$Z\,R/25\,V_o$	Helium properties and pressurant tank volume
160	$F_o/1000$	Regulator spring preload
161	$\left[2000 - 2\,K_s\right]/K_s$	Regulator spring rate
191	$W_{2i}/5$	Initial helium mass in propellant tank

TABLE 8-III (Continued)

PROPULSION SYSTEM POTENTIOMETER SCHEDULE

Potentiometer Number	Parameter	Description
Sequencing		
143	$t_2/500$	Time at which engine starts
144	$t_6/500$	Time at which engine stops
145	$t_7/500$	Time at which engine burn stops
146	$\dot{t}/500$	Clock input

TABLE 8-IV

ANALOG COMPONENT ACCURACIES

Reference Voltage		$\pm 0.01\%$
Potentiometers −	Setting	$\pm 0.01\%$
	Resolution	12,000 turns
Resistors		$\pm 0.001\%$
Capacitors		$\pm 0.002\%$
Thermal Stability		$\pm 0.0015\%$
Oven Temperature		$45°C \pm 0.5°C$
Open Loop Gain of Operational Amplifiers		$> 10^8$
Balance		$< 100\ \mu v$
Random Drift		$< 50\ \mu v$
Long Term Drift		$< 100\ \mu v$ 24 hours
Noise		< 1 mv p-p @ 60 H_z

TABLE 8-V

MISSION DUTY CYCLES

Burn No.	First Duty Cycle Burn Time (sec)	Second Duty Cycle Burn Time (sec)
1	10.2	10.2
2	20.2	10.2
3	420.2	361.2
4	20.2	157.2
5	14.65	166.2
6	–	66.2

Total guaranteed accuracy of all components used in this analog is approximately 1%. However, in practice it has been found that the total accuracy is about 3 times better than 1%.

8.2 DESCRIPTION OF MISSION DUTY CYCLES I AND II AND PROPULSION SYSTEM PHYSICAL CONSTANTS

The two duty cycles that were analyzed by the propulsion model are summarized in Table 8-V. The first duty cycle consists of five separate engine burns of varying duration each, the second duty cycle consists of six burns. For each successive burn in the two duty cycles the propellant and helium masses for both the fuel and oxidizer circuits were reinitialized to the final masses of the preceding burn. The propulsion system physical constants utilized in the mission duty cycle simulations are presented in Table 8-VI. The helium and propellant loadings establish the initial conditions of the integrators. At the end of the first burn, the remaining propellant and helium masses are noted and these values established the reinitialized conditions of the integrators for the beginning of the second burn. The same procedure was followed for each successive burn until the mission duty cycle was completed, or one or both propellants were depleted.

8.3 PROPELLANT UTILIZATION RESULTS FOR LOW, NOMINAL, AND HIGH DROOP REGULATOR CHARACTERISTICS

The propellant and pressurant utilization for each burn for each mission duty cycle was determined with analog computer and a sample of this data is presented in Figure 8-3. In effect, for each run the propellant and pressurant masses as well as the propellant tank and pressurant tank pressures were monitored during the run. This data is dynamically very uninteresting because of the slow chart speed required to put the entire run on a reasonable size piece of paper. Consequently, no additional analog computer printouts are presented. The initial propellant and pressurant loading for each duty cycle and the final propellant and pressurant loadings at the end of each run for each duty cycle are tabulated in Table 8-VII.

In comparing the final fuel loading for the first duty cycle, it is noted that the values are 29.4, 33.6, and 30.0 pounds for the nominal, high droop ox. reg./low droop fuel reg., and low droop ox. reg./high droop fuel reg. configurations. Thus, the maximum variation is 4.2 pounds. Referring back to the initial amount of fuel loaded, which was 230.6 pounds, it is apparent that the residual fuel variation constitutes approximately 1.8%. Putting it a different way, if the mission duty cycle had been such as to use up all of the fuel, an additional 1.8% of fuel would have been loaded to allow for propellant residuals resulting from the unit-to-unit variables of the pressure regulator. Similarly, the percentage of residual fuel for mission duty cycle No. II was 0.5% and that of the oxidizer for the same duty cycle 0.3%. The maximum oxidizer residual variation for the first duty cycle cannot be read off the data table presented directly since the low droop ox. reg./high droop fuel reg. configuration consumed all of the oxidizer 2.85 seconds prior to scheduled run No. 5 termination. However, by multiplying this 2.85-second time by the nominal oxidizer flowrate and adding this value to the maximum 5.7 pounds residual oxidizer observed, a total oxidizer residual variation of 8.9 pounds is determined. This constitutes a 1.6% variation.

SECOND DUTY CYCLE - BURN NO. 6

Figure 8-3

155
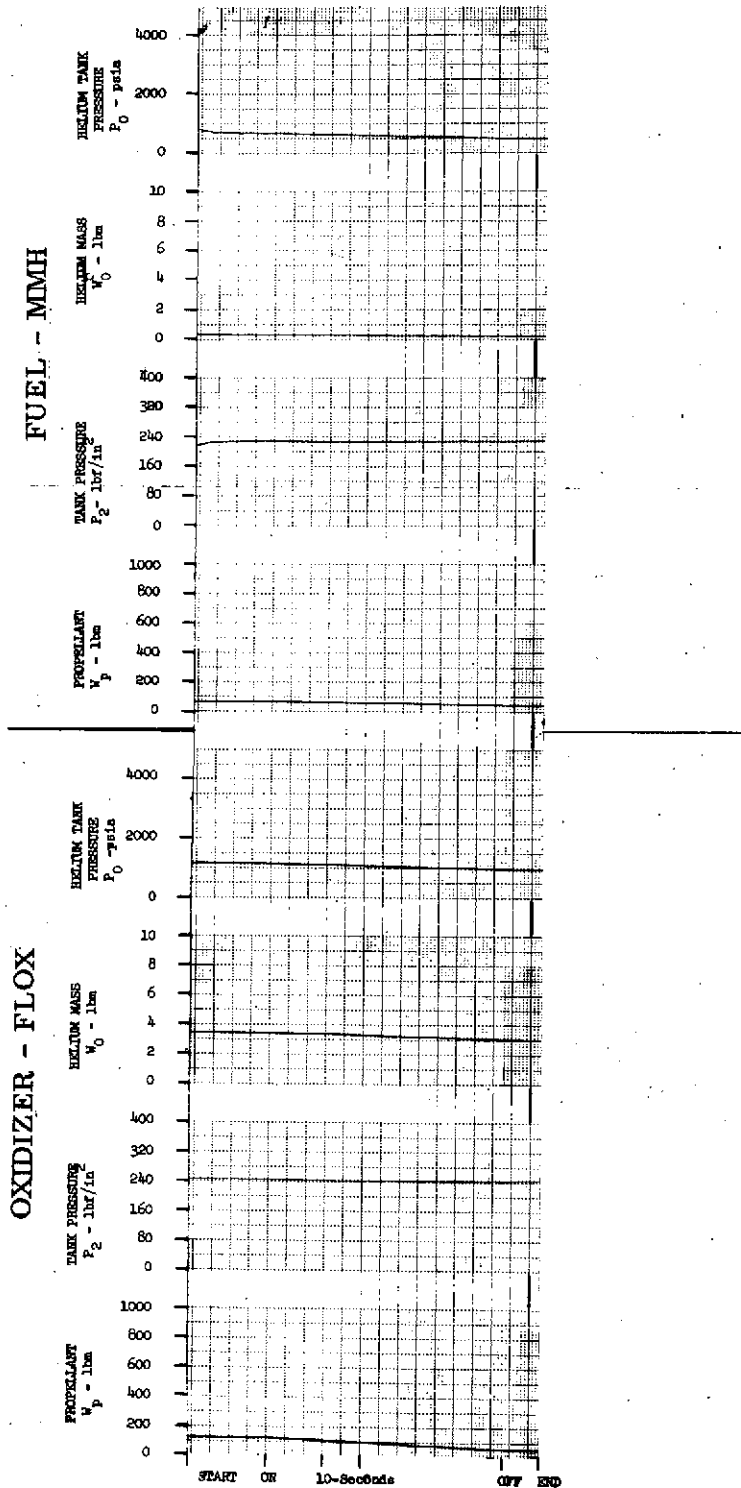
TABLE 8-VI

PROPULSION SYSTEM PHYSICAL CONSTANTS

FIRST DUTY CYCLE

Ullage, Oxidizer	$3,057$ in.^{3}
Ullage, Fuel	608.4 in.^{3}
Oxidizer Volume	$10,518$ in.^{3}
Fuel Volume	$7,320$ in.^{3}
Tank Volume, Oxidizer	$13,575$ in.^{3}
Tank Volume, Fuel	$7,928$ in.^{3}
Pressurant Tank, Oxidizer	$1,638$ in.^{3}
Pressurant Tank, Fuel	732.5 in.^{3}

SECOND DUTY CYCLE

Ullage, Oxidizer	$4,500$ in.^{3}
Ullage, Fuel	$1,282$ in.^{3}
Oxidizer Volume	$17,910$ in.^{3}
Fuel Volume	$11,830$ in.^{3}
Tank Volume, Oxidizer	$22,410$ in.^{3}
Tank Volume, Fuel	$13,112$ in.^{3}
Pressurant Tank, Oxidizer	$2,514$ in.^{3}
Pressurant Tank, Fuel	$1,068$ in.^{3}

TABLE 8-VII

FIRST DUTY CYCLE

Helium and Propellant Utilization

Oxidizer Temper- ature	Fuel Temper- ature	Configuration	Burn No.	Fuel, MMH		Oxidizer, FLOX	
				Propellant (lbm)	Helium (lbm)	Propellant (lbm)	Helium (lbm)
150°R	530°R	Nominal	Initial	230.6	0.996	559.4	6.596
			1	226.8	0.947	549.2	5.738
			2	219.1	0.921	527.3	5.521
			3	44.0	0.425	44.8	2.577
			4	35.5	0.333	22.0	2.537
			5	29.4	0.295	5.7	2.465
142°R	557°R	High Droop	1	228.0	0.962	550.1	5.707
		Ox. Reg.	2	220.9	0.940	528.7	5.487
		Low Droop	3	47.8	0.478	44.1	2.362
		Fuel Reg.	4	39.5	0.387	20.5	2.350
			5	33.6	0.353	3.8	2.291
158°R	503°R	Low Droop	1	226.7	0.946	547.6	5.741
		Ox. Reg.	2	218.6	0.920	524.3	5.512
		High Droop	3	43.1	0.405	35.9	2.569
		Fuel Reg.	4	34.6	0.297	12.5	2.544
			5	30.0	0.265	0.0*	2.514

* Run terminated after 11.80 seconds of engine burnout of scheduled 14.65 seconds burn due to oxidizer depletion

TABLE 8-VII (Continued)

SECOND DUTY CYCLE

Helium and Propellant Utilization

Oxidizer Temperature	Fuel Temperature	Configuration	Burn No.	Fuel, MMH		Oxidizer, FLOX	
				Propellant (lbm)	Helium (lbm)	Propellant (lbm)	Helium (lbm)
155°R	530°R	Nominal	Initial	368.0	1.467	952.0	9.598
			1	362.2	1.347	939.8	8.359
			2	356.2	1.325	927.5	8.125
			3	208.1	0.891	512.1	5.529
			4	143.8	0.654	332.4	4.420
			5	75.8	0.408	143.3	3.272
			6	48.7	0.251	68.7	2.850
142°R	557°R	High Droop	1	364.2	1.359	939.2	8.265
		Ox. Reg.	2	360.3	1.345	926.7	8.014
		Low Droop	3	211.5	0.933	511.9	5.190
		Fuel Reg.	4	146.6	0.707	332.8	4.000
			5	77.9	0.462	145.0	2.783
			6	50.7	0.332	71.3	2.323
158°R	503°R	Low Droop	1	364.2	1.348	940.5	8.380
		Ox. Reg.	2	360.2	1.333	929.2	8.156
		High Droop	3	210.0	0.874	513.0	5.610
		Fuel Reg.	4	144.8	0.623	333.1	4.520
			5	76.0	0.366	143.5	3.396
			6	48.9	0.224	69.2	2.977

The propellant residuals determined are considered quite reasonable and within the goals of the space storable propulsion system. However, in examining the data in Table 8-VI, it is noted that the propellants remaining after the nominal condition runs actually fall out of the range as established by what was thought to be the conditions reflecting the least amount of propellant used and the most amount of propellant used. This phenomena is apparently due to the fact that the worst case and the best case is rather difficult to define since the regulator droop curve as shown in Figure 5-33 overlapped certain inlet pressures. Thus, what may constitute the most droop at one inlet pressure is not the most droop at another inlet pressure and the amount of propellant utilized during the mission has been a function of how much of the mission is operated at any particular inlet pressure. Nevertheless, the data obtained on propellant residuals is still considered reasonable and conservative since the tolerances on the unit-to-unit variables have all been added up arithmetically rather than combined on a root mean square basis to achieve worst case conditions. To attain a better definition of propellant residuals, additional sensitivity studies would have to be performed and considerable more potential duty cycles would have to be evaluated. Since the Jupiter Orbiter Mission is not defined that well at the present time, these additional efforts are better performed when the Jupiter Orbiter Mission has been more firmly established.

9.   RECOMMENDATIONS AND CONCLUSIONS

The design for pressure regulating components program has resulted in the conceptual design and analysis of a pressure regulator which is well suited for the requirements of the space storable propulsion system. The final regulator design constitutes a major advance in the state-of-the-art of regulator technology. The design includes a number of unique features such as:

- Completely friction free (all flexure guided)

- Solid damping and gas damping

- Fluorine and hydrazine compatible

- Wide temperature capability (-420°F to level limited only by propellant reactivity, above 300°F)

- Redundant Bellows

- No coil or other reference spring required

- Simple, highly reliable design

The final advanced pressure regulator design was modeled in the propulsion system to determine the residual propellants remaining after these missions as well as the minimum amount of pressurant gas which has to be loaded for typical Jupiter orbiter missions. To determine the residual propellant quantities, regulator configurations featuring the greates droop and the slowest inherent response as well as regulator configurations featuring the least droop and fastest inherent response as determined by estimated unit-to unit variables were identified and these regulator configurations were utilized to simulate two

typical flight missions. Results from these simulations indicated residual propellant requirements to be less than 3% of the initial propellant loaded for mission No. 1 and less than 0.6% for mission No. 2. These values are considered very acceptable. However, the results of the mission simulations also disclosed unexpectedly that the most droop and the least droop regulator cases modeled may not constitute the extreme propellant utilization situations. Rather, the interactions of the variables that affect the droop characteristics of the regulator were proven to be other than straightforward, such that what constitutes the most droop over the entire flowrate and operating pressure range may not be the most droop over an inlet pressure range of say 4000 to 1000 psia which is the operating pressure range for more than 80% of the entire mission. Thus, it was concluded that additional sensitivity studies would be required wherein each of the possible variables is allowed to vary over its maximum range independently and the effects on the residuals of this variation are determined. This more extensive sensitivity study was considered to be beyond the intended scope of the design for pressure regulating components progrom presented herein.

Upon completion of the analytical efforts in support of this program and as a result of discussions with the JPL technical manager, as well as analyses performed by The Marquardt Company in support of other pressure regulator technology programs, a recommendation for the performance of additional analytical tasks is being made. The first of these tasks is the analysis of a special situation which could conceivably occur during the initial charging of the propellant system. Because of the surface tension propellant acquisition systems employed in the propellant tank it appears possible that the inlet tubing to the pressure regulator upstream to the pressurant isolation valve could be filled with liquid at the time the pressure oscillation valve is initially opened. Under that condition, the pressure regulator would be wide open and the liquid propellant would then be forced through the regulator poppet/seat interface with a pressure of 4000 psi. Once the liquid upstream of the poppet/seat interface has been forced through the poppet/seat interface and at the very moment that the pres   rant reaches the poppet/seat interface, it is expected that some pressure rise will occ · on the downstream side of the poppet/ seat interface. If at that instant the actuator s   ısing cavity is also filled with liquid, it appears that a significant pressure overshoot   ıy occur while the remaining liquid in the regulator outlet tubing is being pushed into ᴜıe propellant tank. The magnitude of this pressure rise was not determined during the study report herein and should be reviewed during future efforts.

The second analytical task that appears worthwhile is the imposition of the random vibration spectrum converted into an equivalent sinusoidal acceleration in the direction of the poppet and actuator movement to determine if the regulator stability is affected by vibration to any appreciable degree. Since the vibration environment for the Jupiter Orbiter spacecraft is quite low, it is expected that no significant instabilities will be encountered. However, a check appears worthwhile.

A review of the possibility of causing ice to form in the reference cavity when the system is chilled in the earth's atmosphere should also be performed to determine if such formation is detrimental to the regulator. In the event it is considered to be a problem corrective action such as the installation of a check valve or similar barrier should be instituted.

Another task considered desirable is a comparison of regulator design layouts featuring the poppet/seat and enclosing body turned 90 or 180 degrees to the actuator shaft. This arrangement may offer a more desirable regulator package.

Finally, the experimental sealing closure programs performed to evaluate compatible sealing closures featuring high cycle life have generally been concerned only with such fluorinated oxidizers as chlorine pentafluoride and chlorine trifluoride and were therefore performed at ambient temperatures. Although the reactivity of the fluorine at cryogenic temperatures is known to be greatly reduced, there are some reasons, such as the formation of solid fluorides versus the formation of liquid or gaseous fluorides at ambient temperature, which appear to make the experimental verification of the sealing capability of the proposed poppet/seat interface at cryogenic temperature, while exposed to fluorine, worthwhile.

In conclusion it is evident that the systematic pursuit of a pressure regulator technology program by the Jet Propulsion Laboratory in support of the Jupiter Orbiter Mission has resulted in a significant advance in pressure regulator technology. While additional analytical and experimental tasks are recommended herein, it is evident that the pressure regulator concept developed as a result of this effort will be an extremely accurate device featuring high reliability and long service life and will be capable of minimizing the required pressurant loadings and the residual propellants to the degree necessary for the Jupiter Orbiter Mission.

10. SYMBOLS

NOMENCLATURE

Symbol	Description	Units
a	Sonic velocity	
a/b	Lever ratio	–
A	Area	
A_B	Bellows effective area	$in.^2$
A_L	Feed line cross-sectional area	$in.^2$
A_T^*	Motor exhaust throat area	$in.^2$
A_R	Regular outlet port area	$in.^2$
A_o	Gas damping orifice area	$in.^2$
A_s	Poppet seating area	$in.^2$
A_{SE}	Effective seat flow orifice	$in.^2$
b	Lever length	
B	Solid damping factor	lbf-sec/in.
C	Coefficient	
C	Damping orifice annular clearance	in.
C_D	Discharge coefficient	–
C_m or C_M	Flow function	$lbm-°R^{1/2}/lbf-sec$
D_s	Poppet seating diameter	in.
D_{SE}	Poppet/seat hole diameter	in.
D_{ST}	Poppet stem diameter	in.
e	Napierian base	
e_i	Propellant valve input electrical signal	volts
F	Force	
F_o	Spring preload	lbf
g	Acceleration due to gravity, 386.09	$in.-lbf/lbm-sec^2$
h	H/2	
H	Σ peak-to-valley height	

162

Symbol	Description	Units
K	Constant	
K_1	Empirical flow force factor	-
K_2	Filter pressure drop constant (laminar)	$in.^3/lbf\text{-}sec$
K_3	Lumped propellant flow impedance	$lbf\text{-}sec^2/in.^2\text{-}lbm$
K_4	Rate of change of motor chamber pressure with propellant flowrate	$lbf\text{-}sec/in.^2\text{-}lbm$
K_s	Spring rate	$lbf/in.$
K_{ss}	Spring rate of bellows stop	$lbf/in.$
L	Damping orifice length or Seat land width	$in.$
ℓ	Length	$in.$
M	Mach number	-
m	Mass	lb_m
P	Pressure	lbf/in^2
P_1	Inlet pressure	$lbf/in.^2$
P_2	Outlet pressure	$lbf/in.^2$
P_3	Motor chamber pressure	$lbf/in.^2$
P_{01}	Regulator inlet pressure after first shock reflection	$lbf/in.^2$
P_{02}	Final regulator inlet pressure	$lbf/in.^2$
P_o	Pressurant tank pressure	$lbf/in.^2$
$\dot{P}_o$	Pressurant tank pressure rate	$lbf/in.^2\text{-}sec$
P_{oi}	Pressurant tank initial pressure	$lbf/in.^2$
$\dot{P}_2$	Outlet pressure rate	$lbf/in.^2\text{-}sec$
P_2'	Lower bellows cavity pressure	$lbf/in.^2\text{-}sec$
$\dot{P}_2'$	Lower bellows cavity pressure rate	$lbf/in.^2\text{-}sec$

Symbol	Description	Units
P_2''	Upper bellows cavity pressure	$lbf/in.^2$
$\dot{P}_2''$	Upper bellows cavity pressure rate	$lbf/in.^2\text{-sec}$
P_{2i}	Initial outlet pressure	$lbf/in.^2$
P_{2i}'	Lower bellows cavity initial pressure	$lbf/in.^2$
P_{2i}''	Upper bellows cavity initial pressure	$lbf/in.^2$
P_{21}	Internal regulator volume pressure	$lbf/in.^2$
$\dot{P}_{21}$	Internal regulator volume pressure rate	$lbf/in.^2\text{-sec}$
P_{21_i}	Initial internal regulator volume pressure	$lbf/in.^2$
$(P_2)_{ref}$	Set-point pressure (nominal)	$lbf/in.^2$
P_{2t}	Final pressure of helium in propellant tank at end of the last burn	lbf/in^2
Q	Volumetric flowrate	ft^3/sec
R	Gas constant (helium), 4632	$in.\text{-}lbf/lbm\text{-}°R$
R_e	Gas constant of motor chamber	$in.\text{-}lbf/lbm\text{-}°R$
S	La Placian operator	$1/sec$
t	Real time	sec
$\dot{t}$	Clock input	–
t_1	Initial shock travel time	sec
t_2	Reflected wave travel time, or tune at which engine starts	sec
t_6	Time at which engine stops	sec
t_7	Time at which engine burn stops	sec
T	Temperature	$°R$
T_e	Motor exhaust gas temperature	$°R$
T_1	Inlet temperature	$°R$
T_{2f}	Final helium temperature in propellant tank at the end of the last burn	$°R$
T_{2i}	Initial temperature of helium in propellant tank at the beginning of the next burn	$°R$
T_o	Pressurant tank temperature	$°R$
$\dot{T}_o$	Pressurant tank temperature rate	$°R/sec$

NOMENCLATURE
(Continued)

Symbol	Description	Units
T_{oi}	Initial helium temperature in the pressurant tank at the beginning of the next burn	°R
u	Gas velocity	ft/sec
V	Volume	ft^3
V_e	Motor chamber volume	$in.^3$
V_o	Pressurant tank volume	$in.^3$
V_p	Propellant velocity in feed line	ft/sec
$\dot{V}_p$	Propellant acceleration in feed line	$in./sec^2$
V_{pi}	Initial propellant velocity in feed line	$in./sec$
V_R	Internal regulator volume	$in.^3$
V_T	Ullage volume	$in.^3$
V_2'	Lower bellows cavity volume	$in.^3$
V_2''	Upper bellows cavity volume	$in.^3$
ΔV_1	Voltage drop of diode 01	volts
ΔV_2	Voltage drop of diode 02	volts
ΔV_3	Voltage drop of diode 03	volts
ΔV_4	Function generator offset at zero input	volts
W	Weight, shock velocity	lbf
$\dot{W}$	Helium flowrate through poppet/seat interface	lbm/sec
W_B	Bellows mass	lb_m
W_{BF}	Bellows flexure mass	lb_m
W_{BP}	Bellows endplate mass	lb_m
W_{BS}	Bellows mass & spring mass	lb_m
W_L	Lever mass	lb_m
W_o	Pressurant tank mass	lb_m
W_p	Fluid mass in feed line	lb_m

NOMENCLATURE
(Continued)

Symbol	Description	Units
$\dot{W}_{p2}$	Liquid-filled damper flowrate	lbm/sec
W_P	Poppet mass	lbm
$\dot{W}_P$	Propellant flowrate	lbm/sec
W_{PF}	Poppet flexure mass	lbm
W_{PR}	Pushrod mass	lbm
W_{PRF}	Pushrod flexure mass	lbm
W_T	Total moving mass	lbm
$\dot{W}_2'$	Lower bellows cavity flowrate	lbm/sec
$\dot{W}_2''$	Upper bellows cavity flowrate	lbm/sec
W_{of}	Final helium pressure in the pressurant tank at the end of the last burn	lbf/in^2
X	Bellows position	in.
X_P	Poppet position	in.
Y	Valve position	in.
$\dot{Y}$	Bellows velocity	in./sec
Y_i	Bellows initial position	in.
$\dot{Y}_i$	Bellows initial velocity	in./sec
$\ddot{Y}$	Bellows acceleration	$in./sec^2$
Y_{max}	Maximum bellows position	in.
ΔY	Clearance between bellows and lever when poppet is closed and bellows is on closed stop	in.
Z	Compressibility factor	

GREEK SYMBOLS

Δ	Increment	
γ	Ratio of specific heats	
μ	Propellant viscosity	lbm/in.-sec

166

NOMENCLATURE
(Continued)

Symbol	Description	Units
ρ	Specific weight	lb_m/ft^3
ρ_P	Propellant density	$lbm/in.^3$
σ	Seat stress	psi
τ	Time constant	sec
τ_1	Motor time constant	sec
τ_2	Propellant valve time constant	sec

SUBSCRIPTS

a	actuator
b	bellows
c	circular
f	friction, final
D	discharge, delay
h	specific heat
i	initial
He	helium
m	mass flow
o	oxidizer, initial
p	poppet face, propellant
R	regulator
s	spring, seating
t	thermal
u	unidirectional
v	valve, const. vol.
1	upstream, initial
2	downstream
3	combustion chamber

11. REFERENCES

1. T. Brintzenhoff, "User's Guide for PSOP-B and PSOP-C", Jet Propulsion Laboratory internal document, February 1, 1972.

2. NASA-Manned Spacecraft Center, "Metals and Metal Couples - Restriction on Use", Standard No. 63, November 3, 1967.

3. P. E. Uney and D. A. Fester, "Material Compatibility with Space Storable Propellants," MCR-72-26, Martin Marietta Corporation, March 1972.

4. I. J. Eberstein and I. Glassman, "Consideration of Hydrazine Decomposition," Laboratory Report 490, Princeton University, December 1959.

5. A. E. Axworthy, et al, "Research on Hydrazine Decompowition," AFRPL-TR-61-146, Rocketdyne, July 1969.

6. R. J. Salvinsky, et al, "Advanced Valve Technology, Volume II - Materials Compatibility and Liquid Propellant Study," 06641-6014-R000, TRW Systems, November 1967.

7. E. L. White, W. K. Boyd and W. F. Berry, "Compatibility of Materials with Rocket Propellants and Oxidizers," Memorandum 201, Definse Metals Information Center, January 1965.

8. S. Kleinberg, et al, "The Properties and Handling of Fluorine," ASD-TDR-62-273, Air Products Inc., Allentown, October 1963.

9. G. R. Pfeifer, H. Wichmann and Dr. R. Kratzer, "Advanced ACS Valve Sealing Surface Compatibility Investigation," The Marquardt Company, AFRPL-TR-71-84, September 1971.

10. Verlag Chemie, "Gmelins Handbuch der Anorganischen Chemie," Weinheim, Germany.

11. Crane, "Flow of Fluids Through Valves, Fittings and Pipe", Technical Paper No. 410.

12. H. Wichmann, "Advanced ACS Valve Development Program", AFRPL-TR-69-250.

13. J. A. Perry, ITT, "Critical Flow through Sharp Edged Orificies," ASME 481-A-146.

14. Wm. Griffel, P.E., "Elastic Energy Methods," Picatinny Arsenal.

168

15. Bendix, Utica, N. Y., "Free Flexural Pivot Engineering Data" .

16. N. O. Myklestad, "Fundamentals of Vibration Analysis", McGraw-Hill.

17. W. Flügge , "Handbook of Engineering Mechanics", McGraw-Hill.

18. SAE TR-63, "Manual on Design and Manufacture of Coned Disc Springs", February 1955.

19. Stylarg Bulletin DS2-70, "Belleville Spring Design Manual".

20. H. K. Metalcraft Mfg. Corporation, "The Design of Spring Valves".

21. Gerhard Schremmer, "Endurance Strength and Optimum Dimensions of Belleville Springs", Rochester Institute of Technology, ASME 68-WA/ED-9.

22. Internal Memo by Lt. E. Lantzer, AFRPL, 1971.

23. P. J. Axworthy to H. Wichmann telecon June 22, 1972, regarding decomposition of hydrazine

12. NEW TECHNOLOGY REPORT

As part of Marquardt's preproposal and proposal efforts which led to the award of Contract No. 953383, Mr. H. Wichmann of the Marquardt Company was responsible for the preparation of a preliminary design layout for a pressure regulator which had a number of unique features. These unique features were achieved by employing components which had previously been demonstrated in support of other fluid system component technology programs; however, the combination of these components in a regulator design is believed to be a first. The unique regulator features are:

A. Friction free operation resulting in nearly limitless regulator life, the elimination of hysterisis, the elimination of self generated contamination, and an improvement in regulator accuracy. This was accomplished by utilizing flexure guidance (both rotary and linear metallic flexures) for all moving elements.

B. Fluorine compatibility and extended service life achieved through the elimination of all elastic and plastic materials and the utilization of ceramic and metalic materials only as well as the incorporation of a fluorine compatible poppet/seat configuration.

C. Solid and pneumatic damping only obtained from the solid damping characteristics of the flexures, bellows, and springs and by using the actuator bellows in combination with a control orifice to achieve pneumatic damping.

APPENDIX A

CALCULATION OF SEAT IMPACT FORCES

PREPARED BY
DICKENS
CHECKED BY

THE MARQUARDT COMPANY

CLASSIFICATION

REPORT
FLOX PRESS. REG. PROPOS.

DATE
7 JAN 1972

PAGE
1. OF

FLOX PRESS. REG. PROPOSAL

CALCULATION OF IMPACT FORCES ON SEAT

DETERMINATION OF TOROIDAL SEAT THICKNESS

$a = 1.32/4 = .33$ in   TO CENTER OF TOROID.

$b = 1/4 = .25$ IN   MEAN R

MATERIAL INCO 718 $T = 70°F$, $N = 50,000$ cycles

FOR $R = 0$, $Fend = 105$ K max

ROARK pg 306, case 26   TORUS

S_2 HOOP $= \dfrac{pb}{2t}$

$t = \dfrac{(4000-240)(.25)}{2 \times 105000} = .0045$ too small

$S_{1 MAX} = \dfrac{pb}{t}\left(\dfrac{2a-b}{2a-2b}\right)$

$t = \dfrac{(4000-240)(.66-.25)(.27)}{(105K)(.66-.50)} = .024$ MIN

USE $t = .030$ NOM.   (OK FOR BURST $P = 8000 psi$)*

FOR DEFLECTION UNDER LOAD AT CENTER SPLIT TORUS

ANALYZE PER ROARK pg 306, case 27

$\dfrac{\Delta}{SEAT} = \dfrac{10.88 \, Pb \sqrt{1-v^2}}{2\pi \, E t^2} = \dfrac{10.8(.25)(.954)P}{2\times(30)10^6(.0009)}$

$\underline{\Delta = .000152 \, P}$

* See pg 1.1   M.S. = .19

A-1

PREPARED BY
DICKENS

THE MARQUARDT COMPANY

REPORT
FLOX PRESS. REG. PROP.

CHECKED BY

CLASSIFICATION

DATE
10 JAN 1972

PAGE
1.1   OF

FLOX PRESS. REG PROPOSAL

CHECK OF TOROIDAL DOME THICKNESS

CHECK AS SPLIT TORUS - LOAD ON CENTER

CENTER LOAD $P = p \left(\frac{\pi}{4}\right)(.40)^2$

$$= (4000 - 240)(.126) = 473^H$$

Roark p 306, case 27)

$a = .33$ IN
$t = .030$ IN
$b = .25$ IN.

$$S' = \frac{2.99 \, P \sqrt[3]{\frac{ab}{t^2}}}{2\pi t a \sqrt[3]{1 - v_c^2}}$$

$$= \frac{2.99 (.473) \, 4.5}{2\pi (.030)(.33)(.992)}$$

$$= \underline{102000 \, psi} \qquad CLOSE \, ENOUGH \, !$$

$$S_2 = \frac{2.15 \, P \sqrt[3]{1 - v_c^2} \, \sqrt[3]{\frac{ab}{t^2}}}{2\pi a t}$$

$$S_2 = \frac{2.15 (.970)(102000)}{2.99 (.992)} = \underline{71800 \, psi} \qquad AT \, INSIDE \, FOR$$

BURST M.S.   (INCO 718 - $F_{tu} = 189,000 \, psi$ MIN)

$$f_{b \, MAX} = \frac{8000 (102000)}{3760} = 217000 \, psi$$

$$F_{bu} = 1.45 (189000) = 260,000 \, psi \quad (PLASTIC \, BENDING)$$

$$\underline{MS = \frac{260}{217} - 1 = .19}$$

A-2

PREPARED BY
DICKENS

THE MARQUARDT COMPANY

CHECKED BY

CLASSIFICATION

REPORT
FLOX PRESSURE REG. PROP

DATE
7 JAN 1972

PAGE
2 OF

FLOX PRESS REG. PROPOSAL

CALCULATION OF IMPACT FORCES ON SEAT

POPPET VELOCITY AT IMPACT = 10 IN/SEC

FROM COMPUTOR ANALYSIS

MASS OF POPPET (KENNAMETAL INSERT - $d = .56 \#/in.^3$)

INSERT $= \frac{\pi}{4}(.21)^2(.04)(.560) = .000775^{\#}$

CARRIER (INCO 718) $= [\pi(.25)(.07)(.04) + \frac{\pi}{4}(.2)^2(.033)](.288) = .00096$

$= .0010^{\#}$

TOTAL INSERT + CARRIER $= .001 + .00078 = .00178^{\#}$

SEAT WGT

KENNAMETAL INSERT   WEIGHT APPROX .00055$^{\#}$

INCO 718 SEAT MASS WEIGHT $= \frac{\pi}{4}(.22)^2 \times .10 \times .288 = .0011^{\#}$

TOTAL SEAT WGT $= .0011 + .00055 = .00165^{\#} \rightarrow .0017^{\#}$

K.E. OF POPPET AT IMPACT

$KE = \frac{1}{2}MV^2 = \frac{.00178}{2 \times 386}(10)^2 = .00023$ LBS·IN BASIC

CORRECTING FOR MASS OF SEAT

$V_e = \frac{.00178(10)}{(.00178 + .0017)} = 5.11$ IN/SEC

K.E. OF COMBINED MASS $= \frac{1}{2}(\frac{.00348}{386})(5.11)^2 = .000118$ LBS IN

A-3

FORM TMC 685   REV. 3-70

PREPARED BY DICKENS

THE MARQUARDT COMPANY

CHECKED BY

CLASSIFICATION

REPORT FLOX PRESS. REG. PROPOS

DATE 7 JAN 1972

PAGE 3 OF

FLOX PRESS. REG. PROPOSAL

IMPACT FORCES ON SEAT

DEFLECTION OF SEAT = .0000152 P   (1g 1)
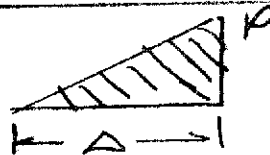
K.E POPPET + SEAT =   AREA = $P\Delta/2$

$\Delta = .0000152 P$

$KE = \dfrac{P\Delta}{2} = \dfrac{.0000152 P^2}{2}$

$.000116 = \dfrac{.0000152 P^2}{2}$

$\left(\dfrac{.000236}{.0000152}\right)^{\frac{1}{2}} = P$

$\underline{3.94^{\#} = P}$ IMPACT

BEARING AREA LOCAL

$A_{br} = \dfrac{\pi}{4}\left[(.080-.005)^2 - (.063+.005)^2\right] = .00079 \ in^2$

$\underline{f_{br} = \dfrac{3.94}{.00079}} = \underline{4970 \ psi}$ IMPACT

PRESSURE FORCE $= \dfrac{\pi}{4}(.060-.005)^2(4000-240) = \underline{16.6^{\#} P}$

$\underline{f_{br} = \dfrac{16.6}{.00079}} = \underline{21000 \ psi}$ BEARING

TOTAL BEARING STRESS = 4970 + 21000 = $\underline{25970 \ psi}$ TOTAL

JPL FLOX REGULATOR

SEAT STIFFNESS CALCULATIONS

IMPACT FORCE ALLOWED = $25^{\#}$

$\text{PRESSURE FORCE} = \frac{\pi}{4}(.083)^2(4000 - 240) = 20.3\ \#$

$\text{BEARING AREA} = \frac{\pi}{4}[(.083)^2 - (.067)^2] = .0019\ in^2$

$f_{br} = (25 + 20.3)/.0019 = 23800\ psi$

KENNAMETAL $F_{bry} =$

$M.S. =$

K.E. OF POPPET MASS   —   V = 15 IN/SEC AT IMPACT

MASS POPPET $= .0028\ \#/386$

WEIGHT SEAT + INSERT $= .0017\ \#$

$\text{K.E. of POPPET} = \frac{1}{2}MV^2 = \frac{1}{2}\left(\frac{.0028}{386}\right)(15)^2 = .816 \times 10^{-3}$

CORRECTING FOR MASS OF SEAT FOR MOMENTUM EXCHANGE

$V_e = \frac{.0028}{(.0028 + .0017)} \times 15 = 9.34\ in/sec$

K.E. OF COMBINED MASS $= \frac{1}{2}\left(\frac{.0045}{386}\right)(9.34)^2 = .508 \times 10^{-3}$

Plate Deflection $\frac{473}{615000} = .0007''$

A-5

PREPARED BY
DICKENS

CHECKED BY

THE MARQUARDT COMPANY

CLASSIFICATION

REPORT
JPL FLOX REG

DATE
6 MAY 1972

PAGE
4/12 OF

JPL FLOX REGULATOR

SEAT STIFFNESS CALCULATIONS

FOR POPPET MASS $= .0028^{\#}/386$, $V_1 = 15 \text{ IN/SEC}$

$\underline{K.E.}$ COMBINED POPPET & SEAT $= .508 \times 10^{-3}$ LBS-IN

$KE = \dfrac{P\Delta}{2}$

$AREA = \dfrac{P\Delta}{2}$

$P_{ALLOW} = 25^{\#}$ IMPACT

$\Delta = \dfrac{1}{K} P$
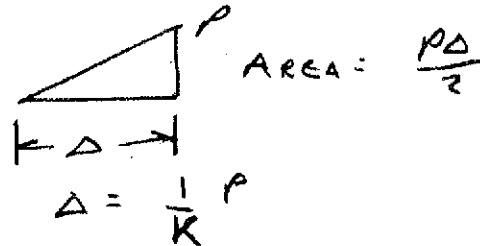
$.508 \times 10^{-3} = \dfrac{P^2}{2K} = \dfrac{(25)^2}{2K}$

$\underline{K} = \dfrac{625}{2 \times .508 \times 10^{-3}} = \underline{615\,000 \ ^{\#}/\text{IN}}$

FOR SEAT AS SPLIT TORUS

PER ROARK pg 306, CASE 27

$\Delta /_{SEAT} = \dfrac{10.88 \ P b \sqrt{1 - v_e^2}}{2 \pi E t^2}$

$b = .25$ "ASSUMED

FOR $\dfrac{P}{\Delta} = K = \dfrac{2 \pi E t^2}{10.88 \sqrt{1 - v_e^2} \ b} = 615\,000 \ ^{\#}/_{\text{b}}$

$t^2 = \dfrac{615\,000 \ (10.88) \sqrt{1 - (.3)^2} \ (.25)}{2 \pi \ 30 \times 10^6}$

$t^2 = .00716$

$\underline{t = .0845 \longrightarrow .085 \text{ IN}}$

A-6

PREPARED BY
DICKENS

CHECKED BY

THE MARQUARDT COMPANY

CLASSIFICATION

REPORT
JPL FLOX REG

DATE
6 MAY 1972

PAGE
4.3 OF

J.PL FLOX REGULATOR

SEAT STRENGTH CALCULATIONS   INCO 718 HT/Aged

STRESSES DUE TO PRESSURE + CYCLES

FOR N = 10^5, F_{END} = 65,000 psi MAX FULLY REVERSED
               = 95,000 psi MAX UNIDIRECTIONAL

CHECK AS SPLIT TORUS. $P = p \frac{\pi}{4}(.4)^2 =$

ROARK, P306, case 2 $= (4000-240)(.126) = 473^{\#}$

$$S_1 = \frac{2.99 P \sqrt[3]{\frac{ab}{t^2}}}{2\pi\, a t \sqrt[6]{1-v_e^2}}$$

$a = .33$ (conservative)
$b = .25$
$t = .085$

$$= \frac{2.99(473)(2.25)}{2\pi(.33)(.085)(.992)}$$

$$= 18,200 \text{ psi UNIDIRECTIONAL}$$

F_{END} = 95,000 psi $\underline{M.S. = \frac{95}{18.2} - 1 = LARGE}$

FOR HOOP STRESS AT INSIDE

$$S_2 = \frac{2.15\, P \sqrt[3]{1-v_e^2}\; \sqrt[3]{\frac{ab}{t^2}}}{2\pi\, a t}$$

$$S_2 = \frac{2.15(473)(.970)(2.25)}{2\pi(.33)(.085)} = 12600 \text{ psi ok}$$

BURST M.S. $F_{TU} = 180,000$ psi

$f_{b\,MAX} = \frac{8000}{3760} \times 18,200 = 38,800 \text{ psi}$

$f_{bu} = 1.45 \times 180,000 = 260,000$ psi $\underline{M.S. = \frac{260}{38.8} - 1 = LARGE}$

A-7

APPENDIX B

FLEXURE STRESS ANALYSIS

JPL Flox Regulator

Poppet Flexure   INCO718 + Aged

Criteria

O.D. = 1.00, ID = .260, OPEN PATTERN

Axial Spring Rate = 500 #/in OR LESS

Radial Spring Rate = 600 #/in OR MORE

Stroke = .010 in plus $\dfrac{.50\#}{K}$ PRECOAD STROKE

$\approx$ .011 in. TOTAL

Temp. Ambient To -320°F

Side Load = .06 # For 100'j'

CONFIGURATION "A"

FORM TMC 688 REV. 8-70

PREPARED BY
DICKENS

CHECKED BY

THE MARQUARDT COMPANY

CLASSIFICATION

REPORT
JPL FLOX REG.

DATE
3 MAY 1972

PAGE
1.2 OF
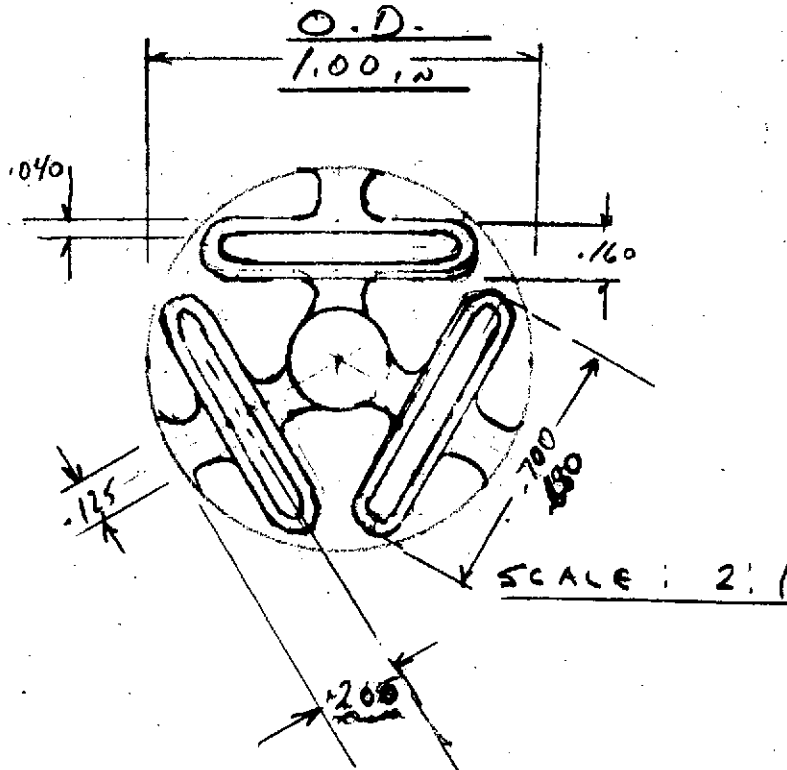
JPL FLOX REGULATOR

POPPET FLEXURE
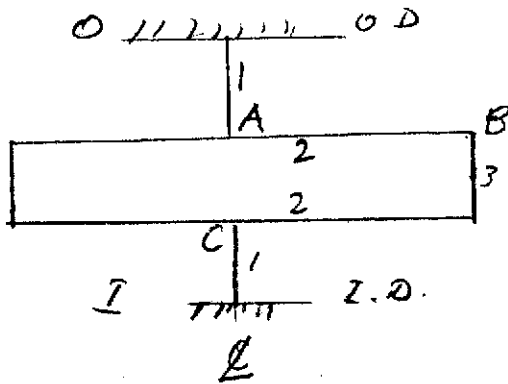
DEFLECTION 0 TO 1 = .011 IN.

FOR AXIAL LOADS + DEFL.

$$I_1 = \frac{.12}{12}(t)^3 = .01 t^3$$

$$I_2 = \frac{.040}{12}(t^3) = .00333 t^3$$

$$I_3 = I_2$$

$$L_1 = .105$$

$$L_2 = .60 \ (\text{TOTAL})$$

$$L_3 = .120 \ (.080 \text{ IN FOR TORSION})$$

FOR UNIT LOAD P/LOOP
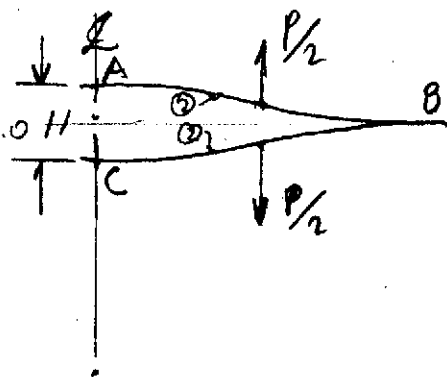
FOR ①

$$\delta_1 = 2\left[P\frac{L_1^3}{3EI}\right]$$

$$\delta_1 = \frac{2}{3}\frac{P(.105)^3}{30 \times 10^6(.01 t^3)} = \frac{2.565 \, P \times 10^{-9}}{t^3}$$

FROM OFFSET DUE TO ③

$$M_1 = \frac{P}{2} \times \frac{③}{2} \times 2 = \frac{P}{2}(.120) = .060 P$$

$$\delta_{1-2} = 2\left[.060\,P\frac{L_1^2}{2EI}\right]$$

$$= \frac{.060\,P(.105)^2}{30 \times 10^6(.01 t^3)} = \frac{2.2\,P \times 10^{-9}}{t^3}$$

$$\text{TOTAL } \delta_1 + \delta_{1-2} = (2.565 + 2.2)\frac{P \times 10^{-9}}{t^3} = \frac{4.765\,P \times 10^{-9}}{t^3}$$

JPL FLOX REGULATOR

Poppet Flexure

$$\delta_2 = 4 \times \left[\frac{P}{2} \left(\frac{L_2}{4} \right)^3 / 3EL \right] = \frac{P}{32} \frac{(L_2)^3}{3EL_2}$$

$$= \frac{P(.60)^3}{96 \times 30 \times 10^6 (.00333\, t^3)}$$

$$\underline{\delta_2 = .0225 P \times 10^{-6} / t^3}$$

δ_3 DEFLECTION DUE TO TORSION ON ②

$$\theta_C \text{ AT END} = \frac{P}{2} \times \frac{L_3}{2} \times \frac{L_2}{2} / KG$$

$$= \frac{\frac{P}{2} \times \frac{.120}{2} \times \frac{.60}{2}}{11.5 \times 10^6 \times .01\, t^3}$$

$$= \frac{.009\, P}{.115 \times 10^6\, t^3}$$

$$= .078\, P \times 10^{-6} / t^3$$

$$\delta_3 = 2 \left[\theta \times \frac{L_2}{2} \right] = \frac{.078 P \times 10^{-6} \times .120}{t^3} = \frac{.00936 \times 10^{-6}\, P}{t^3}$$

$K = \frac{at^3}{4.0} = .25 \times .040\, t^3$
$= .01\, t^3$

$G = 11.5 \times 10^6$

δ_2 DEFLECTION DUE TO TWIST OF ③

$$M_3 = \frac{P}{2} \times \frac{L_2}{4} \quad , \quad \theta_3 = \frac{M_3 \frac{L_2}{2}}{KG}$$

$$\theta_3 = \frac{\frac{P}{2} \left(\frac{.60}{4} \right)(.040)}{.115\, t^3 \times 10^6}$$

$$\theta_3 = \frac{.0261\, P \times 10^{-6}}{t^3}$$

$K = .25 (.040)\, t^3 = .01\, t^3$
$G = 11.5 \times 10^6$
$\frac{L_2}{2} = \frac{.08}{2} = .040$

For ② $\theta_2 = M_2 \frac{L_2}{2} / EI_2 = \theta_3$ (Reduction of Fixity)

$$M_2 = \theta_3 EI_2 / \frac{L_2}{2} = \frac{.0261 P \times 10^{-6}}{t^3} \times \frac{30 \times 10^6 (.00333\, t^3)}{.30}$$

B-3

PREPARED BY
DICKENS

CHECKED BY

THE MARQUARDT COMPANY

CLASSIFICATION

REPORT
JPL FLOX REGULATORS

DATE
4 MAY 1972

PAGE
1.4   OF

JPL FLOX REGULATOR

Poppet Flexure

Deflection of ② due to twist of ③

$$M_2 \text{ (at end of ②)} = .026 P \times 10^{-6} \times \frac{30 \times 10^6 (.00333)}{.30}$$

$$= .026 \times .333 P$$

$$= .00867 P$$

$$\delta_2 = 2\left[\frac{M_2(L_2/2)^2}{2EI}\right] = \frac{.00867 P(.3)^2}{30 \times .00333 t^3 \times 10^6}$$

$$= .0078 P \times 10^{-6}/t^3$$

Deflection of ② due to $P/2$

$$\delta_3 = 2\left[\frac{P/2 (L_3/2)^3}{3EI}\right] = P(.06)^3 / 3 \times .1 t^3 \times 10^6 = \frac{.720 P \times 10^{-9}}{t^3}$$

$$\text{Total } \delta_1 + \delta_2 + \delta_3 = \frac{P}{t^3}\left[4.765 \times 10^{-9} + 22.5 \times 10^{-9} + 7.8 \times 10^{-9} + 9.36 \times 10^{-9} + .720 \times 10^{-9}\right]$$

$$\Delta = \frac{P \times 10^{-9}}{t^3}(45.145)$$

$$R = \frac{1}{\Delta} = \frac{t^3}{45.145 \times 10^{-9}} = \frac{22.1 \times 10^6 \times t^3}{} / \text{Loop}$$

Per plate $R = 3 \times 22.1 \times 10^6 t^3 = 66.3 \times 10^6 t^3 \ \#/\text{in}$

For axial spring rate = $500 \ \#/\text{in}$ max

$$\frac{500}{66.3 \times 10^6} = t^3$$

$$.0195 \ \text{in} = t \text{ max.}$$

B-4

PREPARED BY DICKENS

THE MARQUARDT COMPANY

REPORT J PL FLUX REGULATOR

CHECKED BY

CLASSIFICATION

DATE 4 MAY 1972   PAGE 1-5   OF

JPL FLUX REGULATOR

POPPET FLEXURE

RADIAL STIFFNESS

FOR ① $\quad S = \dfrac{PL}{AE} = \dfrac{2 \times P \times .105}{.125 \times t \times 30 \times 10^6} = \dfrac{.056}{t} \times 10^{-6} P$

② $\quad \delta = \dfrac{2\left(P_1\left(\frac{L_2}{4}\right)^3 2\right)}{3 \times 30 \times 10^6 \, I} \qquad I = \dfrac{t}{12}(.040)^3 = 5.33 \, t \times 10^{-6}$

$\qquad = \dfrac{4 P_1 (.60)^3}{64 \times 90 \times 5.33 \, t} = \dfrac{28.1 \times 10^{-6} P_1}{t}$

TOTAL RADIAL DEFLECTION PER UNIT LOAD / LOOP

$\underline{\delta_{TOT} = \dfrac{28.16 \times 10^{-6} P_1}{t}}$

FOR TOTAL LOAD P / PLATE
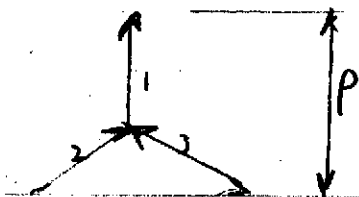
LOAD / LOOP = $\dfrac{P_{TOT}}{3} = P_1$

BASED ON COMPATIBILITY OF DEFLECTIONS

THEREFOR $\delta = 28.16 \dfrac{P}{3t} \times 10^{-6} = 9.33 \dfrac{P \times 10^{-6}}{t}$

$\underline{RADIAL\ RATE = .107 \times 10^6 \, t}$

$\underline{FOR\ .020\ t \qquad R = 2140 \ ^{\#}/_{\eta}}$

PREPARED BY DICKENS

THE MARQUARDT COMPANY

REPORT JPL FLOX REG

CHECKED BY

CLASSIFICATION

DATE 4 MAY 1972

PAGE 1.6 OF

JPL FLOX REGULATOR

POPPET FLEXURURES

STRESSES $t = .020$ Inco 718, H74 Aged

FOR AXIAL $R = 500^\#$,   STROKE $= .011"$

$P_{TOTAL} = 5.5^\#$ AXIAL

LOAD / LOOP $= \dfrac{5.5}{3} = \underline{1.83^\#}$

ON CONNECTOR

$M_{MAX} = 1.83 \times .185 = .349$ IN$^\#$

$fb = \dfrac{.349 \times 6}{.125(.02)^2} = \underline{41800\, psi}$

ON LOOP SIDES

$P = 1.83/2 = .915^\#$

$M_{MAX} = \dfrac{.60}{4} \times .915 = .1375$ IN$^\#$ CONSERVATIVE

$fb = \dfrac{6 \times .1375}{.040(.020)^2} = \underline{51500\, psi}$

TORSION $= .915 \times \left(\dfrac{.160}{2} - \dfrac{.040}{2}\right) = .055$ IN$^\#$

$\tau = \dfrac{Tq}{Kat^2} = \dfrac{.055}{.246(.040)(.020)^2}$ $K_a = .246$ FOR $a/b = 2/1$

$= \underline{14000\, psi}$

$\sigma_e = \left[(\sigma_N)^2 + 3\tau^2\right]^{\frac{1}{2}} = \left[(51.5)^2 + 3(14.0)^2\right]^{\frac{1}{2}} \times 1000 = \underline{57,000\, psi}$

N ALLOWABLE 5×10^5 FULLY REVERSED CYCLES   Inco 718

MIL-HAND-BK 5A   Fig 6.3.8.2.8(a)   1 Dec 1968

B-6

PREPARED BY

Dickens

CHECKED BY

THE MARQUARDT COMPANY

CLASSIFICATION

REPORT
JPL FLOX REG

DATE
4 MAY 1972

PAGE
1.7   OF

JPL FLOX REGULATOR

POPPET FLEXURES $t = .020$

STRESSES FOR RADIAL LOAD $= .06^{\#}$

$$\text{LOAD}/\text{LOOP} = \frac{P}{3} = \frac{.28}{3} = .093^{\#} \quad (pg \; \underline{5})$$

M MAX ON LOOP ELEMENTS

$$M = \frac{.093}{2} \times \frac{.6}{4} = .00695 \, IN^{\#}$$

$$f_b = \frac{.00695(6)}{.020(.040)^2} = 1300 \, psi \quad NEG.$$

$$\left(f_b = f \frac{l^2}{t^2} = \frac{P}{t} S \times K \right)$$

J.P.L FLOX REG.

PUSH ROD — AXIAL GUIDE FLEXURES

$O.D = 1.0$

$I.D = .260$

$RATE = 500 \ \#/_{in} \quad TOTAL \quad AXIAL$

$\quad = 12,000 \ \#/_{in} \quad TOTAL \quad RADIAL$

STROKE = .010 in

SIDE LOAD TOTAL = $1.2^{\#}$ FOR 100 g'

1. ### USE SAME CONFIGURATION FOR POPPET FLEXURE

FOR SIX PLATES $\quad R/_{PLATE} = \dfrac{500}{6} = 83 \ \#/_{in}$

FOR CONFIG. ON Pg 1.1 $\quad R = 66.3 \times 10^6 \ t^3 \ \#/_{in}$

$$t^3 = \frac{83}{66.3 \times 10^6} = 1.25 \times 10^{-6}$$

$$\underline{t = .0108 \ in} \rightarrow .010$$

RADIAL RATE $= .107 \times 10^6 \ t \quad (pg \ 1.5)$

$RATE/_{PLATE} = .107 \times 10^6 (.01) = 1070 \ \#/_{in}$

FOR SIX PLATES $R = 6 \times 1070 = 6420 \ \#/_{in} \quad \underline{N.G}$

FOR $\underline{t = .008}$ RADIAL RATE $= .107 \times 10^6 (.008) = 855 \ \#/_{in} / PLATE$

FOR $12000 \ \#/_{in}$, $N = 12000 / 855 = \underline{14 \ PLATES}$

AXIAL RATE $= 14 \times 66.3 \times 10^6 (.008)^3 = \underline{475 \ \#/_{IN}}$

PREPARED BY
DICKENS

CHECKED BY

THE MARQUARDT COMPANY

CLASSIFICATION

REPORT
JPL Flox Reg

DATE
4 MAY 1972

PAGE
2.2 OF

JPL FLOX REG

PUSH ROD AXIAL GUIDE FLEXURES — Inco 716, HT & Aged

$t = .008$, STROKE $= .010$, RATE $= \dfrac{475}{14} = 34\,\#/\text{PLATE}$

$\text{LOAD}/\text{LOOP} = .010 \times \dfrac{34}{3} = .113\,\#$

MAX STRESS ON LOOP SIDES (Ref ps. 16)

$$\sigma_e = \dfrac{.113}{1.83}\left(\dfrac{.020}{.008}\right)^2 * 57000 = 22000\ psi$$

$\underline{N_{ALLOWABLE} = \infty}$ (MIL-HAND-BK-5A)

M.S = LARGE

FOR RADIAL LOAD STRESSES   FOR SIDE LOAD $= 1.2\,\#$ TOTAL

$f b = \dfrac{93.7\,(\text{LOAD}/\text{PLATE})}{S\,t}$

$S = \text{RATIO}\ \dfrac{O.D.}{1.0} = 1.0$

$t = \text{THICKNESS} = .008$

$\text{LOAD}/\text{PLATE} = \dfrac{1.2}{14} = .0856\,\#$,

$\underline{f b = \dfrac{93.7\,(.0856)}{1.0 \times .008} = 1005\ psi}$ SMALL

PREPARED BY DICKENS

THE MARQUARDT COMPANY

REPORT JPL FLOX REG.

CHECKED BY

CLASSIFICATION

DATE 5 MAY 1972

PAGE 3-1 OF

JPL FLOX REG

BELLOWS GUIDANCE FLEXURE(S) (3 Lobe)

FOR FLEXURE CONFIGURATION SHOWN (pg 1-1)

DEFLECTION PARAMETERS ARE: (AXIAL)

$$\delta_1 = 2.565 \times 10^{-9} / t^3 \frac{x}{\#} \, \ell \frac{(L_1^3 / .105^{-9})}{W / .12} = \frac{2.565 \times 10^{-9}}{t^3} \times S^2 / \#$$

$\underline{S = SCALE\ FACTOR}$

$$\delta_{1-2} = \frac{2.2 \times 10^{-9}}{t^3} \times \frac{L^3}{W} = \frac{2.2 \times 10^{-9}}{t^3} \times S^2 / \#$$

$$\underline{\delta_1, \delta_{1-2} = \frac{S^2 \times 10^{-9}}{t^3} (2.565 + 2.2) = \frac{4.765 \times 10^{-9} \, S^2}{t^3}}$$

$$\delta_{2_1} .0225 \times 10^{-6} / t^3 \times \frac{L_2^3}{W_2} = \frac{22.5 \times 10^{-9}}{t^3} \times S^2$$

$$\delta_{22} = \frac{M_2 (L_2/2)^2}{KI} = \frac{\theta_9 E L_2}{L_2/2} \frac{(L_2/2)^2}{E I_2} = K \frac{L \times L_2}{W} \left(\frac{L_2}{2}\right) = K S^2$$

$$= 7.8 \times 10^{-9} / t^3 \times S^2 / \#$$

$$\underline{\delta_{2_1} + \delta_{22} = \frac{S^2 \times 10^{-9}}{t^3} (22.5 + 7.8) = \frac{30.3 \times 10^{-9}}{t^3} \frac{S^2}{t^3} / \#}$$

$$\delta_{3_1} = \frac{.720 \times 10^{-9}}{t^3} \times \frac{(L \times L_2)^3}{W} = .720 \times 10^{-9} S^2 / t^3 / \#$$

$$\delta_{32} = - \frac{}{t^3} \frac{}{W} \quad 9.36 \times 10^{-9} S^2 / t^3$$

$$Total\ \delta = \frac{S^2 \times 10^{-9}}{t^3} (4.765 + 30.3 + .720 + 9.36) = \frac{10^{-9}}{t^3} (45.145 \, S^2) / \#$$

$$\underline{Rate = t^3 \, 10^6 (22.1) / S^2 / LOOP} \rightarrow \underline{66.3 \times 10^6 \, t^3 / S^2 / PLATE}$$

$\underline{AXIAL}$

PREPARED BY
DICKENS

CHECKED BY

THE MARQUARDT COMPANY

CLASSIFICATION

REPORT
JPL FLOX REG.

DATE
5 MAY 1972

PAGE
J.2   OF

J.P.L. FLOX REG

BELLOWS GUIDANCE FLEXURES

FOR FLEXURE CONFIGURATION SHOWN (pg J.1)

DEFLECTION PARAMETERS FOR RADIAL RATE

PRINCIPAL CONTRIBUTOR IS ③

$$\delta = \frac{25.1 \times 10^{-6}}{t} \frac{L^3}{h^3} = \frac{25.1 \times 10^{-6}}{t} \times 1$$

THEREFORE FOR EQUAL DIMENSIONAL SCALING

$$\delta = \frac{1}{R} = \underline{SAME \ FOR \ ALL \ SIZES}; \ FOR \ SAME \ THICKNESS$$

$$\underline{R = .107 \times 10^6 t.}$$

STRESS PARAMETERS FOR RADIAL LOAD

$$f_b = Load/\delta \times \frac{KL}{tL^2} = \frac{LOAD \times K}{tL} \qquad LET \ L = S = \frac{0.2}{1.0}$$

$$f_b = \frac{K \ LOAD}{S(t)}$$

FOR 1.0 O.D. , $t = .020$; $P = .06$ #/PLATE, $f_b = 281$ psi

$$K = \frac{f_b \ S(t)}{LOAD} = \frac{281 \ (1.0)(.020)}{.06} = 93.7$$

$$\underline{f_b = \frac{93.7 \ (LOAD/PLATE)}{S(t)}}$$

PREPARED BY Dickens

THE MARQUARDT COMPANY

REPORT JPL Flox Reg.

CHECKED BY

CLASSIFICATION

DATE 5 MAY 1972

PAGE 3.3 OF

JPL Flox Reg.

BELLOWS GUIDANCE FLEXURE (CONFIG- pg 1.1)

RADIAL + AXIAL SPRING RATES/PLATE

O.D.	t	t^3	$S = \frac{O.D.}{I.D.}$	S^2/t^3	R_{RADIAL} (#/in)	R_{AXIAL} (#/in)
1.00	.020	8×10^{-6}		$.125 \times 10^6$	2140.0	530.0
	.010	1 "	1.0	1.0×10^6	1070.0	66.3
	.008	.51 "		1.96×10^6	856.0	33.5
2.00	.030	27×10^{-6}		$.148 \times 10^6$	3210.0	446.0
	.020	8 "	2.0	.50	2140.0	132.6
	.010	1 "		4.0	1070.0	16.6
	.008	.51 "		7.84	856.0	8.5
3.00	.040	64×10^{-6}		$.1407 \times 10^6$	4280.0	471.0
	.030	27 "	3.0	.30	3210.0	220.0
	.020	8 "		1.125	2140.0	59.0
	.010	1 "		9.00	1070.0	7.96
4.00	.050	125×10^{-6}		$.1278 \times 10^6$	5350.0	520.0
	.030	27 "	4.0	.593	3210.0	112.0
	.020	8 "		2.00	2140.0	33.15
	.010	1 "		16.0	1070.0	4.15

B-12

PREPARED BY
DICKENS
CHECKED BY

THE MARQUARDT COMPANY

CLASSIFICATION

REPORT
JPL FLox REG
DATE
5 MAY 1972
PAGE
3.4 OF

J.P.L FLOX REG

BELLOWS GUIDANCE FLEXURE(S)

LOAD = K R_{AX} STROKE (AXIAL)

$$f_b = K \cdot \frac{LOAD \times L/.1375}{W/.040 \, t^2}$$

$\underline{S = SCALE \; FACTOR}$

BUT $\frac{L}{W} = \frac{S}{S} = 1$ FOR SCALE FACTOR

$$2 = K \; LOAD \times \frac{L}{W} t^2$$

BUT $\frac{L}{W} = 1.0$ FOR EQUAL SCALE

LET $\sigma_e = K \; LOAD / t^2$

$= K \; RATE \; STROKE / t^2$ (Ref pg 3.1)

$$\sigma_e = (K) \frac{66.3 \times 10^6 \, t^3}{S^2} \times \frac{STROKE}{t^2} = \frac{66.3 \times 10^6 \, t \; STROKE \times K}{S^2}$$

FOR 1.00 OD, t = .020 STROKE = .011, $\sigma_e = 57000\text{p}$, $S = 1$
(Ref pg 1.6)

$$57000 = \frac{66.3 \times 10^6 (.020)(.011)}{1} K$$

$$K = \frac{57000}{14600} = 3.90$$

$$\underline{\sigma_e = 259 \times 10^6 \, t \; Stroke / S^2}$$

ALLOWABLE σ_e FOR 10^5 cycles Inco 718

$\sigma_e = 65000 \; \text{psi}$

$$\underline{Allowable \; STROKE = \frac{65000 \times S^2}{259 \times 10^6 \, t}} = \left(\frac{251 \, S^2}{t \times 10^6} \right)$$

$S = SCALE = \frac{O.D.}{1.0}$

JPL FLOX REGULATOR

BELLOWS GUIDANCE FLEXURE(S)

ALLOWABLE STROKE VS. O.D. + THICKNESS

$$A.S. = 251 \left(\frac{S^2}{t} \right) 10^{-6}$$

O.D.	S	S^2	t	S^2/t	ALLOW-STROKE (MAX)
1.00	1	1	.030	33.3	.00835 IN
			.020	50	.0125 IN
			.010	100	.0251 IN
			.008	125	.0314 IN
2.0	2	4	.030	133	.0334
			.020	200	.0502
			.010	400	.100
			.008	500	.1255
3.0	3	9	.040	225	.0565
			.030	300	.0753
			.020	450	.1130
			.010	900	.226
4.0	4	16	.050	320	.0803
			.040	400	.100
			.030	533	.134
			.020	800	.200
			.010	1600	.400

FORM TMC 685 REV. 3-70

PREPARED BY DICKENS

THE MARQUARDT COMPANY

REPORT JPL FLOX REG

CHECKED BY

CLASSIFICATION

DATE 6 MAY 1972

PAGE J.8 OF

JPL FLOX REG

RADIAL BENDING STRESSES ON BELLOWS GUIDANCE FLEXURES

LOAD = .3 # FOR 100 g

$$\text{MAX STRESS} = \frac{93.7\,(LOAD/PLATE)}{S(t)} \qquad \text{WHERE } S = \frac{O.D.}{1.0}$$

$$f_b = \frac{93.7 \times .3}{S(t)} = \frac{28.1}{S(t)}$$

ALLOWABLE F_{by} = 150,000 psi = F_{ty}

O.D.	S	t	S(t)	$f_b = \frac{28.1}{S(t)}$
1.00	1	.040	.040	703.0 psi
		.030	.030	940
		.020	.020	1406
		.010	.010	2810
		.006	.008	3520
2.0	2	.050	.10	281
		.040	.08	352
		.030	.06	
		.020	.04	703
		.010	.02	1406
3.0	3	.050	.150	
		.040	.12	
		.030	.09	
		.020	.04	
		.010	.03	940 psi
4.0	4	.050	.20	
		.040	.16	
		.030	.12	
		.020	.08	
		.010	.04	703 psi

CONDITION NOT CRITICAL

Radial & Axial Spring Rates
Flexure Configuration "A"
One Plate Only
Modulus = 30×10⁶

FORM TMC 911-2 REV. 11-71

THE **Marquardt** COMPANY
CCI Aerospace Corporation
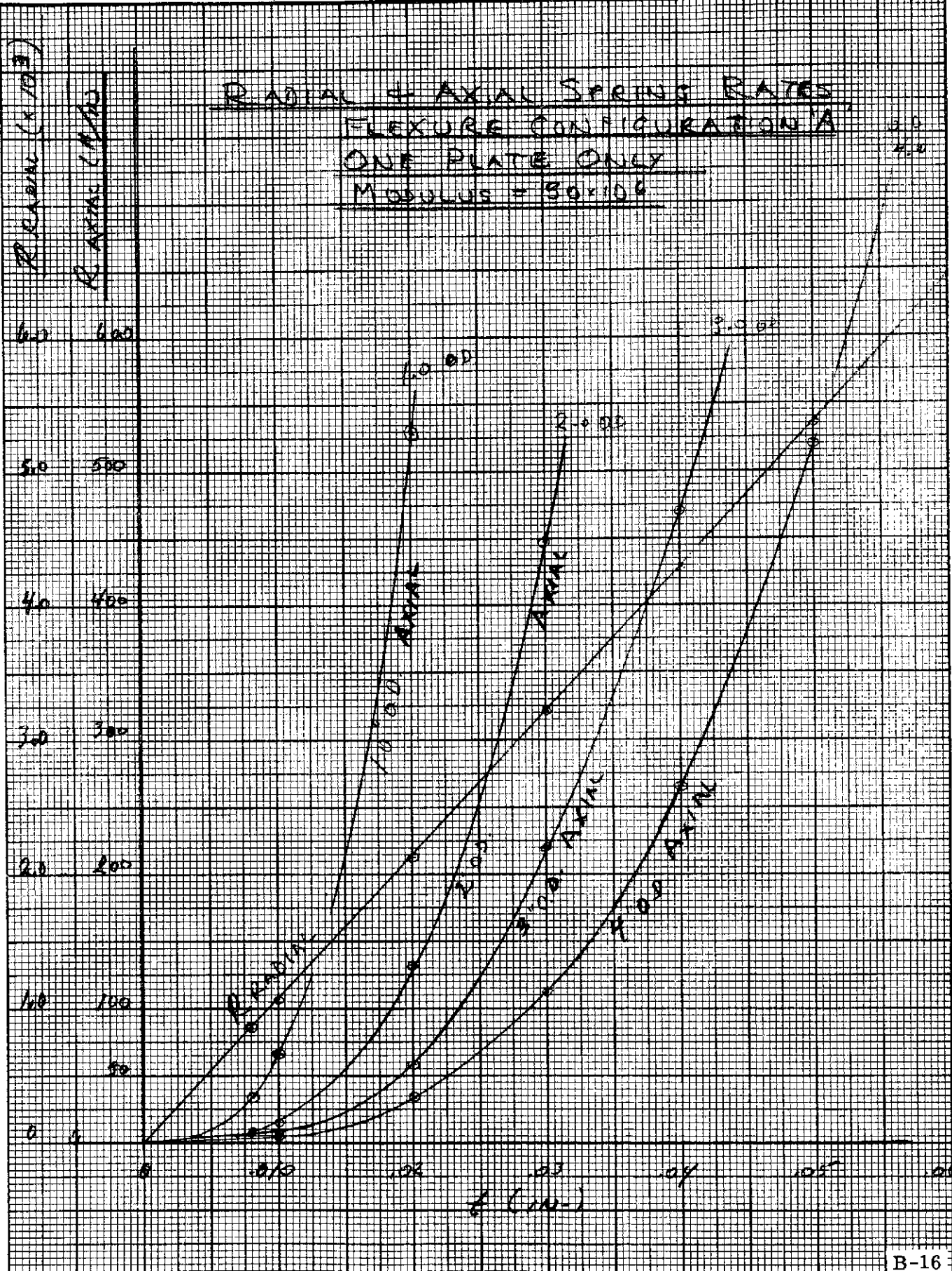
PREPARED BY: DICKENS
CHECKED BY:
PAGE: 3.7
DATE: 5 MAY 1972

ALLOWABLE AXIAL STROKE vs THICKNESS FLEXURE CONFIGURATION 'A'
Inco 718 HT 4 Aged
$N_{END} = 10^5$ CYCLES

B-17
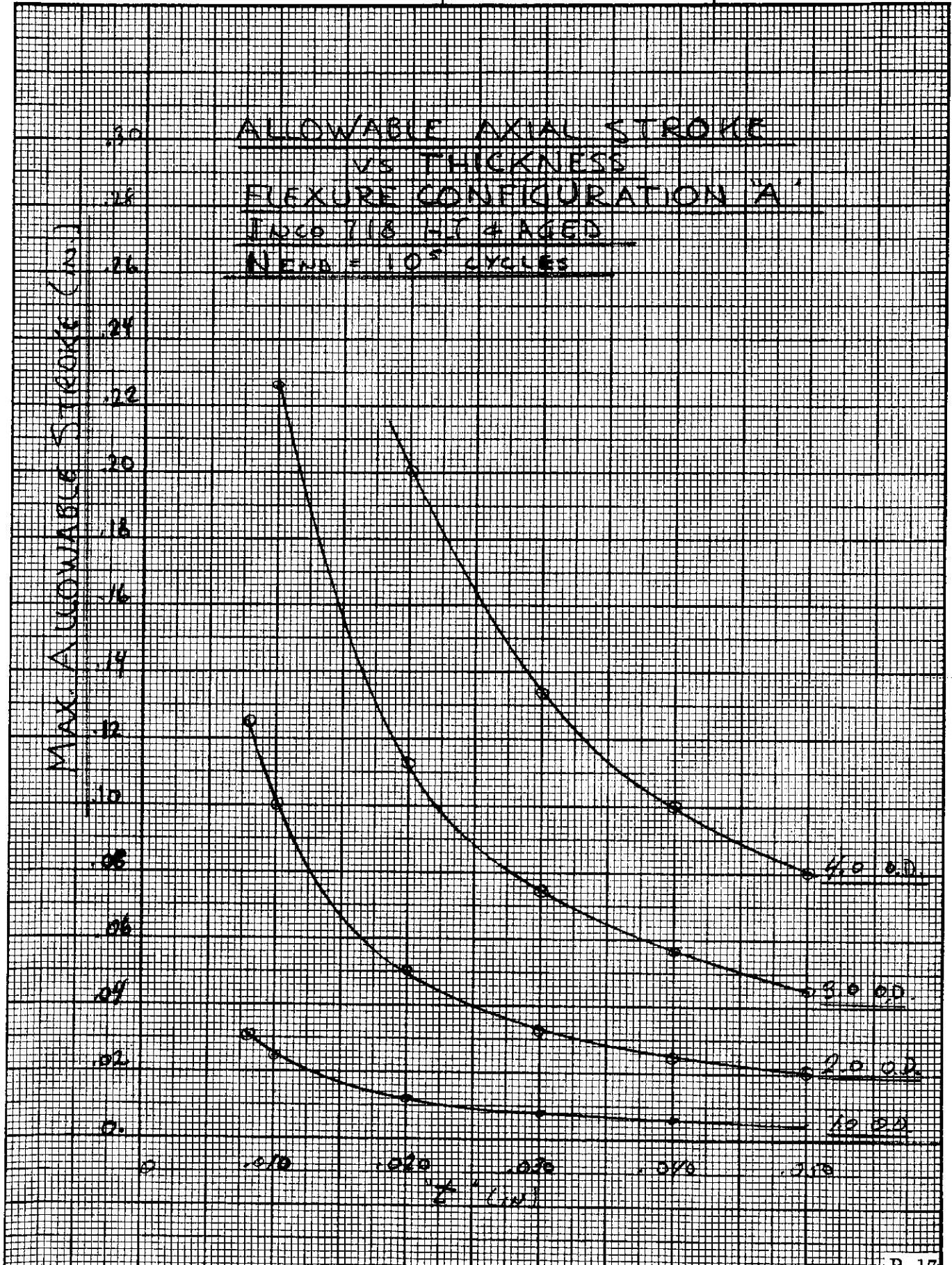
FLEXURES   360° TYPE
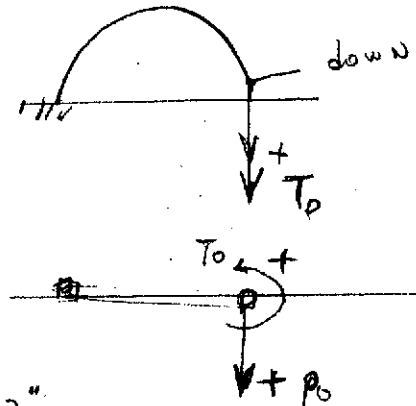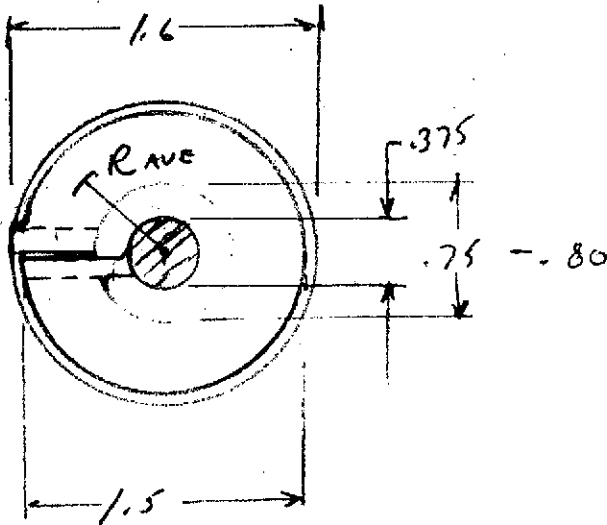
ASSUME $R_{AVER} = \dfrac{\left(\dfrac{1.5}{2} + \dfrac{.75}{2}\right)}{2} = .563"$

LET STROKE $= \pm .100$ IN

TREAT AS TWO SEMI-CIRCULAR BEAMS

FOR AXIAL Δ OF .100 TOTAL, <u>END OF SEMI-CIRCLE</u>

<u>DEFLECTS .050 IN.</u>

$$\Delta = \frac{P_0 R^3}{4EI}(B_1 + \lambda B_2) + \frac{T_0 R^2}{4EI}(\lambda B_5 - B_1)$$

Ref PROD ENGRG JAN 7, 1963 pg 78

$$\theta = 0 = +\frac{P_0 R^2}{4EI}(\lambda B_3 - B_1) + \frac{T_0 r}{4EI}(\lambda B_7 + B_1)$$

FOR SEMI-CIRCLE, $\phi = 180° = 3.14$ rad
$\theta = 0.0$ rad
$R = .563$

PREPARED BY
DICKENS

CHECKED BY

THE MARQUARDT COMPANY

CLASSIFICATION

REPORT
FLEXURES - JPL VALVE

DATE
2 MAY 1972

PAGE
3,2 OF

FLEXURES —360° TYPE

FOR $\frac{1}{2}$ CIRCLE

$\phi = \pi = 3.14 \, rad$
$\theta = 0.0 \, rad$

$B_1 = 2(\phi - \theta)\cos\theta + \sin\theta - \sin(2\phi - \theta)$

$\underline{B_1} = 2(3.14) + 0 - 0 = \underline{6.28}$

$B_2 = 3\sin\theta + \sin(2\phi - \theta) + 2(\phi - \theta)\cos\theta + 4(\phi - \theta) - 4\sin\phi - 4\sin(\phi - \theta)$

$\underline{B_2} = 0 + 0 + 2(3.14) + 4(3.14) - 0 - 0 = \underline{18.84}$

$B_3 = 4\cos(\phi - \theta) - \cos(2\phi - \theta) - 2(\phi - \theta)\sin\theta + \cos\theta - 4$

$\underline{B_3} = -4 - 1 - 0 + 1 - 4 = \underline{-8}$

$B_5 = 4\sin\phi - 3\sin\theta - \sin(2\phi - \theta) - 2(\phi - \theta)\cos\theta$

$\underline{B_5} = 0 - 0 - 0 - 2(3.14)1 = \underline{-6.28}$

$B_7 = 2(\phi - \theta)\cos\theta + \sin(2\phi - \theta) - \sin\theta$

$\underline{B_7} = 2(3.14) + 0 - 0 = \underline{6.28}$

$\lambda = \frac{EI}{GK} = \frac{1}{.38}\frac{I}{K}$

$I = \frac{.375}{12}(t^3) = .0312\, t^3$

$K \simeq .31(.375)(t^3)$
$= .116\, t^3$

$\underline{\lambda = \frac{.0312 t^3}{.38(.116)t^3} = .707}$

FORM TMC 685 REV. 3-70

JPL FLOX REGULATOR

BELLOWS GUIDE FLEXURES

360° TYPE — 1.50 O.D.

FOR CONFIGURATION SHOWN ON PAGE —

$$R_{AXIAL} = 1.365 \, t^3 \times 10^6 \; \#/in$$

$$R_{RADIAL} = .228 \, t \times 10^6 \; \#/in \qquad RADIAL \; IN \; X - DIREC.$$

$$R_{RADIAL} = .504 \, t \times 10^6 \; \#/in \qquad RADIAL \; IN \; Y - DIREC.$$

EFFECTS OF SCALE

ASSUME PLANE DIMENSIONS ARE DIRECT FUNCTION OF SCALE

$$SCALE = \frac{O.D.}{1.50}$$

$$R_{AXIAL} = \frac{1.365 \, t^3 \times 10^6}{S^2} \; \#/in \qquad *$$

$$R_{RADIAL} = .228 \, t \times 10^6 \; \#/in \qquad - \; X \; DIRECTION$$

$$R_{RADIAL} = .504 \, t \times 10^6 \; \#/in \qquad - \; Y \; DIRECTION$$

$$\left(R_R = \frac{1}{\Delta} = \frac{1}{f\left(\frac{R^3}{W^3}\right)\frac{1}{t}} = \frac{1}{K\left(\frac{SR}{SW}\right)^3 \frac{1}{t}} = Kt \right)$$

$$* \; BASED \; ON \quad R_A = \frac{1}{\Delta} = \frac{1}{f\left(\frac{R^3}{Wt^3}\right)} = \frac{1}{f\left(\frac{(SR)^3}{SWt^3}\right)} = \frac{1}{fK\left(\frac{S^3}{S}\right)} = \frac{1}{KS^2}$$

PREPARED BY
DICKENS

THE MARQUARDT COMPANY

CHECKED BY

CLASSIFICATION

REPORT
JPL - FLOX REG.

DATE
8 MAY 1972

PAGE
7.4 OF

JPL FLOX REGULATOR

EFFECT OF SCALE SIZE ON 360° TYPE FLEXURE

FOR AXIAL RATE

$$R = 1.365 \, t^3 \times 10^6 / S^2$$

$$S = \frac{O.D.}{1.50}$$

O.D	S	S^2	t	t^3	$R_{AX} = \dfrac{1.365 \, t^3 \times 10^6}{S^2}$ /PLATE
1.5	1	1	.006	.216 ×10⁻⁶	.295 #/ɪ
			.008	.51 "	.695 "
			.010	1.00 "	1.365 "
			.020	8.0 "	10.90 "
			.030	27.0 "	36.90 "
			.040	64.0 "	87.5 "
3.0	2	4	.008	.51 ×10⁻⁶	.174 #/ɪ
			.010	1.00 "	.341 "
			.020	8.0 "	2.730 "
			.030	27.0 "	9.22 "
			.040	64.0 "	21.90 "
			.060	216.0 "	73.8 "
4.0	2.67	7.1	.010	1.0 ×10⁻⁶	.192 #/ɪ
			.020	8.0 "	1.54 "
			.030	27.0 "	5.20 "
			.040	64.0 "	12.30 "
			.060	216.0 "	41.60 "

RADIAL RATE $\cong \dfrac{(.228 + .504)}{2} \, t \times 10^6$ AVER. FOR ALL O.D.

t	$R_{RADIAL} = .366 \, t \times 10^6$
.006	2200 #/ɪ /PLATE
.060	22,000 #/ɪ /PLATE

FORM TMC 686 REV. 3-70

PREPARED BY
DICKENS

THE MARQUARDT COMPANY

CHECKED BY

CLASSIFICATION

REPORT
JPL - FLOX REG.

DATE
8 MAY 1972

PAGE
3.5 OF

J.P.L FLOX REGULATOR

AXIAL RATE OF 1.00 OD 360° TYPE FLEXURE

$$R = 1.365 \, t^3 \times 10^6 / s^2$$

$$S = \frac{OD}{1.5} = \frac{1.0}{1.5} = .667$$

$$S^2 = .444$$

O.D	t	t^3	$R_N = \dfrac{1.365 \, t^3 \times 10^6}{.444}$ /PLATE
1.0	.006	$.216 \times 10^{-6}$	.665 #/1.
	.008	.51 "	1.570
	.010	1.0 "	3.065
	.020	8.0 "	24.60
	.030	27.0 "	83.0
	.040	64.0 "	197.0

APPENDIX C

BELLOWS STRESS ANALYSIS

He Regulator

Bellows Analysis - (SS P)

I.D. 1.74 "   MATL INCO 718
O.D. = 2.09 "
D_{EFF} = 1.93 "

N = 20 convolution
t = .006
TOTAL RATE = 105 #/"

FREE H = 3.4 "
INSTALL H = 1.9 "

STROKE = .036 "

From Roark pg 306, case 28

$$\Delta = (1.813 \, b)^3 \sqrt{1-v^2} \, Pn / \pi E t^3 a$$

$b = \dfrac{O.D - I.D}{4} = .0875$

$v = .3$

$n = 20$

$t = .006, \quad t^3 = .216 \times 10^{-6}$

$a = \dfrac{I.D}{2} + .0875 = .965$

$\Delta_1 = 3.4 - 1.9 = 1.5$

$\Delta_2 = 1.5 \times .03 = 1.53$

$E = 30 \times 10^6$

$$P_1 = \frac{\Delta \pi E t^3 a}{n (1.813 \, b)^3 (1-v^2)^{\frac{1}{2}}} = \frac{1.5 \, \pi \, (20) 10^6 (.216) 10^{-6} (.965)}{4.0 \times 10^{-3} (.956) \times 20}$$

$$= \underline{386 \, \#} \quad \text{Too High - does not agree} \\ \underline{\text{with rate}}$$

USE $P_1 = 105 \times 1.5 = \underline{158 \#}$

$P_2 = 105 \times 1.53 = \underline{161 \#}$

He REGULATOR

FOR 161# LOAD

Roark pg. 306 case 28

$$S_1 = \frac{1.63 P}{2\pi ta \sqrt[6]{1-v^2}} \sqrt[3]{\frac{ab}{t^2}}$$

$$= \frac{1.63 (161)}{2\pi(.006)(.965)(.99)} \left(\frac{.965 \times .0875}{36 \times 10^{-6}}\right)^{\frac{1}{3}}$$

$$= 7300 (13.3)$$

$$= 97500 \text{ psi} \quad \underline{(Low - See \ below)}$$

FOR 158 # LOAD

$$S_1 = \frac{158}{161} \times 97500 = 95600 \text{ psi}$$

CIRCULAR MEMBRANE STRESS

$$S_2 = \frac{.925 P \sqrt[3]{1-v_e^2}}{2\pi ta} \sqrt[3]{\frac{ab}{t^2}}$$

$$= \frac{.925 (161)(.969)}{2\pi(.006)(.965)} (13.3)$$

$$= 3970 (13.3)$$

$$= 53000 \text{ psi}$$

CHECK   LET P = 161#

plate Roark pg 221 case 18

$$Max S = \beta \frac{W}{t^2} = \frac{.03(161)}{36 \times 10^{-6}}$$

$$= 133000 \text{ psi} \quad MAX$$

$$\frac{a}{b} = \frac{2.09}{1.93} = 1.08$$

$$\beta = .03$$

C-2

PREPARED BY: DICKENS
THE MARQUARDT COMPANY
CHECKED BY:
CLASSIFICATION:
REPORT: He REGULATOR
DATE: 23 JUNE 72
PAGE: 3 OF

He REGULATOR

FATIGUE CAPABILITY OF SSP BELLOWS — INCO 718

MAX S_1 = 133,000 psi FOR 161 A $\qquad$ $F_{tu} = 180$ KSi

$F_{ty} = 150$ KSi

$$S_2 = \frac{158}{161} \times 133000 = 131000 \text{ psi}$$

MEAN STRESS = 132,000 psi

ALT. STRESS = ±1,000 psi

GOODMAN - DIAGRAM MIL-HANDBK 5A
DEC/1968

45 KSi

ALT STRESS

1 KSi

132 KSi   180 KSi

MEAN STRESS
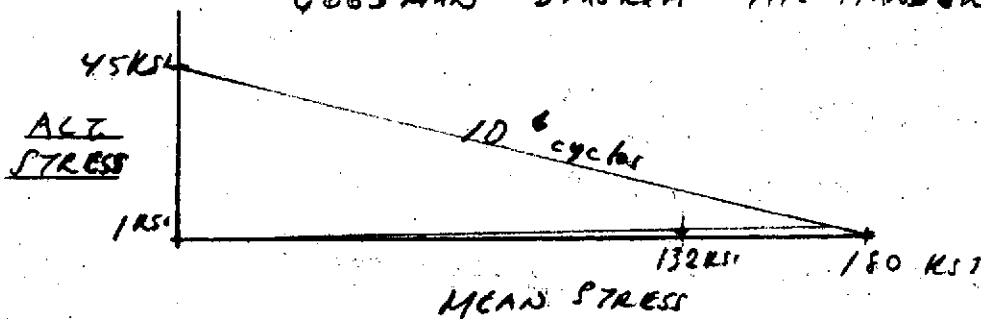
SCALE 1" : 50 KSi

$$M.S. = \frac{17}{13.2} - 1 = .29$$

FOR MAX COMPRESSION — $P = 105(3.4 - 1.5) = 200$ #

$$f_{b\,max} = \frac{200}{158} \times 133000 = 169000 \text{ psi}$$

$$F_{by} = 1.22 \times 150,000 = 183,000 \text{ psi}$$

$$M.S. = \frac{183}{169} - 1 = .08$$

He REGULATOR-

BELLOWS ANALYSIS - GARDNER

$ID = 1.60$
$OD = 2.105$
$D_{EFF} = 1.86$

MAT'L INCO 718 HT + AGED
$F_{TY} = 150,000$ psi

$N = 30$
$t = .008$ in
$RATE = 105$ #/in

$FREE \ H = 2.0$
$INSTAL. \ H = 1.7$

$STROKE = .030$ in

$P_1 = (2.0 - 1.7)105 = \underline{31.5}$ #

$P_2 = 31.5 + .03(105) = \underline{34.65}$ #

ANALYZE PER ROARK pg 221 case 18

$MAX \ S = \beta \dfrac{\omega}{t^2}$

$a/b = \dfrac{2.05}{1.86} = 1.10$

$\beta = .03$

$= \dfrac{.03 (34.65)}{(.008)^2}$

$= \underline{16,300 \ psi} \quad MAX$

$MIN \ S = \dfrac{31.5}{34.65} \times 16300 = 14800 \ psi$

$\left[\begin{array}{l} MEAN \ S = (16300 + 14800)/2 = \underline{15550 \ psi} \\ ALT \ S = \underline{750 \ psi} \end{array} \right.$

$F_N = 65,000 \ psi$ FOR 10^5 cycles

$\underline{M.S = LARGE}$

FOR MAX COMP $P = (2.0 - .3)105 = 178$ #

$S_{MAX} = (178/34.65) \times 16300 = \underline{83600 \ psi}$

C-4

PREPARED BY DICKENS

THE MARQUARDT COMPANY

REPORT He REGULATOR

CHECKED BY

CLASSIFICATION N-60350-10

DATE 26 JUNE 1972

PAGE 5 OF

He REGULATOR

BELLOWS ANALYSIS - SS p - $t = .006$ INCO 716

FOR 240 psi EXTERNAL - CONSTANT

$F_{ty} = 150,000$ psi
$F_{tu} = 160,000$ psi

O.D. = 2.090
I.D. = 1.74
MEAN D = 1.985
$t = .006$

FROM ROARK pg. 306, case 29 ,   AT RADIUS

MAX BENDING STRESS $S_1 = \dfrac{.955 \, p}{\sqrt[3]{(1 - \nu^4)}} \sqrt[3]{\left(\dfrac{ab}{t^2}\right)^2}$

a = MEAN RADIUS
$= \dfrac{1.985}{2} = .955$

$b = \dfrac{t}{2}\left(\dfrac{OD - ID}{2}\right) = .0875$

$t = .006, \quad t^2 = 36 \times 10^{-6}$

$S_1 = \dfrac{.955(240)}{.969} \sqrt[3]{\left(\dfrac{.955 \times .0875}{36 \times 10^{-6}}\right)^2}$

$S_1 = 23.6 \left(2320\right)^{\frac{2}{3}}$

$\underline{S_1 = 41400 \text{ psi}}$ USE

CHECK FROM BELLOWS EQUATION

$\underline{S = \dfrac{p(OD - ID - t)^2}{16 \times 1.25 \,(t)^2}} = \dfrac{240(.344)^2}{20 \times (36)(10^{-6})} = \underline{39700 \text{ psi}}$

He REGULATOR

BELLOWS ANALYSIS - GARDNER $t = .008$ INCO 718

$F_{TY} = 150 K$
$F_{TU} = 180 K$

FOR 240 psi EXTERNAL CONSTANT

$O.D = 2.05$
$I.D = 1.60$
$MEAN = 1.825$
$t = .008$

FROM ROARK pg 306, case 29, AT RADIUS

MAX BENDING STRESS $= S_1 = \dfrac{.955 P}{\sqrt[3]{(1-v^2)}} \sqrt[3]{\left(\dfrac{ab}{t^2}\right)^2}$

$a = $ MEAN RADIUS $= \dfrac{1.825}{2}$

$= .9125$

$b = \dfrac{1}{2}\left(\dfrac{OD - ID}{2}\right) = .1125$

$t^2 = 64 \times 10^{-6}$

$S_1 = \dfrac{.955\,(240)}{.969} \sqrt[3]{\left(\dfrac{.9125 \times .1125}{64 \times 10^{-6}}\right)^2}$

$= 236\,(1600)^{2/3}$

$= 32100 \text{ psi}$

CHECK FROM BELLOWS EQUATION

$S = \dfrac{p\,(O.D - I.D - t)^2}{16 \times 1.25\,(t)^2} = \dfrac{240\,(.442)^2}{20\,(64)10^{-6}} = 36,500 \text{ psi}$ USE

C-6

He Regulator

Bellows Analysis - SSP - $t = .006$ Inco 718 HT/Age

Combined 240 psi Pressure and .030 Stroke 10^5 cycles

Mean Stress - $41400 + 132000 = 173400$ psi* (pg 3, 5)

Alt. Stress = ± 1000 psi   (pg 3)

From Fig 6.3.8.2-8(a) Mil-Hand Bk 5A, Dec 1968

$$M.S. = \frac{5.25}{4.85} - 1 = .08$$

Bellows Analysis - Gardner - $t = .008$ Inco 718 HT/Age

Combined 240 psi Pressure and .030 Stroke - 10^5 cycles

Mean Stress = $36500 + 15550 = 52050$ psi (Ref pgs 4, 6)

Alt. Stress = ± 750 psi   (pg 4)

From Fig 6.3.8.2-8(a) Mil-Hand Bk 5A, Dec 1968

$$M.S. = \frac{5.10}{1.45} - 1 = \underline{LARGE}$$

Note:

* 173400 psi Stress at Bending Yield of Material

APPENDIX D

SPRING OPTIMIZATION

SPRING OPTIMIZATION - HELIUM REGULATOR
BASED ON WEIGHT

- 4 LEVER RATIOS
- FOR EACH LEVER RATIO
  1. SINGLE COIL SPRING
  2. ZERO TWIST
     a. TWO COIL SPRINGS IN SERIES OPPOSITE HELIX
     b. MACHINED SPRING — TWO SECTIONS OPPOSITE HELIX
  3. OPTIMIZED SPRING CONFIGURATION

	LEVER RATIO			
	1	2	3	4
O. DIA. (MAX)	2.85	1.95	1.60	1.35
STROKE (INCHES)	.010	.020	.030	.040
PRELOAD (POUNDS)	1850	953	646	488
SPRING RATE (MAX)	4588	1058	388	188

D-1

PREPARED BY
ALEX MARDERIAN

THE MARQUARDT COMPANY

REPORT

CHECKED BY

CLASSIFICATION

DATE
JUNE 6 1972

PAGE
2 OF

STRESS CRITERIA

10^6 CYCLES OPERATION

MATERIAL — CUSTOM 455 STEEL

$\gamma = 0.28$ LBS/IN^3

$E = 29 \times 10^6$ PSI

$G = 11 \times 10^6$ PSI

$\sqrt{} = 0.30$

ASSUME SHEAR YIELD $= 0.57 \times$ MINIMUM TENSILE ULTIMATE.

— FOR COIL SPRINGS
COLD DRAWN & AGE HARDENED

WIRE DIA. OVER 0.150" $\sigma_{TU} = 260,000 / 290,000$ PSI

$\longrightarrow$ $\sigma_{sy} = 0.57(260,000) = 148,500$ PSI

— FOR MACHINED SPRINGS
AGE HARDENENED

$\sigma_{TU} = 220,000$ PSI MIN.

$\longrightarrow$ $\sigma_{sy} = 0.57(220,000) = 125,000$ PSI

SHOT PEEN ALL SPRINGS.

D-2

1.0 LEVER RATIO = 1

1.1 SINGLE COIL SPRING
$\qquad$ 2.850 O. DIA.
$\qquad$ .500 WIRE DIA.
$\qquad$ 2.350 MEAN DIA.

$\qquad$ RATE = 4500 LB/IN.

PRELOAD = 1850 LB.
@ .010" TRAVEL LOAD = 1900 LB.
$\qquad$ DEFLECTION TO 1850 LB. PRELOAD = 0.410"
— ALLOW .020" TRAVEL BEYOND MIN. OPERATING
$\qquad$ HEIGHT TO GO TO SOLID HEIGHT.
LOAD AT SOLID HEIGHT = 2300 LB.

$D/d = 4.70 \qquad K = 1.31$

AT SOLID $\begin{cases} \sigma_s = \dfrac{2.55\,(2300)\,(2.35)}{(0.50)^3} \times 1.31 \\[2mm] \sigma_s = 145,000 \text{ PSI.} \end{cases}$

PRELOAD = 1850 LB $\qquad \sigma = 117,000$ PSI
@.010" TRAVEL = 1900 LB $\qquad \sigma = 120,000$ PSI

MEAN STRESS = 118,500 PSI
ALTERNATING STRESS = 1,500 PSI.

$$N = \frac{G\,d^4}{8\,D^3\,R} = \frac{11\times10^6\,(62.5\times10^{-3})}{8\,(2.85)^3\,(4.5\times10^3)} = 0.82$$

ACTIVE COILS = 0.82

TOTAL COILS = 2.82

WEIGHT $= (2.35\,\pi)\,(2.82)\left[\dfrac{\pi(.5)^2}{4}\right] 0.28 = 1.13$ LBS

$\left(\text{WEIGHT PENALTY} - 2 \text{ DEAD COILS} = .81 \text{ LBS.}\right)$

WORKING WEIGHT = 0.32 LBS.

PREPARED BY
ALEX MARDERIAN

THE MARQUARDT COMPANY

REPORT

CHECKED BY

CLASSIFICATION

DATE
JUNE 6 1972

PAGE
4 OF

1.2 TWO COIL SPRINGS IN SERIES
OPPOSITE HELIX
DIMENSIONS SAME AS ITEM 1.1
STRESSES SAME A ITEM 1.1

RATE /SPRING = 9,000 LB/IN

ACTIVE COILS = 0.41

TOTAL COILS = 2.41

WEIGHT ONE SPRING = $2.35 \, \pi (2.41) \left(\frac{\pi}{4} (0.5)^2 \right) .28 = .99$

NEIGHT PENALTY /SPRING (2 DEAD COILS) = .83

WORKING WEIGHT = .16

2 SPRINGS

TOTAL WEIGHT = 1.98 LBS

WEIGHT PENALTY (2 DEAD COILS) = 1.66 LBS

WORKING WEIGHT = .32 LBS

1.3 MACHINED SPRING TWO SECTIONS IN
     SERIES — OPPOSED HELIX

1.3.1 1ST ITERATION

$b = h = 0.5$ $b/h = 1.0$ O. DIA = 2.85"
                                       RATE = 4500 LB/IN

$D = 2.35$ $D/b = 4.7$

$\lambda = 1.275$

$$\tau = \frac{1.275 \ (1900)\ (2.35 + .50)(.50 + .50)}{(.50)^2 (.50)^2} = 111,000 \ PSI$$

TOTAL ACTIVE COILS REQ'D $\mu = .179$

$\longrightarrow$ BOTH SECTIONS $N = \dfrac{.179 \ (.5)^2 (.5)^2 (11 \times 10^6)}{(2.35)^3 \ (4.5 \times 10^3)} = \underline{\underline{2.11}}$

WT OF ACTIVE COILS $= (2.35 \pi)(2.11)[(.50)^2].28 = 1.09$ LBS.
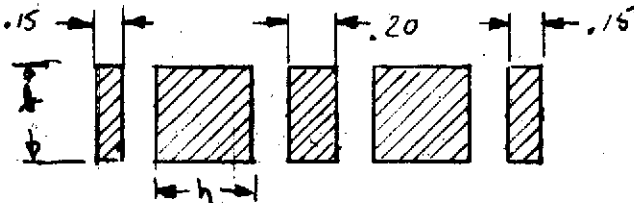
WT OF DEAD MTL $= 0.50 \left[\frac{\pi}{4} \left[(2.85)^2 - (1.85)^2\right]\right] 0.28 = 0.46$

$\begin{cases} TOTAL \ WEIGHT = & 1.55 \ LB. \\ \\ WEIGHT \ PENALTY = & .46 \ LB. \\ (DEAD \ MTL) & \\ WORKING \ WEIGHT = & 1.09 \ LB \end{cases}$

D-5

PREPARED BY
ALEX MARDERIAN
CHECKED BY

THE MARQUARDT COMPANY

REPORT

CLASSIFICATION

DATE JUNE 6 1972

PAGE 6 OF

$6.3.2$ 2ND ITERATION

$h = .625$ $\quad$ $b/h = 0.64$ $\qquad$ 2.85" O.DIA.

$b = .400$ $\qquad$ 4500 LB/IN.

$$D = 2.85 - .40 = 2.45"$$

$$D/b = 6$$

$$\lambda = 1.32$$

$$\sigma = \frac{1.32\,(1900)\,(2.45 + .40)\,(.625 + .40)}{(.625)^2\,(.40)^2}$$

$$\sigma = 117,000 \text{ PSI}$$

$$\mu = .165$$

TOTAL ACTIVE COILS = N

$$N = \frac{.165\,(.625)^2\,(.40)^2\,(11 \times 10^6)}{(2.45)^3\,(4.5 \times 10^3)}$$

$$N = 1.71$$

WT. ACTIVE COILS = $2.45\,\pi\,(1.71)(.625)(.40)(.28) = .92$

DEAD WT. $= .50\left[\frac{\pi}{4}\left((2.85)^2 - (2.05)^2\right)\right].28 = .46$

TOTAL WEIGHT = 1.38

WEIGHT PENALTY = $.46$
(DEAD WEIGHT)

WORKING WEIGHT = $.92$

PREPARED BY
ALEX MARDERIAN

THE MARQUARDT COMPANY

REPORT

CHECKED BY

CLASSIFICATION

DATE JUNE 7 1972

PAGE 7 OF

1.3.3. 3RD ITERATION

$h = 0.70$ $b = .365$ O.DIA. = 2.850

$D = 2.485$

$b/h = .52$ $D/b = 6.6$

$\lambda = 1.37$ $\mu = .15$

$$\sigma = \frac{1.37\,(1900)(2.85)(1.22)}{(.70)^2\,(.365)^2}$$

$\sigma = 139,000\ PSI$ ← TOO HIGH

1.4. OPTIMUM — FROM THIS STUDY
MACHINED SPRING PER ITEM 1.3.2

PREPARED BY
ALEX MARDERIAN

CHECKED BY

THE MARQUARDT COMPANY

CLASSIFICATION

REPORT

DATE JUNE 7 1972

PAGE 8 OF

2.0 LEVER RATIO = 2

2.1 SINGLE COIL SPRING.
  1.950 O. DIA.
  .340 WIRE DIA.   RATE = 1050 LB/IN.

  1.610 MEAN DIA.

    PRELOAD = 953 LB.
  @ .020" TRAVEL LOAD = 974 LB.

  ALLOW .070" TRAVEL BEYOND MIN. OPERATING HGT
  TO GO TO SOLID HGT.

  LOAD @ SOLID HGT = 1050 LB.

    $D/d = 4.75$ $K = 1.31$

STRESS @ SOLID HGT.

$$\tau = \frac{2.55\,(1050)(1.61)(1.31)}{(.34)^3} = 144,000 \text{ PSI}$$

  PRELOAD = 953 LB. $\tau = 131,000$ PSI
  @ .020" TRAVEL = 974 LB $\tau = 134,000$ PSI

  MEAN STRESS = 132,500 PSI
  ALTERNATING STRESS =   1,500 PSI

→ $N = \dfrac{(11.0\times10^6)(.34)^4}{8\,(1.61)^3\,(1.05\times10^3)} = \underline{4.19}$ ACTIVE COILS

  TOTAL COILS = 6.19

  $(1.61\,\pi)\,N\left[\dfrac{\pi}{4}(.34)^2\right].28 = .129\,N$

  TOTAL WEIGHT = .80 LB.

  WEIGHT PENALTY (DEAD COILS) < .26 LB.

  WORKING WEIGHT = .54 LB

D-8

PREPARED BY
ALEX MARDERIAN

THE MARQUARDT COMPANY

REPORT

CHECKED BY

CLASSIFICATION

DATE
JUNE 7 1972

PAGE
9 OF

2.2 TWO COIL SPRINGS IN SERIES

DIM'S. & STRESSES SAME AS ITEM 2.1

PER SPRING
$$\left\{\begin{array}{l} \text{RATE /SPRING} = 2100 \text{ }^{LB}/_{IN.} \\ \text{ACTIVE COILS} = 2.095 \\ \text{TOTAL COILS} = 4.095 \end{array}\right.$$

$$(1.61\,\pi)N\left[\frac{\pi}{4}(.34)^2\right].28 = .129\,N$$

	ONE SPRING (REF)	TWO SPRINGS
TOTAL WEIGHT	.53	1.06
WEIGHT - DEAD COILS	.26	.52
WORKING WEIGHT	.27	.54

PREPARED BY
ALEX MARDERIAN

THE MARQUARDT COMPANY

REPORT

CHECKED BY

CLASSIFICATION

DATE
JUNE 7 1972

PAGE
10   OF

2.3. MACHINED SPRING
    2- SECTIONS IN SERIES   OPPOSITE HELIX

2.3.1 1ST ITERATION
    1.950 0.DIA.   RATE = 1050 LB/IN.
    $b = h = .350''$ $D = 1.600''$
    $b/h = 1.0$ $D/b = 4.7$
    $\lambda = 1.275$
    $\mu = .179$

$$\sigma = \frac{1.275 (1000)(1.950)(.700)}{(.35)^2 (.35)^2} = 116,000 \text{ PSI.} \leftarrow \text{OK}$$

TOTAL ACTIVE COILS REQ'D, ~ BOTH SECTIONS

$$N = \frac{.179 (.35)^2 (.35)^2 (11 \times 10^6)}{(1.60)^3 (1.05 \times 10^3)} = 7.0$$

WEIGHT OF COILS $= (1.60 \, \pi)(7.0)\left[.35\right]^2 .28 = 1.21$

LENGTHS OF RINGS $= 0.50''$
    .15" EACH END
    .20" CENTER

DEAD WEIGHT $= \frac{\pi}{4}\left[(1.95)^2 - (1.25)^2\right].50 (.28) = .25$

TOTAL   WEIGHT $=$ 1.46   LB

DEAD   WEIGHT $=$ .25   LB

WORKING   WEIGHT $=$ 1.21   LB.

D-10

FORM TMC 685 REV. 3-70

PREPARED BY
ALEX MARDERIAN

THE MARQUARDT COMPANY

REPORT

CHECKED BY

CLASSIFICATION

DATE
JUNE 7 1972

PAGE
11 OF

2.3.2 2ND ITERATION

1.950 O.DIA.

$R = 1050$ LB/IN

$b = .280''$ $b/h = .64$

$D = 1.670$ $D/b = 6$ $\lambda = 1.32$

$h = .440$ $\mu = .164$

$$\sigma = \frac{1.32 \,(1000)\,(1.95)\,(.720)}{(.280)^2 \,(.440)^2} = 122,000 \text{ PSI}$$

TOTAL ACTIVE COILS — BOTH SECTIONS

$$N = \frac{.164 \,(.28)^2 \,(.44)^2 \,(11 \times 10^6)}{(1.67)^3 \,(1.05 \times 10^3)} = 6.0$$

WEIGHT OF COILS $= (1.67 \,\pi)\,(6.0)(.28)(.44)(.28) = 1.08$

DEAD WEIGHT $= \frac{\pi}{4}\left[(1.95)^2 - (1.39)^2\right].56 \,(.28) = .21$

TOTAL WEIGHT $= 1.29$ LB.

DEAD WEIGHT $= .21$ LB.

WORKING WEIGHT $= 1.08$ LB.

FORM TMC 685 REV. 3-70

PREPARED BY
ALEX MARDERIAN

THE MARQUARDT COMPANY

REPORT

CHECKED BY

CLASSIFICATION

DATE
JUNE 7 1972

PAGE
12 OF

2.3.3 3RD ITERATION

1.950 O.DIA.   R = 1,050 LB/N

$\mathscr{b} = .440$ b/h = 1.57

D = 1.510   D/b = 3.4

h = .280   λ = 1.27

                                          μ = .163

$$\sigma = \frac{1.27(1000)(1.95)(.720)}{(.44)^2(.28)^2} = 118,000 \, PSI.$$

TOTAL COILS - BOTH SECTIONS = N

$$N = \frac{.163(.44)^2(.28)^2(11\times10^6)}{(1.510)^3(1.05\times10^3)} = 7.5$$

HEAVIER THAN 2ND ITERATION

2.3.4,   4TH ITERATION

1.95 O.DIA.

$\mathscr{b} = .26$ b/h = .55

D = 1.69   D/b = 6.5

h = .48   λ = 1.35   μ, = .154

$$\sigma = \frac{1.35(1000)(1.95)(.74)}{(.48)^2(.26)^2} = 125,000 \, PSI.$$

$$N = \frac{.154(.48)^2(.26)^2(11\times10^6)}{(1.69)^3(1.05\times10^3)} = 5.2 \quad \text{TOTAL ACTIVE COILS.}$$

WEIGHT OF COILS = $1.69\pi(5.2)(.26)(.48)(.28) = .96$

DEAD WEIGHT = $\frac{\pi}{4}\left[(1.95)^2 - (1.41)^2\right].50(.28) = .20$

TOTAL WEIGHT = 1.16 LB.

DEAD WEIGHT = .20 LB,

WORKING WEIGHT = .96 L.B.

D-12

FORM TMC 688 REV. 9-70

PREPARED BY
ALEX MARDERIAN

THE MARQUARDT COMPANY

REPORT

CHECKED BY

CLASSIFICATION

DATE
JUNE 7 1972

PAGE
13   OF

2.4. OPTIMUM CONFIGURATION

    2.2. TWO COIL SPRINGS IN SERIES   1.06 LB,

    2.3.4 4TH ITERATION MACHINED SPG.   1.16 LB,

PREPARED BY

ALEX MARDERIAN

THE MARQUARDT COMPANY

REPORT

CHECKED BY

CLASSIFICATION

DATE JUNE 7 1972

PAGE 14 OF

3.0 LEVER RATIO = 3

3.1 SINGLE COIL SPRING

1.600 O. DIA.

.280 DIA. WIRE

1.320 MEAN DIA.

$D/d = 4.7$ $K = 1.31$

RATE = 380 LB/IN

PRELOAD = 650 LB.

@ .030" TRAVEL LOAD = 662 LB

LOAD @ SOLID HGT = 690 LB. (.100" TRAVEL BEYOND PRELOAD)

$\sigma_S = $ STRESS @ SOLID HGT $= \dfrac{2.55\,(690)(1.32)(1.31)}{(.28)^3} = 139{,}000\,PSI.$

$$\left[\begin{array}{ll} \text{PRELOAD} = 650\ LB & \sigma = 131{,}000\ PSI \\ \text{LOAD @ .030" TRAVEL} = 662\ LB & \sigma = 133{,}000\ PSI \\ \\ \text{MEAN STRESS} = & 132{,}000\ PSI \\ \text{ALTERNATING STRESS} = & 1{,}000\ PSI \end{array}\right.$$

$$N = \frac{(11.0 \times 10^6)\,(.28)^4}{8\,(1.32)^3\,(0.380 \times 10^3)} = 10 \text{ ACTIVE COILS}$$

TOTAL COILS = 12

$$0.28\left[(1.32\,\pi)\ N\left[\frac{\pi}{4}(.28)^2\right]\right] = .071$$

TOTAL WEIGHT = .85 LB

WEIGHT OF DEAD COILS = .14 LB

WORKING WEIGHT = .71 LB.

PREPARED BY
ALEX MARDERIAN

THE MARQUARDT COMPANY

REPORT

CHECKED BY

CLASSIFICATION

DATE
JUNE 7 1972

PAGE
15 OF

3.2 TWO COIL SPRINGS IN SERIES   OPPOSITE HELIX

SAME DIM'S. & STRESS AS ITEM 3.1
RATE/SPRING = 766 LB/IN.

ACTIVE COILS/SPG. = 5

TOTAL COILS/SPG = 7

	ONE SPRING (REF)	TWO SPRINGS
TOTAL WEIGHT	.50	1.0
WT. DEAD COILS	.14	.28
WORKING WEIGHT	.36	.72

PREPARED BY

ALEX MARDERIAN

CHECKED BY

THE MARQUARDT COMPANY

REPORT

CLASSIFICATION

DATE   JUNE 7 1972   PAGE   16   OF

3.3 MACHINED SPRING.   TWO SECTIONS   OPPOSITE HELIX

3.3.1 1ST ITERATION
  1.600   O. DIA. $R = 380$ LB/IN.
  $b = .250$ $b/h = .78$
  $D = 1.350$ $\lambda = 1.31$
  $h = .32$ $D/b = 5.4$ $\mu = .176$

$$\tau = \frac{1.31 \,(670)(1.60)(.570)}{(.25)^2 \,(.32)^2} = 125,000 \text{ psi.}$$

$$N = \frac{.176 \,(.25)^2 (.32)^2 \,(11 \times 10^6)}{(1.35)^3 \,(.38 \times 10^3)} = 13.25$$

WEIGHT COILS $= 1.35 \,\pi \,[13.25](.25)(.32)(.28) =$ 1.26 LBS

DEAD WEIGHT $= \frac{\pi}{4} \left[(1.60)^2 - (1.10)^2\right] .50(.28) =$ .15 LBS

TOTAL WT $=$ 1.41 LBS

4.0 LEVER RATIO = 4

    4.1 SINGLE COIL SPRING

        1.35 O. DIA,   180 LB/IN

        .240 DIA, WIRE

        1.110 MEAN DIA,

$$\frac{D}{d} = 4.6 \qquad K = 1.31$$

        PRELOAD = 490 LB

@ .40 TRAVEL LOAD = 497 LB,

@ .140 TRAVEL LOAD = 515 LB, SOLID HgT,

@ SOLID HgT $\sigma = \dfrac{2.55 \, (515)(1.11)(1.31)}{(.24)^3} = 138,000 \text{ PSI}$

$$N = \frac{(11 \times 10^6)(.24)^4}{8\,(1.11)^3\,(.180 \times 10^3)} = 18.5 \text{ ACTIVE COILS}$$

TOTAL COILS = 20.5

$$1.11 \, \pi \, (N) \left[\frac{\pi \, (.24)^2}{4} \right] .28 = .044 \, N$$

TOTAL WEIGHT — .90 LBS

WEIGHT - DEAD COILS — .09 LBS

WORKING WEIGHT — .81 LBS.

STRESS @ PRELOAD = 131,000 PSI

STRESS @ .040 TRAVEL = 133,000 PSI

MEAN STRESS = 132,000 PSI

ALTERNATING STRESS = 1,000 PSI

D-17

PREPARED BY

ALEX MARDERIAN

CHECKED BY

THE MARQUARDT COMPANY

CLASSIFICATION

REPORT

DATE

JUNE 7 1972

PAGE

18 OF

4.2 Two Coil Springs in Series — Opposite Helix

Same Dim's & Stress As Item 4.1

Rate/Spring = 360 LB/IN.

9.25 Active Coils /SPG.
11.25 Total Coils /SPG

	ONE SPRING (REF.)	TWO SPRINGS
TOTAL WEIGHT	.50	1.00
DEAD COIL WEIGHT	.09	.18
WORKING WEIGHT	.41	.82

D-18

FORM TMC 685 REV. 3-70

PREPARED BY
ALEX MARDERIAN

CHECKED BY

THE MARQUARDT COMPANY

CLASSIFICATION

REPORT

DATE JUNE 7 1972

PAGE 19 OF

4.3 MACHINED SPRING - 2 SECTIONS, OPPOSITE HELIX

4.3.1 1ST ITERATION
1.350 O. DIA.   180 LB/IN.

$b = .200$ $b/h = .67$
$D = 1.150$ $D/b = 3.8$
$h = .310$ $\lambda = 1.87$ $\mu = .167$

$$\sigma = \frac{1.37 \,(500)\,(1.35)\,(.510)}{(.20)^2 (.31)^2} = 123,000 \text{ PSI}$$

$$N = \frac{.167 \,(.20)^2 (.31)^2 (11 \times 10^6)}{(1.15)^3 (.180 \times 10^3)} = 25.7 \quad \text{TOTAL COILS}$$

WEIGHT COILS $= 1.15 \, \pi \,(25.7)(.20)(.31)(.28) = \qquad 1.61$ LBS.

DEAD WT. $= \frac{\pi}{4}\left[(1.35)^2 - (1.15)^2\right].50(.28) = \qquad .09$

TOTAL WEIGHT $= 1.70$ LBS.

PREPARED BY
ALEX MARDERIAN

THE MARQUARDT COMPANY

REPORT

CHECKED BY

CLASSIFICATION

DATE JUNE 8 1972

PAGE 20 OF

5.0 ADDITIONAL WEIGHT REQ'D. FOR ACCOMODATING LONG SPRINGS.

FOR LEVER RATIOS = 2, 3, 4 WEIGHT PENALTY FOR SPRING LENGTHS OVER 2.00"

FOR LEVER RATIOS = 1 WEIGHT PENALTY FOR SPRING LENGTHS OVER 1.00"

ASSUME A CYLINDRICAL HOUSING.

PRESSURE = 500 PSI

$$\sigma = \frac{PR}{t} + \frac{F_s}{2\pi R t}$$

LEVER RATIO	R	F_s	σ	@ 10,000 PSI t
1	1.75	2000	$\frac{1057}{t}$	.011
2	1.25	1000	$\frac{752}{t}$	.008
3	1.05	700	$\frac{631}{t}$	.006
4	.95	500	$\frac{559}{t}$	.006

STRESS IS NOT THE PROBLEM

DEFLECTION DICTATES THE DESIGN

ASSUME:
MIN. THICKNESS FOR FABRICATION = .025
$$\lambda = \Delta L / L = \frac{\sigma}{E}$$

LEVER RATIO	σ	λ	ΔL IN 2"
1	42,280	.0014	.0014 (IN 1.00")
2	30,080	.0010	.0020
3	25,240	.0008	.0016
4	22,360	.0007	.0014

DESIGN TO MINIMIZE THIS DEFLECTION WOULD BE TOO HEAVY.

THIS DEFLECTION MUST BE CALIBRATED INTO SPRING ASSEMBLY INSTALLATION

D-20

PREPARED BY
ALEX MAROERIAN

THE MARQUARDT COMPANY

REPORT

CHECKED BY

CLASSIFICATION

DATE
JUNE 8 1972

PAGE
21 OF

5.0 WEIGHT PENALTY (CONT'D)

$$\text{WEIGHT PENALTY} = 2\pi R t \left[L - L_{REQ} \right] 0.28$$

R = HOUSING RADIUS $-\left[(\text{SPRING DIA.} + 0.10) \div 2 \right]$

L_{REQ} = 2.00" FOR LEVER RATIOS 2, 3, 4

= 1.00" FOR LEVER RATIO = 1

CASE ① SINGLE COIL SPRING

② TWO COIL SPRINGS IN SERIES — OPPOSITE HELIX

③ MACHINED SPRING.

$t = .025"$

LEVER RATIO	R	①		WEIGHT PENALTY — LBS ②		③	
		L INCH.	LBS	L	LBS	L	LBS
1	1.475	1.5	.03	4.0	.19	2.8	.12
2	1.025	2.2	.01	5.2	.14	3.8	.08
3	.85	3.5	.06	7.5	.21	6.5	.17
4	.70	5.2	.10	10.8	.27	11.2	.28

APPENDIX E

BELLEVILLE SPRING ANALYSIS

PREPARED BY
ALEX MARDERIAN

THE MARQUARDT COMPANY

REPORT

CHECKED BY

CLASSIFICATION

DATE
JULY 6 1972

PAGE

OF

BELLEVILLE WASHER STACK
— USE WITH SSP BELLOWS

LET: $\dfrac{O.\,DIA.}{I.\,DIA.} = 2.0$ $O.\,DIA. = 1.70$

$a = .85$

$h = 0.625\,t$

FLAT $\Big\{$

$$\sigma = \frac{48 \times 10^6\,h}{a^2}\left[.4h + 1.37t\right]$$

$$\sigma = 72.72 \times 10^6\,t^2$$

$$P_1 = 72.72 \times 10^6\,h\,t^3 = 45.45 \times 10^6\,t^4$$

LET: $t = .062$ $h = .0388$

P_1 (FLAT) = 668 LB.

σ (FLAT) = 280,000 PSI

$$P = 72.72 \times 10^6\,\delta\left[(.0388 - \delta)\left(.0388 - \tfrac{\delta}{2}\right).062 + .000238\right]$$

δ INCHES	P — LBS
.010	211
.015	305
.020	393
.025	473 ⎤ *
.030	545 ⎦
.035	618
.0388	669

*INSTANTANEOUS RATE PER WASHER $\dfrac{72}{.005} = 14,400$ LB/IN

REQ'D RATE = 380 LB/IN

NO. OF WASHERS REQ'D = 38

TOTAL WEIGHT = 1.20 LB.

TOTAL HEIGHT = 3.83"

PREPARED BY

ALEX   MAROERIAN

CHECKED BY

THE MARQUARDT COMPANY

REPORT

CLASSIFICATION

DATE

JULY 6 1972

PAGE

1 OF 3

BELLEVILLE WASHER STACK
 —USED WITH GARDNER BELLOWS

LET: $\dfrac{O.DIA.}{I.DIA.} = 2$ $\qquad O.DIA = 1.56''$ $\qquad I.DIA. = 0.78''$

$h = 0.5\,t$ $\qquad a = 1.56/2 = 0.78$
h = FREE HEIGHT
t = THICKNESS
STRESS WHEN FLAT

$$\sigma = \frac{48 \times 10^6 h}{a^2} (.61\,h + 1.37\,t)$$

$$\sigma = 66.075\,t^2$$

IF: $\sigma = 300,000$ PSI $\qquad$ THEN: $t = .067''$
$\qquad\qquad\qquad\qquad\qquad\qquad h = .0335$

$$P = \frac{E\,\delta}{(1-r^2)(M)\,a^2}\left[(h-\delta)\left(h-\frac{\delta}{2}\right)t + t^3\right]$$

$r = 0.3$ $\quad M = 0.69$ $\quad a = .78$ $\quad t = .067$

δ = DEFLECTION

δ - INCHES	P - LBS
.010	271
.015	385
.020	503
.025	605
.030	715
.0335	785

DEFLECTION TO   650 LB. PRELOAD = .027''
DEFECTION TO   661.4 LB. @ FULL STROKE = .0275''

$.0275/.0335 = 0.82 \;(< .85)$

INSTANTANEOUS RATE PER WASHER = $11.4/.0005 = 22,800$ LB/IN.

REQ'D. RATE = 380 LB/IN.

NO. OF WASHERS REQ'D = 60

TOTAL WEIGHT = 1.73 LBS.

TOTAL HEIGHT = 6.030''

E-2

PREPARED BY
ALEX MARDERIAN

THE MARQUARDT COMPANY

REPORT

CHECKED BY

CLASSIFICATION

DATE
JULY 6 1972

PAGE
2 OF 3

BELLEVILLE WASHER STACK
- USE WITH GARONER BELLOWS

LET: $O.DIA/I.DIA. = 3.00$ $O.DIA. = 1.56"$ $I.DIA. = .52"$

$M = .78$ $C_1 = 1.425$ $C_2 = 1.74$ $a = .78"$

IN FLAT CONDITION $\begin{cases} \sigma = 69.47 \times 10^6 \left[.7125 \, h + 1.74 \, t \right] h \\ P = 69.47 \times 10^6 \, h \, t^3 \end{cases}$

LET: $\frac{h}{t} = 0.50$
$t = .069$
$h = .0345$

$\begin{cases} \sigma = 347,000 \; PSI \\ P = 785 \; LB. \end{cases}$

$P = \dfrac{E \, \delta}{(1-r^2) M a^2} \left[(h - \delta)\left(h - \frac{\delta}{2}\right) t + t^3 \right]$

$E = 30 \times 10^6$ $M = .78$ $r = 0.3$ $h = .0345$
$t = .069$

$P = 69.47 \times 10^6 \, \delta \left[(.0345 - \delta)(.0345 - \frac{\delta}{2})(.069) + .000329 \right]$

δ - INCHES	P - LBS
.010	257
.015	375
.020	486
.025	590
.030	695
.0345	788

DEFLECTION TO 650 LB. PRELOAD = .0278"
DEFLECTION TO 661.4 LB @ FULL STROKE = .0285
   $.0285/.0345 = .83 \; (< .85)$

INSTANTANEOUS RATE PER WASHER $= \dfrac{11.4}{.00065} = 21,000 \; LB/IN$

RATE REQ'D $= 380 \; LB/IN$

NO. OF WASHERS $= 55$

TOTAL WEIGHT $= 1.93 \; LB.$

TOTAL HEIGHT $= 5.69"$

E-3

PREPARED BY ALEX MARDERIAN

THE Marquardt CORPORATION

CHECKED BY

BELLEVILLE WASHER LOAD VS DEFLECTION

USE WITH GARLOCK BELLOWS

$$K = \frac{O.DIA.}{I.DIA.} \qquad O.DIA = .456"$$

K = 2

K = 3

LOAD = LBS

DEFLECTION - INCHES

E-4

K+E ALBANENE® LA3227
TRACING PAPER
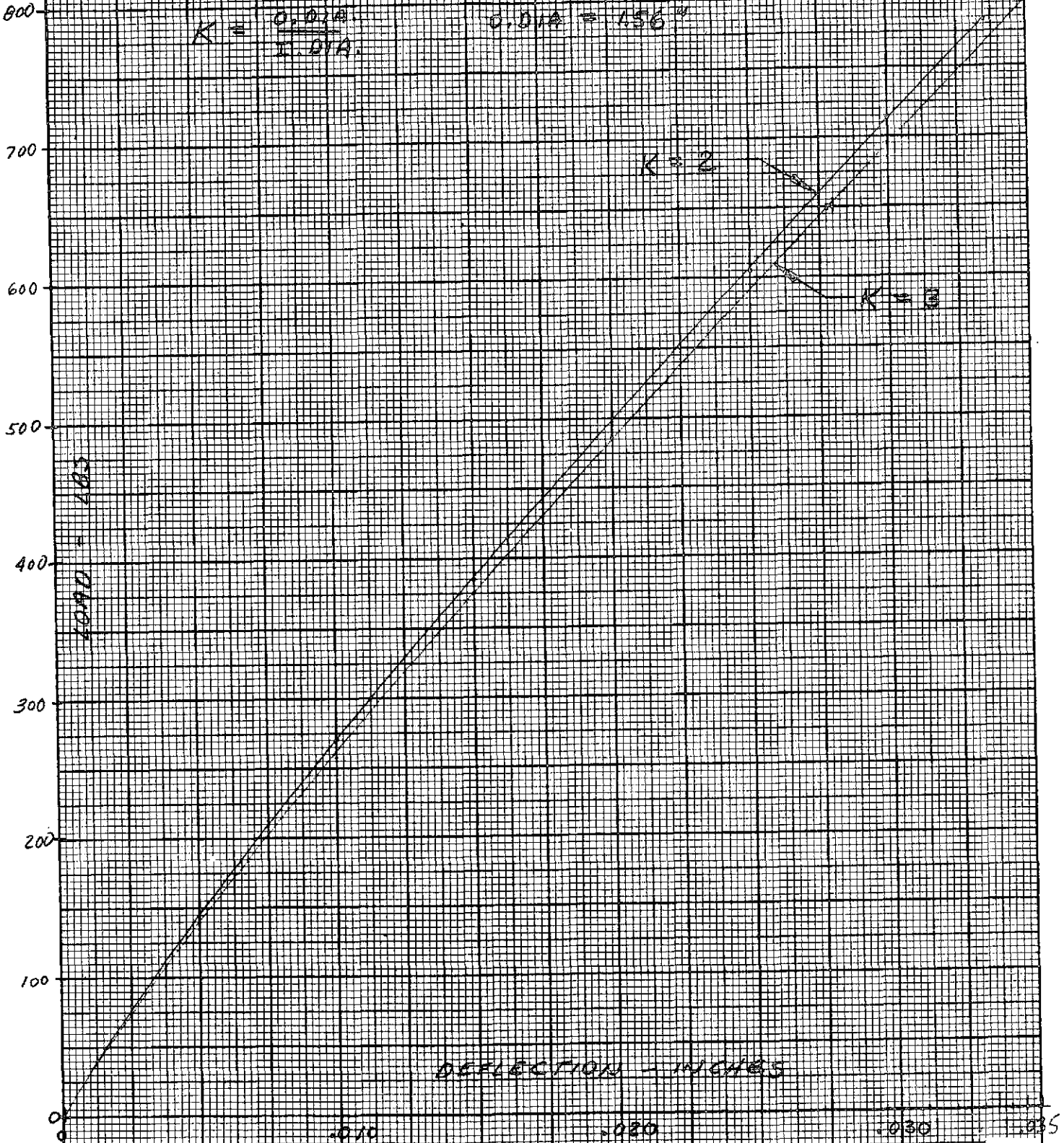
APPENDIX F

DIAPHRAGM ANALYSIS

PREPARED BY
ALEX MARDERIAN

THE MARQUARDT COMPANY

REPORT

CHECKED BY

CLASSIFICATION

DATE
JULY 13 1972

PAGE
1 OF

DIAPHRAGM & PISTON
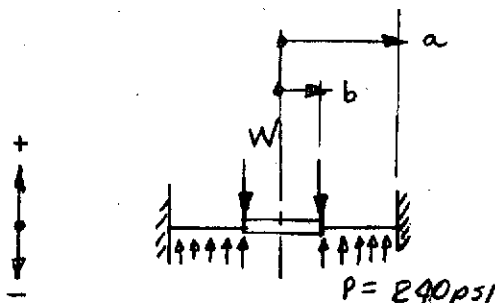
$$\begin{cases} m = \dfrac{1}{\nu} = \dfrac{1}{.294} = 3.4 \\ m^2 = 11.6 \end{cases}$$

$$W = \rho \, \gamma \, (a^2 - b^2)$$

$$a = 1.00 \qquad \log \tfrac{a}{b} = 1.1$$
$$b = .33''$$

$$P = 240\,psi$$

CASE I   PRESSURE LOAD ALONE

OUTER EDGE
$$\begin{cases} \sigma_r = \dfrac{3P}{4t^2}\left[a^2 - 3b^2 + \dfrac{4b^4}{a^2-b^2}\log\tfrac{a}{b}\right] \\ \sigma_r = \dfrac{134.8}{t^2} \end{cases}$$

INNER EDGE
$$\begin{cases} \sigma_r = -\dfrac{3P}{4t^2}\left[(a^2+b^2) - \dfrac{4a^2b^2}{a^2-b^2}\log\tfrac{a}{b}\right] \\ \sigma_r = -\dfrac{110}{t^2} \end{cases}$$

$$\begin{cases} \delta = +\dfrac{3P(m^2-1)}{16\,m^2 E\,t^3}\left[a^4 + 3b^4 - 4a^2b^2 - 4a^2b^2\log\tfrac{a}{b} + \dfrac{16a^2b^4}{a^2-b^2}\left(\log\tfrac{a}{b}\right)^2\right] \\ \delta = +\dfrac{.555\times10^{-6}}{t^3} \end{cases}$$

CASE II   W LOAD ALONE $W = 240\,\gamma\,(.9) = 216\,\gamma$

OUTER EDGE
$$\begin{cases} \sigma_r = \dfrac{3W}{2\pi t^2}\left[1 - \dfrac{2b^2}{a^2-b^2}\log\tfrac{a}{b}\right] \\ \sigma_r = \dfrac{259.8}{t^2} \end{cases}$$

INNER EDGE
$$\sigma_r = \dfrac{3W}{2\pi t^2}\left[1 - \dfrac{2a^2}{a^2-b^2}\log\tfrac{a}{b}\right]$$
$$\sigma_r = -\dfrac{468}{t^2}$$

$$\begin{cases} \delta = \dfrac{3W(m^2-1)}{4\pi\,m^2 E\,t^3}\left[a^2 - b^2 - \dfrac{4a^2b^2}{a^2-b^2}\left(\log\tfrac{a}{b}\right)^2\right] \\ \delta = -\dfrac{1.787\times10^{-6}}{t^3} \end{cases}$$

F-1

PREPARED BY
ALEX MARDERIAN

CHECKED BY

THE MARQUARDT COMPANY

CLASSIFICATION

REPORT

DATE
JULY 13 1972

PAGE
2 OF

DIAPHRAGM & PISTON (CONT'D)

CASE III BALANCED PISTON — HANDBOOK

INNER EDGE $\sigma_r = \dfrac{3P}{4t^2}\left[\dfrac{4a^4}{a^2-b^2}\,Log\,\dfrac{a}{b}\;-3a^2+b^2\right]$

$$\delta = \dfrac{-3p\,(m^2-1)}{16\,E\,m^2\,t^3}\left[3a^4-4a^2b^2+b^4+4a^2b^2\,Log\,\dfrac{a}{b}\;-\dfrac{16\,a^4b^2}{a^2-b^2}\left(Log\,\dfrac{a}{b}\right)^2\right]$$

$\sigma_r = -\dfrac{358}{t^2}$

CHECK: SUBTRACT STRESSES
CASE I & II

$\sigma_b = -\dfrac{40}{t^2} - \left(-\dfrac{468}{t^2}\right) = \dfrac{358}{t^2}$

$\delta = -\dfrac{1.232\times10^{-6}}{t^3}$

CHECK: ADD δ IN CASES I & II

$\delta_I = +.555$
$\delta_{II} = -1.787$
——————
-1.232

$\angle ET\;\sigma_r = 150,000\;PSI$ THEN: $t = .049$	$\angle ET\;\sigma_r = 300,000\;PSI$ THEN $t = .0345$
CASE I $\;\begin{cases}\delta = \dfrac{+.555\times10^{-6}}{t^3}\\[4pt]\delta = +.005''\end{cases}$	CASE I $\;\delta = +.0135''$
CASE II $\;\begin{cases}\delta = -\dfrac{1.787\times10^{-6}}{t^3}\\[4pt]\delta = -.015''\end{cases}$	CASE II $\;\delta = -.0435''$
CASE III $\;\delta = -.010''$	CASE III $\;\delta = -.030''$

PREPARED BY

ALEX MARDERIAN

CHECKED BY

THE MARQUARDT COMPANY

REPORT

CLASSIFICATION

DATE July 13 1972

PAGE 1 OF 2

CORRUGATED DIAPHRAGM

w_0 = CENTER DEFLECTION
p = PRESSURE PSI.

<u>1.0</u> 1ST APPROXIMATION
UNSUPPORTED AT THE CENTER
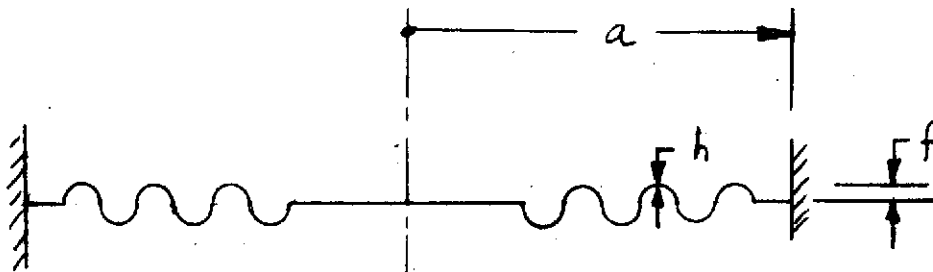
$$\sigma_M = 0.423 \left[\frac{E p^2 a^2}{h^2} \right]^{\frac{1}{3}}$$

OUTER EDGE STRESS $= \dfrac{\sigma_M}{2} + \dfrac{E}{(\frac{a}{h})^2} \left[\dfrac{4}{(1-\nu^2)} \dfrac{w_0}{h} \right]$

$E = 30 \times 10^6$

$1 - \nu^2 = 1 - (0.3)^2 = 0.91$

$p = 240$ psi

$\sigma_M = 0.423 \left[E p^2 \left(\dfrac{a}{h} \right)^2 \right]$

$\sigma_M = 0.423 \left[(30 \times 10^6)(.24 \times 10^3)^2 \left(\dfrac{a}{h} \right)^2 \right]^{\frac{1}{3}}$

$\sigma_M = 6090 \left(\dfrac{a}{h} \right)^{\frac{2}{3}}$

$0.5 \, \sigma_M = 3045 \left(\dfrac{a}{h} \right)^{\frac{2}{3}}$

$\sigma_b = \dfrac{30 \times 10^6}{(\frac{a}{h})^2} \left[\dfrac{4}{.91} \dfrac{w_0}{h} \right]$

$\sigma_b = \dfrac{132 \times 10^6}{(\frac{a}{h})^2} \dfrac{w_0}{h}$

$\sigma = 3045 \left(\dfrac{a}{h} \right)^{\frac{2}{3}} + \dfrac{132 \times 10^6}{(\frac{a}{h})^2} \dfrac{w_0}{h}$

PREPARED BY

ALEX MARDERIAN

THE MARQUARDT COMPANY

REPORT

CHECKED BY

CLASSIFICATION

DATE *July 13 1972*

PAGE 2 OF 2

CORRUGATED DIAPHRAGM (CONT'D)

$$8 \left(\frac{w_0}{h}\right)\left[\frac{2}{3(1-v^2)} + \left(\frac{f}{h}\right)^2\right] + \frac{6}{7}\left(\frac{w_0}{h}\right)^3 = \frac{P}{E}\left(\frac{a}{h}\right)^4$$

$$8 \left(\frac{w_0}{h}\right)\left[0.731 + \left(\frac{f}{h}\right)^2\right] + \frac{6}{7}\left(\frac{w_0}{h}\right)^3 = 8 \times 10^{-6}\left(\frac{a}{h}\right)^4$$

<u>4.4</u> 1ˢᵀ ITERATION

LET: $a/h = 150$ $\frac{w_0}{h} = 10$

$$\sigma = 3045 \left(150\right)^{2/3} + \frac{132 \times 10^6}{(150)^2} \times 10$$

$$\sigma = 145,000 \ PSI.$$

$$8 \left(\frac{w_0}{h}\right)\left[.731 + \left(\frac{f}{h}\right)^2\right] + \frac{6}{7}\left(\frac{w_0}{h}\right)^3 = 8 \times 10^{-6}\left(\frac{a}{h}\right)^4$$

$$80 \left[.731 + \left(\frac{f}{h}\right)^2\right] + 857 = 4050$$

$$\frac{f}{h} = 6.26$$

$\underline{a}$	$\underline{h}$	$\underline{w_0}$	$\underline{f}$
1.00	.0067	.067	.042

F-4

CIRCULAR PLATE – CLAMPED EDGE

σ_M MEMBRANE STRESS AT CENTER

(TIMOSHENKO) $\dfrac{w_0}{h} + 0.488\left(\dfrac{w_0}{h}\right)^3 = \dfrac{3}{16}\dfrac{P a^4}{E h^4}(1-\nu^2)$

(NADAI) $\sigma_M = 0.423\sqrt[3]{E P^2 \left(\dfrac{a}{h}\right)^2}$ { MEMBRANE STRESS AT CENTER

σ_D = OUTER EDGE STRESS

$\sigma_D = \dfrac{0.8\,\sigma_M}{1.6} + \dfrac{E}{\left(\frac{a}{h}\right)^2}\left[\dfrac{4}{1-\nu^2}\left(\dfrac{w_0}{h}\right)\right]$

$\sigma_D = 0.5\,\sigma_M + \sigma_B$

$\nu = 0.3$

$E = 28 \times 10^6$

h = THICKNESS

w_0 = CENTER DEFLECTION

a = RADIUS

P = UNIT PRESSURE

$\dfrac{a}{h}$

1000

100

σ_B

$\dfrac{w_0}{h}$

PRESSURE – P.S.I.

σ_B values: 10,000 20,000 30,000 40,000 50,000 60,000 70,000 80,000 90,000 100,000 125,000 150,000

σ_M values: 13,000 15,000 23,000 25,000 33,000 40,000 50,000 60,000 70,000 80,000 90,000 100,000 125,000 150,000 175,000 200,000

ALEX MARDERIAN
12 AUG. 1964

F-5

PREPARED BY
ALEX MARDOERIAN

THE MARQUARDT COMPANY

REPORT

CHECKED BY

CLASSIFICATION

DATE
July 14 1972

PAGE 1 OF 1

NESTED SPRINGS TO BE USED WITH DIAPHRAGM

$D/d = 7.0$ $K = 1.213$ $G = 11.2 \times 10^6$

$$\tau = \frac{4P}{\pi d^2}\left[1 + 2\frac{DK}{d}\right] = \frac{22.89\,P}{d^2}$$

$$R = \frac{Gd}{8\left(D/d\right)^3 N} = \frac{4081.6\,d}{N}$$

LET: O.DIA. OF OUTER SPRING $\cong 2.10''$
TOTAL MAX LOAD $\cong 700$ LB.
TOTAL RATE = 490 LB/IN.

OUTER SPRING

$D_o = 1.834$
$d_o = .262$

O.DIA. = 2.096
I.DIA. = 1.572

$$\tau = 333.46\,P_o$$

$$R_o = \frac{1069.4}{N_o}$$

$P_o = 457$ LB
$\tau = 152,000$ PSI

$R_o = 320$ LB/IN

ACTIVE COILS = 3.34
TOTAL COILS = 5.34
SOLID HGT = 1.400
PRELOAD HGT = 1.500
WEIGHT = .36 LB.

$f_c = 324$ CPS

INNER SPRING

$D_f = 1.337$
$d_i = .191$

O.DIA = 1.528
I.DIA. = 1.146

$$\tau = 627.45\,P_i$$

$$R_i = \frac{779.6}{N_i}$$

$P_i = 243$ LB
$\tau = 152,000$ PSI

$R_i = 170$ LB/IN

ACTIVE COILS = 4.58
TOTAL COILS = 6.58
SOLID HGT = 1.260
PRELOAD HGT = 1.360
WEIGHT = .24 LB

$f_c = 324$ CPS

LET: $N_i = \frac{.262}{.191}\,N_o$

$R_o + R_i = 490$
$N_o = 3.34$
$N_i = 4.58$

TOTAL WEIGHT = 0.60 LB.

F-6

FLAT DIAPHRAGM. — USING MEMBRANE THEORY

MEMBRANE STRESS $\sigma_M = 0.423 \left[E p^2 \left(\frac{a}{h}\right)^2 \right]^{1/3}$

OUTER EDGE STRESS $= 0.5 \sigma_M + \sigma_b$

$$\sigma_b = \frac{E}{\left(\frac{a}{h}\right)^2} \left[\frac{4}{1-r^2} \left(\frac{w_0}{h}\right) \right]$$

$a =$ OUTSIDE RADIUS
$h =$ THICKNESS
$w_0 =$ CENTER DEFLECTION
$v = 0.3$
$E = 30 \times 10^6$
$p =$ PRESSURE

$$\left\{ \begin{array}{l} \sigma_M = 0.423 \left[(30 \times 10^6)(.24 \times 10^3)^2 \left(\frac{a}{h}\right)^2 \right]^{1/3} \\[2mm] \sigma_M = 6090 \left(\frac{a}{h}\right)^{2/3} \end{array} \right.$$

$$\left\{ \begin{array}{l} \sigma_b = \frac{30 \times 10^6}{\left(\frac{a}{h}\right)^2} \left[\frac{4}{.91} \quad \frac{w_0}{h} \right] \\[3mm] \sigma_b = \frac{132 \times 10^6}{\left(\frac{a}{h}\right)^2} \times \frac{w_0}{h} \end{array} \right.$$

OUTER EDGE STRESS $\sigma = 3045 \left(\frac{a}{h}\right)^{2/3} + \frac{132 \times 10^6}{\left(\frac{a}{h}\right)^2} \times \frac{w_0}{h}$

CENTER DEFLECTION $= w_0$

$$\frac{w_0}{h} + 0.488 \left(\frac{w_0}{h}\right)^3 = \frac{3 \, p \, a^4 \, (1 - v^2)}{16 \, E h^4} = 1.50 \times 10^{-6} \left(\frac{a}{h}\right)^4$$

$$\frac{w_0}{h} + 0.488 \left(\frac{w_0}{h}\right)^3 = 1.5 \times 10^{-6} \left(\frac{a}{h}\right)^4$$
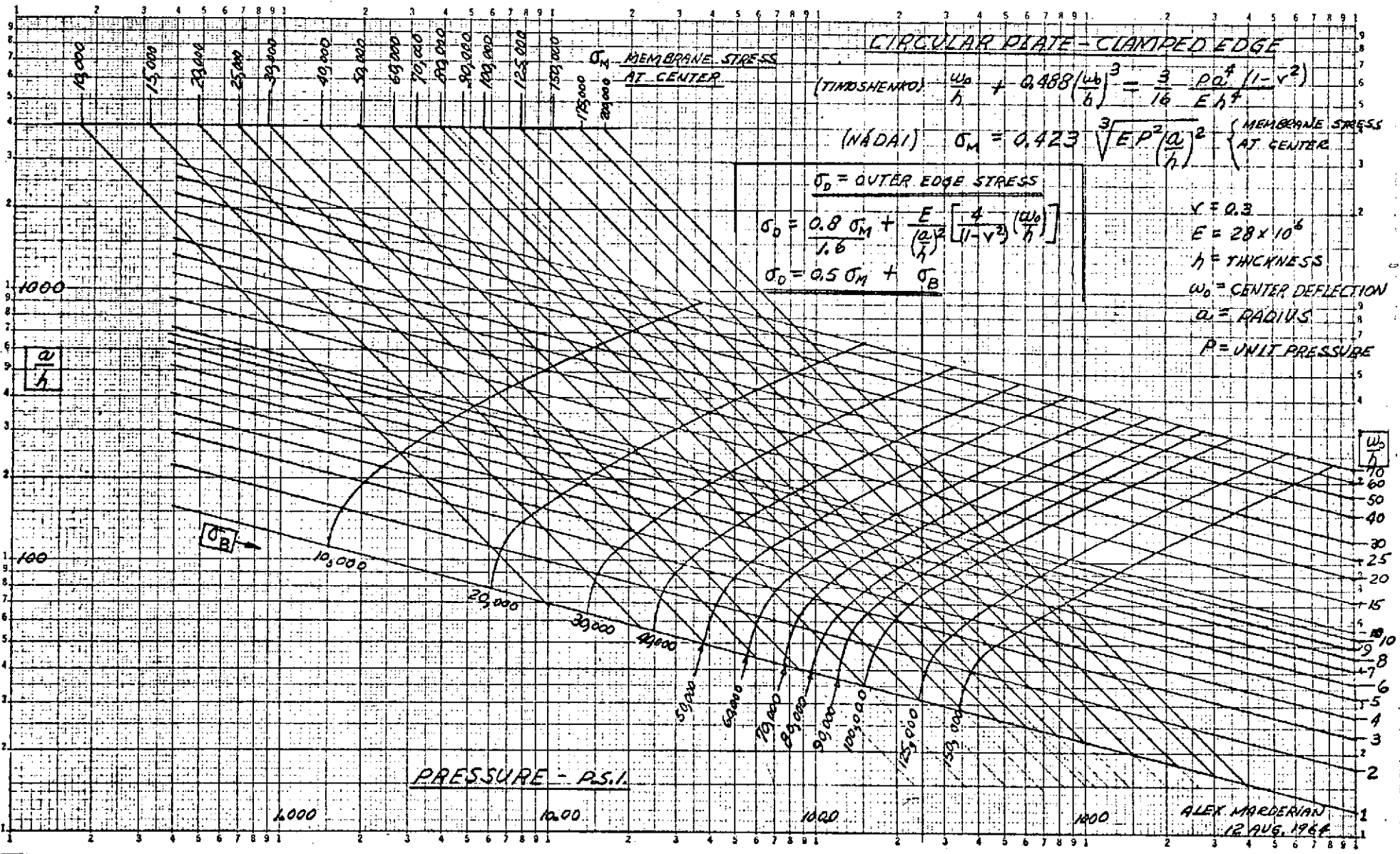
LET: $\frac{a}{h} = 115$ $\frac{w_0}{h} = 8$

$\sigma = 152,000$ PSI

IF: $a = 1.000''$ ← OUTSIDE RADIUS
THEN: $h = .0087''$ ← THICKNESS
$w_0 = .0696''$ ← CENTER DEFLECTION

LET: $\frac{a}{h} = 150$ $\frac{w_0}{h} = 10$

$\sigma = 145,000$ PSI

$\sigma_b = 59,000$ PSI
$\sigma_M = 86,000$ PSI

IF: $A = 1.00$
THEN: $h = .0067''$ $w_0 = .067''$

F-7

APPENDIX G

GREATER MARGIN BELLOWS

STRESS ANALYSIS & SPRING ANALYSIS

PREPARED BY
DICKENS

CHECKED BY

CLASSIFICATION

THE MARQUARDT COMPANY

REPORT
He REGULATOR

DATE 7 July 1972 PAGE 8 OF

He REGULATOR

BELLOWS ANALYSIS - S.S.P (Rev. 2, 3)

3:1 LEVER RATIO

	SSP #2	SSP #3
ID	1.63	1.73
OD	2.11	2.11
De	1.89	1.93
N (convolutions)	19	19
t	.010	.010
MATL	INCO 718	INCO 718
RATE (TOTAL)	202 #/in ?	360 #/in
FREE H	3.40 in	3.40
INSTALL H	1.90	1.90
STROKE	±.030	±.030
Pext	240 psi	240 psi

$$\text{RATE}_2 = \frac{4.3 \, E \,(OD + ID)\, t^3}{(OD - ID - t)^3 \, N}$$

$$= \frac{4.3 \times 30 \,(2.11 + 1.63)(10^{-6}) 10^6}{(2.11 - 1.63 - .010)^3 \, 19}$$

$$= \frac{129 \,(3.74)}{(.47)^3 \,(19)} = \underline{244 \, \#/in}$$
$$\quad\quad .104$$

$$\text{RATE}_3 = \frac{129 \,(3.63)}{19 \,(.37)^3} = \underline{510 \, \#/in}$$
$$\quad\quad .051$$

G-1

PREPARED BY
DICKENS

CHECKED BY

CLASSIFICATION

THE MARQUARDT COMPANY

REPORT He REGULATOR

DATE 10 July 1972   PAGE 9 OF

He REGULATOR

For MAX WORKING LOAD

	SSP #2	SSP #3
FREE H.	3.40	3.40
INSTALL H.	1.90	1.90
STROKE	±.030	±.030
R.	244 #/"	510 #/"

$P_{MAX} =$

SSP #2: $244(3.40 - 1.90 - .030)$
$$= \underline{359\ \#}$$

SSP #3: $510(3.40 - 1.90 - .030)$
$$= \underline{750\ \#}$$

$a/b =$
OD/D_{EFF}

SSP #2: $2.11/1.89 = 1.11$

SSP #3: $2.11/1.93 = 1.09$

Roark p 221
case 18

SSP #2:
$$S_{MAX} = \beta \frac{W}{t^2}$$
$$\beta = .033$$
$$S_{MAX} = .033 \frac{(359)}{(.010)^2}$$
$$= \underline{120000\ psi}$$

SSP #3:
$$S_{MAX} = \beta \frac{W}{t^2}$$
$$\beta = .025$$
$$S_{MAX} = .025 \frac{(750)}{(.010)^2}$$
$$= \underline{188000\ psi}$$

$P_{H\ in}$

SSP #2:
$= 359 - .060(244)$
$$= \underline{344.4\ \#}$$

SSP #3:
$750 - .060(510)$
$$= \underline{719.4\ \#}$$

$S_{M\ in}$

SSP #2:
$$\frac{344.4}{359}(120,000)$$
$$= \underline{115,000\ psi}$$

SSP #3:
$$\frac{719.4}{750}(188000) = \underline{180,000}$$

S_{MEAN}

SSP #2:
$(120 + 115)/1000/2$
$$= \underline{117500\ psi}$$

SSP #3:
$(188 + 180)/1000/2$
$$= \underline{184000\ psi}$$

S_{ALT}

SSP #2: $\pm 2500\ psi$

SSP #3: $\pm 2000\ psi$

G-2

PREPARED BY DICKENS

THE MARQUARDT COMPANY

CHECKED BY

CLASSIFICATION

REPORT He REGULATOR

DATE 10 July 1972

PAGE 10 OF

He REGULATOR

PRESSURE STRESSES — $p = 240$ psi

	SSP #2	SSP #3
$S = \dfrac{p(OD - ID - t)^2}{16(1.25)\, t^2}$ (BELLOWS EQUATION)	$\dfrac{240}{20}\left(\dfrac{(2.11 - 1.63 - .01)^2}{(.01)^2}\right)$ $= 26400$ psi	$\dfrac{240}{20}\left(\dfrac{(2.11 - 1.73 - .01)^2}{(.010)^2}\right)$ $= 16400$ psi
COMBINED PRESSURE AND LOAD STRESS		
MEAN STRESS	$= 117500 + 26400$ $= 143900$ psi	$= 184000 + 16400$ $= 200400$ psi
ALT STRESS	$= \pm 2500$	± 2000 psi
MAT'L Inco 718 HTA		
(MIL HANDBK 5A, DEC 1968)		
FATIGUE M.S. 10^5 cycles	$M.S. = \dfrac{5.25}{4.05} - 1 = .30$	$M.S. = \dfrac{5.3}{5.75} - 1 = -.09$
YIELD MARGIN LET $F_{by} = 1.20 \times 150$ $= 180$ KSI	$M.S. = \dfrac{180}{146.4} - 1 = .23$	$M.S. = \dfrac{180}{202.4} - 1 = -.12$

G-3

BELLOWS & SPRING RESIZING

PER AVO DATED: 7-7-72   H. WICHMANN

CASE I

EFFECTIVE AREA	BELLOWS DATA					SPRING	
	O. DIA.	I. DIA.	COMPRESSED LENGTH	FREE LENGTH	RATE	PRELOAD LBS	RATE
2.81 in^2	2.11	1.63	1.90	3.40	202 LB/in	371	290 LB/in

$$F_T = TOTAL\ FORCE = 2.81\ (240) = 674\ LB.$$

$$R_T = TOTAL\ RATE = 492\ LB/IN.$$

$$F_B = BELLOWS\ FORCE = (3.4 - 1.9)(202) = 303$$

$$F_S = SPRING\ FORCE = F_T - F_B = 371$$

$$R_S = SPRING\ RATE = R_T - 202$$

CASE II

EFFECTIVE AREA	BELLOWS DATA					SPRING	
	O. DIA.	I. DIA	COMPRESSED LENGTH	FREE LENGTH	RATE	PRELOAD LBS	RATE
2.81	2.11	1.63	2.85	5.10	134.7 LB/in	371	357 LB/in

$$F_T = 674\ LB$$

$$R_T = 491.7\ LB/IN.$$

$$F_B = (5.10 - 2.85)\,134.666 = 303\ LB$$

$$F_S = 371\ LB$$

$$R_S = (491.7 - 134.7) = 357\ LB/N$$

G-4

PREPARED BY
ALEX MAROERIAN

THE MARQUARDT COMPANY

REPORT

CHECKED BY

CLASSIFICATION
5099

DATE
July 13 1972

PAGE
2 of 4

BELLOWS & SPRING RESIZING (CONT'D)

CASE I
SPRING CALCULATIONS   NESTED SPRINGS

LET: $D/d = 6.8$ $K = 1.22$

$$\sigma = \frac{4P}{\pi d^2}\left[1 + \frac{2DK}{d}\right] = 22.4\frac{P}{d^2}$$

$$R = \frac{Gd}{8(D/d)^3 N} = 4452.5\frac{d}{N}$$ $G = 11.2 \times 10^6$

OUTER SPRING

$D_o = 1.395$
$d_o = .205$

O. DIA. = 1.600
I. DIA. = 1.190

$\sigma = 533.02\, P_o$

$R_o = \frac{912.76}{N_o}$

$P_o = 231\ LB$ MAX.
$\sigma = 123,200\ psi$

$R_o = 192\ LB/IN.$
ACTIVE COILS = 4.8
TOTAL COILS = 6.8
SOLID HEIGHT = 1.394
PRELOAD HGT. = 1.50
WEIGHT = .30 LB.
$f_c = 305$ CPS

INNER SPRING

$D_i = 1.003$
$d_i = .147$

O. DIA = 1.150
I. DIA = .856

$\sigma = 1036.61\, P_i$

$R_i = \frac{654.52}{N_i}$

$P_i = 119\ LB$ MAX.
$\sigma = 123,400\ psi$

$R_i = 98\ LB/IN$
ACTIVE COILS = 6.7
TOTAL COILS = 8.7
SOLID HGT = 1.279
PRELOAD HGT = 1.38
WEIGHT = .14 LB
$f_c = 303$ CPS.

TOTAL WEIGHT = .44 LB.

LET: $P_i = \frac{533.02}{1036.61}\, P_o$
$P_i + P_o = 350$

THEN: $P_o = 231\ LB$ $P_i = 119\ LB.$

LET: $N_i = \frac{.205}{.147}\, N_o$

$R_o + R_i = 290\ LB/IN.$

$N_o = 4.77$
$N_i = 6.65$

BELLOWS & SPRING RESIZING (CONT'D)

CASE II
  SPRING CALCULATIONS   NESTED SPRINGS

$$LET: \; D/d = 6.8 \qquad K = 1.22$$

$$\sigma = \frac{4P}{\pi d^2} \left[1 + \frac{2 \, D K}{d} \right] = 22.4 \frac{P}{d^2}$$

$$R = \frac{G d}{8 (D/d)^3 N} = 4452.5 \frac{d}{N} \qquad\qquad G = 11.2 \times 10^6$$

__OUTER SPRING__

$D_0 = 1.395$
$d_0 = .265$

O. DIA. = 1.600
I. DIA. = 1.190

$$\sigma = 533.02 \, P_0$$

$$R_0 = \frac{912.76}{N_0}$$

$P_0 = 231 \, LB \quad MAX.$
$\sigma = 123,200 \, psi$

$R_0 = 236 \, LB/IN.$
    ACTIVE COILS = 3.9
    TOTAL COILS = 5.9
    SOLID HEIGHT = 1.210
    PRELOAD HGT. = 1.31
WEIGHT = .26
$f_c = 375 \, CPS$

INNER SPRING

$D_1 = 1.003$
$d_1 = .147$

O. DIA = 1.150
I. DIA. = .856

$$\sigma = 1036.61 \, P_1$$

$$R_1 = \frac{654.52}{N_1}$$

$P_1 = 119 \, LB \quad MAX.$
$\sigma = 123,400 \, PSI.$

$R_1 = 121 \, LB/IN$
    ACTIVE COILS = 5.4
    TOTAL COILS = 7.4
    SOLID HGT = 1.090
    PRELOAD HGT = 1.19
WEIGHT = .12
$f_c = 376 \, CPS$

TOTAL WEIGHT = .38 LB

$$LET: \; P_1 = \frac{533.02}{1036.61} \, P_0$$

$$P_1 + P_0 = 350$$

THEN: $P_0 = 231 \, LB$ $P_1 = 119 \, LB.$

$$LET: \; N_1 = \frac{.205}{.147} \, N_0$$

$$R_0 + R_1 = 357. \, LB/IN$$

$$N_0 = 3.87$$

$$N_1 = 5.40$$

G-6

PREPARED BY
ALEX MAROERIAN

THE MARQUARDT COMPANY

REPORT

CHECKED BY

CLASSIFICATION
5099

DATE
JULY 13 1972

PAGE
4 OF 4

BELLOWS & SPRING RESIZING (CONT'D)

	WEIGHTS		REF. L14014
	CASE I	CASE II	
BELLOWS	.20 LB,	.30	.90 (GARDNER)
SPRINGS	.44 LB	.38 LB,	1.04 LB
SUB-TOTAL	.64 LB	.68	1.94 LB
Δ HSG. WEIGHT, BELLOWS (LENGTH INCREASE)	0	.10 LB	0
Δ HSG. WEIGHT, SPRING, (LENGTH INCREASE)	0	0	.11 LB
TOTAL	.64 LB	.78 LB	2.05 LB
WEIGHT SAVINGS BASED ON L14014	1.41 LB	1.27 LB,	0

G-7

APPENDIX H

REDUNDANT BELLOWS STRESS ANALYSIS

PREPARED BY
DICKENS

THE MARQUARDT COMPANY

CHECKED BY .

CLASSIFICATION

REPORT
He Regulator Bellows

DATE
2 Aug 1972

PAGE
11 OF

He Regulator Bellows

SSP Bellows - Tandem

$O.D = 2.05.10$ Each
$I D = 1.63$ "
$t = .010$ "
$N = 9$ "
Free Length $= 1.60$ Each

For $p = 480$ psi

$$\text{Max Load} = p\left[\frac{\pi}{4}\left(\frac{2.05 + 1.63}{2}\right)^2\right] = 2.65 \times 480 = 1270 \#$$

$$\text{Rate / Spring} = \frac{4.3\, E\,(OD + ID)\, t^3}{(OD - ID - t)^3\, N}$$

$$= \frac{4.3 \times 30 \times 10^6 \,(3.68)\, 10^{-6}}{(.069)\, 9}$$

$$= 765\, \#/'' \;/ \text{Spring}$$

For two in tandem or parallel

$$R = 2 \times 765 = 1530\, \#/'' \quad \text{Total}$$

For Tension Bellows

Maximum pressure stress for 480 psi

$$\text{Pressure Stress} = \frac{p\,(OD - ID - t)^2}{16\,(1.25)\, t^2}$$

$$= \frac{480\,(.41)^2}{20 \times 10^{-4}}$$

$$= 40300\, \text{psi}$$

H-1

FORM TMC 655 REV. 3-70

PREPARED BY DICKENS

CHECKED BY

CLASSIFICATION

THE MARQUARDT COMPANY

REPORT He REGULATOR BELLOWS

DATE 2 AUG 72

PAGE 12 OF

He REGULATOR BELLOWS — TANDEM APPLICATION

FOR STROKE STRESS

TOTAL PRELOAD = 1270# / 480 psi

$$STROKE = LOAD / RATE = \frac{1270^{\#}}{1530 \#/_{in}} = .83''$$

STRESS FOR STROKE = .83''

$$LOAD / SPRING = .83 \times 765 \#/_{in} = 635^{\#}$$

$$S = P \frac{7.5 \times 10^{6} (OD - ID - t)}{E (OD + ID) t^{2}}$$

$$= \frac{635 (7.5)(.41)}{30 (3.68) 10^{-4}}$$

$$= 177,000 \ psi$$

TOTAL COMBINED STRESS

$$S_{TOTAL} = 40,300 + 177,000 = 217,300 \ psi$$

SSP BELLOWS - He REGULATOR

TANDEM ARRANGEMENT

$O.D. = 2.11$ ID

$ID = 1.56$ IN

$t = .012$

$N = 13$

FREE LENGTH = 2.26 IN /BELLOWS

FOR $p = 480$ psi

$$\underline{LOAD} : \quad p \frac{\pi}{4}\left[\left(\frac{2.11 + 1.56}{2}\right)^2\right] = 2.65 \times 480 = \underline{1270^{\#}}$$

$$RATE/SPRING = \frac{4.3 E (OD + ID) t^3}{(OD - ID - t)^3 N} = \frac{4.3 (30)(3.67)(.012)^3 \, 10^6}{(.535)^3 \, 13}$$

$$= 403 \, ^{\#}/_4 / BELLOWS$$

$$\underline{FOR \; TWO \; BELLOWS \; IN \; TANDEM \; R = 2 \times 403 = 806 \, ^{\#}/}$$

FOR TENSION BELLOWS

PRESSURE STRESS   @ 480 psi

$$\underline{\underline{\sigma}} = \frac{p (OD - ID - t)^2}{20 \, t^2} = \frac{480 (.583)^2}{20 (.012)^2} = \underline{52600 \, psi}$$

FOR LOAD = 1270 /2 = 635$^{\#}$/BELLOWS

$$S = \frac{P (7.5) 10^6 (OD - ID - t)}{E (OD + ID) t^2} = \frac{635 (7.5)(.535)}{30 (3.67)(.012)^2} = \underline{162000 \, psi}$$

$$\underline{TOTAL \; COMBINED \; STRESS = 52600 + 162000 = \underline{214000 \, psi}}$$

FOR 480 psi

H-3

PREPARED BY DICKENS

CHECKED BY

THE MARQUARDT COMPANY

CLASSIFICATION

REPORT He Regulator Bellows

DATE 7 Aug 72

PAGE 14 OF

SSP Bellows - He Regulator

TANDEM ARRANGEMENT

For $p = 480$ psi & STROKE = 240 psi LoAD

FOR $p = 240$ psi, LoAD = $1270/2 = 635\#$ TOTAL

STROKE = $\dfrac{635}{806 \, \#/_{in}} = .787''$

STRESS FOR STROKE = $.787''$, $p = 635/2 = 317 \#/\text{Bellows}$

$\sigma = \dfrac{317}{635} \times 162,000 = 81000$ psi

TOTAL STRESS, PRESSURE + STROKE

$= 56,600 + 81000 =$

$\sigma_{TOT} = 137,600$ psi

$F_{ty} = 150,000$ psi $\times 1.22 = 183,000$ psi

$M.S. \dfrac{183,000}{137,600} - 1 = .33$

APPENDIX I

TORSIONAL SPRING RATE ANALYSIS OF THE

ACTUATOR FOR THE BASELINE REGULATOR

PREPARED BY
DICKENS

THE MARQUARDT COMPANY

REPORT
He REGULATOR

CHECKED BY

CLASSIFICATION
N-60350-10

DATE
15 JUNE 72

PAGE
1   OF

He REGULATOR

STIFFNESS CHARACTERISTICS OF SPRING No. 3

O.D = 1.600
WIRE = .280
N = 12 TOTAL, 10 ACTIVE

FREE H = 5.211 IN
INSTALLED H = 3.500 IN.

$$\beta_o = \frac{2 l_o E I G}{n \pi r (2G + E)} \quad = \quad \text{RATIO OF } \underline{\text{BENDING MOMENT}} \atop \underline{\text{CURVATURE}}$$

WAHL pg. 280

l_o = FREE LENGTH
r = mean coil radius
I = MOMENT OF INERTIA OF SECTION
n = number of ACTIVE COILS

UNDER LOAD $\beta = \beta_o \dfrac{l}{l_o}$ where l = COMPRESSED LENGTH

$$\beta_o = \frac{2(5.211)(29\times10^6)(.000303)(11.0\times10^6)}{10 \pi (.660)(2\times11+29)10^6} = \underline{955\times10^6} \equiv \frac{M}{1/\rho}$$

OR $\theta_{TOT} = \dfrac{n \pi M r}{E I}\left(1 + \dfrac{E I}{G I_\rho}\right)$ $\dfrac{E}{G} = \dfrac{1}{.38} = 2.63$

$\theta_{TOT} = \dfrac{n \pi M r}{E I}(2.315)$ $\dfrac{I}{I_\rho} = \dfrac{1}{2} = .5$

$\theta_{TOT} = \dfrac{10 \pi M (.660)(2.315)}{29\times10^6 (.000303)} = \underline{.00546 M}$
rad

PREPARED BY
DICKENS

CHECKED BY

THE MARQUARDT COMPANY

CLASSIFICATION
N-603S0-70

REPORT
He Regulator

DATE
15 June '72

PAGE
2   OF

He Regulator

Stiffness of Bellows — Bending

Deflection at End for Cantilever Bending

$$\Delta = \frac{5.25\, P L^3}{D_o^2\, n\, r}$$

P = Load
L = Bellows Length = 2.0
D_o = O.D = 2.05
n = Length of one convolution of bellows, in (Axial)
r = Spring rate of one convolution, #/in

Find Equivalent Cantilever Beam Slope at End.   Then Stiffness $= \dfrac{M}{\theta}$

$$\Delta = \frac{5.25\, P\, (2.0)^3}{(2.05)^2\, n\, r}$$

$$n = \frac{2.0}{30} = .0666$$

$$r = 105 \times 30 = 3150 \ \#/_{in}$$

$$\underline{\Delta} = \frac{5.25\, p\, (8.0)}{4.2 \times .0666\, (3150)} = \underline{.0475\, P}$$

For Equivalent Beam 2.0 in Long

$$D = \frac{P L^3}{3\, EI} = .0475\, P$$

$$(EI) = \frac{L^3}{3(.0475)} = \frac{8}{.1425} = \underline{56.1}$$

$$\underline{\theta} = \frac{M_o\, L}{EI} = \frac{M_o\, (2)}{56.1} = \underline{.0357\, M_o}$$

PREPARED BY
DICKENS

THE MARQUARDT COMPANY

CHECKED BY

CLASSIFICATION

REPORT
He Regulator

DATE
15 June 72

PAGE
3   OF

He Regulator

Stiffness of Flexure - Bending
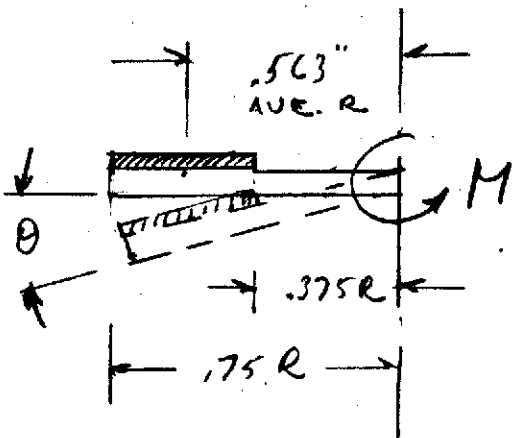
For Unit θ (rad), $\Delta = (.563)\theta$ at .563 in Radius

For Moment Taken Out as Couple

$$P = M/.563 = 1.77 M$$

$$\theta = \frac{PR^2}{4EI}(\lambda B_3 - B_1)$$

$R^2 = (.563)^2 = .316$

$EI = 30 \times .0312 (.020)^3 10^6$
$\qquad = 7.50$

$\lambda = .707$
$B_3 = -8$
$B_1 = 6.28$
$B_7 = 6.28$

$$\theta = \frac{1.77M(.316)}{4 \times 7.5}(.707(-8) - 6.28)$$

$$\theta = .222 M$$

For Unit Torque = Unit Moment

$$\theta = \frac{M_0 R}{4EI}(\lambda B_7 + B_1) = \frac{M_0(.563)(.707+1)6.28}{70} = .201 M_0$$

PREPARED BY DICKENS
CHECKED BY
CLASSIFICATION
THE MARQUARDT COMPANY
REPORT He Regulator
DATE 15 June '72
PAGE 4 OF

He Regulator

STIFFNESS OF FLEXURE - BENDING

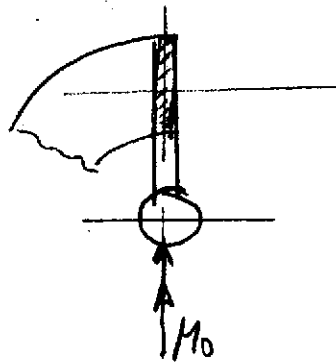For θ due to moment

Proportion Moment taken as couple

$$M' = \frac{.201\, M}{(.201 \times .222)} = .475\, M_0$$

Proportion moment taken as torque

$$T_2 = \frac{.222}{(.201 + .222)} = .525\, M_0$$

Total $\theta = .222 \times .475\, M_0 + .201 \times .525\, M_0 = \underline{.2105\, M_0}$

For stiffness of flex, with arm at 90° to M_0

Approximate θ (treat as bent)

$$\theta = M_0 \left[\frac{2R}{1.57\,EI} + \frac{D}{1.57\,KG} \right]$$

$$EI = 7.5$$

$$KG = .116\, t^3 \times 11.5 \times 10^6$$

$$= .116 (.02)^3 \times 11.5 \times 10^6$$

$$= 10.7$$

$$\theta = M_0 \left[\frac{2(.563)}{1.57 \times 7.5} + \frac{1.126}{1.57(10.7)} \right]$$
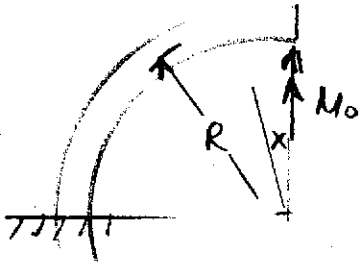
$$\theta = .162\, M_0 \quad (\text{Approx.})$$

But from Pg 5, $\theta = .201\, M_0$

I-4

PREPARED BY
Dickens
CHECKED BY
CLASSIFICATION
THE MARQUARDT COMPANY
REPORT
He Regulator
DATE 15 June '72
PAGE 5
OF

He Regulator

Stiffness of Flexure _ Bending

For Stiffness Due To Edge Mo

Slope at Edge $= \theta$

$\theta = \dfrac{\partial U}{\partial M_0}$

$M = M_0 \cos x$

$T_q = M_0 \sin x$

$$\Sigma U = \left[\int \frac{M^2 R\, dx}{2EI} + \int \frac{T^2 R\, dx}{2GK} \right]$$

$$U = \int_0^{\frac{\pi}{2}} \frac{M_0^2 \cos^2 x \, R\, dx}{2 \times 7.5} + \int_0^{\frac{\pi}{2}} \frac{M_0^2 \sin^2 x \, R\, dx}{2 \times 10.7}$$

$$\theta = \frac{\partial U}{\partial M_0} = \left[\frac{1}{2EI} \int_0^{\frac{\pi}{2}} 2 M_0 (R)(\cos x)^2 dx + \frac{1}{2GK} \int_0^{\frac{\pi}{2}} 2 M_0 (\sin x)^2 R\, dx \right]^2$$

$$\theta = = \left[\frac{(M_0 R)}{7.5} \int_0^{\frac{\pi}{2}} \cos^2 x \, d\alpha + \frac{M_0 R}{10.7} \int_0^{\frac{\pi}{2}} \sin^2 \alpha \, d\alpha \right] 2$$

$$= 2 M_0 R \left[\frac{1}{7.5} \left(\frac{\alpha}{2} + \frac{\sin 2\alpha}{4} \Big|_0^{\frac{\pi}{2}} \right) + \frac{1}{10.7} \left(\frac{\alpha}{2} - \frac{\sin 2\alpha}{4} \Big|_0^{\frac{\pi}{2}} \right) \right]$$

$$= 2 M_0 (.563) \left[\frac{1}{7.5} \left(\frac{\pi}{4} + 0 \right) + \frac{1}{10.7} \left(\frac{\pi}{4} - 0 \right) \right]$$

$$= 1.126 M_0 (.785)(.1333 + .0935)$$

$$\underline{\theta = .201 \, M_0}$$

PREPARED BY
DICKENS
CHECKED BY
CLASSIFICATION
THE MARQUARDT COMPANY
REPORT He REGULATOR
DATE 15 JUNE '72   PAGE 6 OF

He REGULATOR

FROM pgs 4, 5

$\theta = .201 M_0$ FOR M_0 RIGHT ANGLES TO EDGE

$\theta = .210 M_0$ " " PARALLEL TO EDGE

LET $\theta = .205$ FOR M_0 60° TO EDGE

LET $\theta = .205$ FOR AVERAGE VALUE OR STACK AT 120° RELATIVE DISPLACEMENT

THEN $\theta/_{FLEX} = .205 \dfrac{M_0}{3}$ FOR STACK OF 3 FLEX

$$\theta/_{FLEX} = .0683 M_0$$

TOTALS

__FLEXURE__ $M_0/_\theta = 14.63$ in$^{\#}$/rad/FLEX

BELLOWS $M_0/_\theta = \dfrac{1}{.0357} = 28.0$ in$^{\#}$/rad/Bellows

SPRING $M_0/_\theta = \dfrac{1}{.00546} = 183.0$ in$^{\#}$/RAD SPRING

TOTAL STIFFNESS = $14.63 + 28.0 + 183.0 = 225.63$ in$^{\#}$/RAD.

TOTAL STIFFNESS = $M_0/_{\theta°}$ $= 3.94$ in$^{\#}$/°